THE GEOCHEMICAL ASSOCIATIONS OF METALS AND ORGANIC MATTER IN WEST COAST SCOTTISH SEDIMENTS.

by

DAVID O'DONNELL B.Sc.

A Thesis Submitted For The Degree Of

DOCTOR OF PHILOSOPHY

At The University Of Edinburgh.

December 1987.

To My Father

Terry O'Donnell

"Science, beauty, freedom, adventure,

what more could you ask for in life?"

Charles A. Lindberg

ABSTRACT.

Thirteen sediment cores have been collected from a variety of sedimentary environments around the coast of Western Scotland ranging from terrestrially dominated fjords to more marine shelf areas. Eight of these cores have been examined in detail for the minor elements (Cu, Pb, Zn, Zr, Rb, Sc, Sr, Ba, Ni, Cr, Y), Rare Earth elements (La, Ce, Nd), organic components (C, N, S, I, Br,) and porewater components (SO_4^{2-}, alkalinity). In addition, some cores were analysed for $\delta^{15}N$ and also ^{137}Cs (to estimate sediment accumulation rates).

Study of the minor elements associated with the lithogenic fraction (Zr, Rb, Sc, Sr, Ba, Ni, Cr) has highlighted variations in sediment mineralogy and grain-size both spatially and temporally, showing that few of the sediments show steady state accumulation. Indeed, in one core an erosive event can be identified which has been calculated to have removed 18cm of sediment accumulation. In these sediments Ni and Cr have been shown to be associated with the detrital ferromagnesian fraction. Ni can therefore be used as an indicator of lithogenic metal input.

The distibution of the REE (La, Ce, Nd) show enrichments of La and Ce relative to Y and mean shales in the more terrestrially dominated fjords suggesting a possible association with the iron oxide phase.

Organic C, N, S, pore water SO_4^{2-} and alkalinity have been analysed to show the patterns of organic matter degradation in the sediments. C/N ratios have been used to characterise the nature of the organic matter. It is clear that $\delta^{15}N$ values in the sediments are influenced by other factors aside from organic matter provenance, possibly fractionation and biological productivity.

SO_4^{2-} reduction is seen to be a major mechanism of organic degradation, both in the oxic/suboxic biomixed zone and in the anoxic sediment at depth. The incorporation of SO_4^{2-} reduction products at depth is suggested to be a function of the degree of biomixing associated with the flux and quality of the organic matter.

I and Br are shown to be released from the organic matter at depth, but the I/Br ratio shows I to be more labile than Br. Iodine, known to be associated with marine organic matter can therefore be used both as an indicator of marine organic matter and organic diagenesis.

Cu, Pb and Zn show surface enrichment patterns, but these are most marked for Pb and Zn. Ratioing total metals to Ni allows the excess Pb and Zn due to anthropogenic loading to be calculated. Both metals show marked associations with I which vary with depth.

It is concluded that the patterns of heavy metals observed in the sediments are due to diagenetic processes associated with organic matter degradation in a similar manner to I. However, the varying associations of heavy metals to I show the mechanisms of bonding of the Pb and Zn to the organic matter must be different to that of I.

TABLE OF CONTENTS

CHAPTER 1

INTRODUCTION

In recent years, the input of pollutant materials into the marine environment has been causing increasing concern (see Goldberg, 1976(a)). Many of these substances such as, halogenated hydrocarbons (including PCB, DDT and HCB) and certain radionuclides, are alien to the marine environment and enrichment in marine sediments can be attributed directly to a pollutant input (Hom *et al*, 1974; Eisenreich *et al*, 1979; Livingstone and Bowen, 1979; Koide *et al*, 1980; Bopp *et al*, 1981, 1982; Mackenzie, Scott and Williams, 1987). Other pollutant substances for example, heavy metals may show a significant partitioning between natural and anthropogenic phases, however, there is generally a temporal change in the input of pollutant elements that can be recognised. For instance, studies of the distribution of heavy metals, particularly Cu, Pb and Zn, as well as Cd and Hg in the coastal and shallow marine environment (eg Erlenkeuser *et al*, 1974; Bruland *et al*, 1974; Crecelius *et al*, 1975; Goldberg *et al*, 1977; Price *et al*, 1978 and Farmer, 1983) have found them to be enriched in sediments close to the sediment/water interface relative to their concentrations at depth. Many of these studies have been made in areas close to direct pollutant inputs and the enrichment patterns observed in the sediments have therefore been attributed to an increasing anthropogenic loading. Indeed these enrichment patterns have been used by some workers to describe the pollutant history of a number of areas (Erlenkeuser *et al*, 1974; Bruland *et al*, 1974; Goldberg *et al*, 1977, 1978, 1979). However, other studies (Krom, 1976; Price *et al*, 1978; Galloway and Likens, 1979; Hamilton-Taylor, 1979; Malcolm, 1981; Ridgeway, 1984) have found similar metal enrichments in areas more remote from direct industrial discharge. Such trace metals can be released into the atmosphere by the burning of fossil fuels (Bertine and Goldberg, 1971; Swaine, 1977) and other industrial processes (Goldberg, 1976(a); Franzin *et al*, 1979) and their fallout

has been measured over land, sea, and in areas remote from regions of discharge (Lazarus *et al*, 1970; Ranticelli and Perkins, 1970; Nraigu, 1979; Shirahata *et al*, 1980; Shaule and Patterson, 1981; Boutron and Patterson, 1986). These measurements support the theory proposed by Galloway and Likens (1979) that the atmosphere is a major pathway along which heavy metal pollutants may travel to remote sedimentary environments.

Little attention has been paid to the fate of these metals once incorporated into the sediment. A number of workers in remote environments (Elderfield and Hepworth, 1975; Galloway and Likens, 1979; Hamilton-Taylor, 1979; Malcolm, 1981; Ridgway and Price, 1987) have suggested that the patterns of anthropogenic metals in the sediments may be modified by diagenetic processes. In Western Scotland, the only serious studies that have attempted to address this problem (Malcolm, 1981; Ridgway, 1984) have been restricted to one fjord system, Loch Etive.

The aim of this study is to investigate the relationships between heavy metals, sediment lithology (as depicted by trace element comparisons), and organic matter during burial diagenesis in sediments, to try to show that the patterns of anthropogenic metal loading can be diagenetically modified (Elderfield and Hepworth, 1975; Galloway and Likens, 1979; Malcolm, 1981; Ridgway and Price, 1987). To do this a number of sediment cores have been collected from the West Coast of Scotland, which provide a wide range of environments from restricted, terrestrially dominated fjordic systems to more marine dominated sediments of the shelf. To highlight possible spatial variations in the anthropogenic fluxes to the sediments, the sediments were collected over a broad geographical area covering the West coast of Scotland and the Outer Hebrides.

Fundamental to any study of the geochemistry of the sediments is the characterisation of the detrital input material, both spatially and temporally (Shimmield, 1984; Ridgway, 1984). Variations in the detrital input to a sediment can have a marked influence on the patterns of accumulation of heavy metals as well as some control on diagenetic modification. Many studies of sediment diagenesis have assumed that over the period considered, generally the last 100 years, sedimentation as total sediment accumulation has remained constant for a particular sediment and that diagenesis is principally controlled by diffusion within a uniform medium (eg Berner, 1974, 1978, 1980). Measurements of the variability of minor element contents in sediments can be used to identify often small temporal variations in the lithology of the sediments which are often not recognised in mineralogical/grain size analysis (Calvert, 1976; Ridgway, 1984). Such changes can profoundly influence the organic matter in sediments and hence the potential for diagenetic readjustment of authigenic phases (Calvert, 1976). The potential of a sediment for such diagenetic modification is not only influenced by organic content, but also by variations in organic quality, which can be expressed as the ease by which organic matter can be metabolised (Goldhaber and Kaplan, 1975; Berner, 1978; Westrich and Berner 1984). Loosely, this can be regarded as being influenced by variations of terrigenous to marine organic matter as well as their structural changes on burial (Goldhaber and Kaplan, 1975; Lyons and Gaudette, 1979). The relative distribution of the marine and terrigenous organic fractions of sediments has never been satisfactorily identified using isolated geochemical parameters, similarly the propensity of organic matter for degradation by metabolising micro-organisms is difficult to quantify. In this study, the commonly used C/N ratio of organic matter (Bader, 1955; Pocklington and Leonard, 1979) is discussed and used as a basis on which to

compare isotopic variations in the nitrogen content of a sediment which has hitherto being considered a reliable indicator of organic matter provenance (Sweeny *et al*, 1978). Additionally both these methods have been used in conjunction with the minor halides (I and Br) of sediments to obtain an understanding of organic matter degradation.

It is only after appraisal of these factors coupled with sediment accumulation rates that a sensible discussion of the fate of anthropogenically introduced heavy metals can be made.

CHAPTER 2

THE LOCATION, GEOLOGY AND ENVIRONMENTAL SETTING OF THE STUDY AREA

2.1. Introduction

The study area is located on the West coast of Scotland and extends from the Outer Isles in the North, to Oban in the South (see Figure 2.1). Sediment cores were taken from the localities noted in Figures 2.2 and 2.3. The cores were collected during 1984/1985 (Table 2.1) using a lightweight gravity corer, modified to minimise sediment disturbance (Kemp *et al*, 1976). The sediment cores were processed according to the techniques given in Appendix I Section 1. The major emphasis is placed on eight main cores; AB1, CM1, CR1, DN1, DU1, ET1, SH1 and SP1. A further three cores; HO1, NE1, SN1 were collected from the North of the region (see Table 2.1 and Figure 2.2). The data for these sediment cores is given in the appendices. However, this is not as extensive as the former sediments.

2.2. Geology Of The Area.

The rocks of the North-West coast of Scotland and the Hebrides cover a wide span of geological time, from the Archean to the Tertiary (see Figure 2.4). The Isle of Lewis is composed largely of grey tonalitic and granitic gneisses of Lewisian age which have been dated at between 2.8 and 2.9 Ga (Francis *et al* 1971; Moorbath *et al*, 1976). This is the major source of sediment entering Loch Shell. The rocks of the Loch Duich area are also Lewisian, comprising of hornblende and biotite gneiss, garnet and biotite amphibolite, eclogites and diopside-forsterite marble (Harker, 1941). Intercalated with the Lewisian are bands of Moinian psammitic schists. On the Southern shore of Loch Duich is the Glenelg-Ratagan igneous complex which is primarily dioritic in composition with minor granodiorite, syenite, adamellite and some ultrabasics (Nichols, 1950). The head of Loch Duich is bounded by the Strathconon fault

Location	Water Depth (m)	Core Name	Date Collected
Loch Etive:			
Airds Bay	42	AB1	October 1984
Inner Basin	135	ET1	October 1984
Loch Creran	18	CR1	November 1984
Camas an Thais	30	CM1	November 1984
Dunstaffnage Bay	35	DN1	November 1984
Loch Spelve	32	SP1	December 1984
Loch Duich	93	DU1	April 1985
Loch Hourn	130	HO1	April 1985
Loch Nevis	110	NE1	April 1985
Loch Shell	61	SH1	June 1985
Loch Snizort	80	SN1	June 1985

TABLE 2.1: Sediment core localities, core names and collection dates, and water depths.

Loch	Catchment Area Km^2
L. Etive	<1300
L. Creran	166
L. Duich	160
L. Shell	87
L. Spelve	75

TABLE 2.2: Catchment areas of the sea lochs sampled.

Station Location	Precipitation (mm yr^{-1})
L. Etive	2197
L. Duich	2062
L. Spelve	1607
L. Creran	1698
L. Erisort (L. Shell)	1156

TABLE 2.3: Mean annual rainfall over the study area as 30 yr moving average (Meteorological Office Statistics.).

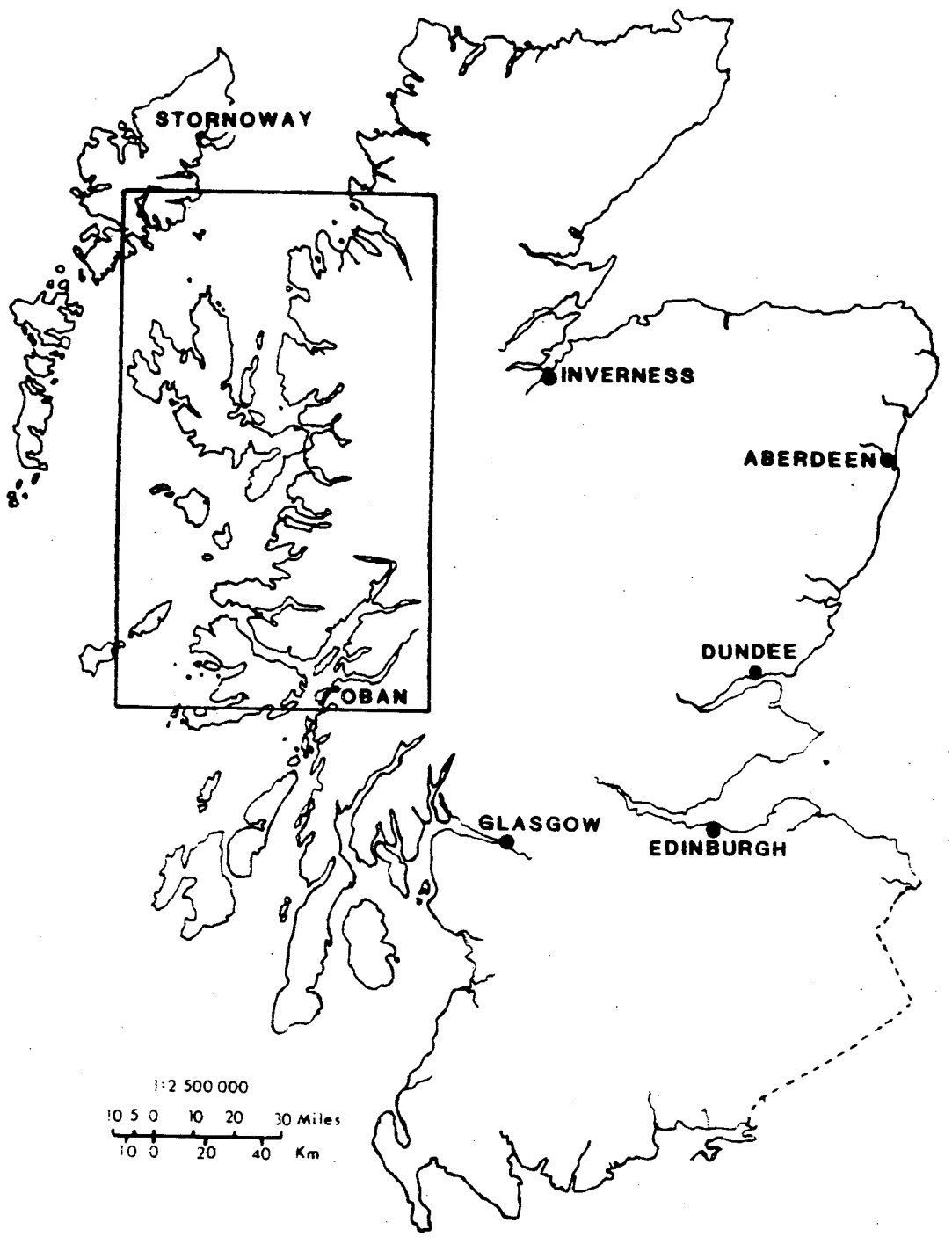

FIGURE 2.1: Location of the study area in Western Scotland.

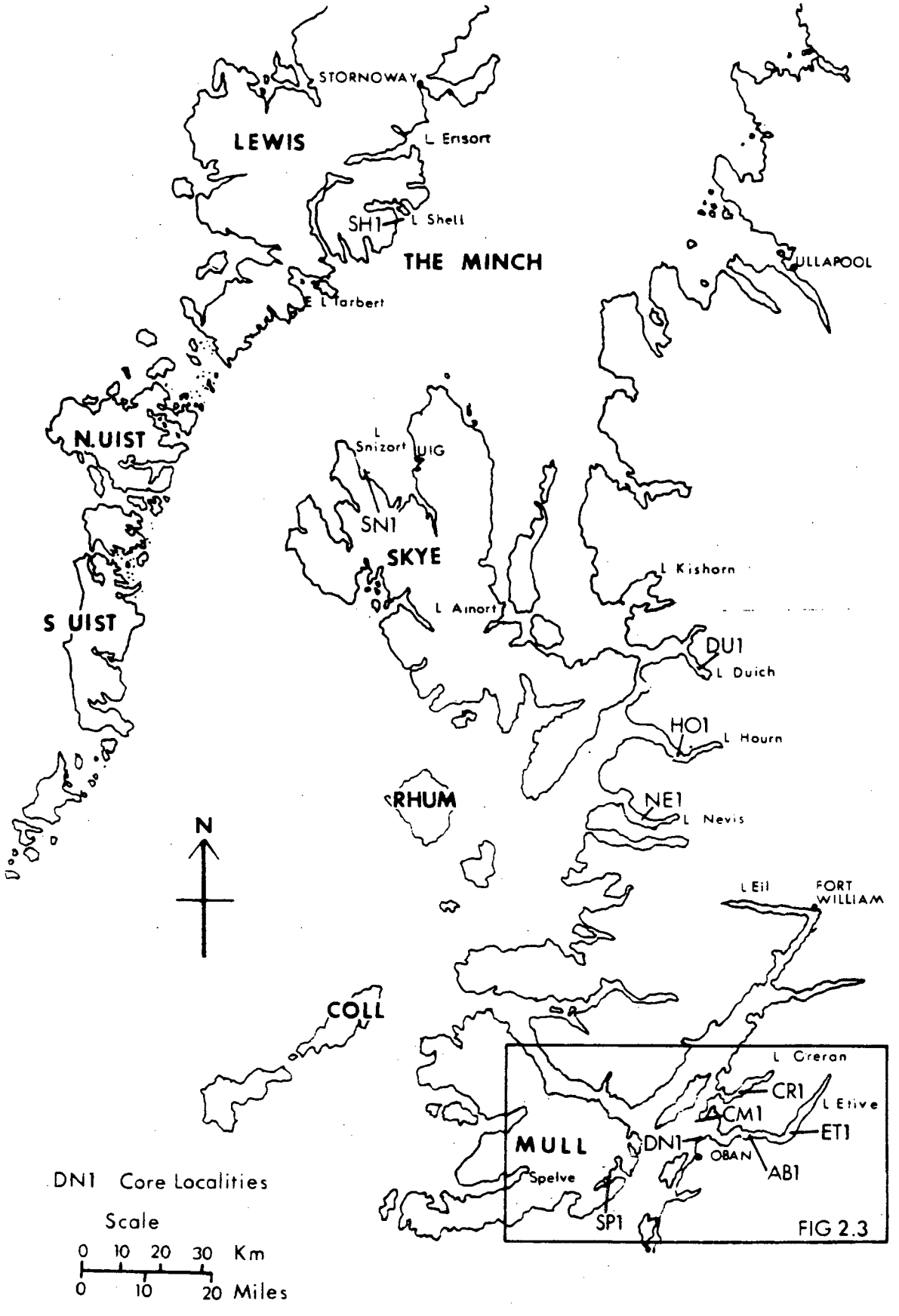

FIGURE 2.2: Sediment core localities in the study area. For inset see Figure 2.3.

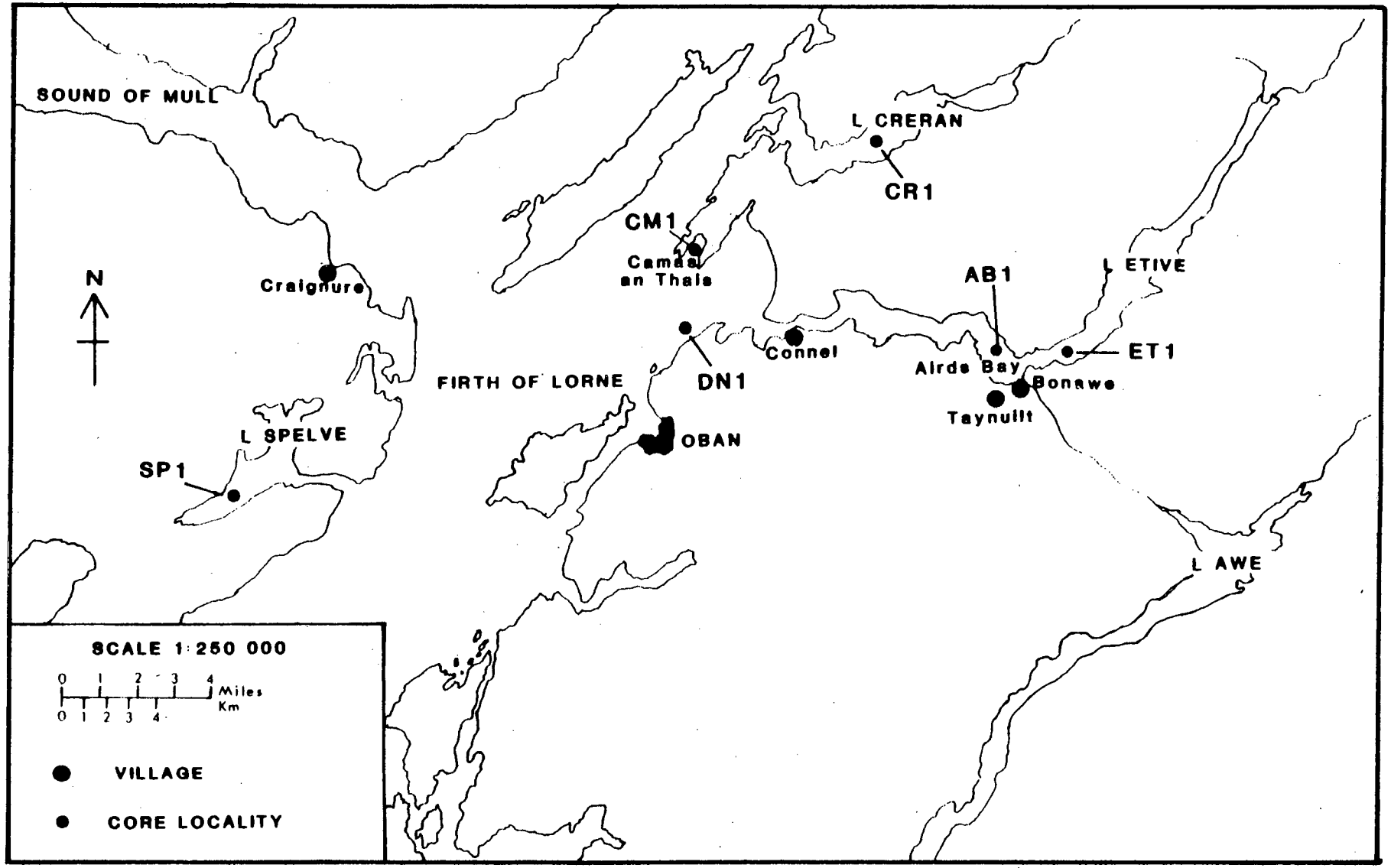

FIGURE 2.3: Enlarged map of Loch Etive and surrounding localities.

which runs North-East South-West and forms the South-Eastern boundary of the Glenelg-Ratagan complex. At its Southern most end, the Strathconon fault crosses the mouth of Loch Hourn. Towards Loch Hourn and Loch Nevis, the rocks become dominantly Moinian comprising pelitic and psammitic schists (Johnson, 1983).

In the South, the Dalradian rocks become important. These are mainly slates, phyllites, limestones, quartzites and grits, with hornblende and epidiorite schists common. West of Bonawe, the shores of Loch Etive are composed of Devonian andesitic and basaltic lavas and tuffs, forming low rolling hills which continue Northwards to Loch Creran. North-East of Bonawe, the surrounding mountains are composed of the Etive Granite, which is Caledonian in age. The Western edge of the Etive Granite is bounded by a fault which runs North-West South-East along the Pass of Brander and continues North-West along Gleann Salach to Loch Creran.

The rocks bordering Loch Spelve on the Isle of Mull are mainly basaltic in nature with associated olivine dolerite, gabbros and agglomerates. These rocks form part of the Tertiary Volcanic Province and have been dated at 59 my (Musset *et al*, 1973, 1980; Walsh *et al*, 1979). On the North-Eastern shore of Loch Spelve, small amounts of Triassic sandstones and grits occur, forming the country rocks through which the volcanics were erupted.

2.3. Geomorphology.

The study area forms the Western margin of the Scottish Highlands and has been greatly modified by the Pleistocene glaciations (Sissons, 1967). Evidence for glaciation in the area is extensive. Sissons (*ibid*) has associated Loch Spelve with a piedmont glacier flowing from the uplands of Mull into the

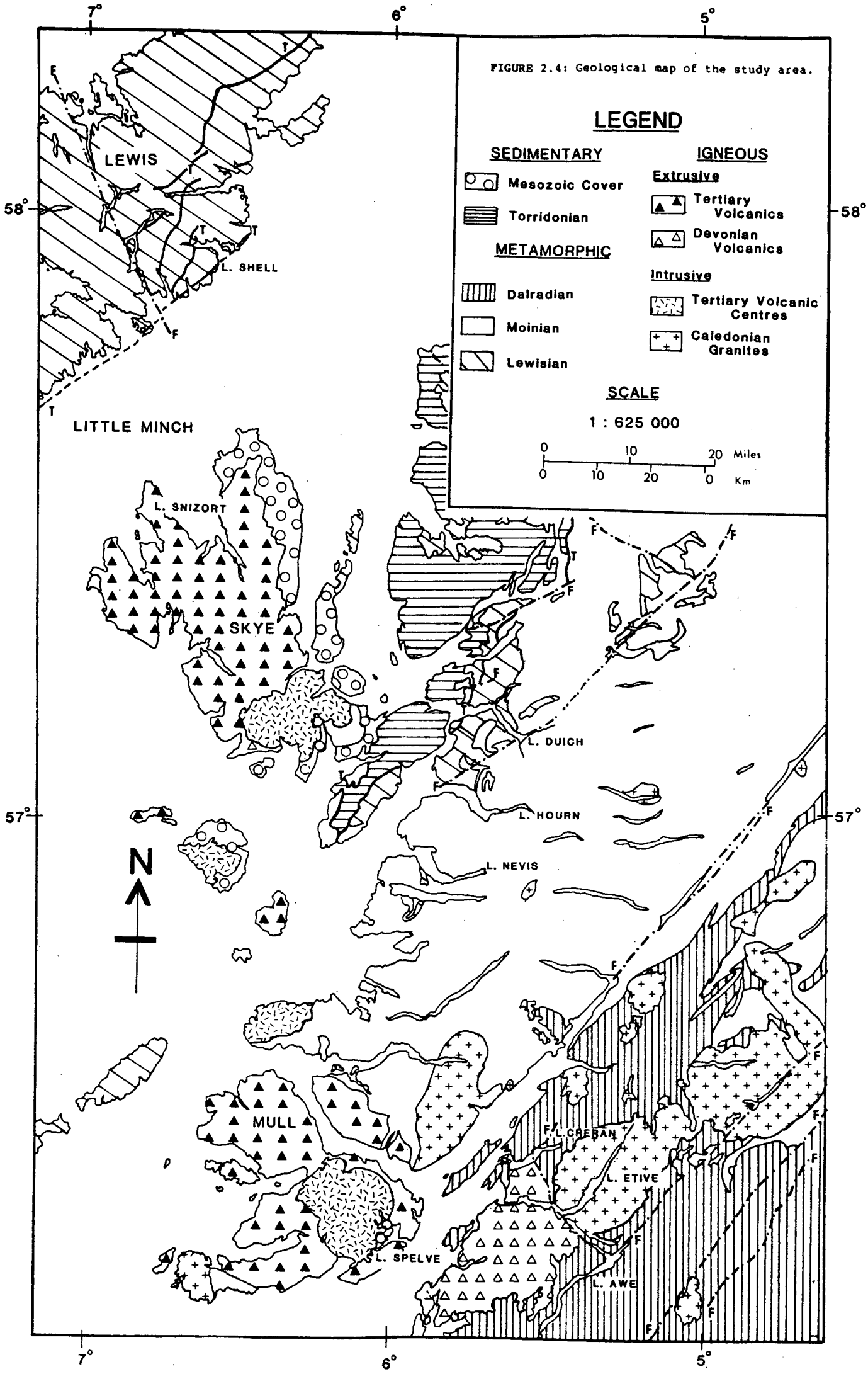

FIGURE 2.4: Geological map of the study area.

Firth of Lorne during the Loch Lomond Stadial c. 11 000 years BP (Peacock *et al*, 1978). Both Loch Etive and Loch Creran are relict glacial valleys and contain extensive glacial outwash features (Sissons, *ibid*). In the North, the confluence of the Glen Lichd and Glen Sheil glaciers caused a considerable overdeepening of the valleys resulting in the fjord system of Loch Duich-Loch Alsh (Krom, 1976).

It has been suggested that the movement of the glaciers was controlled by pre-existing drainage patterns and that many of these pre-existing river valleys picked out lines of structural weakness (Peach and Horne, 1930). It is difficult, however, to distinguish between true glacial erosive features and periglacial water erosive features. Nevertheless, there are a number of lochs and rivers within the area that appear fault controlled. For example in the Loch Etive catchment area, the River Awe, flowing out of Loch Awe and down the Pass of Brander occupies a faulted U-shaped valley suggesting that the valley glacier was following the fault. At the head of Loch Duich, Strath Croe appears to be controlled by the Strathconon fault. The two rivers that flow into the head of Loch Duich, the Sheil and Croe have had very little effect upon the geomorphology of their valleys (Krom, 1976).

The Scottish Highlands were considered by Peach and Horne (1930) to be a deeply dissected plateau with a uniform Eastwards slope. This results in the sea lochs of the area having relatively small catchment areas, see Table 2.2. Examples of this are; Loch Creran and Loch Duich which have catchment areas of 166 Km^2 and 160 Km^2 respectively. The exception is Loch Etive, which has the largest catchment area on the West Coast of Scotland and is in excess of 1300 Km^2 (Malcolm 1981; Ridgway, 1984). The smallest catchment areas of the lochs sampled are Loch Spelve on the Isle of Mull and Loch Shell on the

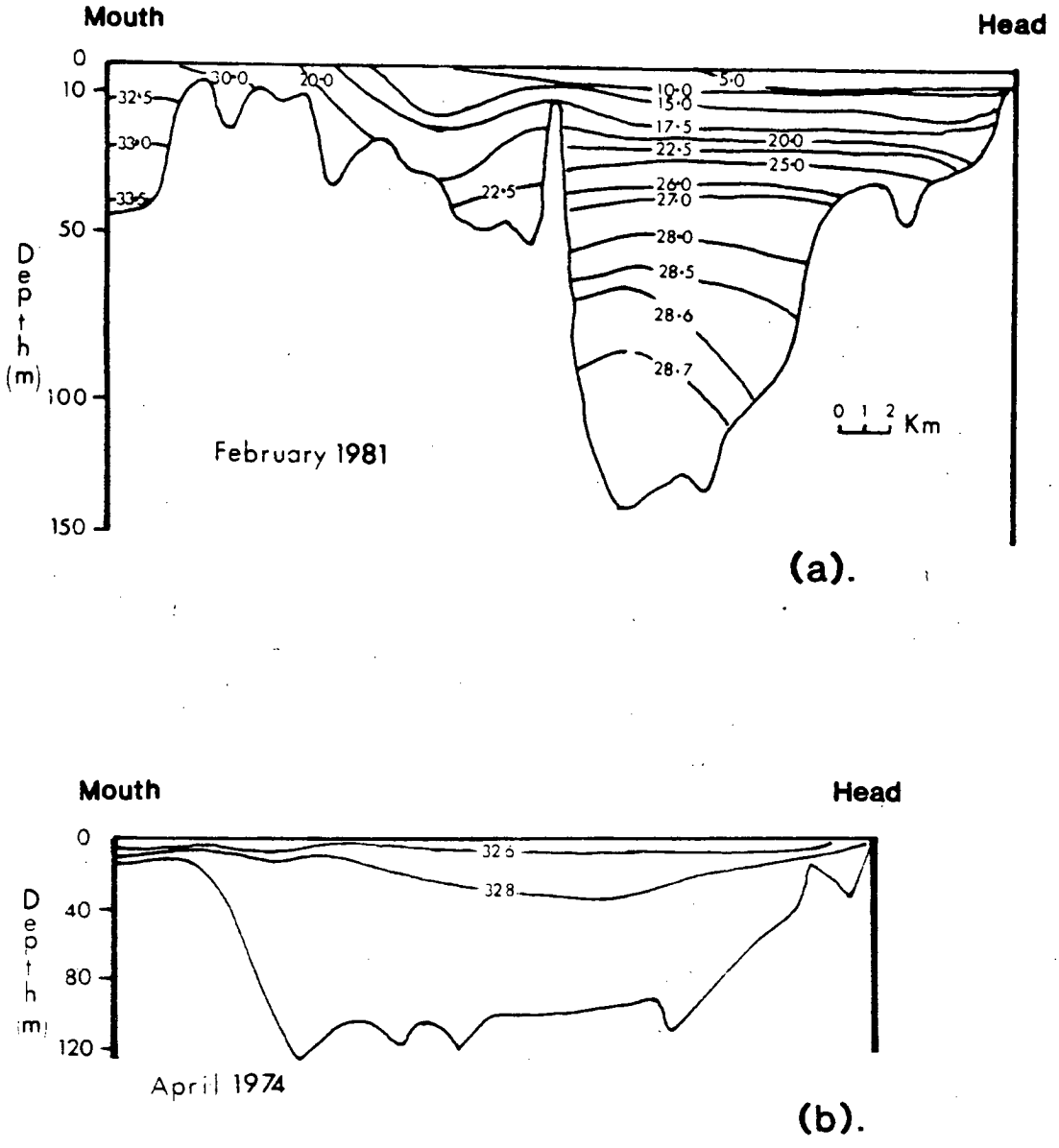

FIGURE 2.5: Salinity/depth profiles for two of the sea lochs studied.

(a) Loch Etive (after Ridgway, 1984)

(b) Loch Duich (after Krom, 1976)

Isle of Lewis (75 Km^2 and 87 Km^2 respectively). This is by virtue of their island locations. The size of catchment area will tend to have an effect upon the amount of terrestrial material entering the lochs. As a result, Loch Etive would be expected to have the greatest terrestrial influence, Loch Duich and Loch Creran correspondingly less. This is reflected in the salinity/depth profiles for Loch Etive (Ridgway, 1984) and Loch Duich (Krom, 1976) seen in Figure 2.5. In Loch Etive, the fresh water entering the loch can be seen as a surface wedge with a maximum thickness of 10m in the inner basin, thinning towards the mouth of the loch. In contrast, the smaller catchment area of Loch Duich results in less fresh water run-off into the loch as shown by a reduced fresh water wedge. The catchment area of Loch Shell is likely to have little effect upon the sediment at core locality SH1 (see Figure 2.2) as this station was outside the loch. Similarly, the Camas an Thais and Dunstaffnage stations (CM1 and DN1) can be regarded as having no catchment areas. However, these sediments may be influenced by the outflow of material from Loch Etive over the Falls of Lora.

2.4. Precipitation.

The proximity of the Highlands to the East and the prevailing moist South-Westerly winds results in a very high annual rainfall. The precipitation pattern over the whole area is broadly similar. The wettest months tend to be September to January and the driest is May (see Figure 2.6). While the rainfall pattern is similar, the mean annual total varies. This is summarised in Table 2.3. The lowest annual average is 1156mm yr^{-1} measured at Loch Erisort on the Isle of Lewis (see Figure 2.2). This is due to the shelter afforded by the

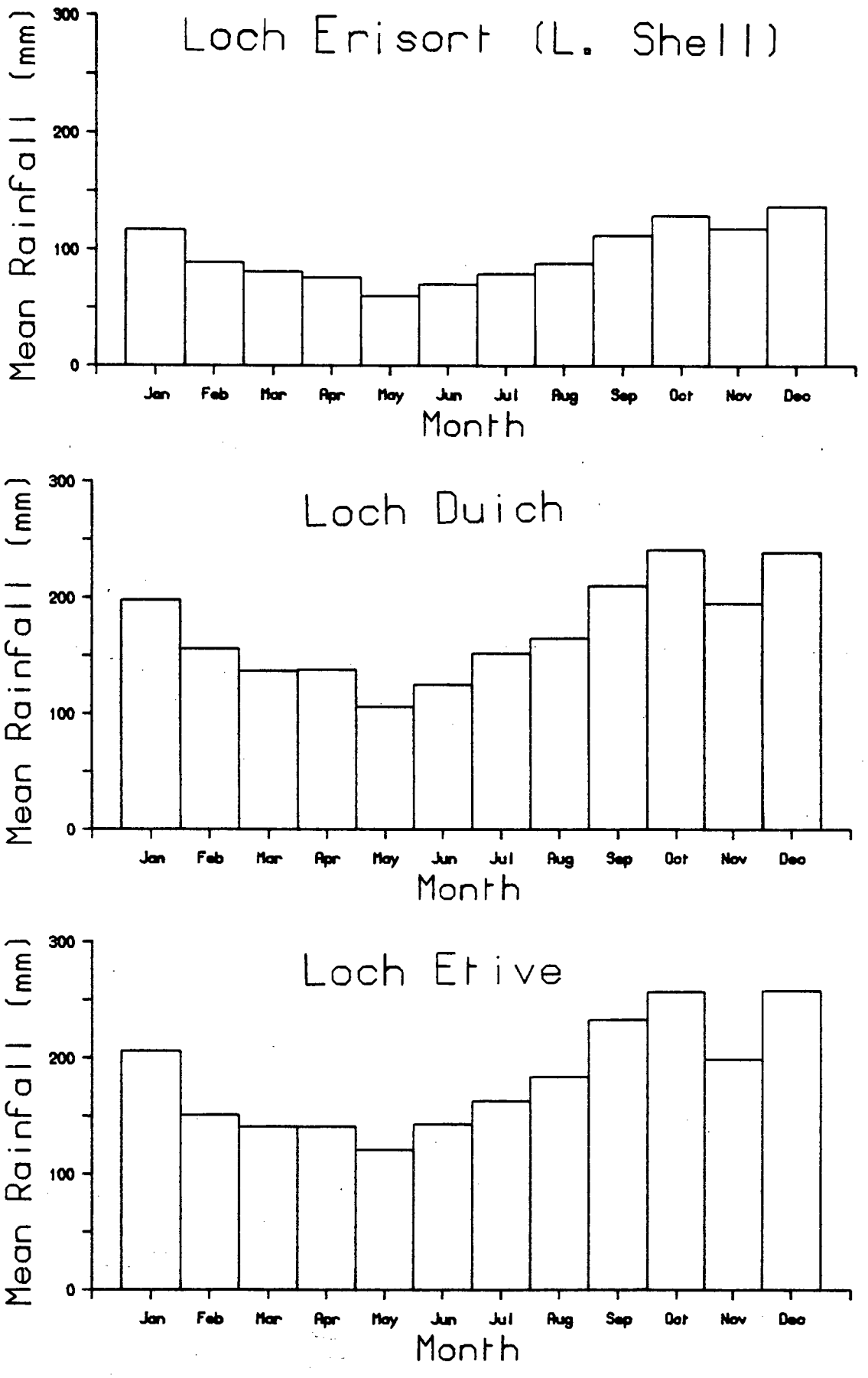

FIGURE 2.6: Precipitation data for three of the localities. Mean monthly totals. (source: Meteorological Office Statistics).

other islands to the South-West. Loch Etive has the highest precipitation, with an annual average of 2197mm yr^{-1} (Meteorological Office 30 year statistics).

This variation in rainfall will also tend to have an effect upon the amount of terrestrial matter entering the lochs through run-off. From this, Loch Etive with the largest catchment area and highest rainfall would be expected to have the greatest terrestrial influence, and Loch Shell with a small catchment area and lowest rainfall the least.

2.5. Population and Industry.

The area as a whole is very sparsely populated, due to the topography and the remoteness. The major centres of population are Oban and Fort William (population about 10,000 in each town). Discounting these centres, the population tends to become sparser Northwards. Along the Southern shore of Loch Etive are the villages of Connel, Bonawe and Taynuilt (population 8500 in total), but in the lochs further North the population is restricted to isolated crofts. On the Outer Hebrides, the major centre is Stornoway on the Isle of Lewis (population c.8000). Around Loch Shell, there is very little settlement, again isolated crofts.

Very little industry is carried out in this region. There is a pulp mill on the North shore of Loch Eil (see Figure 2.2) which is known to discharge cellulose into the loch. This has been examined by Malcolm *et al.* (1986) and the effect was found to be very local. The nearest major industrial centre is Glasgow and the Clyde valley over 100km to the South.

CHAPTER 3

MINERALOGY AND TERRIGENOUS INORGANIC COMPONENTS OF THE SEDIMENTS

3.1. Introduction.

The sediments of the study area are composed of a varied mixture of components derived from different sources. The mineralogical component of the sediments is derived largely from the catchment area of the lochs. As such, the geology and geomorphology of the area may have an influence upon the sediment mineralogy and physical characteristics. It is worth noting that previous studies of the sediment accumulation rates in the region (Ridgway, 1984; see Chapter 8) have shown them to be between 0.5cm yr^{-1} for sediments outside the fjords and up to about 1cm yr^{-1} in the restricted fjords. Thus, the sediment cores collected represent no more than fifty years sediment accumulation and in some instances much less.

In this chapter the bulk mineralogy of the sediments will be discussed along with the porosity. The distribution of the lithogenic elements, Zr, Rb, Ni, Cr, Sc, Ba and Sr will also be considered. The rationale of choosing these elements is that some are unequally partitioned between the sand, clay and carbonate fractions of the sediments. As will be seen in later chapters, variations in the physical characteristics of the sediments can have important effects upon the patterns of diagenesis in the sediment.

In addition, the distribution of Y and the Rare Earth Elements, La, Ce and Nd will be considered. However, these elements appear to bear no relation to the lithogenic input and their distribution is problematic.

3.2. Core Descriptions.

The lithological characters of the cores are sketched in Figure 3.1. The sediments are generally muddy silts, brown, olive green-grey in colour. Most cores display a surface layer of brown flocculant material, but this is absent from DN1 and DU1.

Cores ET1 and AB1 from Loch Etive and DN1 from Dunstaffnage Bay in the Firth of Lorne are relatively uniform with respect to colour changes at depth. Other cores show a more variable history. For example, CR1 from Loch Creran shows several bands rich in shell fragments throughout the core. In general these bands are about 2cm thick, but a thicker band between 5cm and 12cm is prominent. These are very coarse grained and often contain Turritellid gastropods. In Loch Duich (DU1), the grey/brown muddy silt of the upper 10cm gives way to a paler grey silty sediment which continues to about 35cm where there is an irregular boundary to a very pale grey, denser, cohesive clay which occurs in the bottom 12cm of the core.

Burrows were noted in all the cores but the depths to which these extended varied. In ET1 and CM1 burrows were noted at a depth of 25cm-30cm. In SH1, a colour change from grey/brown to homogenous grey at about 20cm was noted immediately below a worm burrow. No live macrofauna was seen in the sediments except for an unidentified worm at 18cm in SH1. However, Ridgway (1984) noted worms present in sediment from the inner basin of Loch Etive. These were identified as *Nephys hombergi*, *Capitella capitata* and *Spirochaetopterus typicus*.

In AB1, ET1, and SP1 there was a distinct odour of H_2S from the bottom sediments

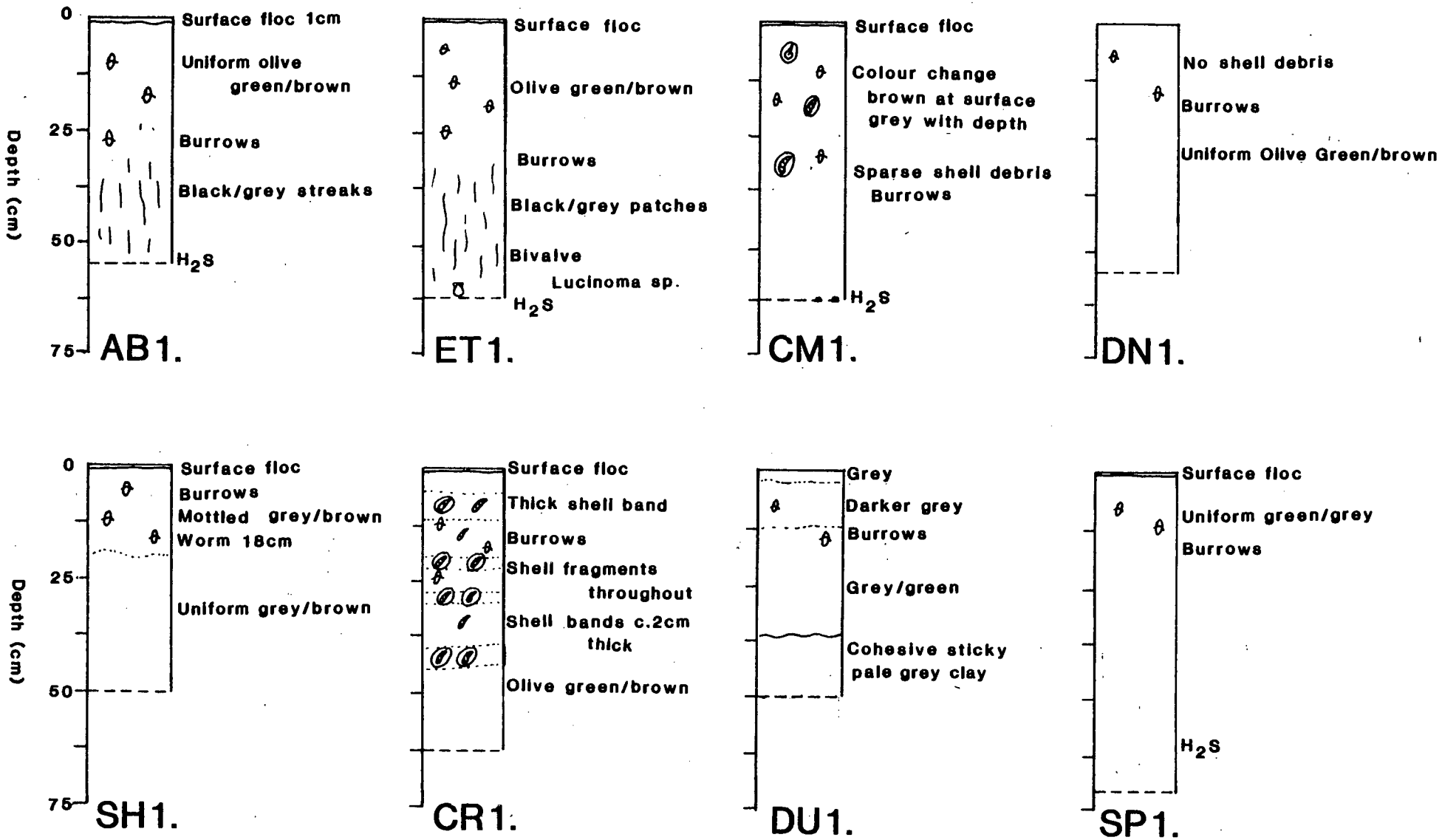

FIGURE 3.1: Summary of the major lithological characteristics observed in the sediment cores.

Whilst some sediments appear to have a uniform lithology, suggesting relatively uniform accumulation, others display irregularities such as shelly horizons and marked colour changes often associated with lithological changes, suggesting that accumulation may not be constant. Such changes must be borne in mind when the diagenetic effects in the sediments are described in later chapters (Chapters 4, 6 and 7)

3.3. Mineralogy.

Sediment samples from the top of the cores collected and also at depth, were analysed mineralogically by X-Ray Diffractometry (XRD. See Appendix I, Section 2.1). The peaks were interpreted using tables prepared by Chao (1969). Quantitative analyses are difficult by XRD, but it was possible to make qualitative comparisons of mineralogy with depth and between cores.

All the sediments analysed show quartz, a suite of feldspars (mostly albite, but containing potassic feldspar, possibly microcline), calcite, and a clay fraction (containing illite, muscovite and chlorite). All samples show a characteristic halite peak reflecting the influence of dried sea salt. Sediments composed of these minerals have been noted by Krom (1976), in Loch Duich and Malcolm (1981) in Loch Etive. These minerals are typical of mechanical weathering in a temperate climate (Biscaye, 1965).

Whilst these minerals occur in all the cores, the relative proportions vary. This can be seen in Figures 3.2-3.5 which shows the variation in peak heights of prominent reflections. This is clearly seen in the surface sediments of cores ET1 and CR1 (Figure 3.2). ET1 is composed mostly of clays with lower amounts of feldspars and quartz and little or no calcite when compared with CR1. The surface sediment from Airds Bay (AB1) is similar to ET1, but appears

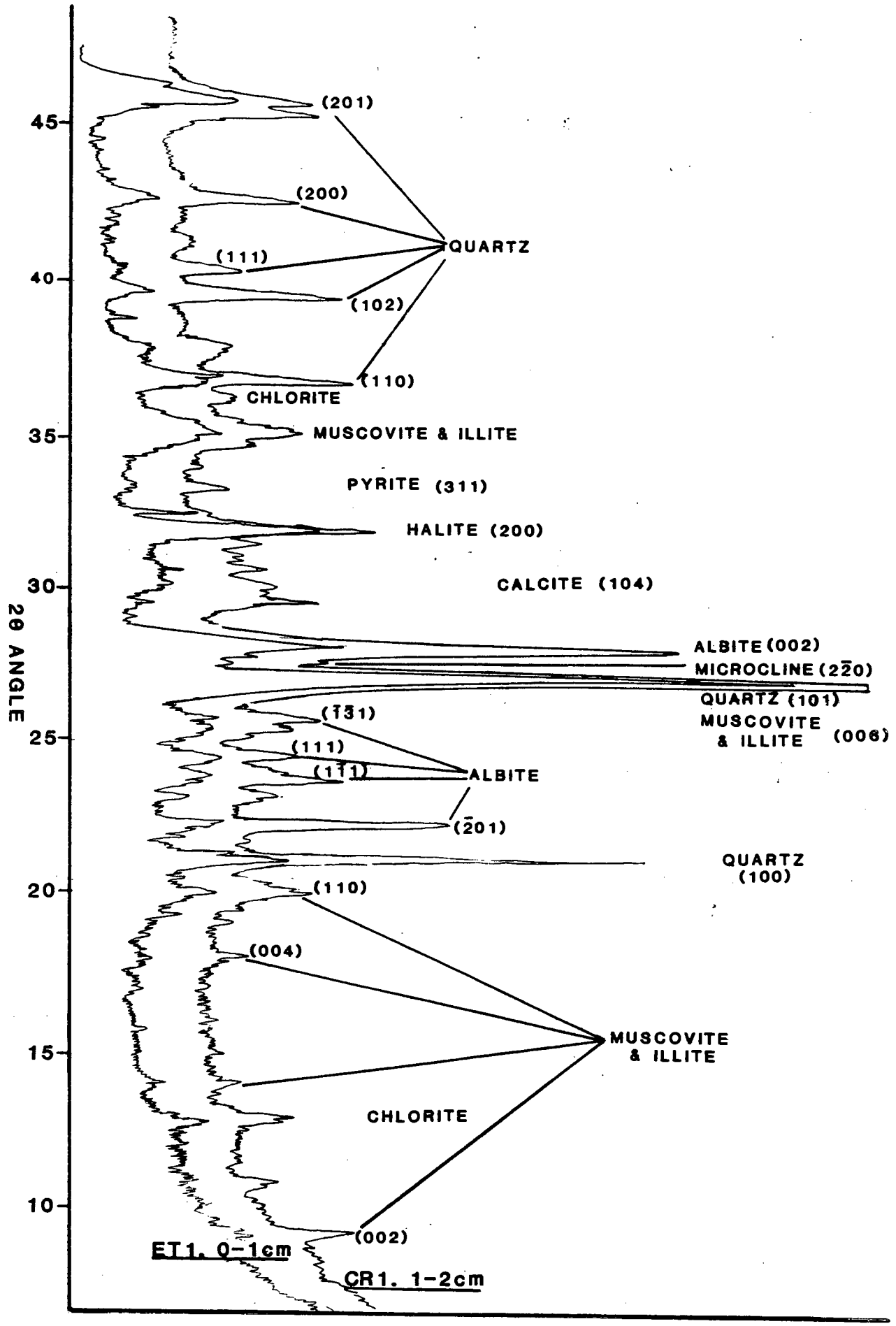

FIGURE 3.2: Comparative XRD traces of the surface sediments from cores CR1 and ET1.

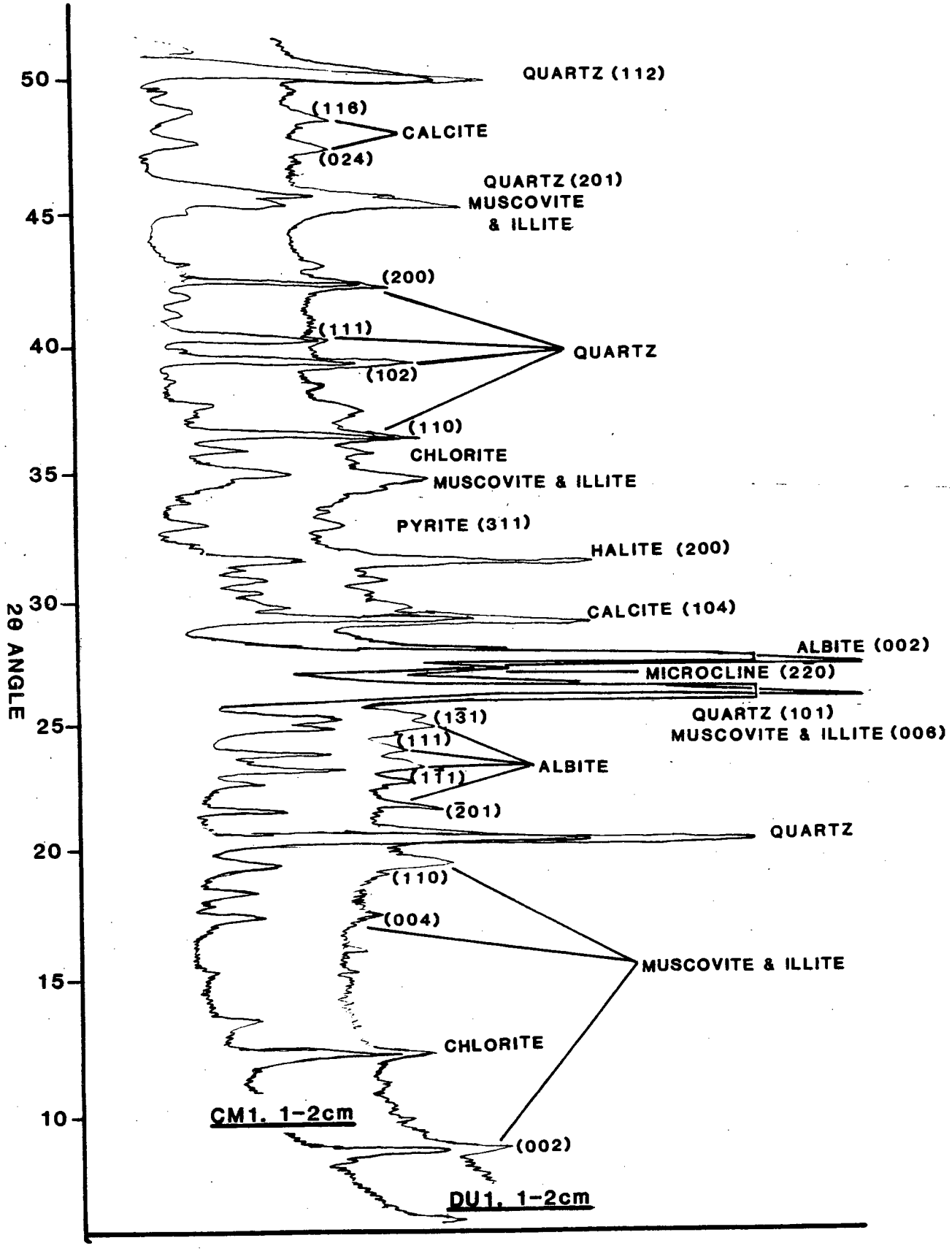

FIGURE 3.3: Comparative XRD traces of the surface sediments from cores CM1 and DU1.

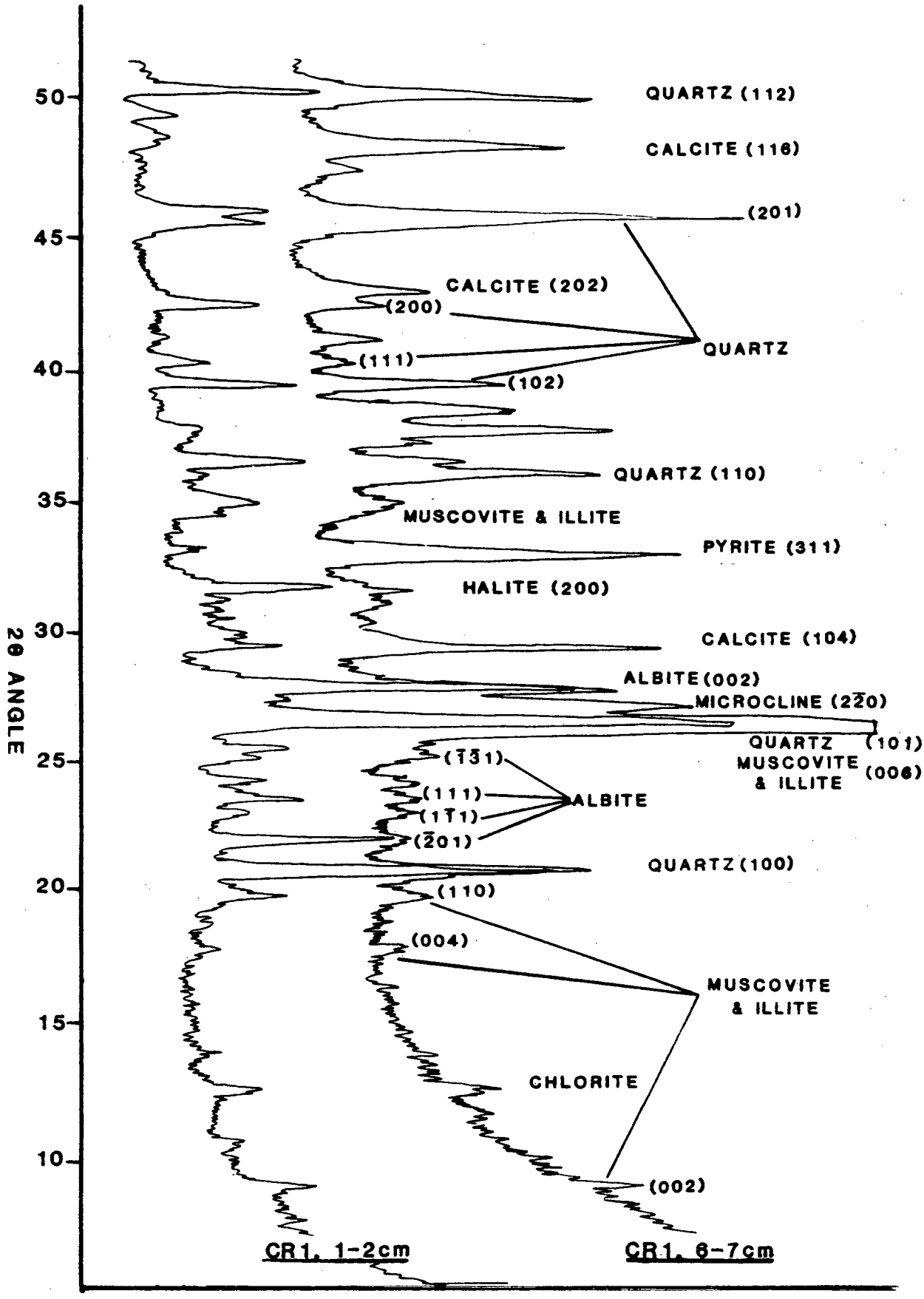

FIGURE 3.4: XRD traces highlighting the mineralogical differences between the shelly (6-7cm) and non shelly (0-1cm) sediments in core CR1.

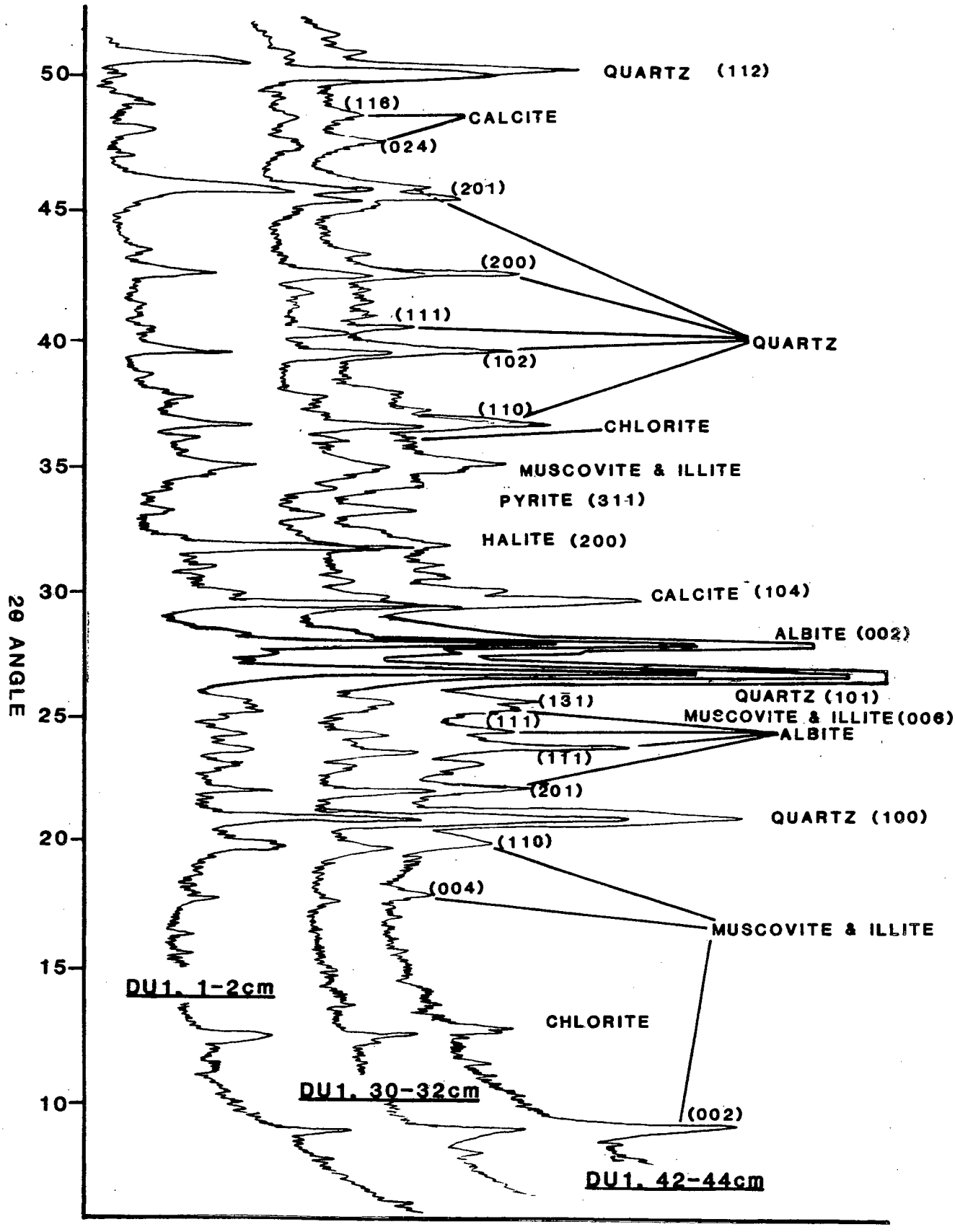

FIGURE 3.5: Representative XRD traces showing the change in mineralogy with depth in core DU1.

to show a slightly higher quartz and feldspar content. In comparison with cores AB1 and ET1, the remaining cores appear to have higher calcite contents. Overall, there appear to be considerable differences in the relative proportions of quartz, feldspars and clay. For instance, Figure 3.3 shows a comparison between CM1 and DU1 surface sediment. CM1 is composed mainly of quartz and albite feldspar, but a significant amount of potassic feldspar is present. DU1 in contrast contains less quartz and relatively more feldspar (dominated by albite) and clay minerals,

At depth the mineralogy of cores ET1 and AB1, in the outer basin, is relatively constant suggesting no major changes in lithology or accumulation rate of the sediment. Other cores show marked changes in mineralogy with depth, possibly suggesting some discontinuity of accumulation or a gradual change over time. This is illustrated for cores CR1 and DU1. Figure 3.4 shows the variation between the sediments of the shell bands and non-shelly horizons in CR1 described above. The shell bands show a marked increase in calcite and quartz relative to the clay fraction and an increase in the relative importance of potassic feldspar over albite. The sediment in the non-shelly horizons is composed mostly of quartz, albite feldspar, and clay, with only minor calcite. In DU1 (see Figure 3.5), the surface sediment contains quartz, feldspar and calcite. At 30-32cm, quartz appears to be more dominant and there is relatively less feldspar and calcite, suggesting a coarser sediment at depth. The light grey clay at the bottom of the core shows more of the feldspar and clay minerals, (chlorite and illite) relative to quartz.

All of the sediments contain pyrite. The peak heights of the different sediments are broadly similar, except ET1 which suprisingly appears to have less pyrite.

3.4. Porosity.

In a sediment of constant lithology, the porosity could be expected to decrease with depth due to the compaction of the sediment with burial. Pettijohn (1975) points out that grain size can affect the porosity of a sediment; coarse sediment tends to have less porosity than finer material. Permeability, however, tends to behave in the opposite manner. The relationship of grain size and porosity will be considered in the sediments studied.

The porosity of the sediments investigated was calculated from measured water contents using equation (3.1) (Berner, 1971). on the formula:

$$\Phi = \frac{Wds}{Wds + (1-W)dw} \qquad (3.1)$$

Where:

Φ = Porosity

W = % Moisture Content x 10^{-2}

ds = Sediment Density (using a mean value of 2.65 gcm^{-3})

dw = Pore Water Density (using a mean value of 1.04 gcm^{-3}

The data calculated are given in Appendix II, Table AII.1 and are illustrated as depth profiles in Figure 3.6. The porosity of the surface sediments is high. This is summarised in Table 3.1 column (a). Core CM1 is unusual in that the surface sediment porosity is low at 0.59%. Table 3.1 column (b) summarises

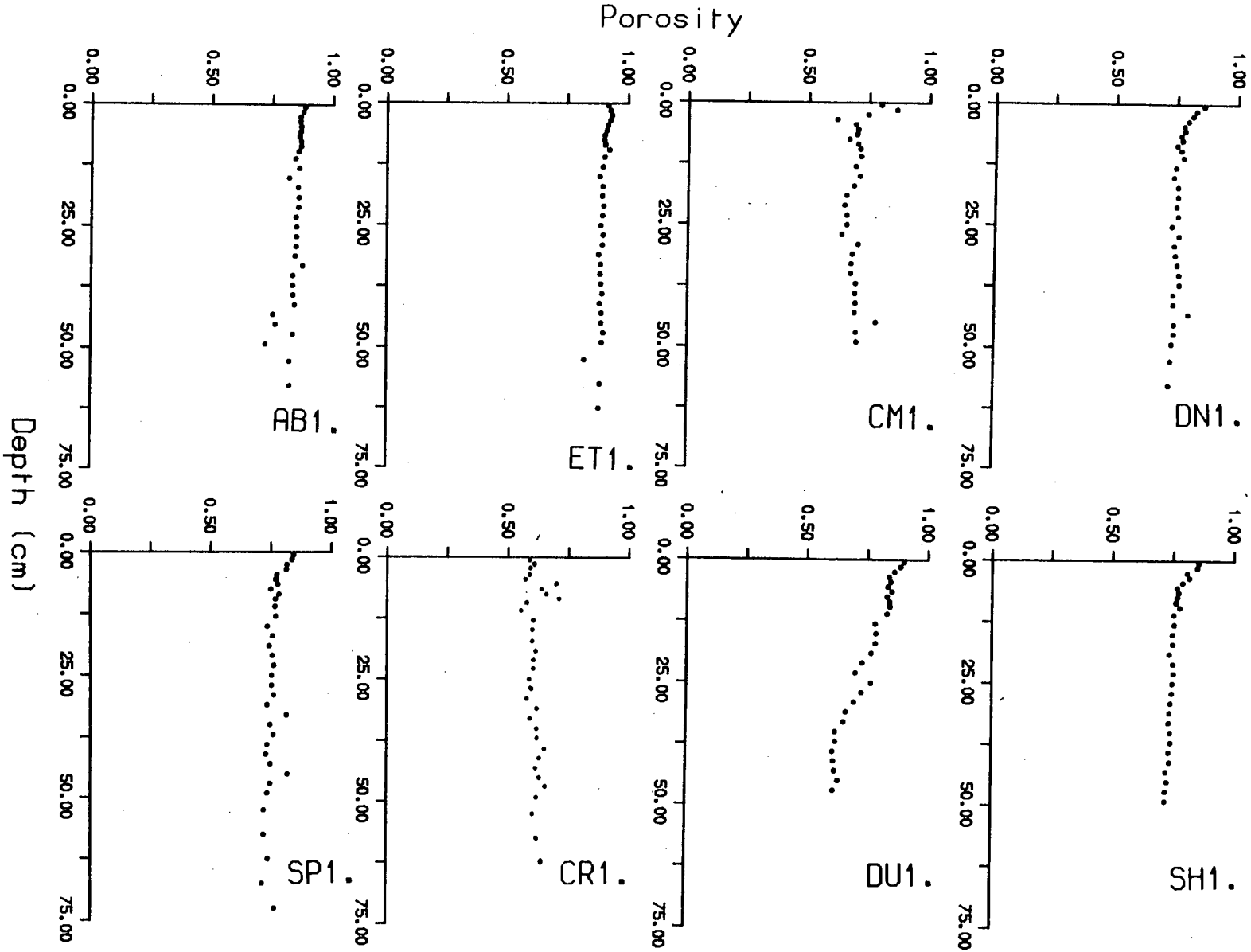

FIGURE 3.6: Porosity patterns in the sediment cores studied.

the mean porosity in the sediments. The highest mean porosities can be found in AB1 (0.84%) and ET1 (0.86%). The lowest is in CM1 (0.62%). This is consistent with the mineralogical evidence that the latter sediments are coarser grained than those of AB1 and ET1.

In general the sediment cores show a decline in porosity with depth, (see Figure 3.6) indicating in some cores compaction of the sediment. Much of the reduction occurs within the uppermost 10cm of sediment. Lower down, the change in porosity with depth is barely discernable in some cores and is not seen in the cores with low mean porosities, for example CM1 and CR1. Both of these cores show slight increases in porosity with depth and the mineralogical data confirms the greater importance of clay minerals at depth. These trends agree with the findings of Füchtbauer and Reineck (1963) that the clay content and associated organic matter content generally increases porosity.

DU1 is unusual in that the sediments show a much greater decrease in porosity with depth than in the other cores. Moreover, there is some evidence of lithological discontinuities at depth as depicted by various breaks in the porosity profile. The porosity at the bottom of the core (37cm-45cm) is 0.60% and is low compared with 0.73% in DN1 and 0.71% in CR1. The change in the porosity profile from one of decrease (0- 37cm) to a constant value (37-45cm) is consistent with the lithological changes described above; the low porosity values at the base of the core are due to the occurence of the cohesive clayey material noted in the core description. The cohesiveness and low porosity of this sediment suggests that this sediment is old and that there is a considerable hiatus in accumulation between this and the overlying sediment. The increase in porosity in the immediate overlying sediment may be partly

Core	Porosity (%)	Mean Porosity (%)
AB1	0.870	0.841
CM1	0.587	0.615
CR1	0.929	0.699
DN1	0.814	0.762
DU1	0.865	0.749
ET1	0.923	0.869
SH1	0.822	0.758
SP1	0.816	0.760

TABLE 3.1: Surface porosities (as a mean of the upper 5cm of sediment) and mean porosities for each core.

Core	Zr (ppm)	Rb (ppm)	Zr/Rb	Ni (ppm)	Cr (ppm)	Ni/Rb
AB1	226	103	2.18	49	97	0.51
CM1	347	85	4.09	27	60	0.45
CR1	277	107	2.59	35	74	0.47
DN1	164	119	1.36	49	100	0.49
DU1	134	118	1.13	53	107	0.50
ET1	172	90	1.92	47	89	0.53
SH1	144	105	1.38	48	96	0.50
SP1	162	110	1.48	49	105	0.47

TABLE 3.2: Surface values of Zr, Rb, Ni, Cr and elemental ratios. All are expressed as a mean value of the upper 5cm of sediment.

influenced by a sediment mixing (biomixing) of old sediment during recent sediment accumulation. This will be considered more fully in Chapters 4 and 9.

3.5. Elemental Chemistry.

Some elements are known to be associated solely with the mineralic fraction of the sediment. It is well known that the arenaceous component of fine grained sediments tends to have very different levels of minor elements than the argillaceous fraction (Calvert, 1976). This is caused, in the former, by the dilution from quartz and in the distribution of feldspars between the coarse and fine grained components of a sediment. Thus the ratioing of element couples which can be empirically ascribed to a particular mineralogy has been useful in showing minor textural differences in a sediment. Several elements when related to Rubidium (Rb) have been used to characterise the physical properties of the sediments (Calvert, 1976; Ridgway, 1984). Due to the closeness of ionic radii, Rubidium (1.49Å) and Potassium (1.33Å) are closely associated in most rocks. Rubidium tends to substitute for Potassium in feldspars, micas and clays (Heier and Billings, 1978). As such, Rubidium predominates in the finer sediment fraction (Calvert, 1976) and can be used in a similar manner to Al as an indicator of the alumina-silicate fraction of a sediment. Variations in the content of other elements expressed as element/Rb ratios can provide evidence of textural change in sediment cores and can express the nature of source rocks of specific areas of Western Scotland.

All of the elements described below were analysed by X-Ray Fluorescence Spectrometry (See Appendix I, Section 2.2). Element data is given in Appendix II, Tables AII.2 and AII.3; all the values are reported on a salt free basis.

3.5.1. Zirconium and Rubidium.

The behaviour of Zirconium (Zr) contrasts with that of Rb. Zr occurs in relatively few minerals and in sediments occurs mainly as detrital zircon (Erlank, 1978). Zircon is resistant to weathering and tends to occur in the coarse fractions of the sediment (Goldschmidt, 1954; Hill and Parker, 1970). The implication of this is that the Zr/Rb ratio is a potentially useful tool in indicating changes in sediment texture.

Rb values range from less than 70 ppm in the shelly horizons in CR1 to over 140 ppm at the base of DU1. Mean Rb values for the upper 5cm of the cores examined are given in Table 3.2. Most of the sediments analysed show values of between 100 and 120 ppm. These values are consistent with previous studies from the area (Krom, 1976; Ridgway, 1984) and with mean values quoted for silty and argillaceous sediments (Heier and Billings, 1978).

The comparatively low values of surface sediments in cores AB1 and ET1 supports greater dilution from quartz compared with other sediments examined. Several cores show uniform Rb with depth, Figure 3.7, implying relatively uniform grain size sediment accumulation. Noticeable exceptions to this are seen in cores CM1, CR1 and DU1 and indicate finer sediment at depth.

Zr values are generally between 140 and 200 ppm. Mean Zr values of the upper sediments (Table 3.2) show high values occur in CM1 surface sediments (350 ppm) and low values of <130 ppm are found in the surface sediments of

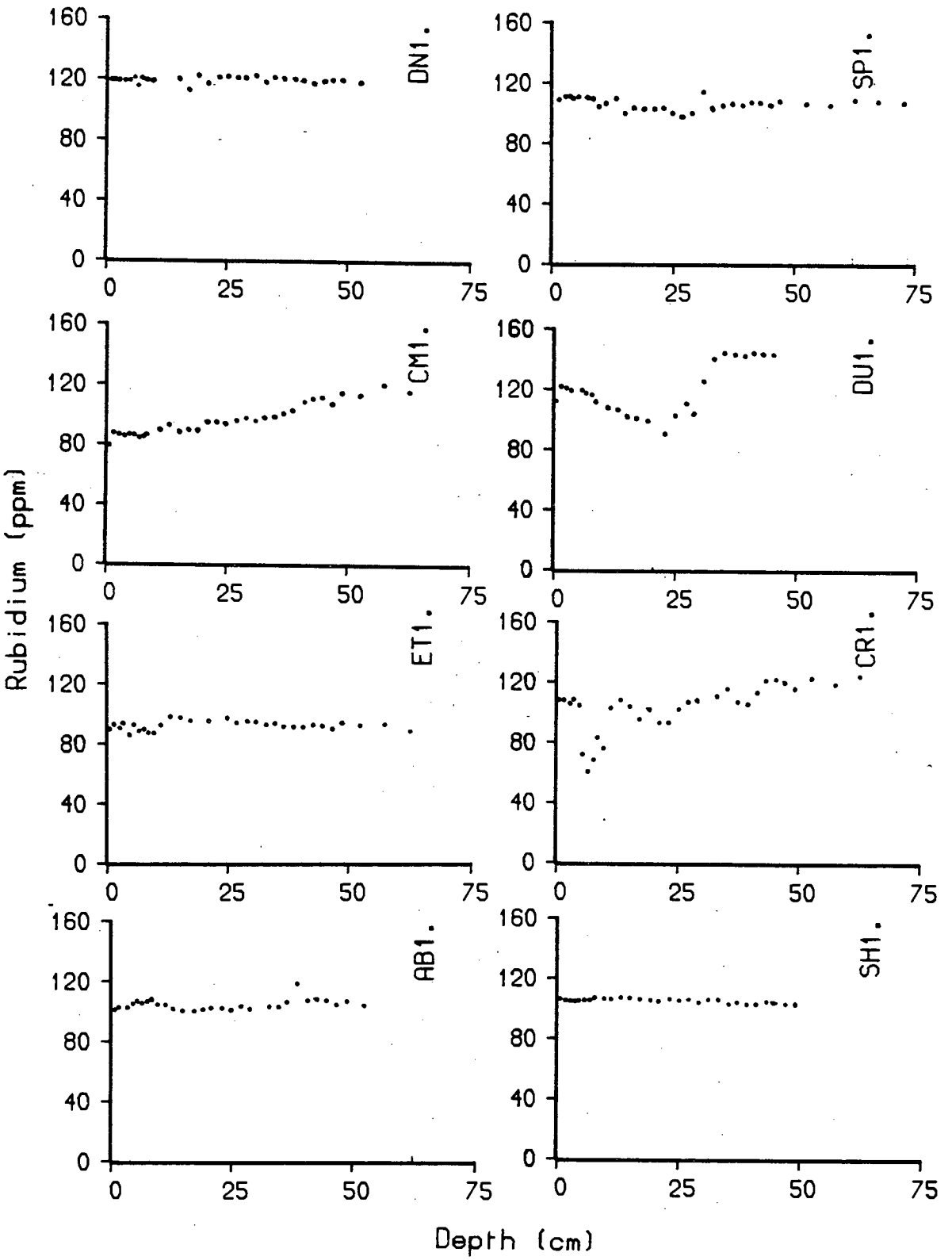

FIGURE 3.7: The patterns of Rb with depth in the sediments.

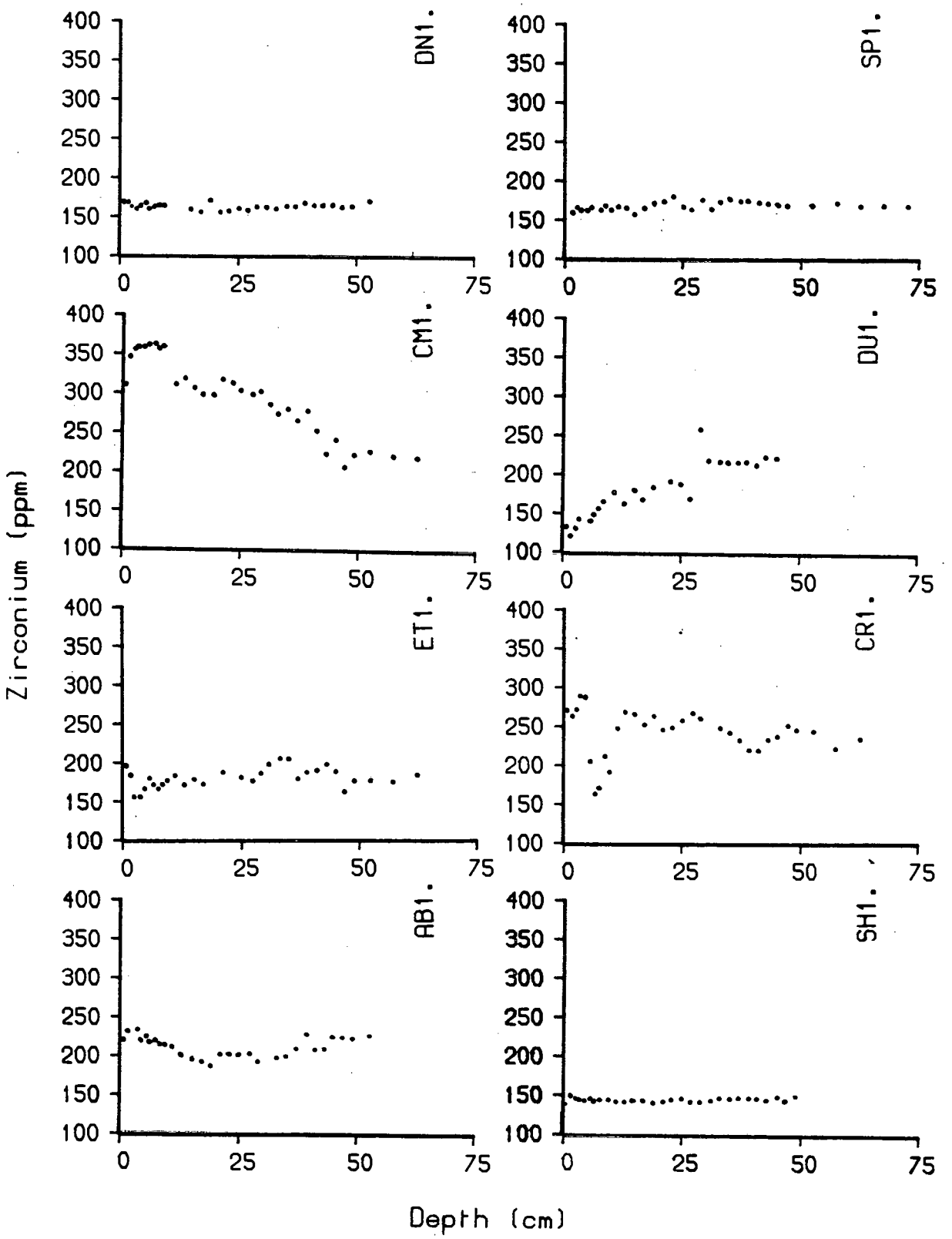

FIGURE 3.8: The patterns of Zr with depth in the sediments.

DU1. Again, these values are consistant with Ridgway (*ibid.*) and Krom (*ibid.*) and are similar to those found in shelf sediments by White (1970). At depth (Figure 3.8) the Zr distributions contrast to that of Rb in that there is an increase in Zr content in cores CM1 and CR1. The distribution of Zr in core DU1 is very complicated. However, Zr/Rb ratios are more significant than the elements themselves for understanding textural and grain size variations.

The Zr/Rb ratios vary significantly from core to core, Figure 3.9. The mean values of the upper 5cm in the cores are summarised in Table 3.2. The surface values vary from 4.09 in CM1 to 1.13 in DU1. ET1, AB1 and CR1 have similar values between 1.92 and 2.59. Cores SH1, SP1 and DN1 have lower surface values of about 1.4.

The patterns of Zr/Rb ratios at depth are very variable. Cores DN1, SH1, SP1, AB1 and ET1 show relatively constant values. However, even in these profiles there are minor depth trends. For instance, SP1 shows a slight increase in the ratio from 1.47 to a maximum of 1.76, before falling to 1.57 at the base of the core. Core ET1 shows an even more irregular profile of Zr/Rb ratios, with changes of Zr/Rb or grain size occuring about 10cm down the core. A similar but less defined trend is also seen in AB1. These irregular ratios of Zr/Rb in ET1 and AB1 imply a number of changes in accumulation over time.

The most defined change in Zr/Rb is observed in core CM1, where there is a greater than twofold decrease in the ratio with depth, implying a considerable change of sediment grain size, becoming finer grained at depth. Core CR1 shows a similar, but less accentuated pattern with notable coarse grained sediments occuring in the carbonate rich horizons, for example 5-12cm.

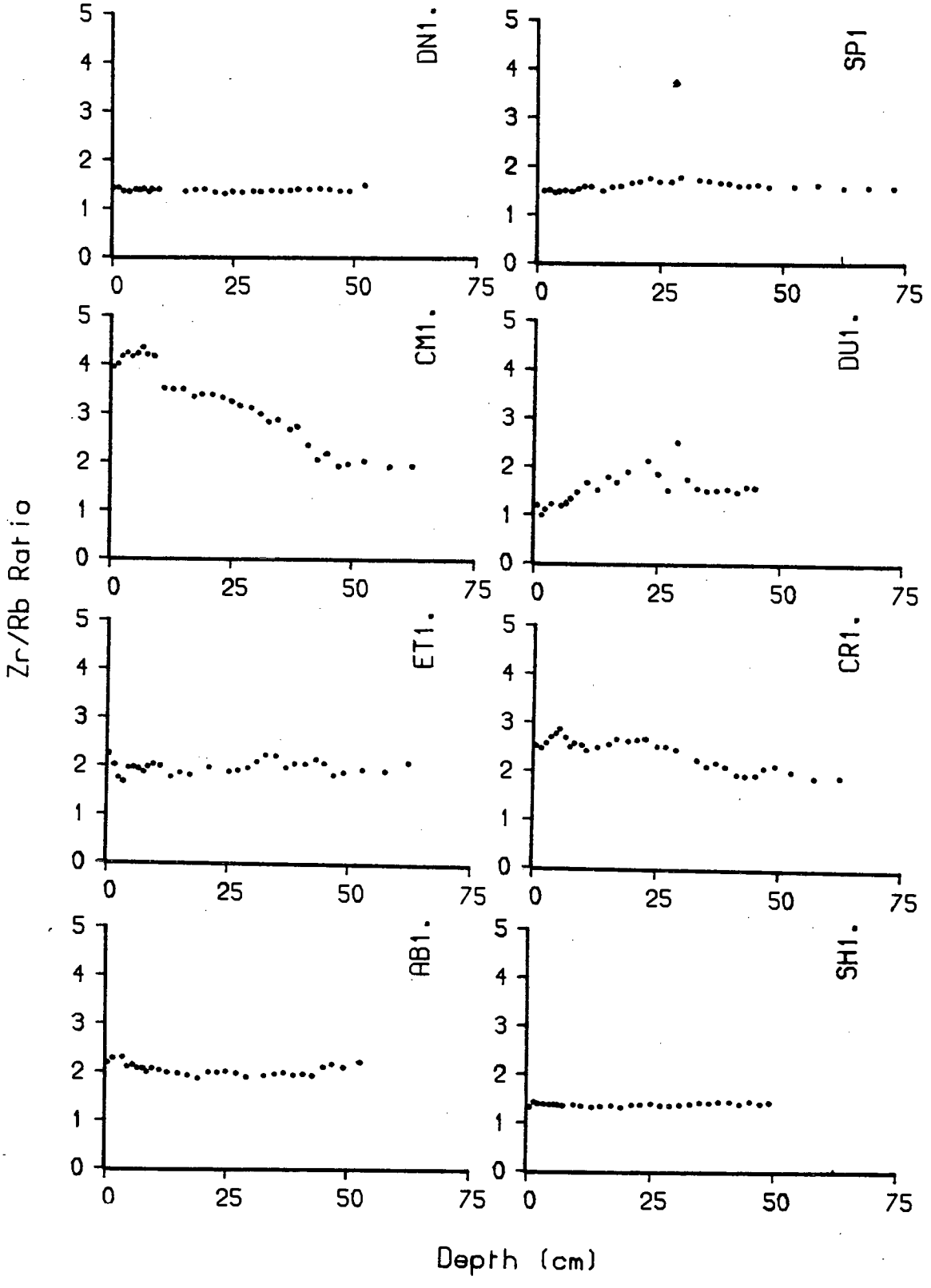

FIGURE 3.9: The patterns of Zr/Rb ratios with depth in the sediments.

In DU1 Zr/Rb ratios increase with depth from a mean of 1.13 in the upper 6cm to a maximum value of 2.47 at 30cm. Below 30cm, there is an abrupt fall in the ratio to 1.54 at 34cm, remaining constant at a mean level of 1.53 to the base of the core.

The wide variation in the Zr/Rb ratio both from core to core, and with depth in some sediments implies a wide variation in sediment type both across the study area and with time. Overall, sediments from the fjords tend to have higher Zr/Rb ratios than the coastal sediments. An exception to this is CM1 which shows a surface Zr/Rb ratio of 4.2. The lowest ratio is seen at the surface of DU1. These trends are supported by the mineralogy of the sediments. CM1 has significantly more quartz than DU1 which is relatively richer in feldspars (see Figure 3.3). An interesting point to note is that CM1 has relatively more potassic feldspar than DU1. It is possible that without this addition, the Zr/Rb ratio would have been even higher.

3.5.2. Nickel and Chromium.

The patterns of Nickel (Ni) and Chromium (Cr) in the sediments (Figures 3.10) and 3.11) tend to be similar implying that both elements occupy similar positions within the sediment. Cr is known to replace Al, Mg, Fe, and Ti especially in chlorites, amphiboles and in spinels and during weathering is concentrated into the clays (Matzat, 1978). This would suggest a similar fate for Ni (Turekian, 1978). Being derived largely from a detrital source (Ridgway, 1984) it is useful to be able to compare their distribution in the sediments with metals such as Copper (Cu), Lead (Pb) and Zinc (Zn) thought to undergo diagenetic mobilisation.

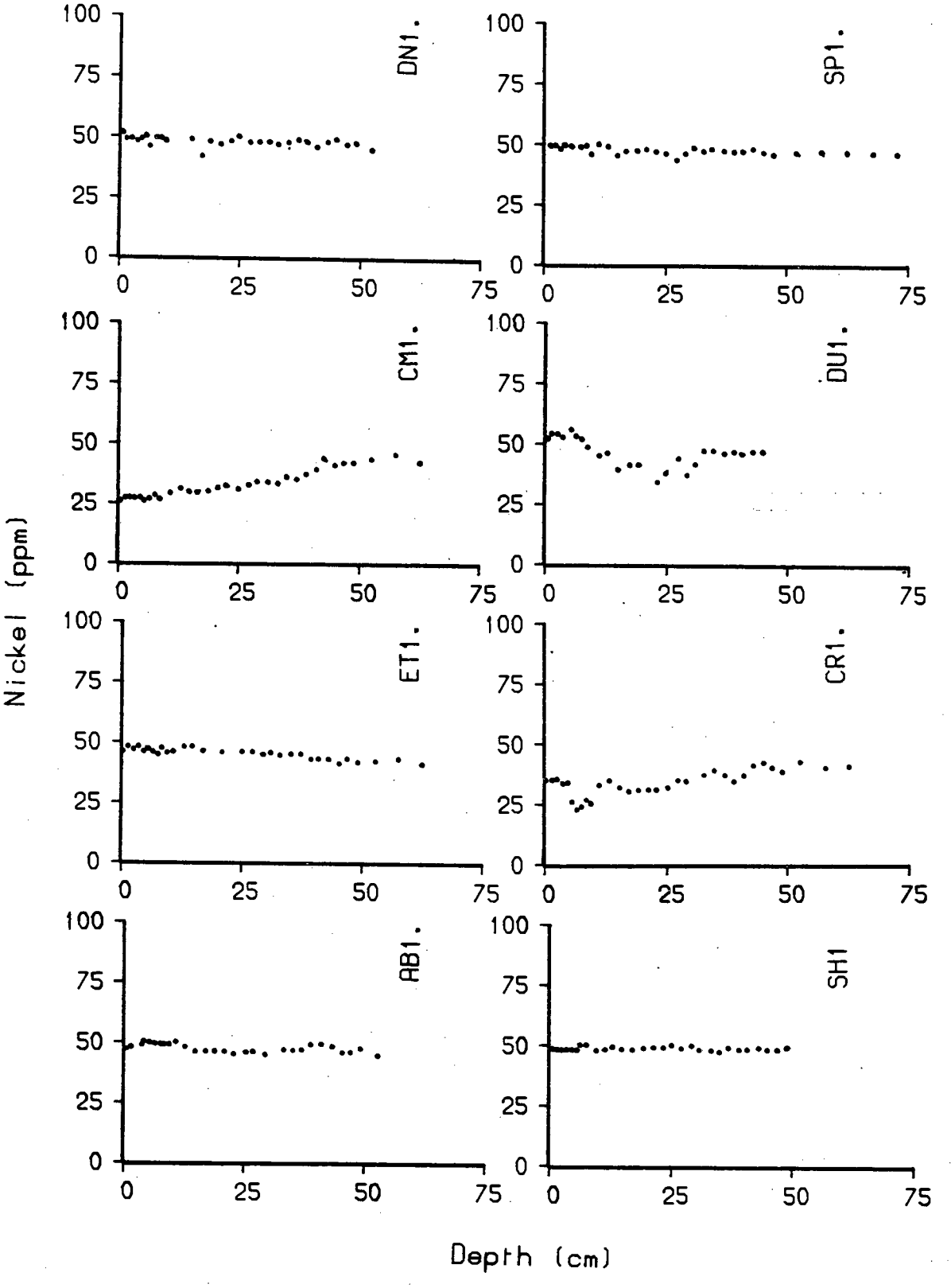

FIGURE 3.10: The patterns of Ni with depth in the sediments.

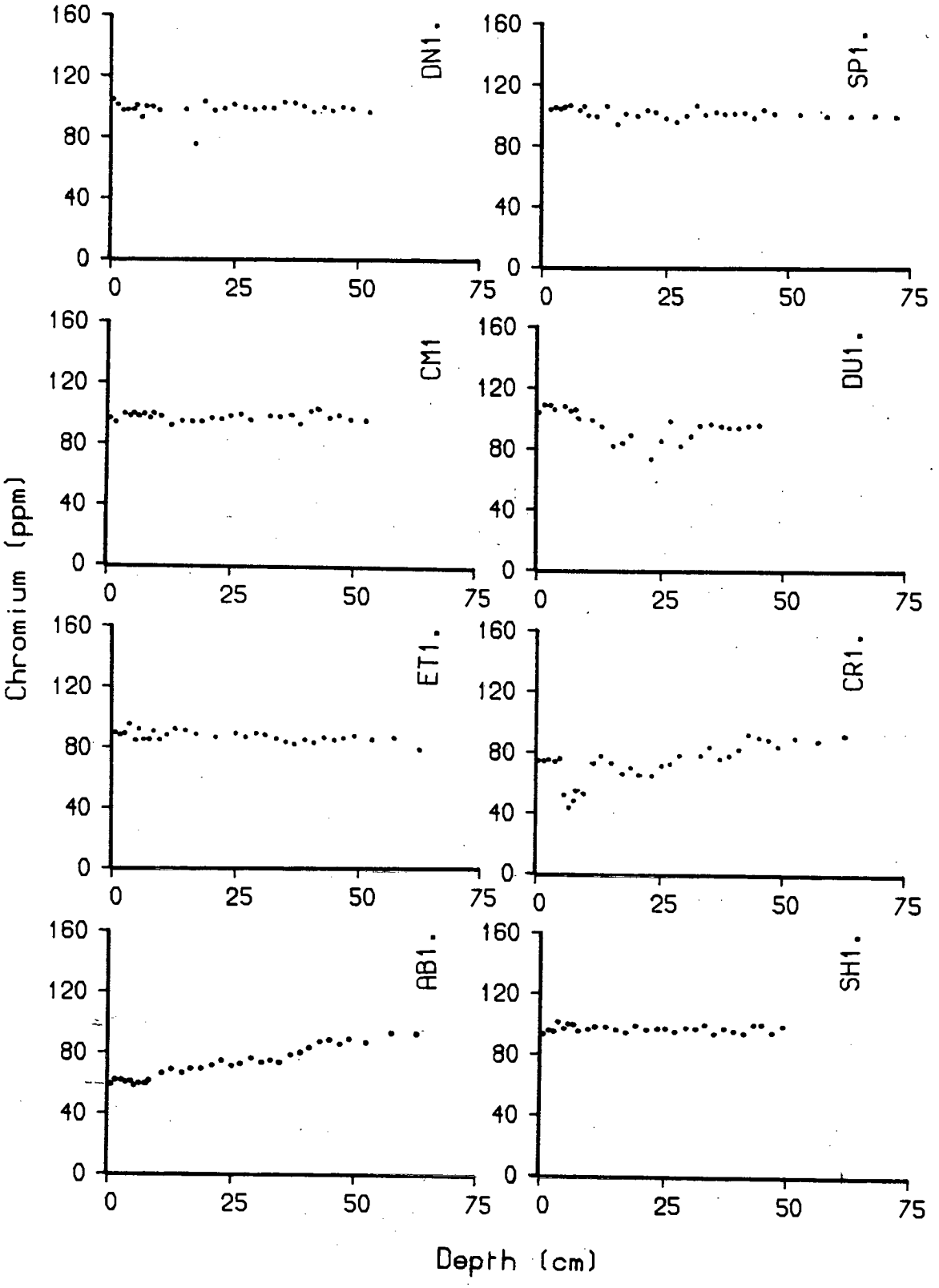

FIGURE 3.11: The patterns of Cr with depth in the sediments.

The surface concentrations of Ni vary from 27ppm in CM1 to 53ppm in DU1. The remaining cores all fall between 35 and 50ppm (see Table 3.2). At depth (see Figure 3.10) concentrations remain relatively constant between 40ppm and 50ppm. This is similar to the average Ni content of 40ppm for nearshore clays given by Potter *et al.* (1963). Similar concentrations of Ni have been noted in Chesapeake Bay by Goldberg *et al.* (1978), in Ranafjord by Skei and Paus (1979), and in the Archachon Basin (El Ghobary and Latouch, 1986). Ni in cores AB1, ET1, DN1, SH1 and SP1 show remarkable uniformity with depth and between cores. However, the Ni concentrations in CM1 increase gradually from 27ppm at the sediment surface to a maximum value of 45ppm at the base of the core indicating a higher clay content. In CR1 the concentration also shows evidence of increasing clay content at depth but the noticeable feature of the core is the marked decrease of Ni values within the shell bands. Core DU1 shows a fall in Ni values from 52ppm at the sediment surface to a low point of 34ppm at 22-24cm. Below 34cm, within the older consolidated clays, the values remain relatively constant about a mean of 47ppm.

Chromium (Cr) values show a similar pattern to Ni. The surface 0-5cm values range from 74ppm in CM1 to 107ppm in DU1. These are summarised in Table 3.2. Crecelius *et al.* (1975) reported mean values of 90ppm from Puget Sound. Ridgway (1984) found similar values from Loch Etive.

The profiles of Cr are shown in Figure 3.11. There is a striking resemblance in the distributions of Ni and Cr in cores ET1, CR1, DN1, DU1, SH1 and SP1 suggesting that both elements are located in the same mineral fraction. However, the overall ratio of Ni/Cr (Figure 3.12) can vary from core to core. For instance, Ni/Cr in cores SP1, DN1, SH1 are very similar whereas,

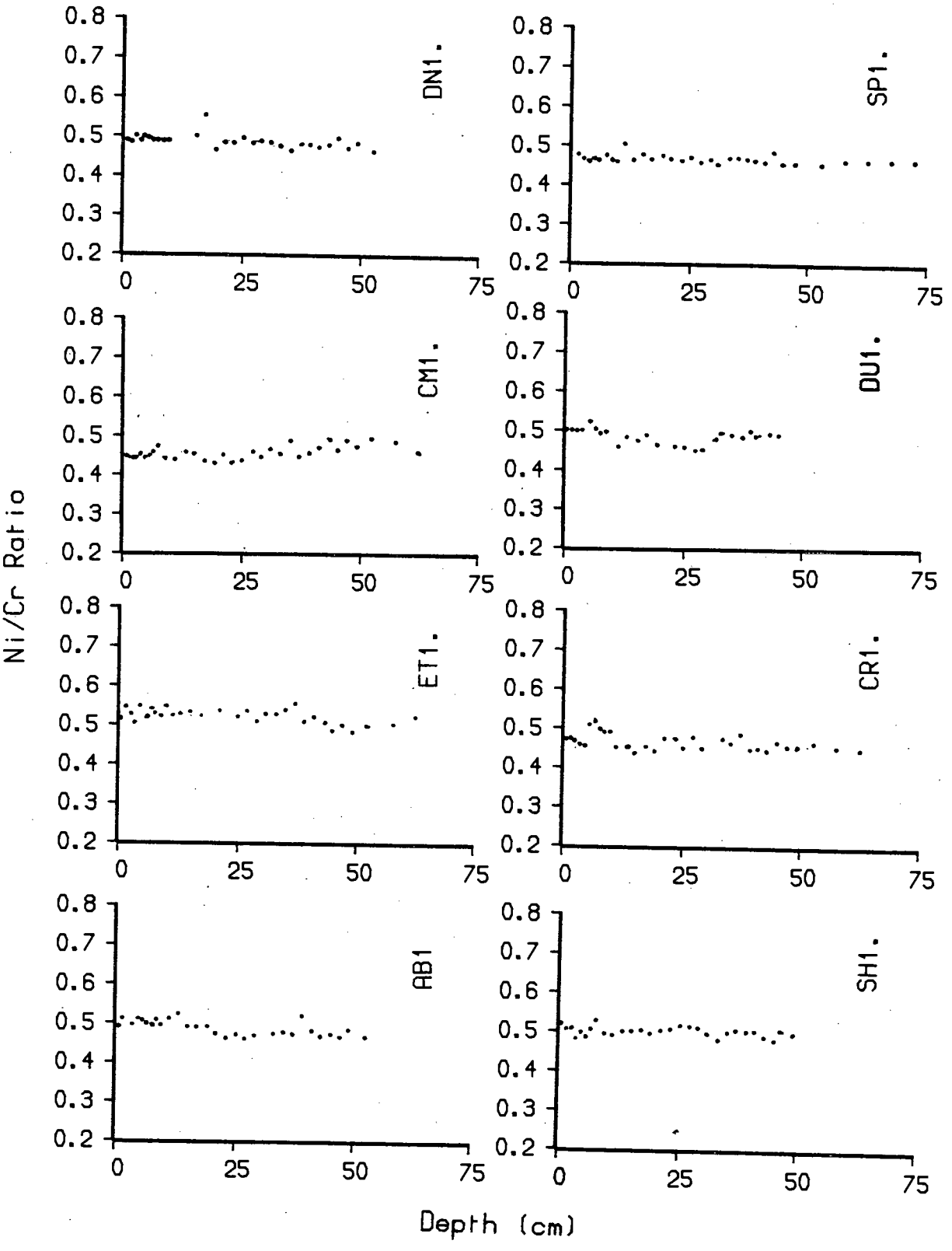

FIGURE 3.12: The patterns of Ni/Cr ratios with depth in the sediments.

cores from Loch Etive, ET1 and AB1, appear to have higher ratios. Two cores, CM1 and CR1 appear to be relatively impoverished in Ni relative to Cr. These cores have been noted from mineralogy and Zr/Rb ratios to be coarser grained than is normal suggesting that although much of the partitioning of Ni and Cr is related to ferromagnesian and alumino-silicates (particularly chlorite), in these sediments some Cr may exist in the resistate fraction, possibly as magnetite. The trends of Ni and Cr with depth in cores CM1, CR1 and AB1, show decreasing Ni/Cr ratios for AB1 and CR1 and an increase for CM1. Shiraki (1978) (quoting Shiraki, 1966) suggested that the ratio of mafic to granitic rocks within the catchment area was important in determining the amount of Cr in a sediment. Within the study area, there is a wide range of rock type from Lewisian granite gneiss to Tertiary flood basalts (See Chapter 2). But, in these sediments, there appears to be little variation in Cr content as a result of the changing rock type.

At depth the patterns of Cr and Ni follow closely that of Rb. This can be seen from Figures 3.13 and 3.14 which show little change in the Ni/Rb and Cr/Rb ratios with depth, although there is some overall variation betweeen cores, CM1 and CR1 having an overall lower ratio than is seen in the other cores. Ni and Cr can therefore be seen to be associated in the clay fraction similar to Rb. In some sediments, Ni and Cr have been shown to have elevated values in the surface sediments (for example, Bruland *et al*, 1974; Bertine and Mendeck, 1978; Bower *et al*, 1978). This has been attributed to anthropogenic input from pollutant sources. The similarities of patterns between Ni, Cr and Rb shows that, in these sediments, this is not the case and that the Ni and Cr are derived from terrestrial weathering sources. The distribution of Ni/Rb ratios will be readdressed when the distribution of Cu, Pb and Zn in the sediments is discussed (Chapter 7).

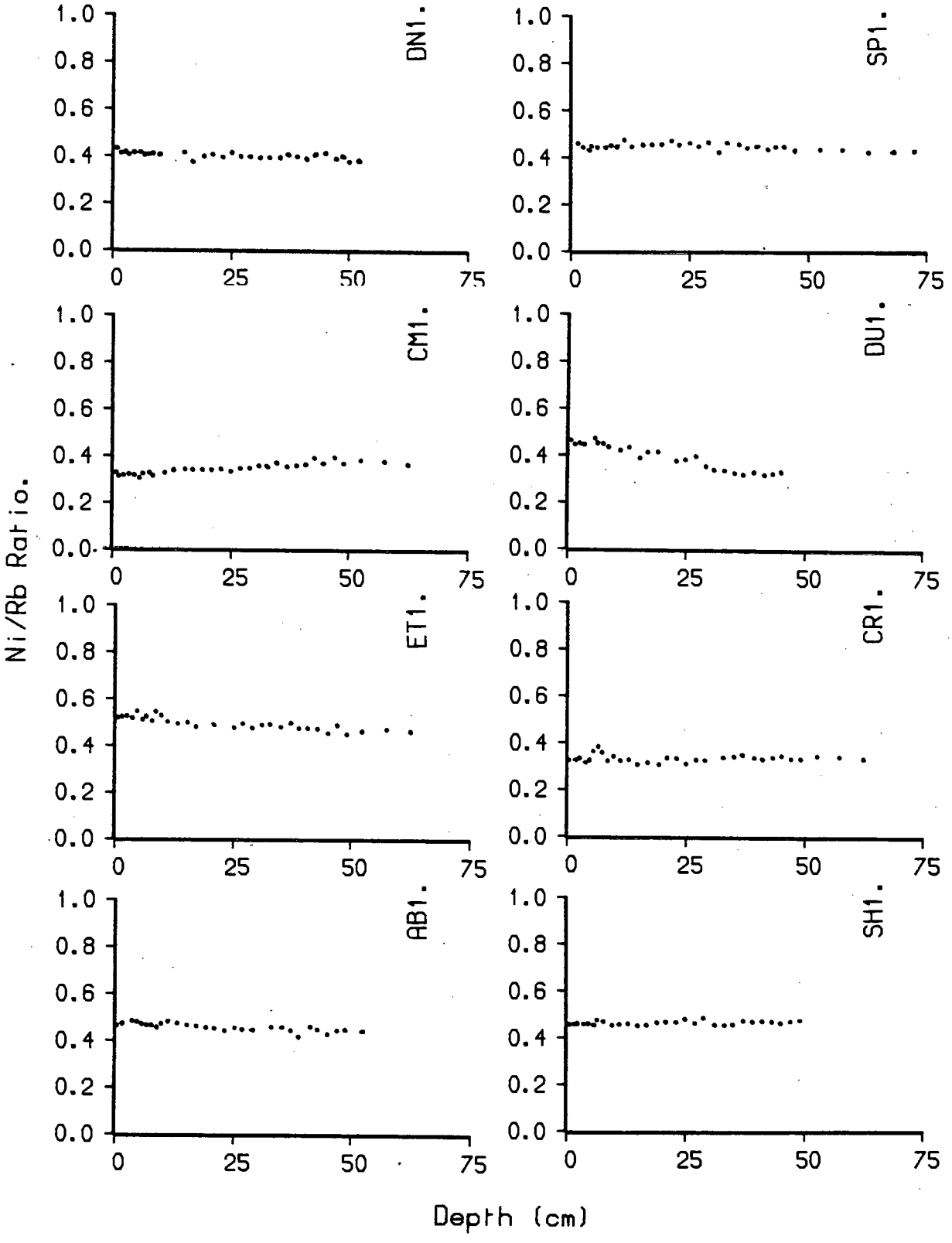

FIGURE 3.13: The patterns of Ni/Rb ratios with depth in the sediments.

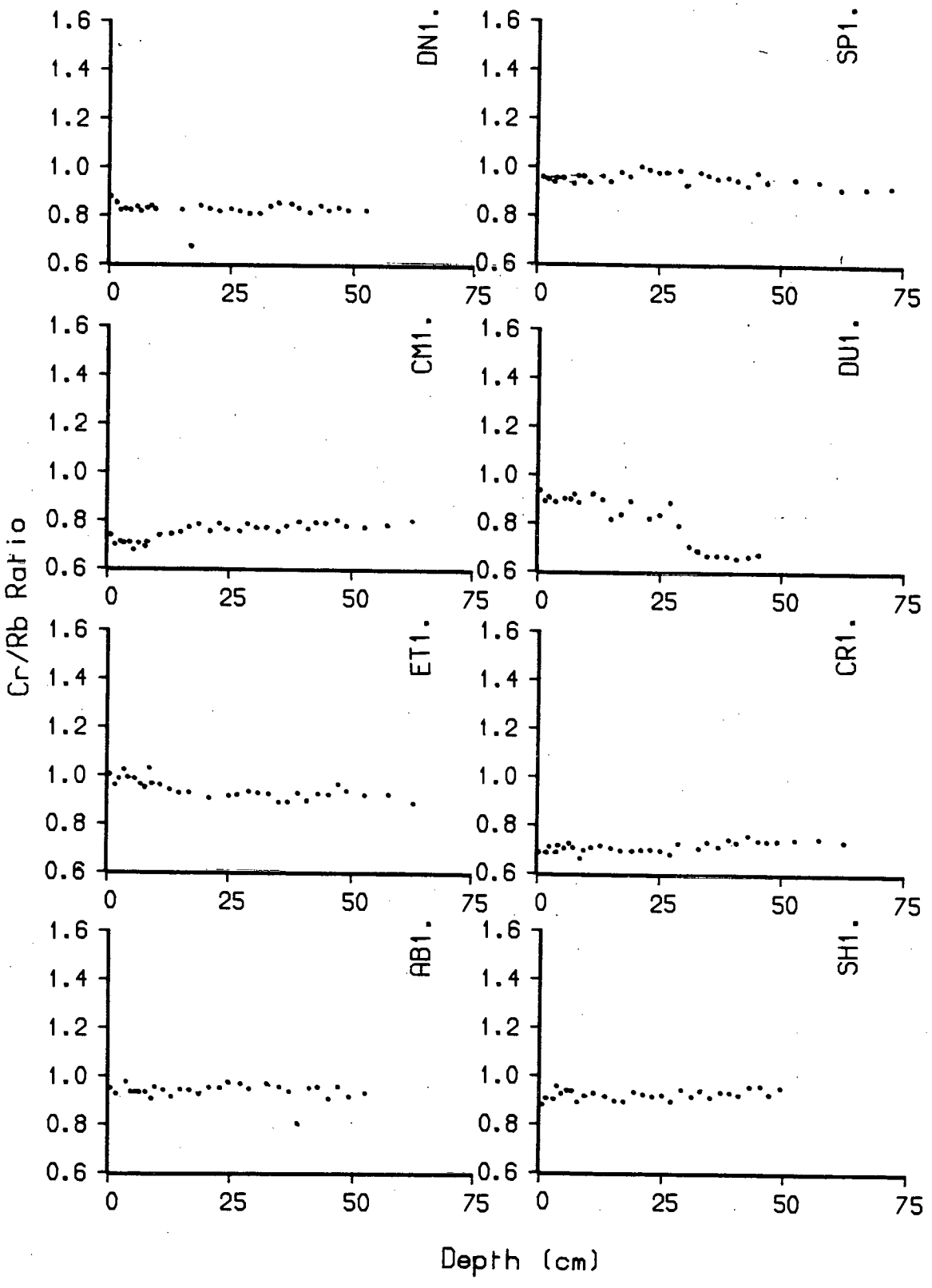

FIGURE 3.14: The patterns of Cr/Rb ratios with depth in the sediments.

3.5.3. Scandium.

Scandium (Sc) is known to be associated with Al in the clay minerals (Frondel, 1978). The concentrations of Sc in the sediments analysed varies from below the detection limit to 17ppm. These compare well to Frondel (1978) who quotes values of between 10 and 25ppm Sc in nearshore clays. Generally, the Sc values are relatively invariant with depth (see Figure 3.15). However, some sediment cores show rather irregular profiles, for example; core CR1. Here, the Sc values approach the analytical detection limits in the shell band between 5cm and 12cm. This is consistent with the fact that carbonates have been shown to contain very little Sc (<1ppm; Frondel, 1978). Core CM1 also shows slightly lower Sc values compared with other cores confirming the contention that CM1 and CR1 contain less alumino-silicates. Comparison of Sc with Rb as Sc/Rb ratios (see Figure 3.16) shows very little change in the ratio from core to core and with depth. The exception to this is in the shell band between 5cm and 12cm in the CR1. The lack of variation between the cores is due to the overall association of Sc and Rb within the same sediment constituents. This association of Sc, Rb and Al, indicates that Rb can be sensibly used as an indicator of the alumino-silicate fraction of the sediments as discussed in section 3.5.1

3.5.4. Barium.

The occurence of Barium (Ba) in rocks and minerals has been reviewed by Puchelt (1978). Ba is generally associated with potassic feldspars and micas. Duchesne (1968) noted that some plagioclases can also contain Ba but, the

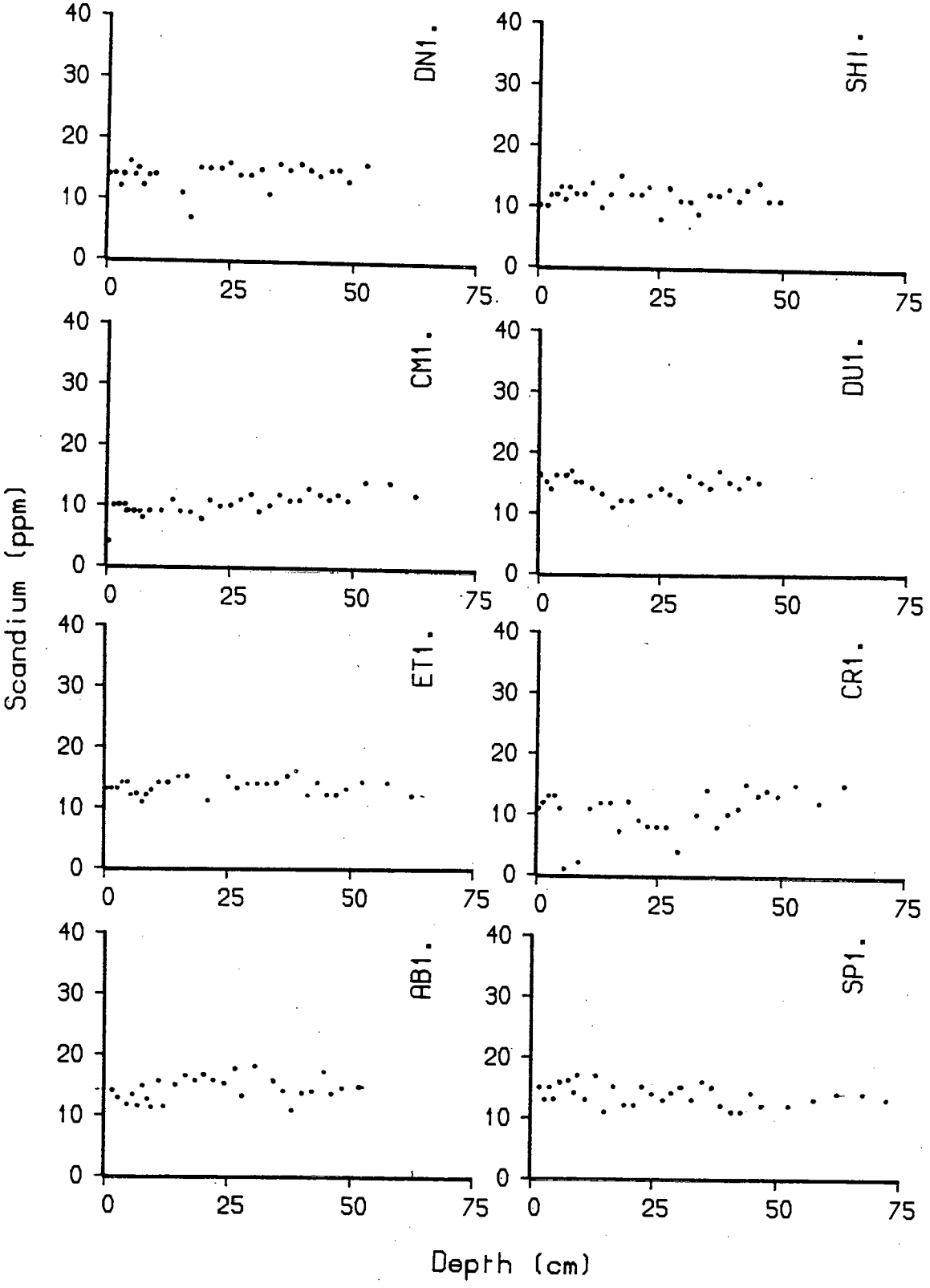

FIGURE 3.15: The patterns of Sc with depth in the sediments.

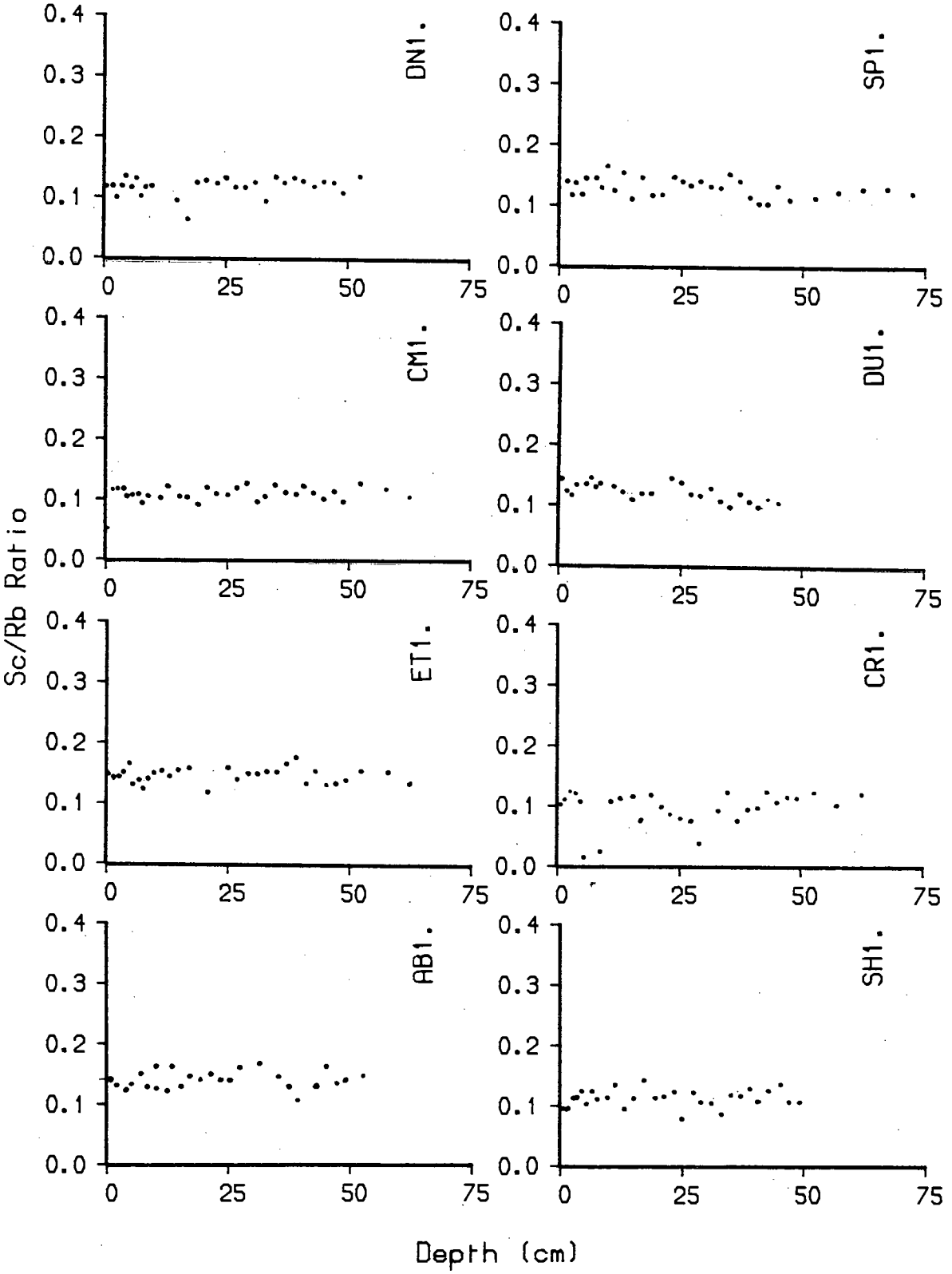

FIGURE 3.16: The patterns of Sc/Rb ratios with depth in the sediments.

concentrations tend to be much lower than in the potassic feldspars. Puchelt (1967; quoted in Puchelt, 1978) noted that in coastal sediments, Ba tends to be higher in the clay fraction than in the sand and silt fraction.

Considering the sediments sampled, the mean surface values (Table 3.3) vary from 304ppm in SH1 to 600 ppm in ET1. Both SH1 and SP1 show relatively low values with cores CM1, CR1 and DN1 having intermediate values between 400 and 450ppm. At depth (see Figure 3.17), the Ba values remain relatively invariant except in cores CR1 and DU1. Core CR1 shows a fall in Ba at the shell band between 5cm and 12cm and DU1 shows a very high Ba concentration in the pale grey clay near the base of the core.

The high Ba values in the sediments may be attributed to higher amounts of feldspars (paticularly potassic) in the sediments. High values noted in core ET1 can be explained by the fact that the sediment in the inner basin of Loch Etive is derived from the granite catchment area. The Ba values in AB1 are lower due to the diluting effect sediment of lower Ba content derived from a non-granitic catchment area. The clay at the bottom of DU1 is relatively fine grained and has a higher proportion of clays and feldspars (see Figure 3.5), thus a higher Ba content would be expected. In CR1 the low Ba content of the shell bands can be accounted for by the coarser sediment as indicated by the Zr/Rb ratios and therefore lower feldspar and clay contents and the diluting effect of the relatively high proportion of carbonate likely to be present (see below, subsection 3.5.5)

3.5.5. Strontium.

The Strontium (Sr) content of the sediments ranges between 209ppm and 790ppm, with most values less than 479ppm. Profiles of Sr with depth are

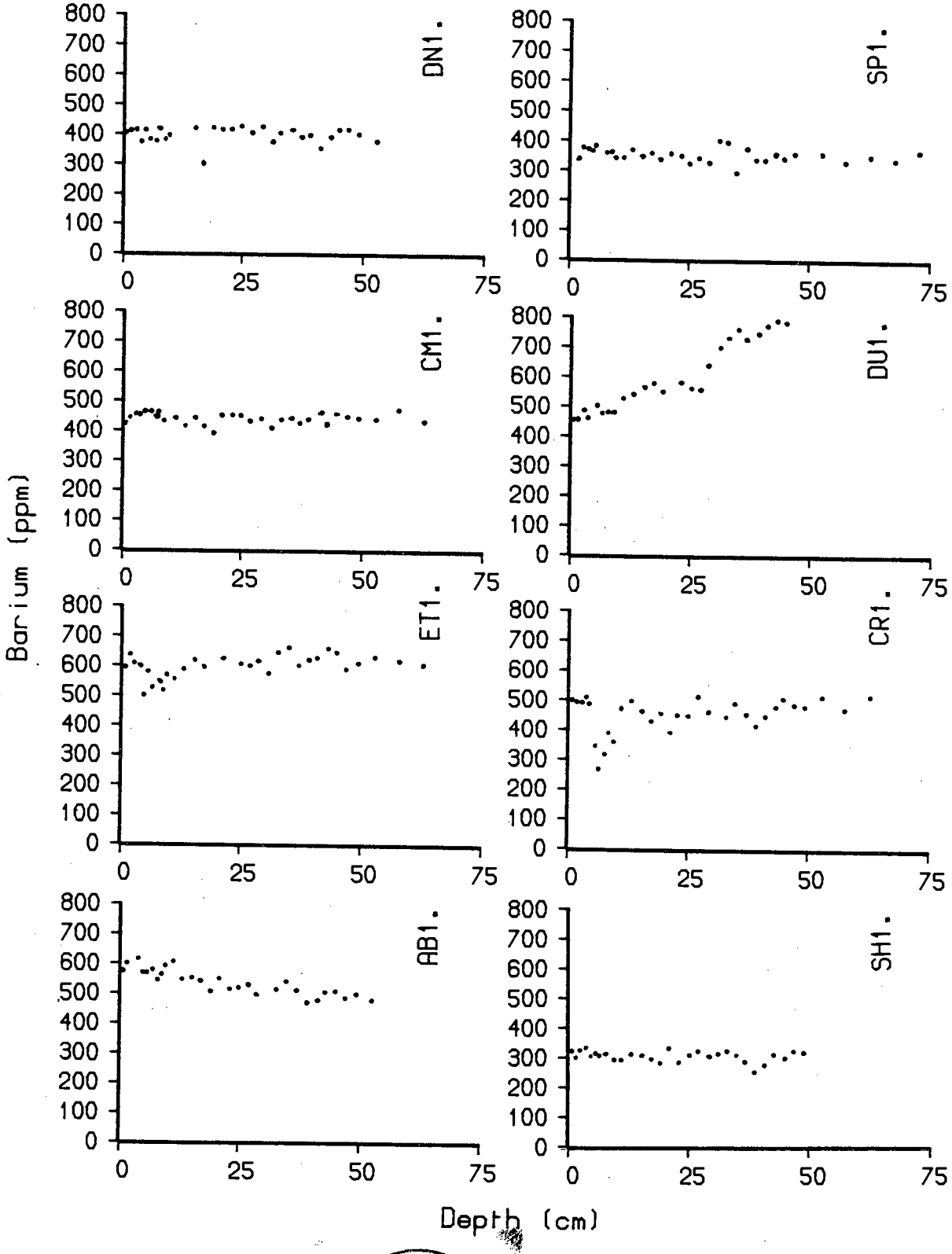

FIGURE 3.17: The patterns of Ba with depth in the sediments.

Core	Ba (ppm)
AB1.	537
CM1.	441
CR1.	451
DN1.	404
DU1.	508*
ET1.	600
SH1.	304
SP1.	352

TABLE 3.3: Mean Ba values (* Mean values of sediment above clay).

Core	Y	La	Ce	Nd	La/Y	Ce/Y	Nd/Y
AB1	27	52	114	42	1.93	4.22	1.56
CM1	25	28	70	26	1.12	2.50	1.04
CR1	25	33	82	29	1.30	3.28	1.16
DN1	25	31	76	29	1.24	3.04	1.16
DU1	29	48	115	45	2.04	4.78	1.70
ET1	27	55	129	46	2.04	4.78	1.70
SH1	22	28	64	25	1.27	2.90	1.14
SP1	24	29	72	29	1.21	3.00	1.21
*N. Am Shales	27	32	73	33	1.19	2.70	1.22
*Europe Shales	32	41	86	42	1.20	2.70	1.31

TABLE 3.4: Mean REE concentrations and REE/Y ratios in the sediment cores, together with mean concentrations and ratios in N. American and European shales (* Data after Haskin and Haskin (1966).

shown in Figure 3.18. The lowest Sr values (269ppm to 209ppm) are seen in AB1. Core CR1 has very high Sr values, up to 790ppm. These are concentrated in the coarse shell bands. In core DU1 the Sr values increase from 336ppm to a maximum of 439ppm at 22-24cm, falling to 270ppm in the pale grey clay below 34cm.

Sr in these sediments is almost entirely partitioned between the alumino-silicate and carbonate constituents of the sediments. Sr is known to be associated with various Na and K feldspars and clay minerals; for example illite (Calvert, 1976; Stueber, 1978). The high values seen in CR1 and SH1 are unlikely to be due solely to the alumino-silicate content of these sediments as carbonate free clays tend to show about 250ppm Sr. Much of the elevated Sr values is almost certainly caused by varying amounts of biogenic carbonate in these sediments. Certainly Figure 3.19 shows that there is a strong negative relationship between the Sr content and alumino-silicate (Rb) content of the sediment, implying mutual dilution of one element by the other; this is especially true in cores CR1 and DU1 which have been shown to have high calcite contents relative to the other constituents. The highest Sr values occur in core CR1 at the major shell band between 5cm and 12cm depth. Although there is no observable shell debris in DU1, appreciably high calcite contents occur in the upper parts of the core which may have different Sr/Ca ratios to that of CR1.

Figure 3.20, shows the correlation between carbonate carbon (C_{CO3}), determined by combustion (see Appendix I, Sections 2.3 and 2.4) and Sr for three cores; CR1, SH1 and ET1. The Sr and C_{CO3} plots confirm that carbonate free sediments tend to have low Sr contents; the regression line based primarily on cores CR1 and SH1 indicates a value of 150ppm Sr. Furthermore,

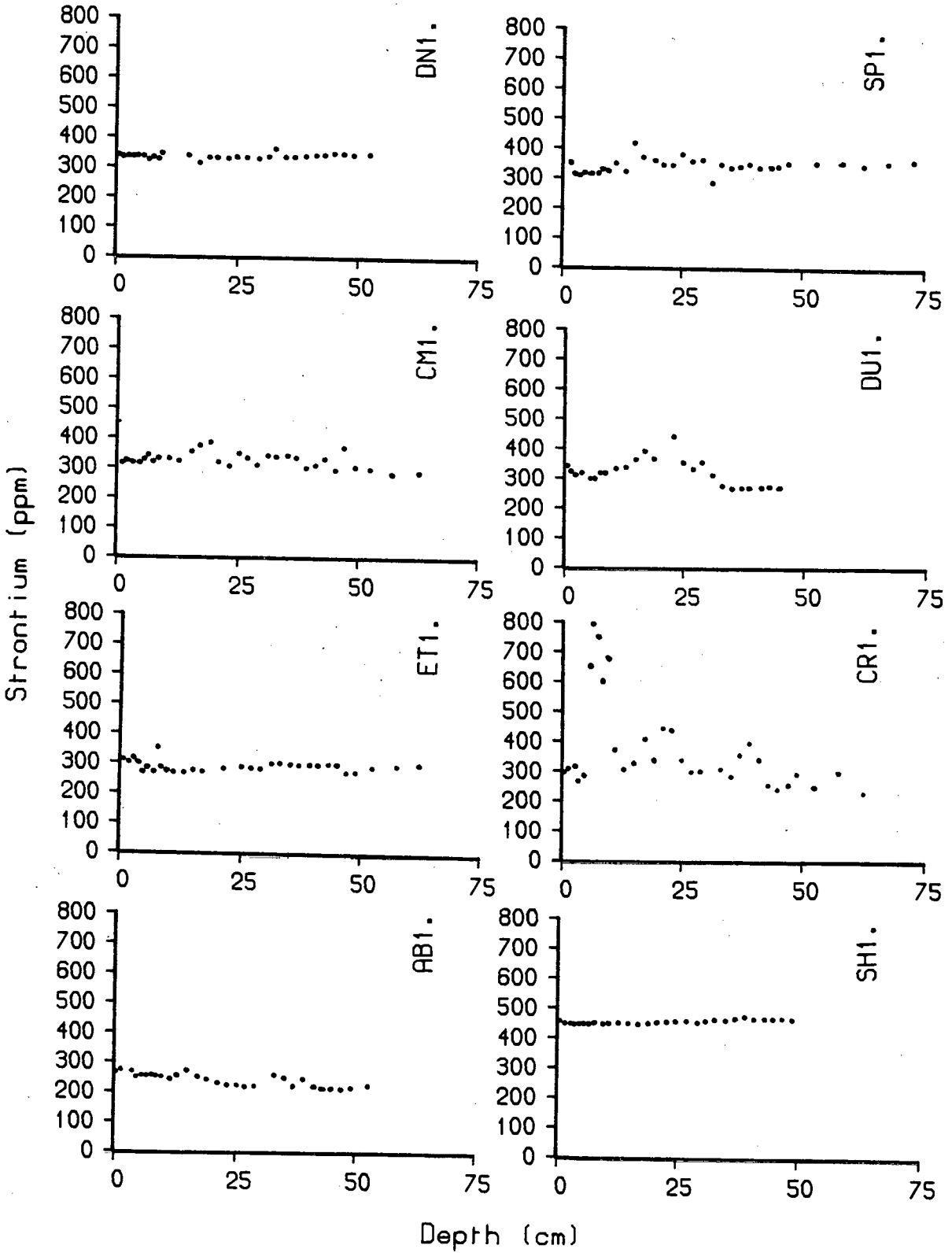

FIGURE 3.18: The patterns of Sr with depth in the sediments.

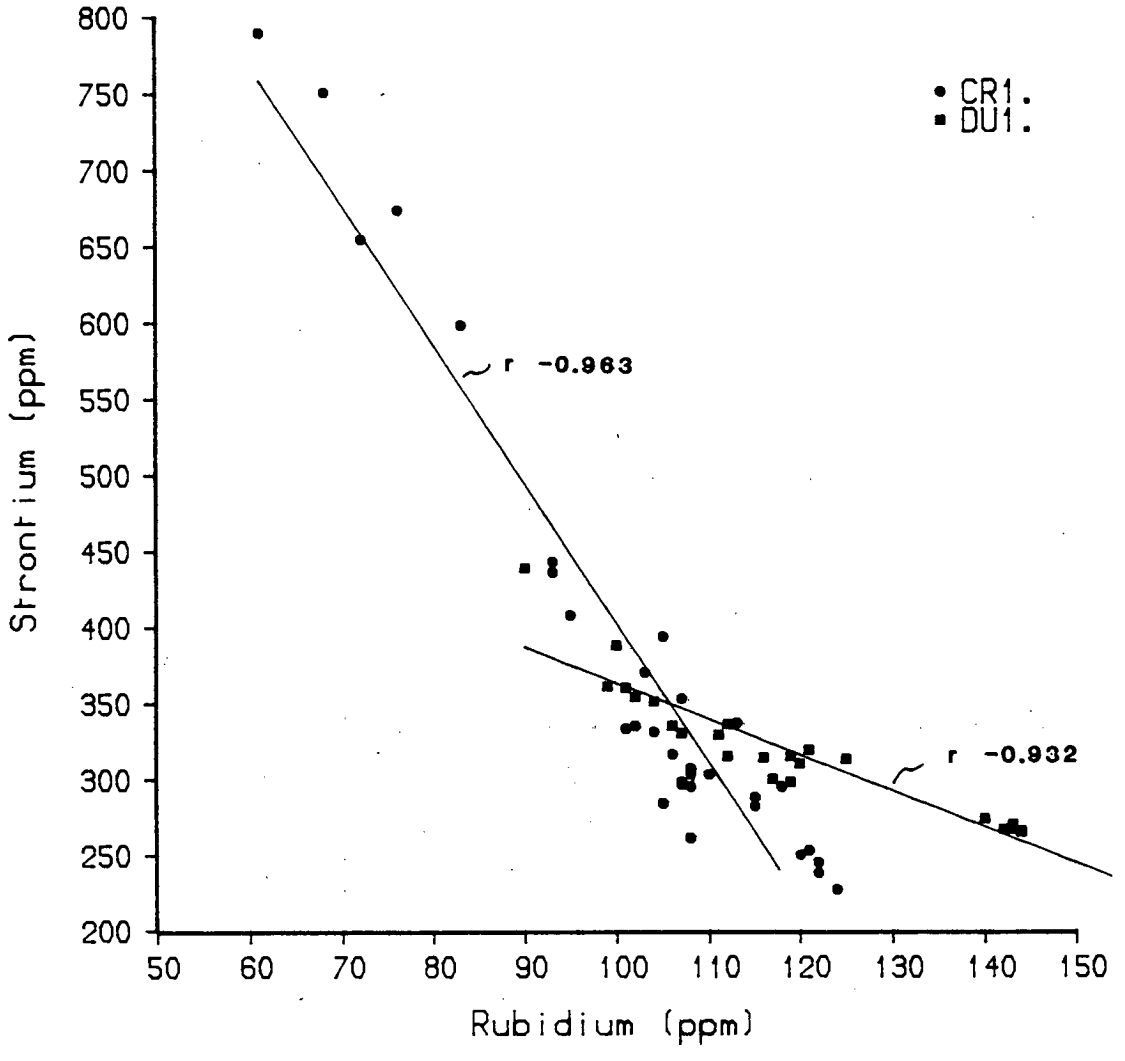

FIGURE 3.19: The relationship of Rb to Sr in cores CR1 and DU1.

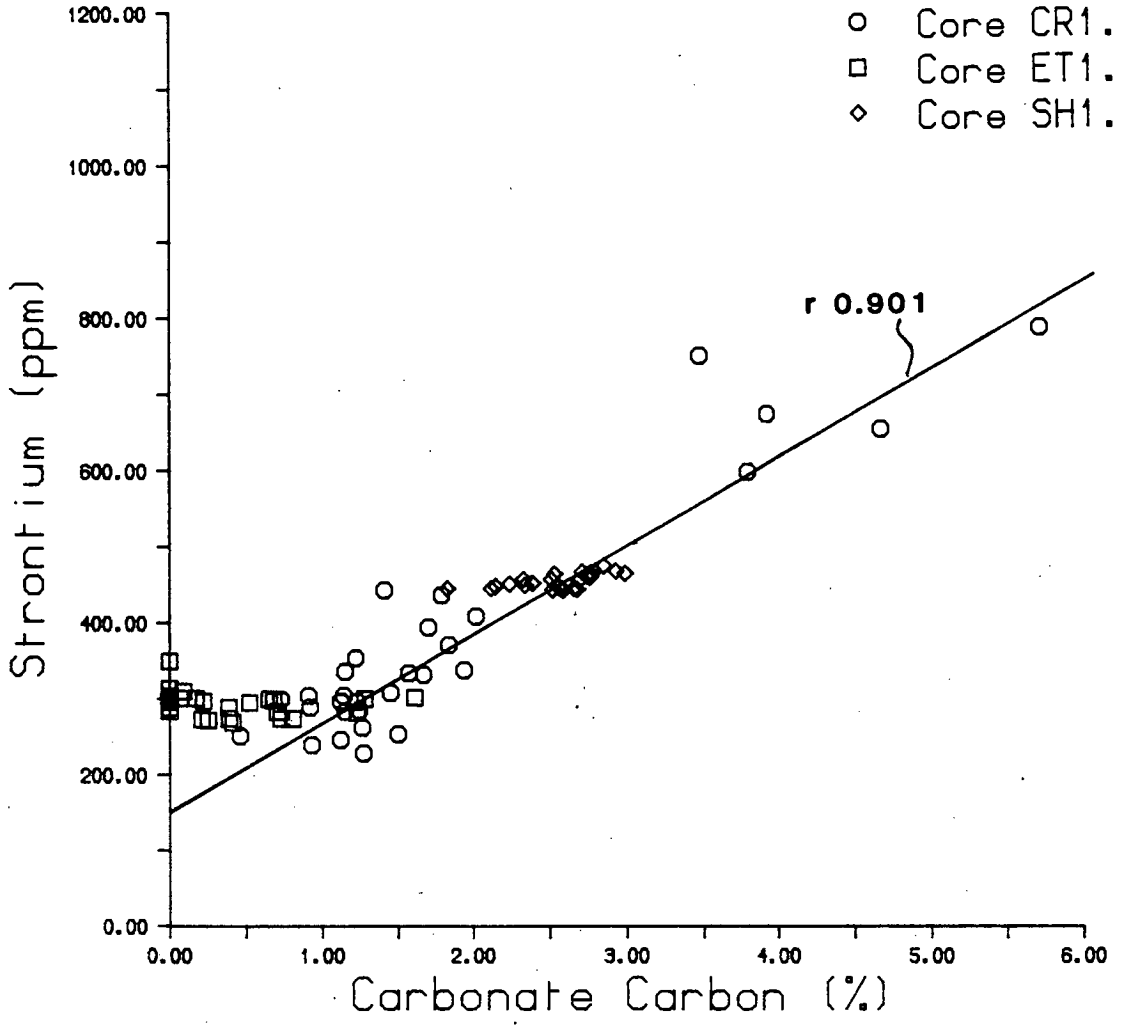

FIGURE 3.20: The relationship of calculated carbonate carbon values (C_{CO3}) to Sr.

the graph confirms the view of Malcolm (1981) that most sediments in Loch Etive contain relatively little carbonate but this will be readdressed in Chapter 4 when organic carbon is considered. The higher Sr/C_{CO3} of the latter sediments may be due to higher Sr in alumino-silicates. Figure 3.20 allows the percentage of C_{CO3} present in carbonate rich sediment to be calculated for a given Sr content mathematically using the standard $y = mx + c$ format and the values for m and c given in Figure 3.20.

The shell band (5-12cm) in core CR1 therefore contains about 50% $CaCO_3$, whilst the non-shelly horizons contain much less carbonate, between 10% and 20% $CaCO_3$. Similarly, the sediments from core SH1 contain about 20% $CaCO_3$. Higher mean Ba values in cores AB1 and ET1 relative to the remaining sediments (see Table 3.3) would tend to support this (Puchelt, 1978).

The conclusion which may be drawn from this is that, where calcite is present, Sr is much more closely associated with this than the feldspars and as such can be used to indicate the presence of shell bands within a sediment. However, in sediments with low calcite values, the Sr is associated with the feldspar fraction.

3.6. Rare Earth Elements.

3.6.1. Results.

Rare Earth data was obtained by X-Ray Fluoresence Spectrometry and is reported on a salt free basis. All the data is listed in Appendix II, Table AII.4. Before the patterns can be discussed, the possibility of their being an artifact of analysis must be considered. The Compton Method of correcting the raw X-Ray Fluorescence response for variations in the absorption effects of

different matrices (see Appendix I, Section 2.2) is not strictly applicable due to the position of the "Lα" lines for La, Ce and Nd beyond the absorption edge of iron and therefore the Compton correction made may not necessarily be a true reflection of the matrix effect. In the analysis of Y, Kα line measurements were made. Hence, in this case, Compton Scatter absorption corrections are not subject to error. However, matrix variations are rarely more than 10% (Fitton, Pers. Comm.) and this cannot account for the Rare Earth Element (REE) variations seen in the sediments. Thus, whilst the contents described below are possibly subject to some error, they probably represent a true reflection of the element variation in the cores.

The Yttrium (Y) patterns in the sediments are similar for all the cores (see Figure 3.21). Surface values are relatively invariant between 25 and 30ppm. In most cores, the values remain constant with depth, however in core CR1 the Y values fall to about 15ppm in the shell band between 5cm and 12cm. These trends broadly follow the trends in alumino-silicates as depicted by Rb. For example, in DU1 the values increase to over 32ppm in the old clay in the bottom section of the core.

Figure 3.22 shows the pattern of Lanthanum (La) in the sediments. In cores; CM1, CR1, DN1, SH1 and SP1, the surface values are relatively similar (between 25 and 35ppm). However, the cores from fjords, AB1, ET1 and DU1 show an increased La content of 50ppm. At depth, the patterns in all the cores remain invariant except for a fall in La concentration between 5cm and 12cm in core CR1, paralleling the pattern of Y.

Similarly, the Cerium (Ce) patterns in the sediments (Figure 3.23) closely follow La in that the fjordic cores; AB1, ET1, and DU1 have much higher

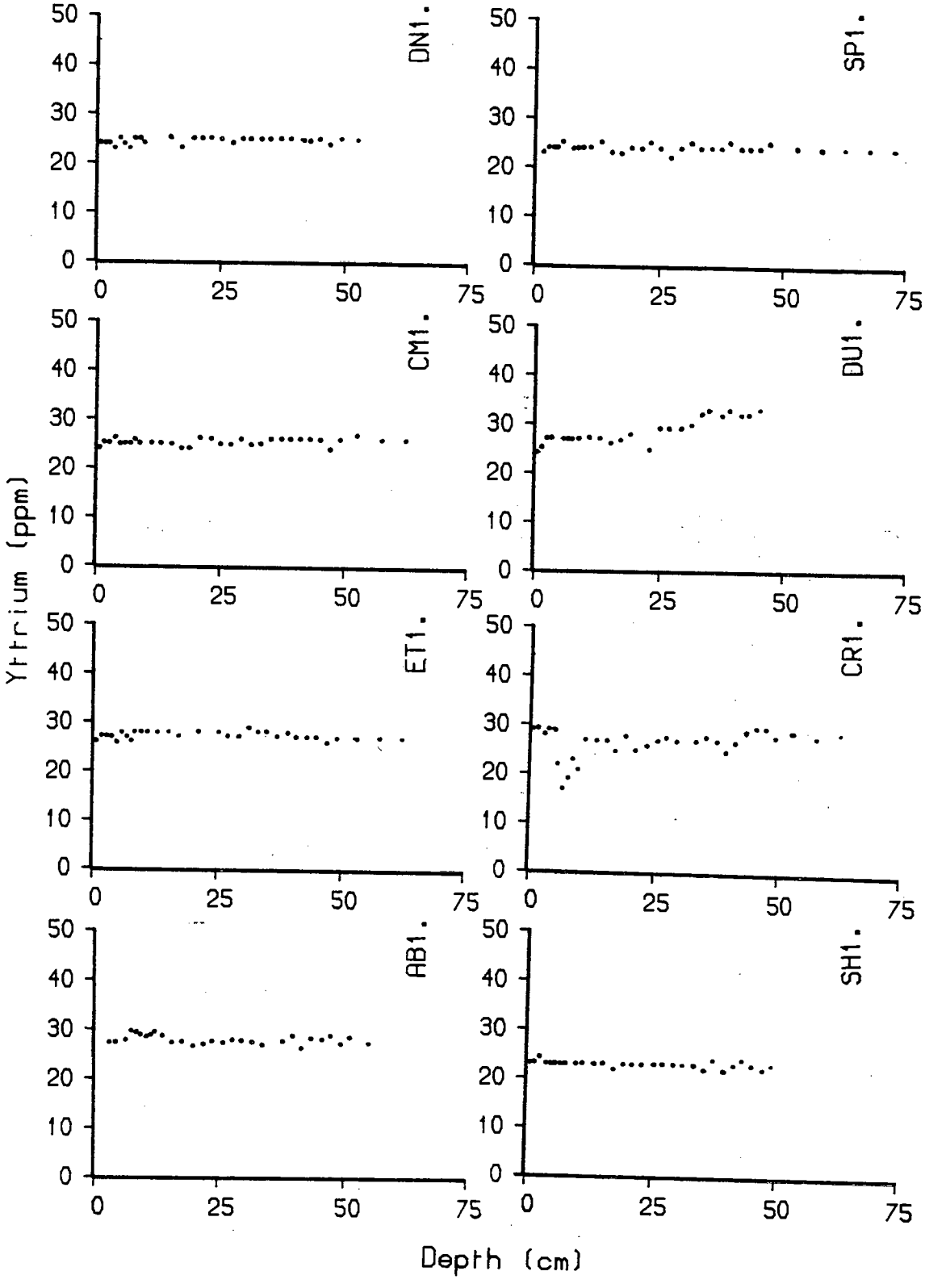

FIGURE 3.21: The patterns of Y in the sediments.

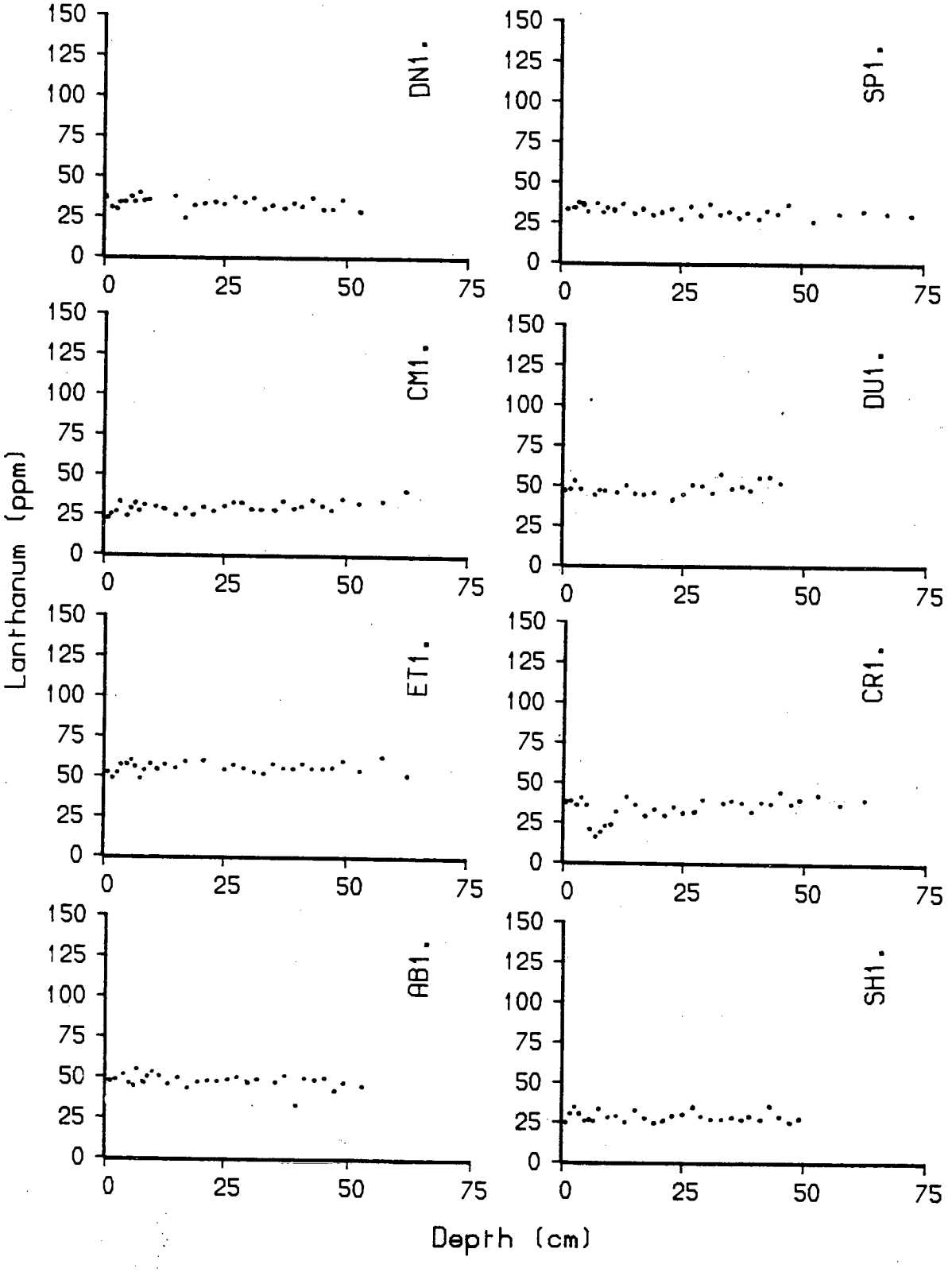

FIGURE 3.22: The patterns of La in the sediments.

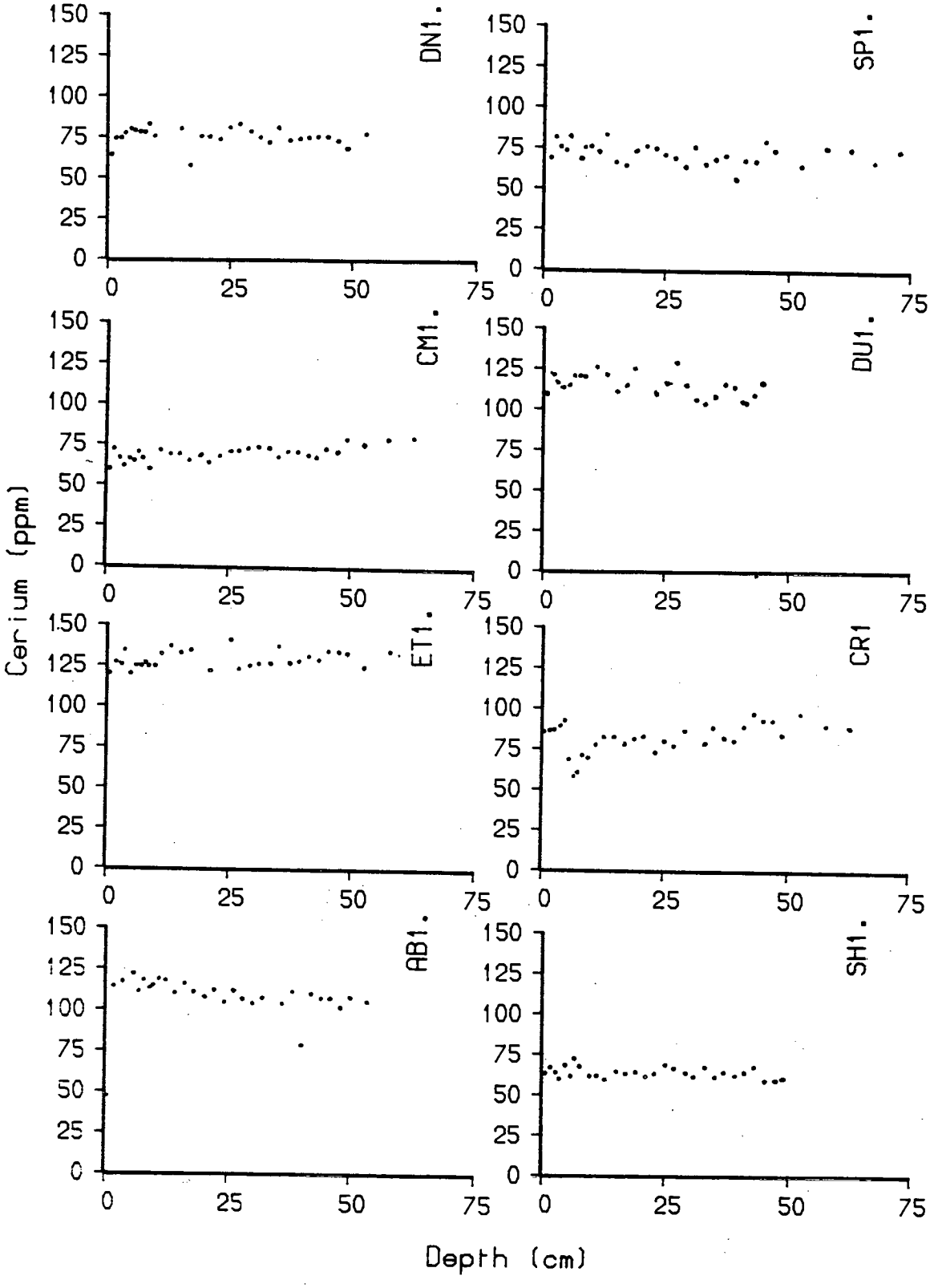

FIGURE 3.23: The patterns of Ce in the sediments.

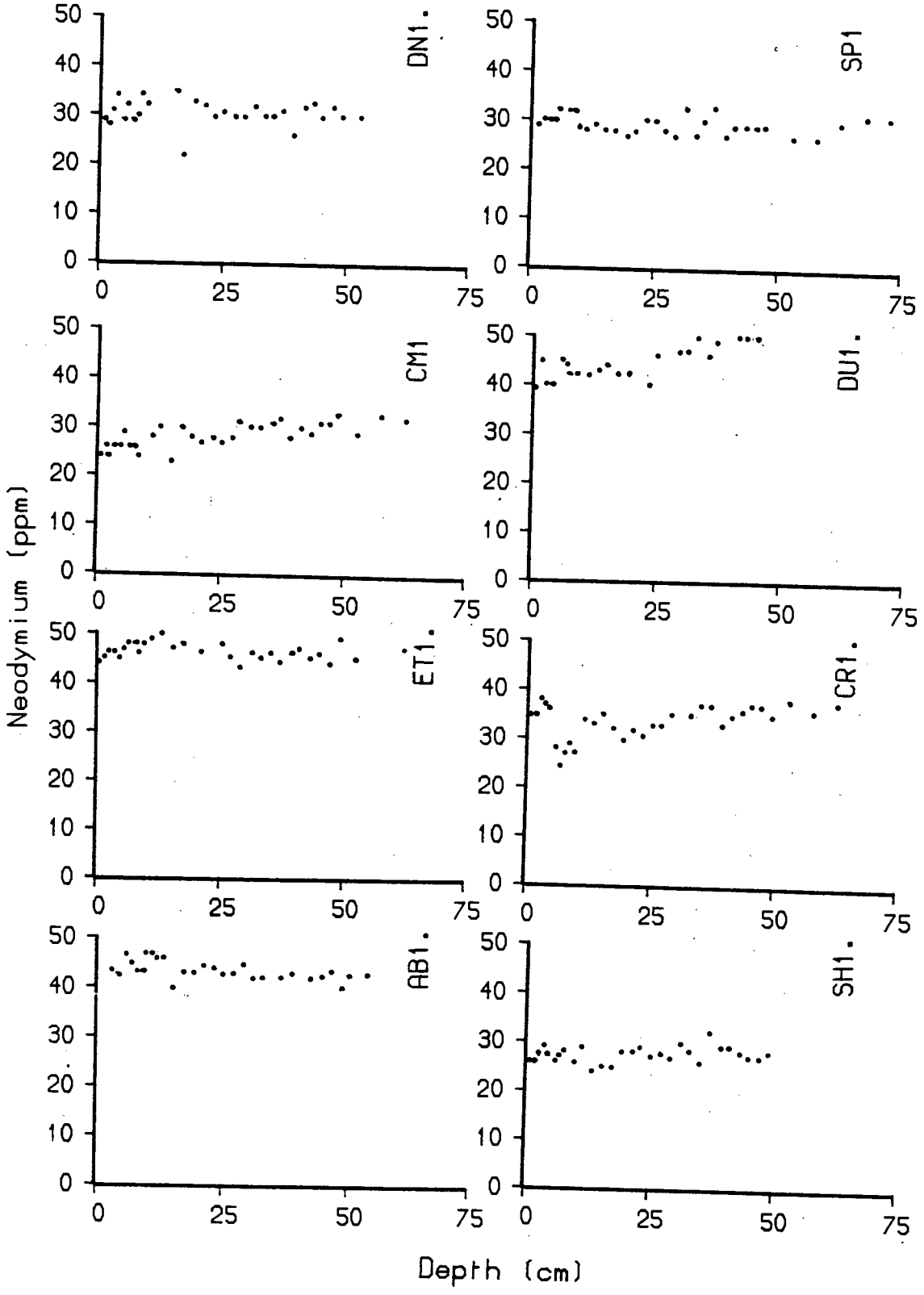

FIGURE 3.24: The patterns of Nd in the sediments.

contents (100-150ppm) than the other cores. The shell band between 5cm and 12cm in core CR1 follows the pattern of Y and La.

The pattern of Neodymium (Nd) (Figure 3.24) in the main follows the pattern of the above elements (La and Ce) being relatively enriched in cores AB1, ET1 but, the increased content in the lower horizons of DU1 tends to follow the pattern of Y.

3.6.2. Discussion.

The mean REE values noted in the sediments for cores CM1, CR1, DN1, SH1 and SP1 compare well with values noted by Haskin and Haskin (1966) for N. American and European shales (see Table 3.4).

The values for La, Ce and Nd noted in cores from Loch Etive and Loch Duich, in contrast to Y, are much higher than those noted from shales (Haskin and Haskin, *ibid*) and other cores from West Scotland (this study). Comparison of the mean REE/Y ratios shows a similar pattern with Loch Etive and Loch Duich being enriched in REE relative to the remaining cores and mean shales (Table 3.4). The sediments from Loch Etive and Loch Duich contain the highest contents of organic matter and the distribution of REE is possibly associated with the distribution of organic matter in the sediments. Ridgway (1984) noted the possibility of the formation of apatite from phosphorous released during organic matter degradation in the sediments of Loch Etive. REE are known to have an affinity for Phosphates (Arrhenius and Bonatti, 1965). Kochenov and Zinov'ev (1960; quoted Herrmann, 1978) found a direct relationship between the Lanthanides and P_2O_5 in fish remains from the Maikop Beds of the Caucasus, particularly from sulphide bearing layers.

It is possible therefore that the anomalous REE patterns from Loch Etive and Loch Duich may be due to the uptake of these elements onto diagenetic apatite. However, Y would also be expected to be enriched. Arrhenius and Bonatti (*ibid*) noted preferential enrichment of Y and Nd over La and Ce in recent pelagic fish bones. A further possibility is an association of REE with $Fe(OH)_3$. All the sediments from the fjordic environments are subject to a large terrigenous input. This is known to contribute iron to the particulate matter and the sediments. The hydrography of the lochs is such that an appreciable amount of Fe is liable to flocculate and sediment out, especially in the inner basin of Loch Etive, which is dominated by terrestrial input. Ridgway (1984) noted an enrichment of Fe relative to Al in sediments from the inner basin of Loch Etive. The sediments from the inner basin (ET1) show the highest REE values relative to Y in comparison to AB1 and DU1. It is possible that the flocculating iron oxides scavenge the REE and transport them to the sediment. The iron oxides, however, are diagenetically mobile in the sediments and are rapidly reduced in anoxic conditions, which would be expected to lead to the release of REE possibly leading to an enrichment in the upper horizons of the sediments. This clearly does not occur as the REE patterns tend to remain relatively constant with depth suggesting that the REE are associated with a non-mobile phase.

CHAPTER 4

ORGANIC COMPONENTS IN THE SEDIMENTS AND PORE WATERS

4.1. Introduction.

It has been seen from a number of studies (Malcolm, 1981; Hunt and Fitzgerald, 1983; Sigg *et al*, 1987) that suspended particulate organic matter plays a significant role in the control of trace metals in marine systems. Similar effects have been noted in sediments (for example, Baturin *et al*, 1967; Jones and Jordan, 1979; Willey and Fitzgerald, 1980; Ridgway, 1984). In order to assess the diagenetic effects of burial on the organic material of the study area, the organic components in the sediment (C, N, and associated S) and in the sediment pore waters (SO_4^{2-}, Titration alkalinity (A_T)) were analysed. However, inference of diagenetic events as observed in patterns of change of these parameters is complicated by the fact that for many of the cores studied the source of organic matter may differ and may represent an admixture of terrestrial and marine organic matter. Variation in the distributions of C, N, S, SO_4^{2-}, A_T may be due to changes in the relative importance of these differing sources and may have a profound influence on the composition of the sediment during burial diagenesis. In order to identify diagenetic effects of organic matter from the variations in organic matter source, it is necessary to attempt to characterise the source of organic matter in the sediments, particularly at the sediment surface. A number of chemical parameters have been employed in the past to distinguish between marine and terrestrial organic matter. These have included; C/N, C/H, Br/C_{org} (organic Carbon), (Bordovskiy, 1965; Pocklington and Leonard, 1975; Mayer *et al*, 1981) and $\delta^{13}C$, $\delta^{15}N$ stable isotope ratios (Cline and Kaplan, 1975; Peters *et al*, 1978; Sweeny *et al*, 1978; Sweeny and Kaplan, 1980).

In this chapter the behaviour of organic carbon (C_{org}) is described especially its role in reducing sulphate to sulphide in sediments. A study of

C/N ratios has also been made in an attempt to identify and quantify the proportions of marine to terrigenous organic matter present in the sediments. The use of $\delta^{15}N$ will be discussed in Chapter 5.

4.2. Results And Discussion.

The sampling and analysis techniques used are described in Appendix I, Sections 2.3, 2.4 and Chapter 5. All of the solid phase data is presented on a salt free basis. The complete data can be found tabulated in Appendix II, Tables AII.5 and AII.6. Carbon, nitrogen and sulphur are expressed as weight %, while C/N is given as atomic ratios.

4.2.1. Organic Carbon.

The sediments can be divided into three distinct groups based on the mean organic Carbon (C_{org}) contents. This is summarised in Table 4.1. The lowest C_{org} content can be found in CM1 with a mean of 0.79% C_{org}; the highest values occur in ET1 (5.57%). DU1 has a very high surface value of 4.62% C_{org}. The values given here are consistant with previously reported mean values of 6.4% from the inner basin of Loch Etive and 4.8% from Airds Bay in the outer basin (Ridgway and Price, 1987). The surface value in DU1 agrees well with 5.1% C_{org} found by Krom (1976).

Table 4:2 shows a comparison of C_{org} values from this study and those from a number of environments worldwide. It can be seen that the values in the sediments studied compare favourably with C_{org} values from coastal and estuarine sediments elsewhere and are significantly greater than those from deep sea sediments.

	org-C (%)	Nitrogen (%)
ET1.	5.57	0.53
AB1.	4.69	--
DU1.	4.62	0.45
DN1.	3.21	--
CR1.	2.11	0.27
SH1.	1.98	0.28
SP1.	1.93	0.28
CM1.	0.79	0.11

TABLE 4.1: Surface values C_{org} and Nitrogen (mean of upper 5cm of sediment).

Locality	org-C (%)	Nitrogen (%)	
Pacific Ocean	0.33-0.39	0.06-0.02	Muller (1977)
Gulf of Maine	4.5-1.1	0.50-0.09	Bader (1955)
Miramichi Estuary	8.00-<1	--	Willey & Fitzgerald (1980)
Saanich Inlet	4.75-1.05	--	Brown *et al.* (1972)
Long Island Sound	0.21-0.06	--	
Bering Sea	1.62-0.93	0.20=0.09	Bordovskiy (1955)
St Lawrence Estuary	16.45-4.9	1.92-0.62	Pocklington & Leonard (1979)

TABLE 4.2: Summary of C_{org} and Nitrogen values from other localities.

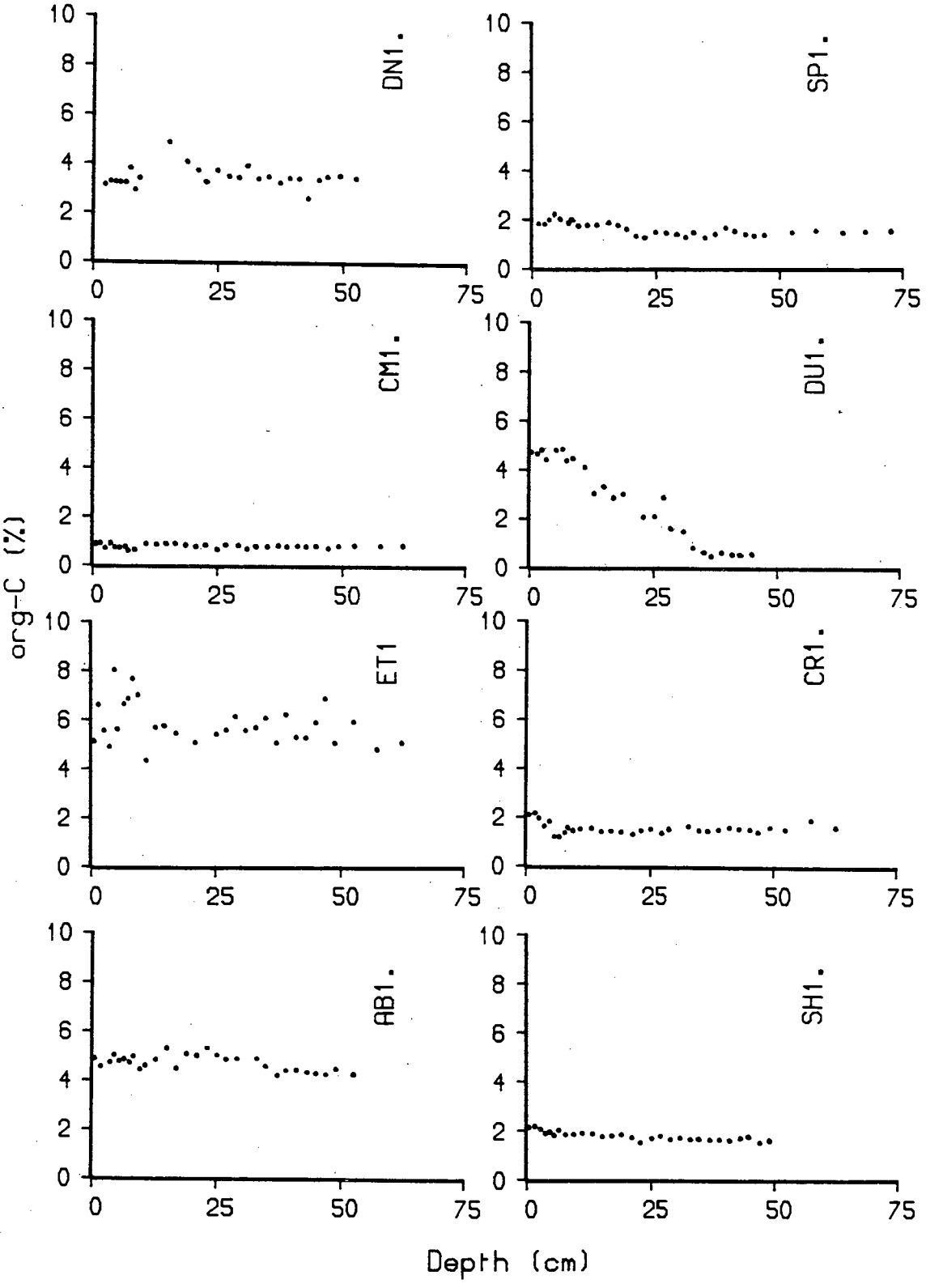

FIGURE 4.1: The patterns of C_{org} with depth in the sediments.

Figure 4.1 shows profiles of C_{org} with depth for eight of the west coast cores. In general the carbon contents are relatively constant with depth but, there are notable exceptions. Core ET1 displays a very irregular depth profile compared to the other cores. This appears to be a real phenomenon as the variations in C_{org} from adjacent depths are well in excess of variations predicted from the error in the analysis method (see Appendix I, Section 2.4). Content and variation in the C_{org} content in ET1 is greatest in the upper 15cm of the sediment. DU1 shows an 89% fall in C_{org} from 4.67% at the surface to 0.5% at 41cm. Low C_{org} at depth correlates well with the fact that there is a lithological change at 40cm to a pale grey, consolidated clay. This was described in Chapter 3, Section 3.2. CR1 displays a slight fall in the upper 8cm from 2.08% C_{org} at the surface to 1.51% by 9cm. However, lower values of 1.2% C_{org} occur between 5cm and 7cm. Below 10cm, the C_{org} remains relatively constant with a mean of 1.35%.

4.2.2. Nitrogen.

Nitrogen (N) in the sediments was determined using a Carlo-Erba 1600 Nitrogen analyser attached to a VG-Micromass 620 mass-spectrometer. This system was also able to produce $\delta^{15}N$ values. For a detailed description of the apparatus and method of analysis see Chapter 5, Section 5.2. The N analyses were not as comprehensive as those of C_{org} and mainly analysed at 2cm or 4cm depth intervals in the sediments.

The patterns of N in the sediments closely follow those of C_{org}. The sediments can be divided into similar groups as C_{org} based on mean N values. This is summarised in Table 4.1. CM1 displays the lowest N values (<0.12%). The highest values can be found in ET1 (0.5%) and the upper sediments of

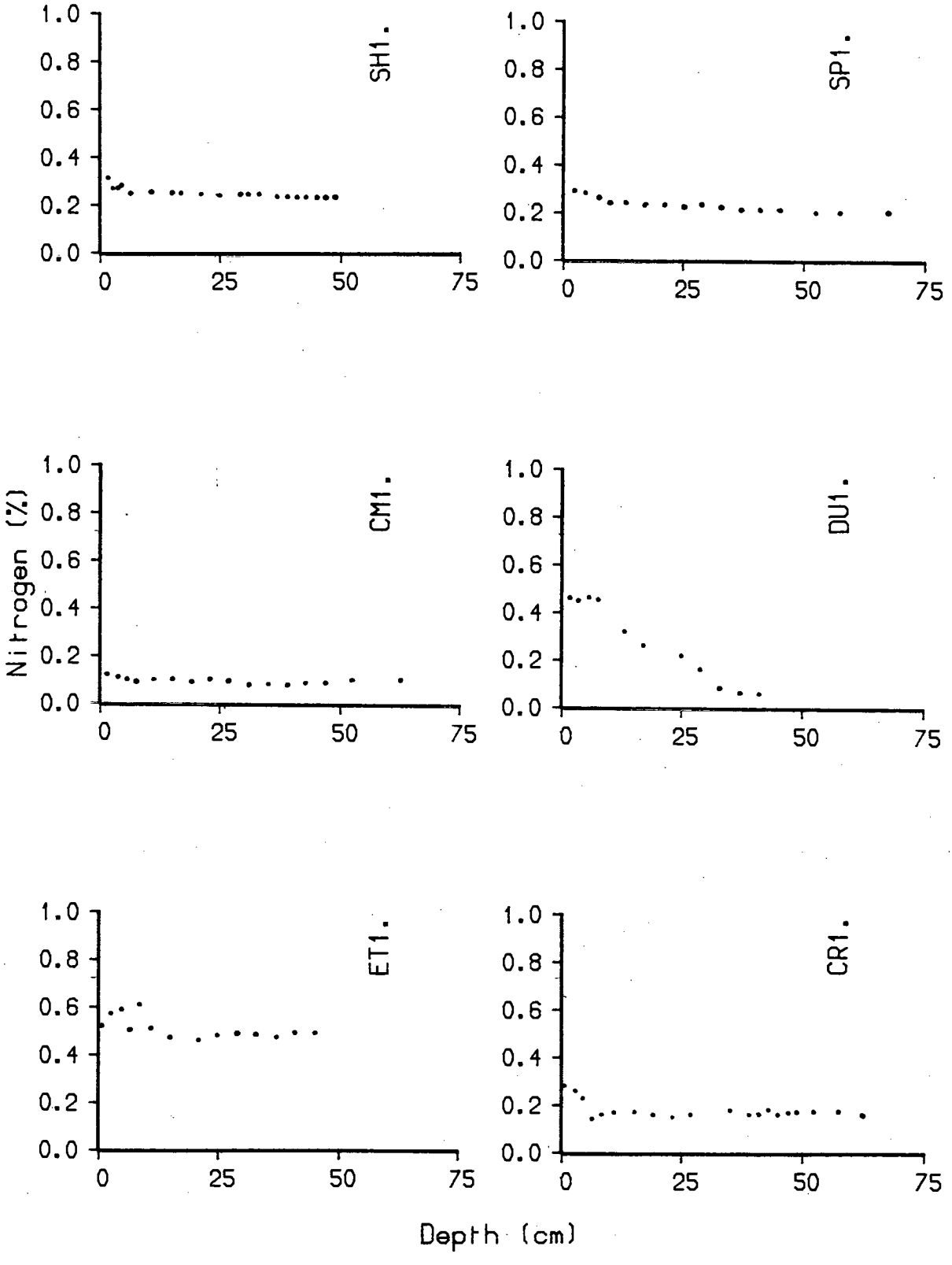

FIGURE 4.2: The patterns of N with depth in the sediments.

core DU1 (0.45%). As with C_{org}, the N data agrees well with previously reported values from the area. Ridgway (1984) found N values of 0.48% in the inner basin of Loch Etive. Malcolm (1981) quotes values of 0.57% for a similar location in Loch Etive. In Loch Duich, Krom (1976) found values of between 0.40% and 0.50% in sediments from the deeper parts of the loch. For comparison, the data is similar to Bader (1955), who quotes N values of between 0.04% and 0.50% for sediments from Puget Sound and the Gulf of Maine respectively. In contrast to and following closely the C_{org} pattern, the data is much greater than the values of 0.03% to 0.08% given by Muller (1977) for deep sea Pacific sediments.

All of the cores show a decline in N values with depth, which is greatest in the uppermost 10cm of the sediments (Figure 4.2). This may reflect the oxic breakdown and the preferential release of N from organic matter (Suess and Muller, 1980; Waples, 1985).

In a similar manner to C_{org}, the sediments from Loch Duich show a very large decrease in N content with depth especially towards the bottom of the core. Here there is an 87% fall in N values from 0.45% at the surface to 0.06% by 41cm, similar to that shown by C_{org}. The variation in N and C_{org} between the high values at the sediment surface and the low values in the consolidated clay may imply a biomixing event between the two sediments during sedimentation. The clay appears to dilute the sediment immediately above, but the influence becomes less with increasing burial leading to gradually increasing N and C_{org} values. CR1 displays a low N value (0.14%) at 6-7cm depth coresponding to the low C_{org} values seen at this position.

4.2.3. Solid Phase Sulphur.

Sulphur profiles of the sediments are shown in Figure 4.3. The S contents range from 0% at the surface of DN1 to 1.1% at depth in Loch Etive. The values found are consistant with other studies of the same area and elsewhere. Ridgway (1984) found S concentrations in Loch Etive of between 1.00% and 2.00% in the inner basin and 0.8% to 1.4% in Airds Bay. Kaplan *et al.* (1963) quote values of 0.20% to 1.00% from sediments of Southern California. Berner (1970), working in Long Island Sound found S concentrations of between 0.30% and 2.20% and similar values were found for the same are by Berner and Westrich (1985).

There is a large variation in the S profiles with depth but there are generally two different patterns of S distribution at depth in the cores examined. For instance, cores AB1, CM1 and CR1 display similar patterns of S build up. In these sediments S content of the uppermost sediment is very low, the greatest increase with respect to depth is seen in the top 15cm, with the maximum content occuring between about 8cm and 15cm which is likely to be occuring below the zone of biomixing (see Section 4.2.4). In AB1 the S tends with depth to continue to increase, but at a much reduced rate reaching a maximum concentration of 1.02% at 31cm depth. CR1 and CM1 however, display relatively constant values below 15cm.

The S profiles from cores SH1, SP1 and DN1 differ from the above sediments in displaying a much more gradual increase in S, from very low values at the sediment surface and attaining a maximum concentration in the deeper horizons of the sediment. These cores tend to have much lower S contents than cores AB1, CM1 and CR1. The lowest values can be seen in

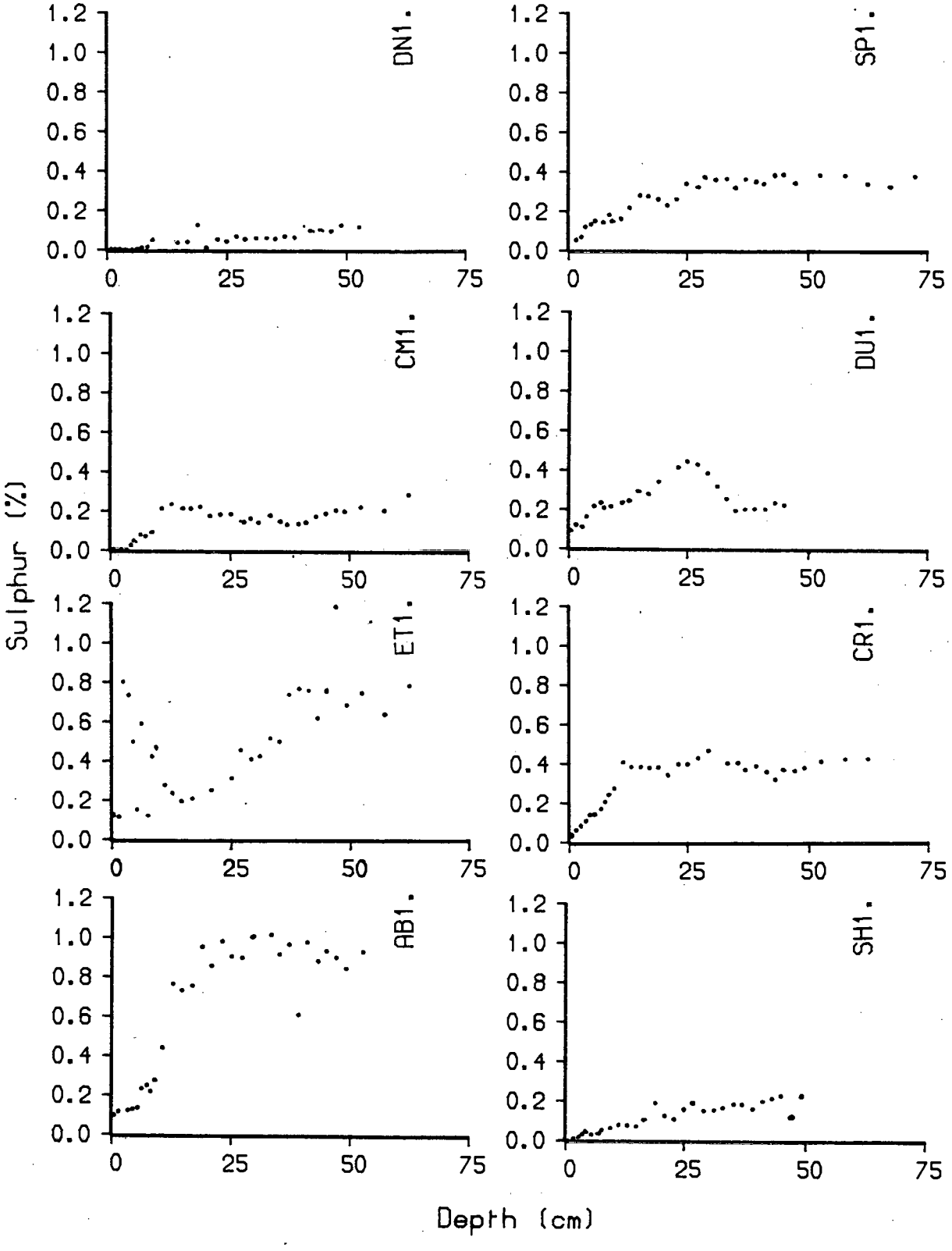

FIGURE 4.3: The patterns of solid phase S with depth in the sediments.

core DN1. There is no detectable S in the top 5cm of this sediment indicating a truly oxic surface. Below this there is a gradual increase to a maximum concentration of 0.12% at 49cm. SH1 and SP1 are similar to DN1 with gradual increases to maxima of 0.22% and 0.38% respectively at 45cm depth.

The S concentration in DU1 after increasing from 0.09% at the sediment surface to 0.45% at 25cm falls rapidly to a mean concentration of 0.21% by 35cm. These low values are coincident with the grey clay at the base of the core. The S distribution of core ET1 is exceptional in that very variable but occasionally very high S contents occur in the upper 10cm of the core and may be related to the overall reducing character of the sediments and the general lack of biomixing (Ridgway, 1984; see also Section 4.5). Below this zone, the S content increases to very high values (1.18%) and tends to follow the pattern seen in the outer parts of the loch (AB1).

4.2.4. Pore Water Sulphate and Alkalinity.

The distribution of S contents, see Figure 4.3 is almost certainly due to the presence of iron sulphide in the sediments. Certainly, pyrite has been identified in the sediments by X-Ray Diffraction and greigite has been noted in sediments from the outer basin of Loch Etive (Thompson, Pers. Comm.). The formation of these is invariably caused by the microbial reduction of sulphate to sulphide in an anoxic environment. For this reason, profiles of pore water SO_4^{2-} have been measured (see Appendix I, Sections 1 and 3.2 for the pore water extraction and analysis methods) to see if there is any relationship, direct or indirect between SO_4^{2-} and the S (Sulphide) content of the sediments.

The surface values of SO_4^{2-} range from 16.6mM in ET1 to 30.6mM in CM1. This is due to the variation in SO_4^{2-} concentration in the overlying waters caused by variations in salinity. In the upper section of all the cores, the SO_4^{2-} values tend to remain relatively constant and close to the SO_4^{2-} content of the overlying water. This zone of constant SO_4^{2-} can be equated with the biomixed layer in the sediments. The biomixing allows the replenishment of SO_4^{2-} from the overlying water to replace that utilised. At depth, the SO_4^{2-} concentration tends to decrease. The extent varies from core to core (see Figure 4.4). The mean surface values and the percentage loss of SO_4^{2-} from the sediments are summarised in Table 4.3. The most noticeable decrease in SO_4^{2-} with depth is seen in Loch Etive, which has the highest C_{org} content. Ambient values approximately that of bottom water are seen in the upper 10cm of cores ET1 and AB1, lower down there is a well defined decrease and at the bottom of ET1, SO_4^{2-} is almost exhausted. Similar values for Loch Etive have been noted by Malcolm (1981) and Ridgway (1984). Sediments from SP1 which have intermediate values of C_{org} also show noticeable SO_4^{2-} depletion in the deeper portion of the core. DU1 is anomalous in this respect. Although the upper sediments are carbon rich, there is no defined SO_4^{2-} reduction. The lack of this trend may be influenced by the occurence of old, possibly abiotic clays near the base. The remaining cores shown in Figure 4.4 show only a limited decrease in pore water SO_4^{2-} with depth. Overall, these trends can be compared with trends noted from similar sediments around the world (Berner, 1964; Sholkovitz, 1973; Goldhaber *et al*, 1977; Jorgensen, 1977; Martens *et al*, 1978; Aller, 1980; Goldhaber and Kaplan, 1980; Klump and Martens, 1987), from pelagic sediments (Toth and Lerman, 1977) and from salt marshes (Lord and Church, 1983; King *et al*, 1985). These are summarised in Table 4.3.

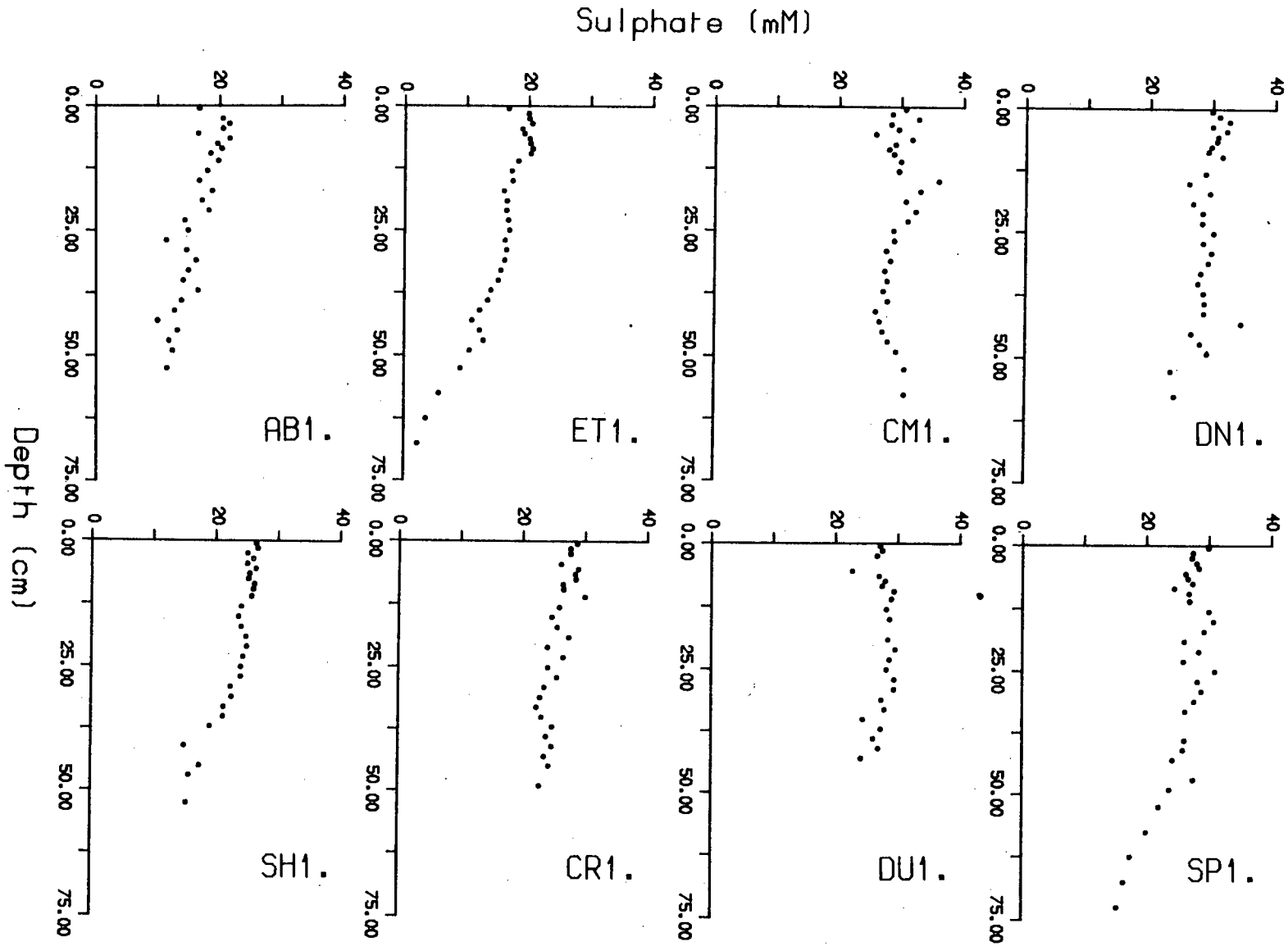

FIGURE 4.4: The patterns of SO_4 in the sediment pore waters.

Core	Surface SO_4 (mM)	%Fall	Depth Interval (cm)
AB1.	19.78	42.26	0-55
CM1.	29.94	0	0-50
CR1.	27.25	16.32	0-50
DN1.	30.93	22.19	0-60
DU1.	27.09	9.85	0-36*
ET1.	19.20	88.38	0-65
SH1.	26.43	58.15	0-55
SP1.	28.18	45.64	0-65

TABLE 4.3a: Surface SO_4 concentrations (mean of upper 5cm) and the percentage fall of SO_4 over the given depth interval.

* DU1 SO_4 fall measured to top of clay.

Location	Surface SO_4 (mM)	% Fall	Depth Interval (cm)	
LDuich	27.6	76.82	0-45	Krom (1976)
LEtive				
(inner)	23.90	95.39	0-65	Malcolm (1981)
(outer)	22.30	53.36	0-65	
LEtive				
(inner)	24.23	78.90	0-65	Ridgway (1984)
(outer)	19.77	--	--	
Long Island	19.5	68.6	0-70	Goldhaber
"FOAM" Site				*et al.*(1977)
LEil	~20	50	0-60	Malcolm *et al.*
				(1986)
Gulf of	27.00	40.7	0-50	Berner (1964)
California				
Cape Lookout	25.00	96.00	0-15	Martens & Klump
				(1984)

TABLE 4.3b: Surface SO_4 values and percent fall for studies in the same locality and worldwide.

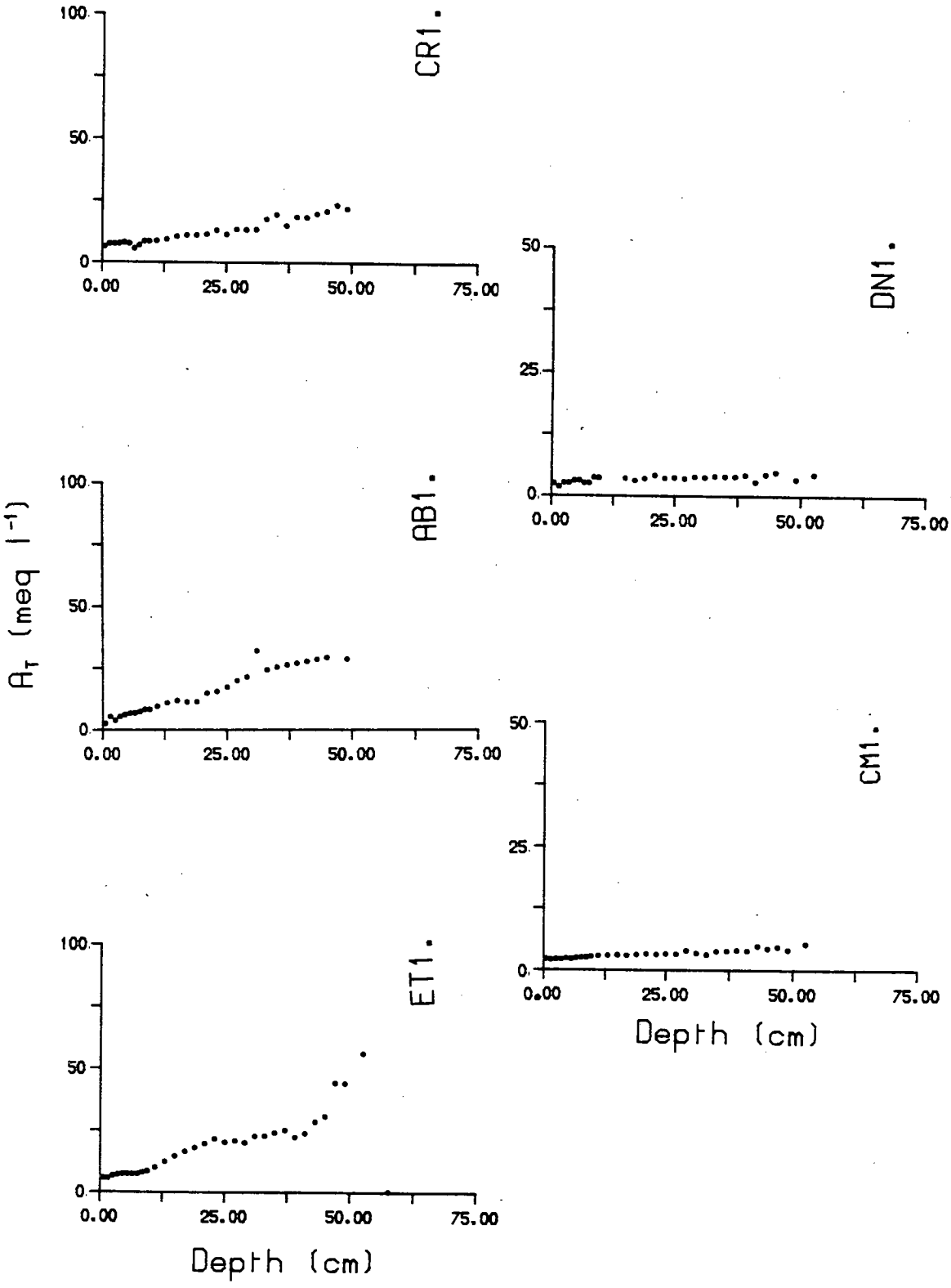

FIGURE 4.5: The patterns of titration alkalinity (A_T) in the sediment pore waters.

Core	A_T increase
ET1.	70.77
AB1.	21.99
CR1.	16.99
CM1.	6.6
DN1.	1.9

TABLE 4.4: Titration alkalinity increase with depth (meq l^{-1}). Increase taken from the mean value of the upper 5cm of the core to the value at the base of the core.

Core	C/N Ratio
ET1.	11.64
DU1.	11.79
CR1.	8.77
CM1.	8.56
SP1.	8.19
SH1.	8.19

TABLE 4.5: Surface C/N ratios (mean of upper 5cm of sediment).

The pattern of SO_4^{2-} change has often been associated with the change in alkalinity (A_T). This relationship will be discussed in Section 4.6. The method of A_T measurement is described in Appendix I, Section 3.1. The data is given in Appendix II, Table AII.6 and Figure 4.5

The titration alkalinity (A_T) concentration across the cores varies from less than 2 meq l^{-1} in the biomixed zone of DN1 to greater than 70 meq l^{-1} at depth in ET1. All the cores show similar surface concentrations of between 2 meq l^{-1} and 6 meq l^{-1}. With depth the cores fall into three distinct groups, based on A_T increase. These are summarised in Table 4.4. DN1 and CM1 show the lowest increase in alkalinity concentration (1.90 meq l^{-1} and 6.60 meq l^{-1} respectively); CR1 and AB1 form a middle group with increases of 16.99 meq l^{-1} and 21.99 meq l^{-1}; the maximum A_T increase occurs in ET1 (70.77 meq l^{-1}). In this core there is a considerable increase in alkalinity towards the base of the core. These concentrations are consistent with those observed in sediments from similar environments (Berner *et al*, 1970; Manheim, 1976; Davies, 1977; Goldhaber and Kaplan, 1980).

4.3. Organic Components and Lithology.

Local grain size variations controlling organic content have been noted by Hunt (1981) in Long Island Sound. In general coarser sediment would be expected to have a lower organic matter content, either through less organic input or by winnowing of the organic containing fine material by erosive currents. This can be seen in CR1 (Figure 4.6). The fall in C_{org} content to 1.2% between 6cm and 9cm corresponds with the coarse sediment of the shell band as identified by the Zr/Rb ratio. The N values show a similar fall at 5-9cm. The S profile shows only a slight deflation in its increase with depth

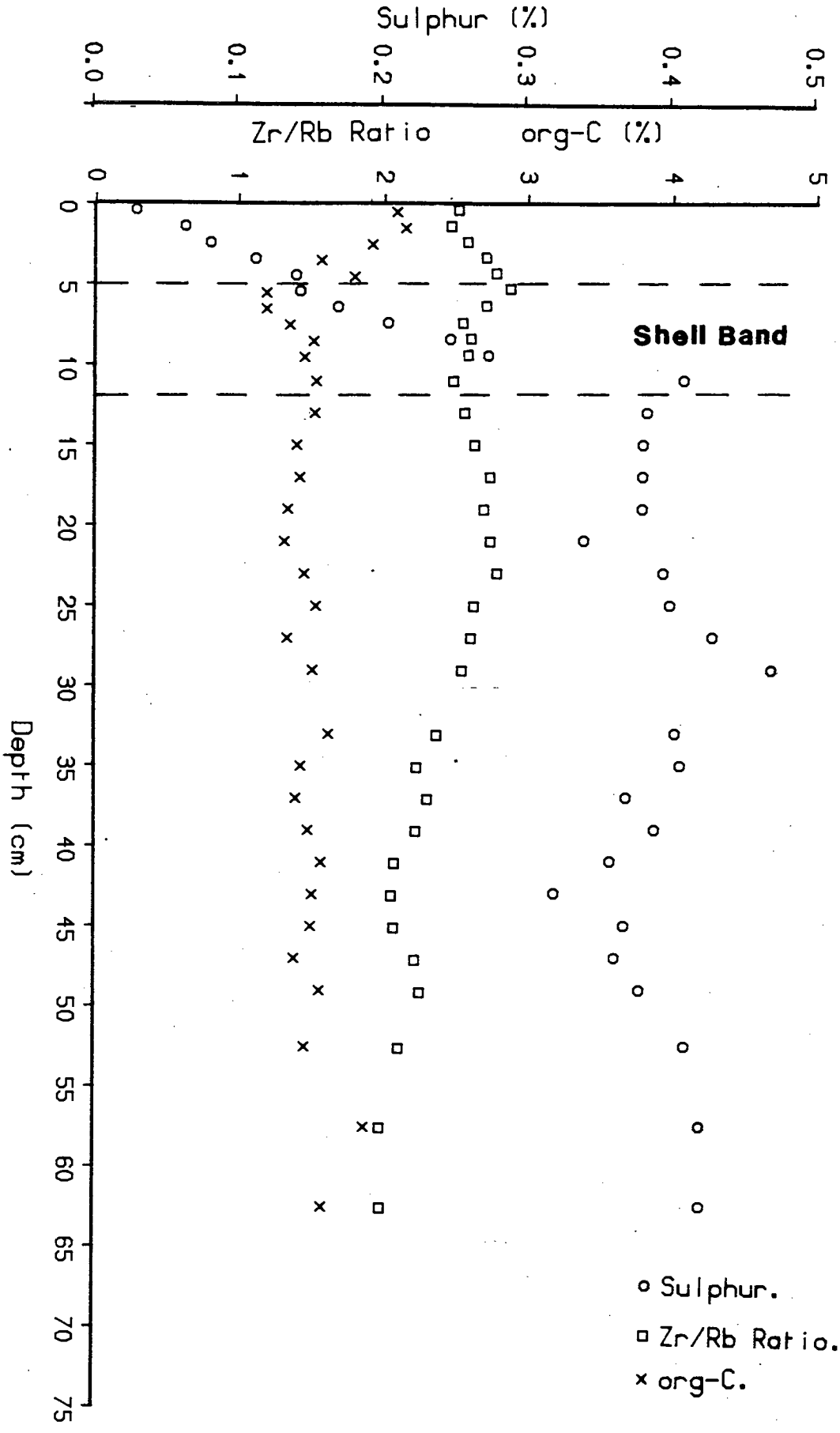

FIGURE 4.6: A comparison of S, C_{org} and Zr/Rb patterns in core CR1 to illustrate the variation in S and C_{org} Patterns in the coarser shell bands.

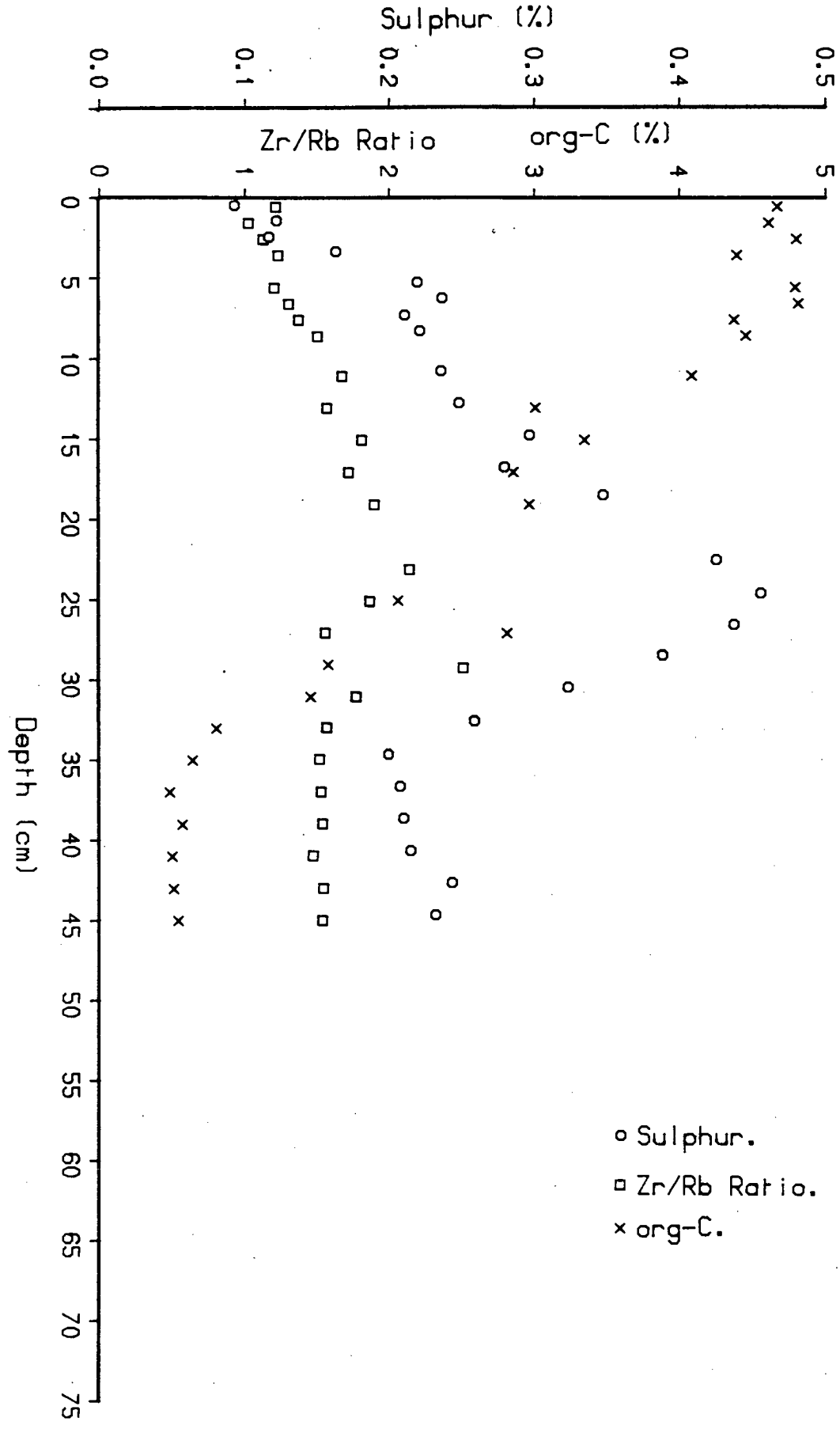

FIGURE 4.7: A comparison of S, C_{org} and Zr/Rb ratio patterns from core DU1 to show the variations in organic content between the upper and lower portions of the core as related to grain size.

at this band (4cm and 6cm). However, at the base of the shell band at 10-12cm, the S becomes near constant with depth at 0.4%. Such a pattern possibly indicates some disconformity in sediment accumulation below and above this shell band. In core DU1 (Figure 4.7), the S profile shows low surface values of S and below a linear increase with depth to 25cm. C_{org} in contrast, shows a well defined decrease over this interval and reaches constant values in the consolidated clay at its base. The pattern of C_{org} for the upper 25cm of the sediment is probably controlled by lithology as seen by its decrease in the coarser grained component as illustrated by the Zr/Rb ratio. The linear decrease in S, C_{org} and to a lesser extent Zr/Rb is probably indicative of biomixing of the old sediment between 25cm and 35cm.

4.4. C/N As An Indicator Of Organic Matter Provenance.

It has been noted that, in general, organic C/N values of marine organic material are lower than those of terrigenous organic matter (Redfield *et al.* 1963; Vaccaro, 1965; Bordovskiy, 1965; Muller, 1977). Thus, C/N ratios have commonly been used to characterise the nature of the organic matter in sediment (Bader, 1955; Bordovskiy, 1965; Pocklington and Leonard, 1979, Berner, 1979).

Redfield *et al.* (1963) summarised marine plankton as having a mean composition in the ratio of; $C_{106}\ N_{16}\ P_{1}$. This gives a C/N ratio for marine plankton of 6.6 (atomic), which has been used in the past as an indicator of marine organic matter. Terrestrial organic matter tends to be enriched in C relative to N and therefore has a higher C/N ratio. This is often greater than 12 (atomic), (Pocklington and Leonard, 1979).

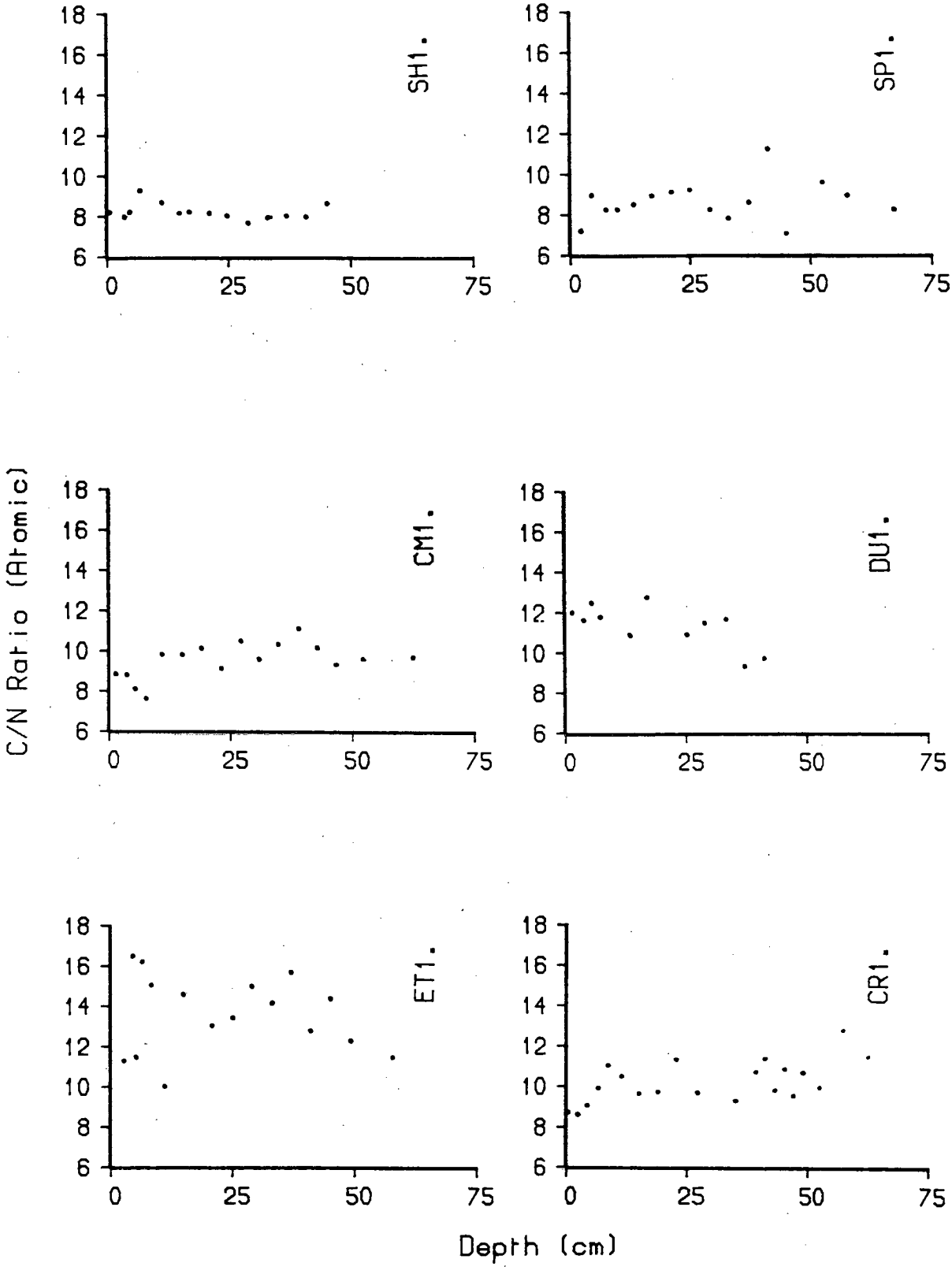

FIGURE 4.8: The patterns of C/N ratios in the sediments.

Table 4.5 shows the C/N atomic ratios of the surface sediments in the cores studied. The lowest ratio is seen in SH1 (8.19). This implies that this sediment has the greatest relative marine influence. The C/N ratios of cores CM1, CR1 and SP1 are slightly higher (8.56, 8.77 and 8.19 respectively), indicating perhaps some influence of terrestrial organic matter. Nevertheless all these values are relatively low and tend to suggest a dominance of marine organic matter in these sediments. This is commensurate with the location of these cores.

Considering the patterns of C/N ratios with depth in these sediments (Figure 4.8), the values tend to be slightly higher than at the surface and much higher than the predicted marine C/N value of 6.6. This suggests possibly a greater terrestrial conribution to the sediments in the past but will be discussed later.

In the fjordic environments such as cores ET1, AB1 and DU1, the surface values are considerably greater than the sediments from the less restricted areas. This implies a greater terrestrial influence in these sediments, which would be expected given the restricted fjordic location. At depth in core DU1, the C/N ratio falls to lower values closer to the cohesive clay in the lower section of the core. This may imply that the older clay is marine in origin.

Using Craib cores (Craib, 1965) collected from Loch Etive (Ridgway, 1984) (see Figure 4.9), a C/N profile along the loch was constructed. This can be seen in Figure 4.10. The head of the Loch (Sta. 1) shows very high C/N values (22). This would be expected from the location as this is likely to receive the greatest influence of terrestrial organic matter. There is a decline in C/N values towards the mouth of the loch, with the outer basin showing values of <14. This is still appreciably higher than the suggested true marine end

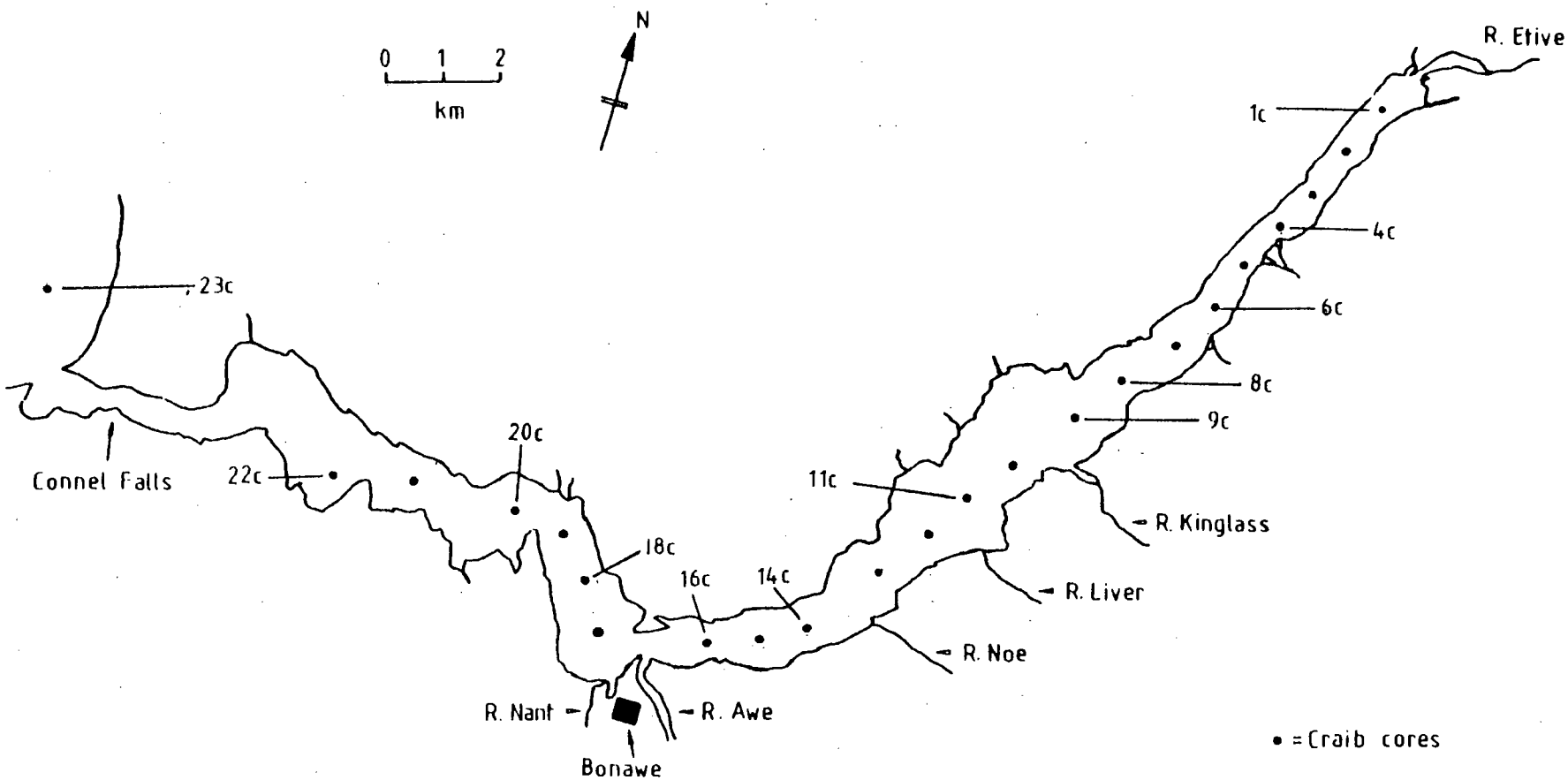

FIGURE 4.9: Craib core localities in Loch Etive. (After Ridgway, 1984).

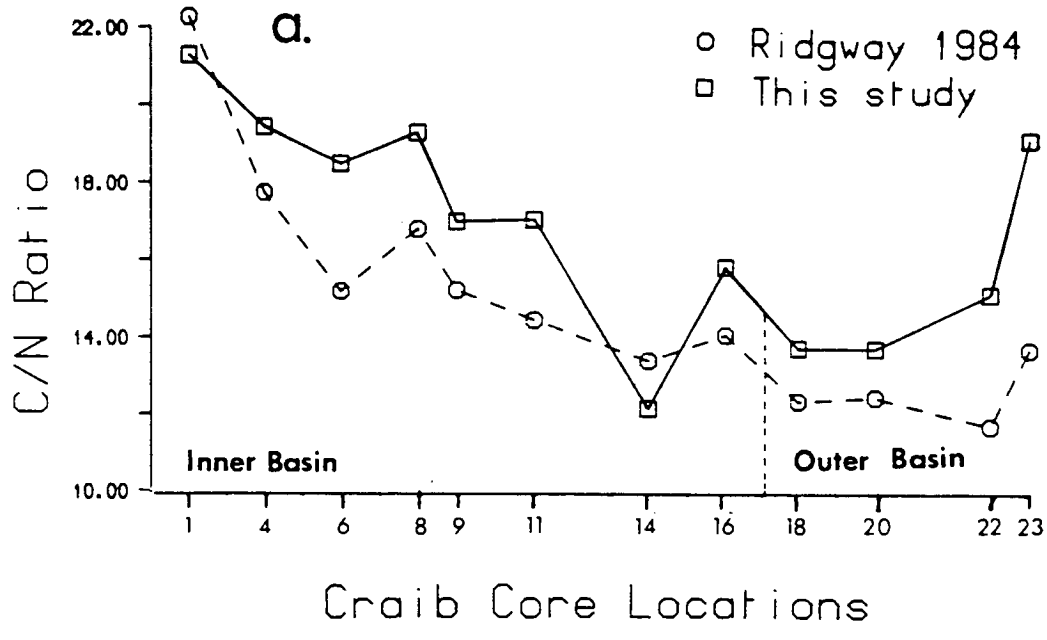

FIGURE 4.10: Longitudinal profiles of the surface C/N values down Loch Etive, comparing data from this study to that of Ridgway (1984).

member value of 6.6, implying that terrestrial influence is still important in the outer basin of Loch Etive. The C/N value in the Firth of Lorne tends to show an increase suggesting a greater terrestrial influence than in the outer basin. A possible explanation for this maybe that the sediments at this locality contain a large amount of terrestrial detritus carried as suspended material from Loch Etive.

However, using C/N ratios as an indicator of organic matter source has a number of drawbacks. Arrhenius (1952) suspected that clay minerals adsorbed a significant amount of NH_4^+. This has been suported by later studies such as Stevenson and Cheng (1972), Muller (1977) and Rosenfeld (1979(a)). Grundmanis and Murray (1982) showed that inorganic NH_4^+ could account for between 12% and 64% total N and that the higher values tended to be in the more oxidising sediments. This led Ridgway (1984) to suggest that the outer basin sediments could have a higher inorganic NH_4^+ content which could account for the lower C/N ratios. However, the clays in these sediments are relatively weathered and unreactive (Price, Pers. Comm.) and therefore there is unlikely to be any uptake of NH_4^+.

Degens and Mopper (1976) noted that the carbohydrate composition of plankton is very variable and a range of C/N values from 5.9 to 9.1 is possible in marine plankton. Thus there may be considerable overlap in the C/N signatures of marine and terrestrial organic material.

In the oceans much of the organic material produced never reaches the sediment as it is broken down in the water column (Ittekot, 1987). It is likely that any marine organic matter reaching the sediment surface will not have a marine C/N signature of 6.6, but will be slightly higher due to organic degradation and the preferential loss of N in the water column. This may

explain why the surface C/N ratios in CM1, SP1 and SH1 which are thought to be dominantly marine in character have values which are greater than 6.6. With depth (see Figure 4.8) other problems occur. During organic breakdown, N is known to be more labile than C. (Rittenberg *et al*, 1955; Muller, 1977; Berner, 1979; Suess and Muller, 1980). This leads to a gradual increase in the C/N ratio with depth and is well illustrated by CR1 and CM1. Both cores show an increase in values in the top 10cm due to organic matter breakdown and the preferential release of N.

To summarise, it is clear from the C/N profile down Loch Etive that C/N ratios are indicative of marine and terrestrial organic matter. However, in sediments with both terrestrial and marine input it is difficult to determine the relative importance of the two components due to the variablitiy of the planktonic ratios and the possibility of prior degradation of the organic matter. At depth in the sediments the increased lability of N over C makes C/N ratios invalid as an organic source indicator.

4.5. Organic Matter Diagenesis.

In organic rich sediments the breakdown of organic matter is brought about by bacterial action. Degradation occurs by way of a number of well documented reactions utilising a characteristic series of oxidants, i.e. O_2, MnO, NO_3, FeO, SO_4^{2-}, CO_2 (Stumm and Morgan, 1970) from which bacteria can gain free energy. The oxidant producing the greatest free energy change (ΔG^o) will dominate. The reactions are summarised in Table 4.6. In anoxic sediments, the low concentrations of the energetically more favoured electron acceptors results in the most dominant reaction being that of SO_4^{2-} reduction (Berner, 1970; Davies, 1977). C_{org} is degraded by a number individual processes

Aerobic Respiration

$$(CH_2O)_{106}(NH_3)_{16}(H_3PO_4) + 138\ O_2 \rightarrow 106\ CO_2 + 16\ HNO_3 + H_3PO_4 + 122\ H_2O$$

$$\Delta G^\circ = -3190\ KJ\ mole^{-1}\ of\ glucose$$

Manganese Reduction

$$(CH_2O)_{106}(NH_3)_{16}(H_3PO_4) + 236\ MnO_2 + 472\ H^+ \rightarrow$$

$$236\ Mn^{2+} + 106\ CO_2 + N_2 + H_3PO_4 + 366\ H_2O$$

$\Delta G^\circ = -3090\ KJmole^{-1}$ Birnessite

$-3050\ KJmole^{-1}$ Nsutite

$-2920\ KJmole^{-1}$ Pyrolusite

Denitrification

$$(CH_2O)_{106}(NH_3)_{16}(H_3PO_4) + 94.4\ HNO_3 \rightarrow 106\ CO_2 + 55.2\ N_2 + H_3PO_4 + 177.2\ H_2O$$

$$(CH_2O)_{106}(NH_3)_{16}(H_3PO_4) + HNO_3 \rightarrow 106\ CO_2 + 42.2\ N_2 + 16\ NH_3 + H_3PO_4 + 148.4\ H_2O$$

$$\Delta G^\circ = -3030\ KJmole^{-1}$$

Iron Reduction

$$(CH_2O)_{106}(NH_3)_{16}(H_3PO_4) + 212\ Fe_2O_3 (or\ 424\ FeOOH) + 848\ H^+ \rightarrow$$

$$4\ 24\ Fe^{2+} + 106\ CO_2 + 16\ NH_3 + H_3PO_4 + 530\ H_2O\ (or\ 74Z\ H_2O)$$

$\Delta G^\circ = -1410\ KJmole^{-1}$ Heamatite

$-2750\ KJmole^{-1}$

$-1330\ KJmole^{-1}$ Limonitic Goethite

Sulphate Reduction

$$(CH_2O)_{106}(NH_3)_{16}(H_3PO_4) + 53\ SO_4^{2-} \rightarrow 106\ CO_2 + 16\ NH_3 + 53\ S^{2-} + H_3PO_4 + 106\ H_2O$$

$$\Delta G^\circ = -380\ KJmole^{-1}$$

Methanogenesis

$$(CH_2O)_{106}(NH_3)_{16}(H_3PO_4) \rightarrow 53CO_2 + 53\ CH_4 + 16\ NH_3 + H_3PO_4$$

$$\Delta G^\circ = -350\ KJmole^{-1}$$

TABLE 4.6

Summary of the chemical reactions by which organic matter is broken down in sediments after Shimmield (1984) (adapted from Froelich *et al*, 1979). The Gibbs free energy changes are calculated at standard conditions and pH 7 and expressed in mM of glucose. The energy gained from the reactions becomes less in the order O_2, MnO, NO_3, FeO, SO_4.

involving the breakdown of biopolymeric organic matter into simple organic molecules by fermentative micro-organisms and the utilisation of these molecules by the SO_4^{2-} reducing bacteria (discussed by Jorgensen, 1982). The equation given in Table 4.6 can be summarised as:

$$2CH_2O + SO_4^{2-2-} \text{ --> } H_2S + 2HCO_3^- \qquad (4.1)$$

2 moles + 1 moles --> 1 mole + 2 moles

The H_2S is precipitated with iron as Fe-monosulphides, Fe-disulphides (pyrite) (Berner, 1970; Pyzic and Sommer, 1981; Berner, 1984; Morse *et al*, 1987).

In general, most sediments with overlying oxic waters have a zone of biomixing due to the action of macro infauna. This zone has been identified by constant SO_4^{2-} values with depth, the concentration being close to that of overlying bottom water. In most of the cores examined biomixing as seen from SO_4^{2-} and A_T values does not occur at depths greater than 10cm. In the past workers have assumed that all of the SO_4^{2-} reduction occured below the aerobic bioturbated zone (eg Berner, 1970; Nissenbaum *et al*, 1972; Sholkovitz, 1973; Sayles and Mannheim, 1975; Krom and Sholkovitz, 1977; Davies, 1977; Martens *et al*, 1978). However, the sediments in this study can show solid phase S precipitating and A_T increasing close to the surface in the biomixed zone, for example in DU1, AB1 and ET1.

Sulphur precipitation indicates SO_4^{2-} reduction must be occuring in these surface horizons although this is not usually indicated by a decrease in pore water SO_4^{2-}. In order to try to explain this, a number of hypothetical situations will be considered.

Figure 4.11(a) illustrates a hypothetical anoxic sediment in which there is no bioturbation in the surface sediment. In this case the S would increase, with the rate of increase falling with depth as the amount of available SO_4^{2-} was used (in the absence of SO_4^{2-} diffusion from the overlying water). Comparison of the SO_4^{2-} values to those of the S being produced would show a 1:1 stoichiometric relationship derived from equation 4.1. This situation clearly does not occur. In these sediments SO_4^{2-} values are relatively constant in the uppermost 10cm of the sediment indicating a zone of biomixing.

If no SO_4^{2-} reduction was occuring in the biomixed region the S profile would approximate to Figure 4.11(b), with no SO_4^{2-} reduction occuring in the biomixed zone and below a build up of S commensurate with the decline of pore water SO_4^{2-}. A third scenario is shown in Figure 4.11(c), which is more realistic and shows the pattern of S contents and SO_4^{2-} depletion as seen in the sediments. Here it is envisaged that SO_4^{2-} reduction does occur in the biomixed zone indicated by S precipitation in the surficial layers. In contrast to Figure 4.11(b), however, SO_4^{2-} profiles show bottom water values well below the zone of active biomixing, implying an addition of SO_4^{2-} to the deeper sediments from the overlying water. This can be achieved by biological irrigation (as opposed to mechanical bioturbation), ionic diffusion, or a combination of both. The importance of irrigation by burrows has been recognised by Goldhaber *et al.* (1977), Rosenfeld (1979(b)), Aller (1980) and

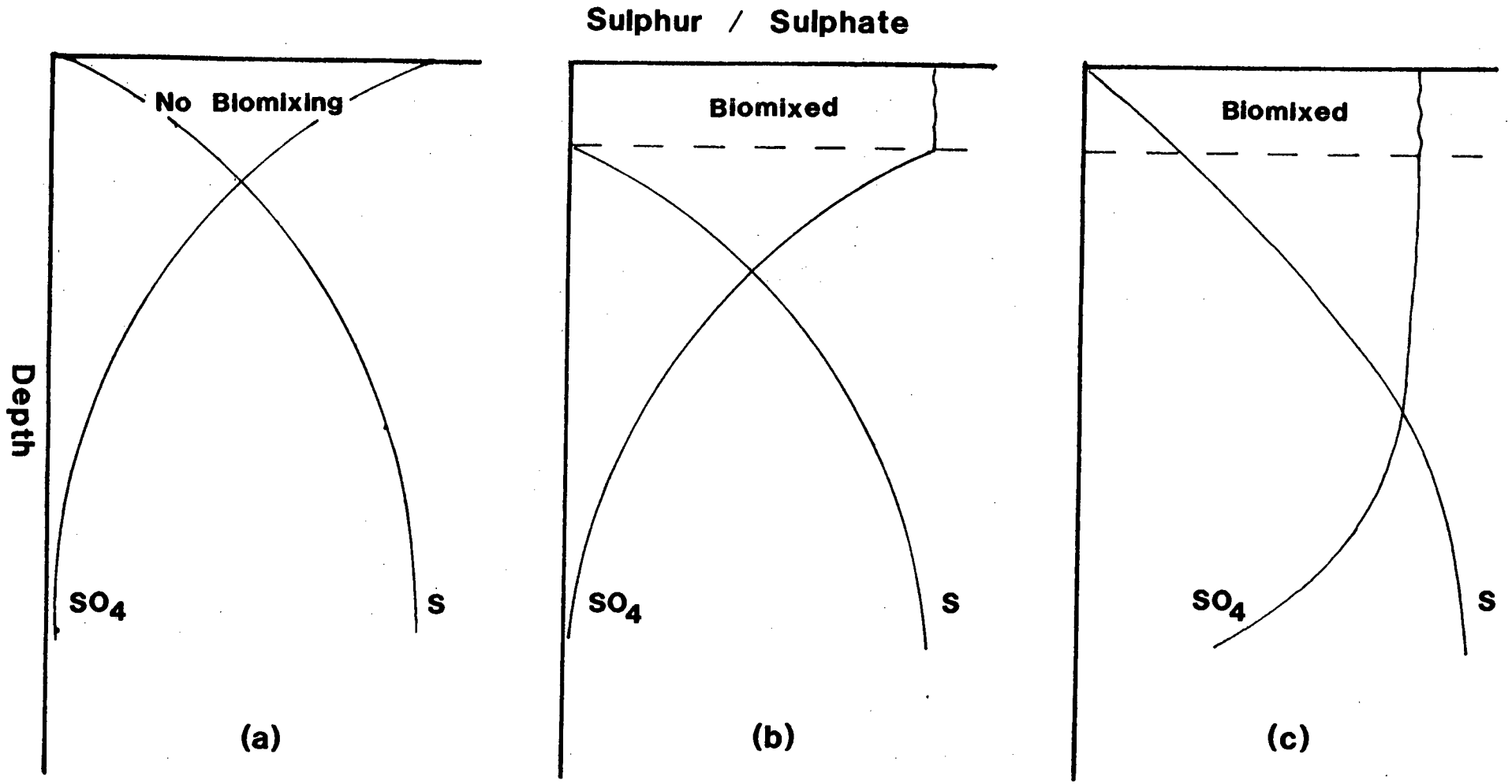

FIGURE 4.11: Hypothetical sediments to illustrate the effect of biomixing on S and pore water SO_4 patterns.

Berner and Westrich (1985). Diffusion rates are difficult to measure in a sediment as the variables involved are hard to quantify. Krom and Berner (1980) from experimental work calculated a diffusion coefficient (D_s) for SO_4^{2-} as 5 x 10^{-6} cm^2s^{-1}. Applying this to Ficks First Law of diffusion (Berner, 1980), the diffusive flux of SO_4^{2-} can be calculated from equation 4.2.

$$J_s = -\Phi D_s . \partial C/\partial X \qquad (4.2)$$

Where:

J_s = Diffusive Flux (mM(mg)cm^{-2})

Φ = Porosity

∂C = Concentration change (mM or mg)

∂X = Depth increment (cm)

The amount of SO_4^{2-} flux through a sediment over a given time can then be calculated from the sedimentation rate (ω) (see Chapter 8). The SO_4^{2-} diffusive fluxes for cores ET1, AB1, and DN1 are summarised in Table 4.7 along with the S inventories. It can be seen from the data that the calculated fluxes of SO_4^{2-} over a fixed 20yr period are sufficient to produce the amount of S in the sediments as seen in the inventories. However, there are a number of problems which must be considered. The assumptions made in the calculation are that;

(a) All of the SO_4^{2-} is utilised in SO_4^{2-} reduction.

Core	SO_4 Flux $mgcm^{-1}$	S Inventory
AB1	44.30	32.32
DN1	14.63	3.04
ET1	16.89	9.06

Table 4.7: Diffusive fluxes of SO_4 and S inventories over a constant 20 yr period.

1).The depth interval is variable, but equates to a constant time period of 20 yrs calculated using sedimentation rates from Chapter 8 and Ridgway (1984)

2).Inventories were calculated from:

$$I = (1-\phi)\rho.EM_i.z$$

Where:

ϕ = porosity

ρ = Density (2.65 gcm^{-3} after Berner (1980))

z = depth (cm)

EM_i = Element gain

(b) SO_4^{2-} reduction proceeds at a constant rate over the whole depth increment being measured.

(c) No SO_4^{2-} reduction occurs in the biomixed zone.

Assumption (a) is reasonable given that SO_4^{2-} reduction is the dominant process in coastal sediments. But assumption (b) may not be true. If the rate of SO_4^{2-} reduction reaches a maximum at a certain depth in the sediment, then calculating the SO_4^{2-} flux over the whole depth increment will lead to an overestimate of the diffusive flux. Furthermore, it is invalid to assume that SO_4^{2-} reduction does not occur in the biomixed zone (assumption c). The locus of SO_4^{2-} reduction will be discussed later.

The conclusion that can be drawn from this is that SO_4^{2-} is introduced to the sediment at depth by both ionic diffusion and irrigation. The contribution of ionic diffusion is difficult to assess, but it is likely that the more dominant mechanism is biological irrigation of the sediment. Goldhaber *et al.* (1977) suggests that vertical transport of pore water SO_4^{2-} by irrigation can be five times greater than by ionic diffusion.

The conditions described in Figure 4.11(b) and (c) can be applied to West Coast sediments. Cores representing Dunstaffnage (DN1) and possibly Camas an Thais (CM1), closely follow the model described in Figure 4.11(b), where S in the surface 10cm is low or lacking, below there is a gradual but limited increase in S precipitation. In these sediments it is difficult to observe the position of SO_4^{2-} depletion due possibly to the irregularity of the SO_4^{2-} analyses. Cores SH1, SP1, ET1 and AB1 show the patterns of S and pore water SO_4^{2-} as seen in Figure 4.11(c). In these sediments, the S profiles show evidence of sulphide in the surface sediments which builds up at depth. SO_4^{2-}

profiles tend to show bottom water concentrations to depths below that assumed for biomixing. For instance; SO_4^{2-} remains at bottom water values to a depth of 20cm in SH1, 30cm in SP1 and 25cm in ET1 implying irrigation of the sediment to at least these depths. In the inner basin of Loch Etive, Ridgway (1984) noted worms down to a depth of 40cm. These were identified by Pearson (Pers. Comm. to Ridgway) as *Spirochaetopterus typicus*. In the outer basin, Ridgway (*ibid.*) saw burrows down to over 40cm and worms of the species *Capitella capitata* and *Nephys hombergi*. Burrows were noted in all of the sediments from this study, continuing to a depth of 30-40cm. In core SH1, an unidentified worm was observed at 20cm along with a colour change from grey-brown to grey. The importance of burrows in irrigation was discussed earlier and has been emphasised by Goldhaber *et al.* (1977); Rosenfeld (1979 (b)), Aller (1980) and Berner and Westrich (1985).

The introduction of pore water SO_4^{2-} at depth in the sediment suggests that the pore water SO_4^{2-} profile does not reflect the true rate of SO_4^{2-} reduction occuring in the sediments. Using an ^{35}S radiotracer technique, Berner and Westrich (1985) and Parkes (Pers. Comm.) were able to measure the rate of SO_4^{2-} reduction independent of pore water SO_4^{2-}. Both have found SO_4^{2-} reduction occuring in the biomixed zone (see Figure 4.12). Berner and Westrich (1985) and Parks (Pers. Comm.) disagree on the position of maximum SO_4^{2-} activity. Berner and Westrich (*ibid.*) working at the "FOAM" site in Long Island Sound (Goldhaber *et al.* 1977) found the maximum SO_4^{2-} activity to be at the base of the biomixed layer and declining slowly with depth, see Figure 4.12(a). Parks suggests different patterns at different localities. He found very high levels of SO_4^{2-} activity in the biomixed zone, below which the activity of SO_4^{2-} reducers rapidly declines with depth, Figure 4.12(b). This is supported by Malcolm *et al.* (1986) with data from Loch Eil. The differences may be

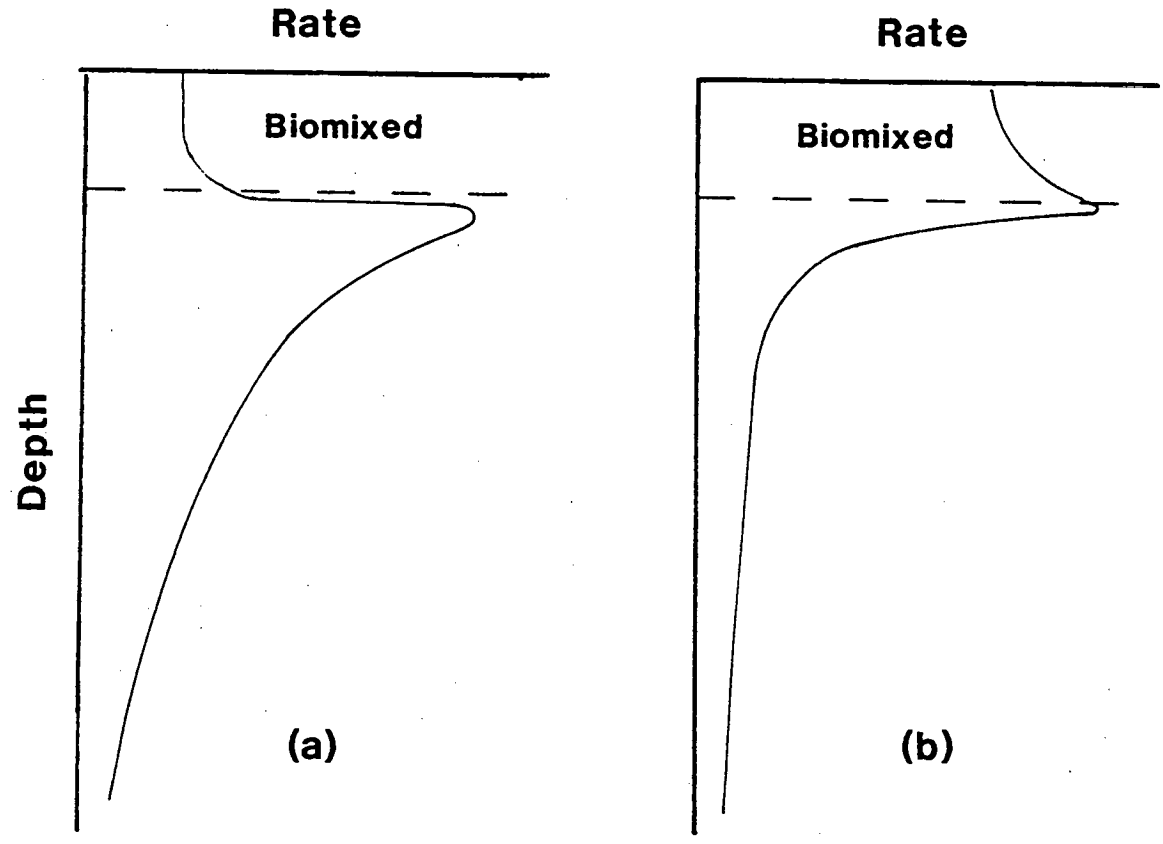

FIGURE 4.12: Representative SO_4 reduction rate profiles as calculated from ^{35}S. (a) Berner and Westrich (1985).

(b) Parkes (Personal Communication.)

explained as the result of variations in the degree of biomixing in the sediments, which is dependent to some degree on the quality of the organic C entering the sediments. This is best explained by envisaging two scenarios; (a) a sediment with an input of reactive marine carbon and (b) a sediment with an input dominated by relatively unreactive terrestrial material.

(a) In a sediment dominated by marine organic matter, the quality of the C_{org} will tend to lead to a high coefficient of bioturbation. Even though the biomixed zone is dominantly oxic, the activity of the SO_4^{2-} reducers is high and much of the organic matter will be consumed close to the surface, both by oxic breakdown and by SO_4^{2-} reduction. The overall oxic nature of the biomixed zone means that the products of SO_4^{2-} reduction (H_2S and sulphides, see Table 4.6) are short lived and tend to be reoxidised, the monosulphides to Fe_2O_3 and the H_2S partly to water and elemental S (S^o) and partly back to SO_4^{2-}. Thus much of the SO_4^{2-} reduction products are not incorporated at depth in the sediment. Such a system can be likened to the model proposed by Parkes (Pers. Comm.) (see Figure 4.12(b)).

(b) In sediments dominated by a high input of terrestrial organic mater, the benthic fauna are less able to utilise the unreactive material and the coefficient of biomixing will tend to be low. Similarly, the rate of SO_4^{2-} reduction will be slower as the time taken to metabolise the unreactive material is longer. SO_4^{2-} reduction will still occur in the biomixed zone, but this is reduced relative to scenario (a). Consequently, the maximum activity of the SO_4^{2-} reducers occurs just below the biomixed zone and activity continues at depth. In this scenario, the products of SO_4^{2-} reduction will have less of a tendancy to be reoxidised and will be incorporated at depth.

This pattern of SO_4^{2-} reduction can be likened to the model proposed by Berner and Westrich (1985) (see Figure 4.12(a)).

These models of SO_4^{2-} reduction can possibly be applied to the West Coast sediments. The sediments from cores CM1, SH1 and SP1 have relatively low C/N ratios as compared to the sediments from core ET1 and possibly the upper sediment of DU1. Given the limitations of C/N, the indication of a greater marine influence would suggest a high degree of biomixing. The amount of S seen in these sediments is much lower and the pattern of S build up is different to that shown in cores ET1 and DU1. The S values remain low or near zero in the biomixed zone, increasing rapidly to a maximum at 14cm in CM1, 20cm in SH1 and 28cm in SP1. This suggests that these sediments conform to the model proposed by Parkes (Pers. Comm.). In these sediments it can be inferred that much of the SO_4^{2-} reduction is not observed as the reduction products are lost.

Conversely, in cores ET1 and possibly DU1 the C/N patterns suggest a greater terrestrial influence. In the inner basin of Loch Etive, the macrofauna is known to be restricted (Pearson, Pers. Comm.) and consequently biomixing will also be restricted. The patterns of S increase in ET1 show very high values at or close to the sediment surface increasing to high concentrations (1.18%) at depth. A similar pattern is seen in DU1, but the S content is not as great. Below the zone of biomixing the pattern of S build up may conform to the pattern of SO_4^{2-} reduction proposed by Berner and Westrich (1985). However, this does not explain the high values seen in the biomixed zone of core ET1. It is possible that the models proposed by Berner and Westrich (*ibid*) and Parkes (*ibid*) may be modified by sedimentation rate. In sediments with a low sedimentation rate any organic material will remain at or close to

the sediment surface over a period of time. Thus much of the degradation products will be lost. In sediments with a high rate of sedimentaion the organic matter will be rapidly buried allowing degradation to occur in the subsurface sediments of the biomixed zone. In Loch Etive the sedimentation rate has been suggested to be high relative to the sediments outside the loch (Chapter 8 and Ridgway, 1984). It is possible that the burial rate of organic matter may account for the degree of S production in the biomixed layer.

4.6. The Relationship Of Pore Water Sulphate To Alkalinity.

The pattern of SO_4^{2-} change in pore waters has been associated with the change in A_T (Sholkovitz, 1973; Goldhaber and Kaplan, 1974). This can be summarised in equation 4.3.

$$\Delta A_T = 2\Delta SO_4^{2-} + \Delta NH_4^{+} - \Delta 2Ca^{2+} \qquad (4.3)$$

Given that in anoxic sediments, the most dominant process of organic breakdown is SO_4^{2-} reduction (Berner, 1970), then the greatest contribution to the right hand side of equation (4.3) is $2\Delta SO_4^{2-}$. This gives a stoichiometric relationship between alkalinity and SO_4^{2-} as very nearly 1:2. Comparison of the West Coast cores to the A_T : SO_4^{-2} model (Figure 4.13) shows that only AB1 conforms to the 1:2 stoichiometric relationship. Cores DN1, CM1 and CR1 show a greater loss of SO_4^{2-} than A_T build up. Conversely, in core ET1 the sediments show a greater build up of A_T than loss of SO_4^{2-}. Below 40cm, this the ratio is in the region of 4:1.

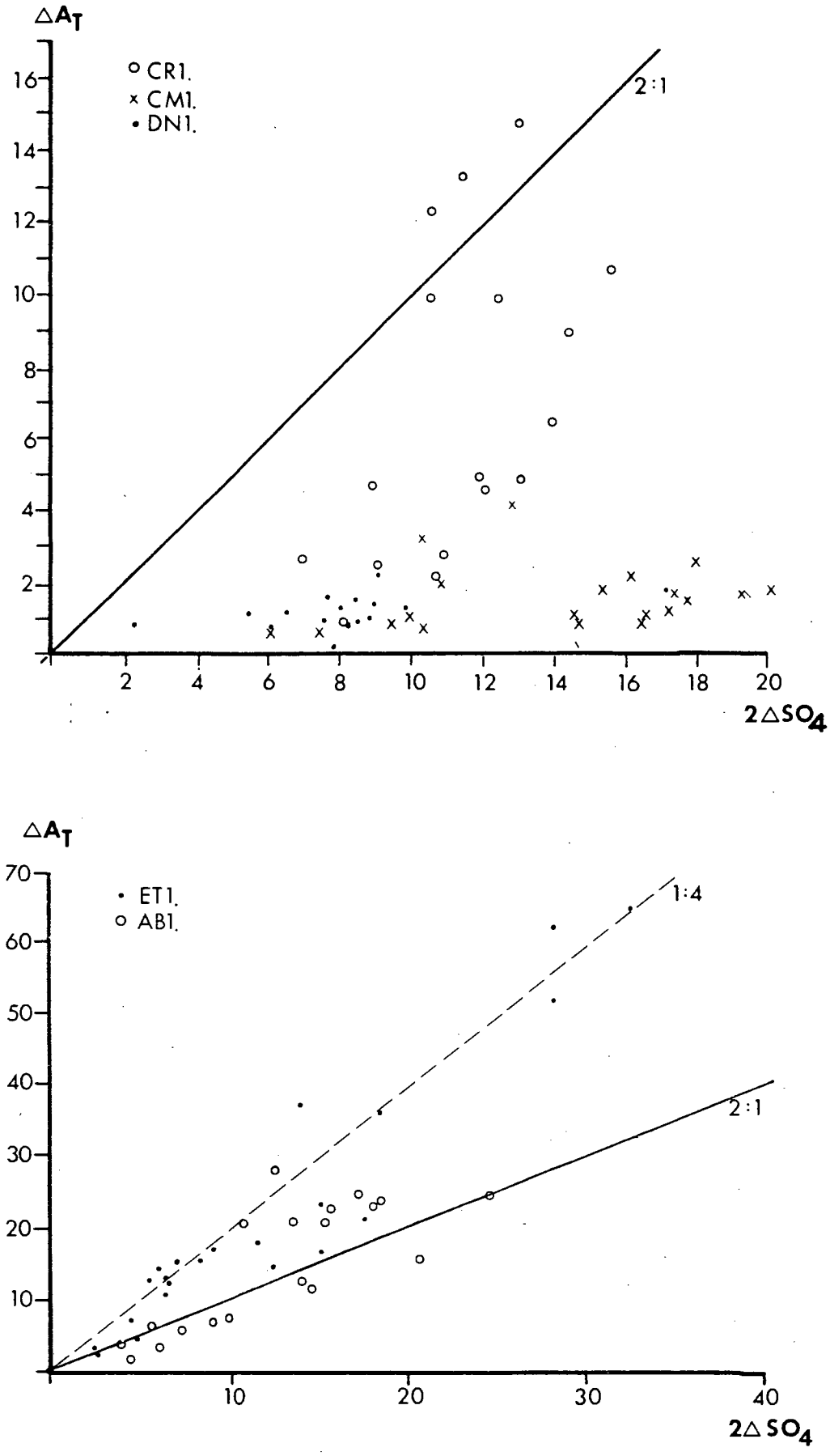

FIGURE 4.13: Plots of $2\Delta SO_4$ against ΔA_T for the sediment cores

Solid line marks the 2:1 SO_4 : A_T stoichiometric relationship.

These variations may be associated with biomixing and the formation of pyrite (Davies, 1977). Sholkovitz (1973) suggested that pyrite can be produced directly from SO_4^{2-} reduction by the reaction given in equation 4.4.

$$6(CH_2O)_c(NH_3)_n(H_3PO_4)_p + 3SO_4^{2-} + 2HFeO_2$$

$$\text{-->}$$

$$6HCO_3 + 6NH_3 + 6H_3PO_4 + FeS_2 + 4H_2O \qquad (4.4)$$

This equation is essentially similar to that given in Table 4.6 but includes an iron component and no attempt is made to estimate the composition of organic matter. Precipitating pyrite by this reaction involves no changes in A_T. Pyrite can also be formed via intermediate meta-stable iron sulphides (e.g. Greigite Fe_3S_4 and Macinawite FeS) in the presence of elemental S (S^o) by the reactions;

$$FeS + S^o \text{ --> } FeS_2 \qquad (4.5)$$

$$Fe_3S_4 + S^\circ \dashrightarrow 3FeS_2$$

(4.6)

Again, these reactions will not affect the A_T of the pore waters. However, Goldhaber (1974; cited Davies, 1977) suggests that pyrite can form in the presence of S° from iron dissolved in pore waters. These reactions (4.7 and 4.8) will decrease alkalinity.

$$4Fe^{3+}+9CH_2O+2H_2O+4SO_4^{2-}+S^\circ \dashrightarrow FeS_2+9HCO_3^-+13H^+$$

(4.7)

1 unit SO_4^{2-} consumed --> 1 unit of A_T consumed

1 unit SO_4^{2-} consumed --> 1 unit of A_T consumed

$$2Fe^{3+}+2CH_2O+2H_2S+SO_4^{2-}+S^\circ \dashrightarrow 2FeS_2+2HCO_3^-+H^+$$

(4.8)

1 unit of SO_4^{2-} consumed --> 4 units of A_T consumed

note that there is much more pyrite in sediments than monosulphides and therefore extra S° is needed in order to convert the monosulphides to pyrite via equations 4.5 and 4.6. Much of this is formed close to the sediment surface from the oxidation of H_2S via reaction 4.9.

$$2H_2S + O_2 \dashrightarrow 2H_2O + 2S^{\circ} \qquad (4.9)$$

To some extent, the amount of S° produced will be dependent upon bioturbation. Two models can be envisaged. Both models involve the precipitation of pyrite and monosulphides via SO_4^{2-} reduction in the biomixed layer, but address the effect of biomixing on the type of sulphide formed. These are summarised in Figure 4.14.

(a) In a sediment with a high coefficient of biomixing (Figure 4.14(a)), the overall oxic condition of the sediment allows any H_2S formed, in the presence of excess O_2 to oxidise to SO_4^{2-} and with more restricted O_2 to S° (see equation 4.9). The presence of S° will transform any meta-stable iron sulphides to pyrite and will also allow the precipitation of pyrite from pore water iron via the reactions summarised in equations 4.7 and 4.8. This will have the effect of reducing the A_T relative to the SO_4^{2-} present (Davies, 1977).

(b) In a sediment with restricted biomixing H_2S will not be as likely to be reoxidised (Figure 4.14(b)). Thus, H_2S will react with any iron present to form monosulphides (Goldhaber and Kaplan, 1974), see equations 4.10 and 4.11.

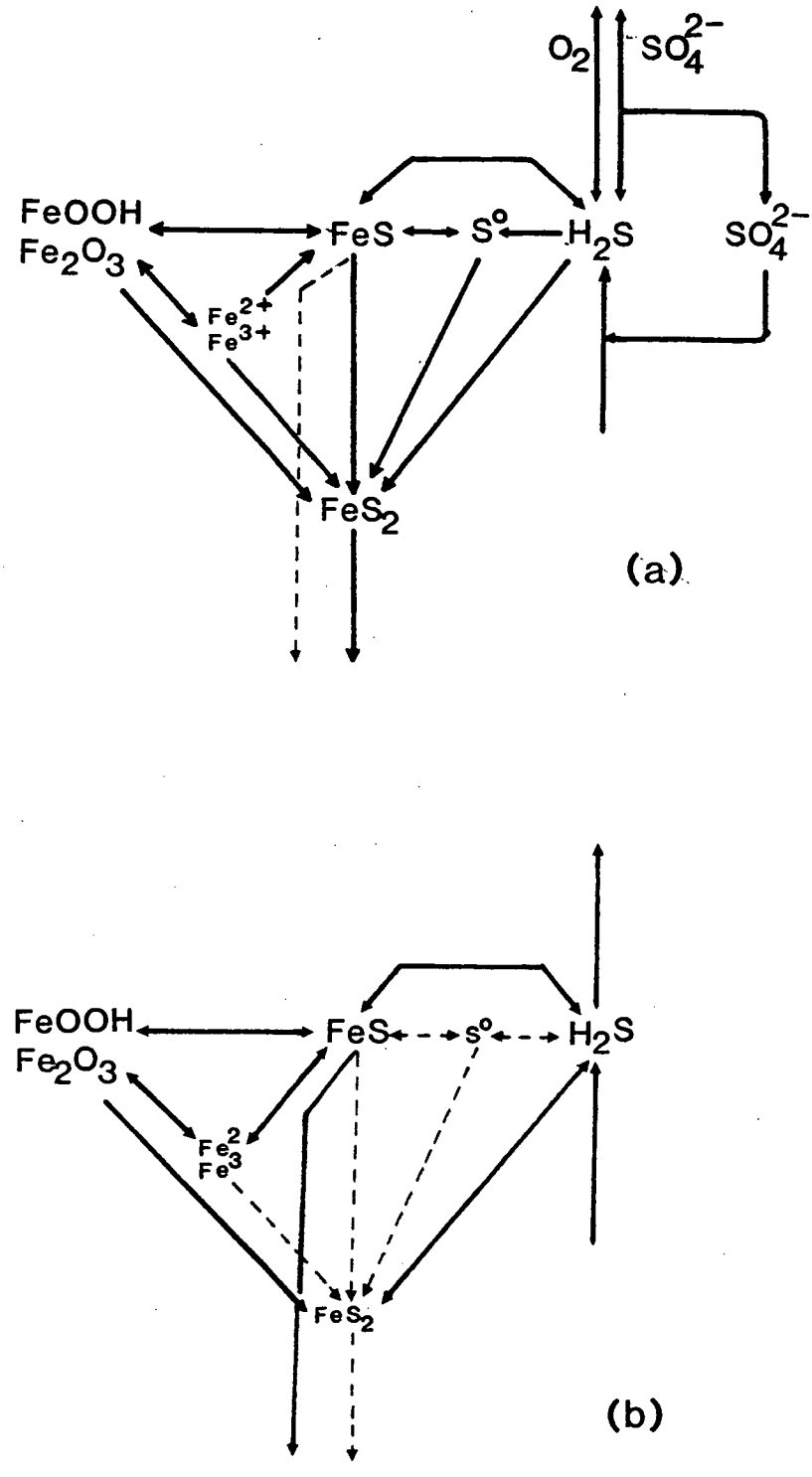

FIGURE 4.14: Summary of the chemical pathways involved in pyrite formation. Major pathways shown in solid lines, minor pathways dotted. (a) corresponds to a poorly biomixed sediment. (b) corresponds to a sediment with a high degree of biomixing.

$$2FeOOH + 3H_2S_{aq} \rightarrow FeS + FeS_2 + 4H_2O \quad (4.10)$$

$$2FeOOH + 3HS^- \rightarrow 2FeS + S^\circ + 3OH^- + H_2O \quad (4.11)$$

Both pyrite and S° will be formed, but the S° is restricted relative to model (a). In the absence of excess S°, the monosulphides will persist and little pyrite will be produced close to the sediment surface. Similarly, the formation of pyrite from pore water iron will be restricted, therefore A_T will remain unchanged. The slower production of S° will however allow pyrite formation at deeper levels in the sediment.

Relating this hypothesis to the sediments studied, it was suggested in Section 4.5 that the sediments from SP1, DN1 and CM1 are likely to have a high degree biomixing. The sediments from these cores all show low A_T increases relative to the loss of SO_4^{2-}. These cores conform to the proposed model (a). The lack of alkalinity can be explained by the precipitation of pyrite from pore water iron. Similar patterns over the same depth range were noted by Davies (1977). However, Davies notes an increase in alkalinity at low SO_4^{2-} concentrations. He attributes this to exchange reactions with clays. It is difficult to see how this could occur as the clay fraction in these sediments is likely to be weathered and unreactive (Price, Pers. Comm.). This being the case, the reason for the alkalinity increase remains unknown.

Core AB1 conforms to the stoichiometric relationship between SO_4^{2-} and A_T. While possessing macro-fauna, the rate of biomixing in the outer basin is unlikely to be as great as that in the sediments from the relatively unrestricted localities (CM1, SP1 and DN1). The implication is that sediments from the outer basin of Loch Etive can be compared to model (b). No loss of alkalinity is observed because very little pyrite is precipitated from pore water iron due to the lack of S^o. The meta-stable sulphides produced remain to much deeper levels in the sediment. This is supported by magnetic susceptibility studies on Airds Bay sediment which would tend to indicate the presence of Greigite to a depth of 90cm (Edwards *et al*, 1987; Thompson, Pers. Comm.)

The sediments from ET1 are unusual in that they show a greater increase in alkalinity than would be expected from the SO_4^{2-} loss. It is difficult to explain how this may occur. Patterns of Sr (Chapter 3) suggest very little carbonate is present, therefore the excess A_T over that produced by SO_4^{2-} reduction is unlikely to be due to carbonate dissolution. A possible explaination is irrigation of SO_4^{2-} at depth. If fresh SO_4^{2-} is introduced at depth to SO_4^{2-} depleted pore water, some A_T will be lost through flushing, but due to the 2:1 stoichiometric relationship more alkalinity will be produced by reduction of the introduced SO_4^{2-} than will be lost. Therefore the total amount of alkalinity will be increased.

CHAPTER 5

$\delta^{15}N$ IN THE SEDIMENTS

5.1. Introduction.

$\delta^{15}N$ in the sediments was investigated in an attempt to use this as a means of identifying the relative proportions of marine and terrestrial organic matter. The values obtained are compared with C/N ratios, which have been proposed as indicators of provenance of organic matter. A number of differences are noted between the patterns shown by the different methods and these will be discussed.

$\delta^{15}N$ has long been used as a source indicator of organic material and a way of measuring N uptake by plants in agronomy and soil science, following the work of Keeny and Bremner (1976), Kohl *et al.* (1971) and Shearer *et al.* (1973, 1979). In the marine environment much work has been done on the $\delta^{15}N$ patterns of particulate organic matter (Cline and Kaplan, 1975; Saino and Hattori, 1980; Altabet and Deuser, 1985; Altabet and McCarthy, 1985, 1986). Cline and Kaplan (1975) used $\delta^{15}N/NO_3^-$ distributions to determine rates of denitrification. However, very little work has been done on the behaviour of $\delta^{15}N$ in sediments (Peters *et al.*, 1978; Sweeny *et al.*,1978; Sweeny and Kaplan, 1980).

In air, the stable isotope ^{15}N forms about 0.37% of the total atmospheric N value, the remainder being composed of the common ^{14}N isotope (Mariotti, 1983). In the case of terrestrial soils the major source of nutrient N is from the atmosphere. In the marine environment the major source is inorganic nitrate, which is enriched in ^{15}N relative to the atmosphere (Cline and Kaplan, 1975; Sweeny and Kaplan, 1980). This may provide a basis for discrimination between marine and terrestrial organic matter. Terrigenous organic material transported to the marine environment is reported to be relatively stable,

implying a refractory nature (Peters, *et al.* 1978); hence little fractionation of terrigenous material in marine systems is likely. In marine organic matter fractionation is known to occur, especially during fallout to the sediment surface (Cline and Kaplan, 1975; Wada and Hattori, 1978; Saino and Hattori, 1980) and this has led to the observations that $\delta^{15}N$ values of marine organic matter tend to be in the range $+7^{o}/_{oo}$ to $+13^{o}/_{oo}$. Terrigenous organic material exhibits values close to the $\delta^{15}N$ of standard nitrogen of the atmosphere, i.e. between $0^{o}/_{oo}$ and $+2^{o}/_{oo}$ (Cline and Kaplan, 1975; Peters *et al*, 1978; Wada and Hattori, 1978; Sweeny *et al*, 1978; Saino and Hattori, 1980; Sweeny and Kaplan, 1980).

5.2. Method Of Analysis.

Total N values and the relative proportions of ^{14}N to ^{15}N were obtained using a standard Carlo-Erba 1400 Nitrogen analyser attached to a VG-Micromass 622 mass-spectrometer in the Department of Soil Science. An accurately known weight of sample of about 20mg (±10%) was injected into the N analyser and combusted at 1030°C. The amount of N_2 gas derived is directly related to the amount of N in the sample. A constant proportion of the N_2 derived was then fed into the mass-spectrometer and the isotopic composition determined by measurements of the ion currents corresponding to mass 28 ($^{14}N\ ^{14}N$) and mass 29 ($^{15}N\ ^{14}N$). The atom % ^{15}N value determined can then be used to calculate a $\delta^{15}N$ value using the ^{15}N content in the atmosphere (0.3663 at % ^{15}N) as a standard, from equation (5.1).

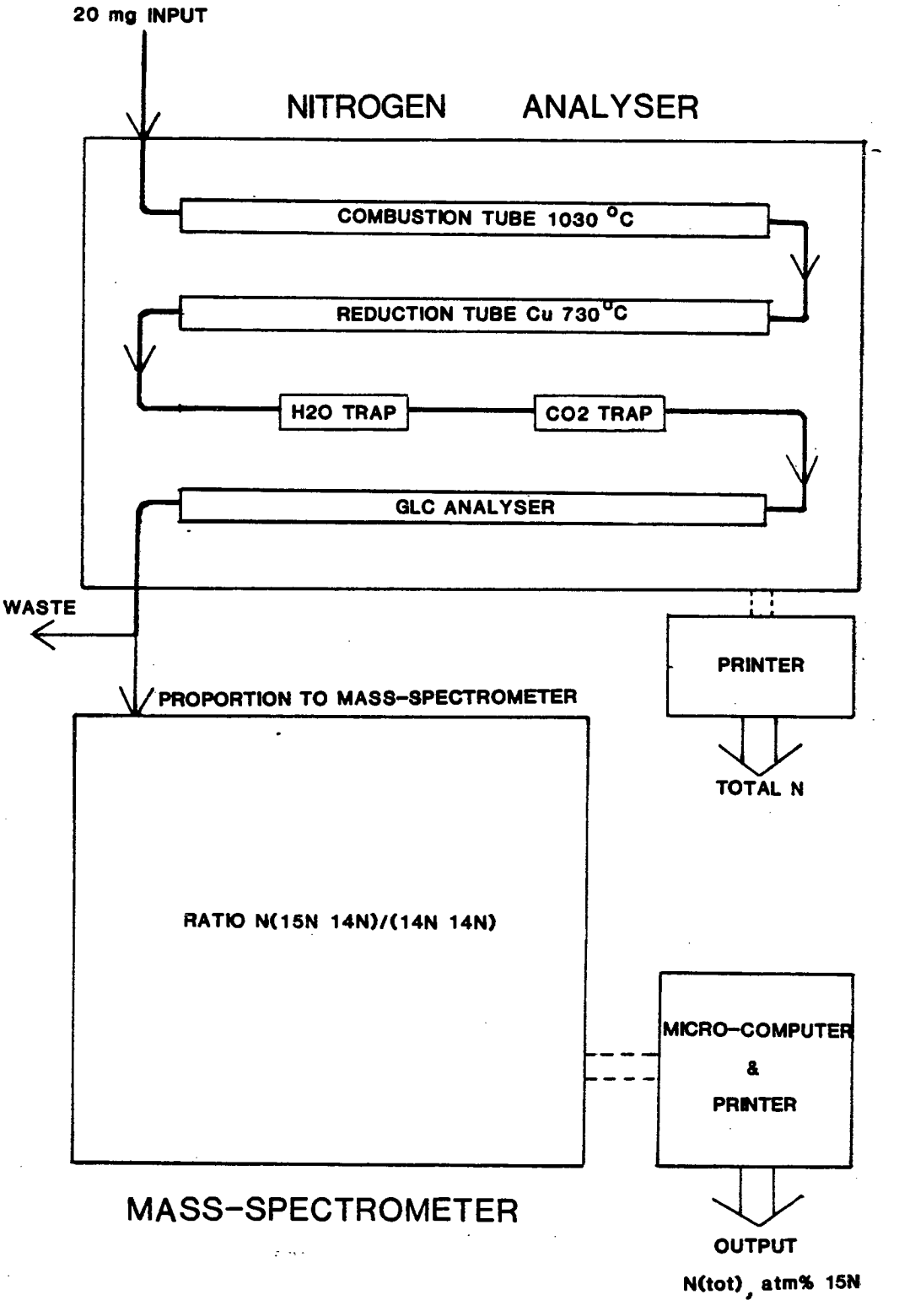

FIGURE 5.1: Flow diagram summarising the major operations of the Carlo-Erba 1400 N analyser and the VG-Micromass 622 mass spectrometer.

$$\delta^{15}N = \frac{(\text{at \% } ^{15}N)_x - (\text{at \% } ^{15}N)_{atm} \cdot 1000}{(\text{at \% } ^{15}N)_{atm}} \qquad (5.1)$$

The operations are summarised in Figure 5.1. Quality control of the data was ensured by analysing each sample in duplicate and running an atmospheric standard and acetanilide reference after every 20 runs (10 samples). Any machine drift was then corrected before the calculation of the ^{15}N atom %. The variation calculated on 18 duplicate samples from Loch Spelve was 0.003 for total N and 2.6×10^{-4} for atom % ^{15}N. This would give an analytical precision in $\delta^{15}N$ of $\pm 1\,^{o}/_{oo}$. The total data are given in Appendix II, Table A11.7.

5.3. Results.

The surface $\delta^{15}N$ values of the cores studied fall in the range $+3\,^{o}/_{oo}$ to $+14\,^{o}/_{oo}$, with the majority of values falling between $+3\,^{o}/_{oo}$ and $+10\,^{o}/_{oo}$ (see Table 5.1). These agree well with the values of between $+2\,^{o}/_{oo}$ and $+10\,^{o}/_{oo}$ reported by Sweeny *et al.* (1978) and Sweeny and Kaplan (1980) for the Santa Barbara Basin. The lowest surface values can be seen in SH1 (Loch Shell) and the highest, $+14\,^{o}/_{oo}$, in CM1 (Camas an Thais). This last value falls outside the range proposed by Sweeny *et al.* (1978) and Sweeny and Kaplan (1980). However, values of greater than $+14\,^{o}/_{oo}$ have been noted from particulate organic matter. Cline and Kaplan (1975) noted $\delta^{15}N$ values of $+18.8\,^{o}/_{oo}$ in the

Core	Surface $\delta^{15}N$ (‰)	Surface C/N
CM1	14.06	8.56
CR1	7.24	8.77
DU1	9.15	11.79
ET1	6.55	11.64
SH1	4.06	8.19
SP1	9.01	8.19

Table 5.1: Surface $\delta^{15}N$ values with corresponding C/N ratios. Both sets of values are means of the upper 4cm of the sediment.

Sta.	%N	$\delta^{15}N$	C_{tot}*	%N*	C/N	C/N*
1	0.318	6.279	5.8	0.380	21.27	22.25
3	0.438	7.098	7.3	0.480	19.42	17.72
5	0.411	6.825	6.5	0.50	18.47	15.16
7	0.454	6.825	7.5	0.52	19.27	16.78
8	0.206	7.644	3.0	0.22	16.97	15.91
10	0.466	6.279	6.8	0.55	17.00	14.40
13	0.503	7.098	5.5	0.48	12.11	13.35
15	0.133	11.193	1.8	0.15	15.78	14.01
17	0.495	7.644	5.8	0.55	13.68	12.29
19	0.571	7.098	6.7	0.63	13.67	12.40
22	0.309	8.190	4.0	0.40	15.07	11.64
23	0.214	8.927	3.5	0.3	19.05	13.62

Table 5.2: Total N, $\delta^{15}N$ and C/N values for core stations in Loch Etive.

* Data from Ridgway (1984)

equatorial Pacific. More recently, in the Western Atlantic, Altabet and McCarthy (1985, 1986) have noted values of +14.4 $^{o}/_{oo}$ from particulate matter in warm core rings associated with the Gulf Stream.

With depth in the sediments, the $\delta^{15}N$ patterns vary considerably from core to core. The patterns can be seen in Figure 5.2. Sediments from Loch Etive (ET1) remain relatively constant with depth, with $\delta^{15}N$ values of between +6 $^{o}/_{oo}$ and +7 $^{o}/_{oo}$. In Loch Spelve, station SP1 shows a gradual increase in $\delta^{15}N$ with depth; within the uppermost 10 cm it increases from +8.8 $^{o}/_{oo}$ to +11.99 $^{o}/_{oo}$, but lower down remains relatively constant between +10 $^{o}/_{oo}$ and +12 $^{o}/_{oo}$. Cores CM1 and SH1 show contrasting patterns. The surface values of CM1 are very high at +14 $^{o}/_{oo}$ and there is an increase to over +16 $^{o}/_{oo}$ in the top 8cm. However, below this depth the values show a fall to +5.6 $^{o}/_{oo}$ (9–10cm) and then continue to decline slowly to almost 0 $^{o}/_{oo}$ at the base. Conversely, in SH1 the surface values are low and remain between +2 $^{o}/_{oo}$ and +4.5 $^{o}/_{oo}$ for the upper 15cm; below there is a rapid rise to +9.7 $^{o}/_{oo}$ (17cm). The bottom section of the core exhibits a steady increase to +13.2 at the base of the core. DU1 (Loch Duich) displays anomalous values at depth. After a slight fall from +9.9 $^{o}/_{oo}$ in the surface sediments, $\delta^{15}N$ values show an increase from +8.6 $^{o}/_{oo}$ at 5–6cm to +13.3 $^{o}/_{oo}$ at 25cm. There is then a rapid increase to over +22 $^{o}/_{oo}$ (37cm). The values then remain constant to the base of the core. In Loch Creran (CR1), the $\delta^{15}N$ values are similar to the pattern seen in cores ET1 and SP1. There is a slight fall in values from the surface (+7.9 $^{o}/_{oo}$) to 4–5cm (+6.5 $^{o}/_{oo}$). Below which there is a gradual increase to +10 $^{o}/_{oo}$ at the base of the core.

Sweeny and Kaplan (1980) have attempted to establish the $\delta^{15}N$ values for the two end members, marine and terrestrial organic matter, in Santa Barbara

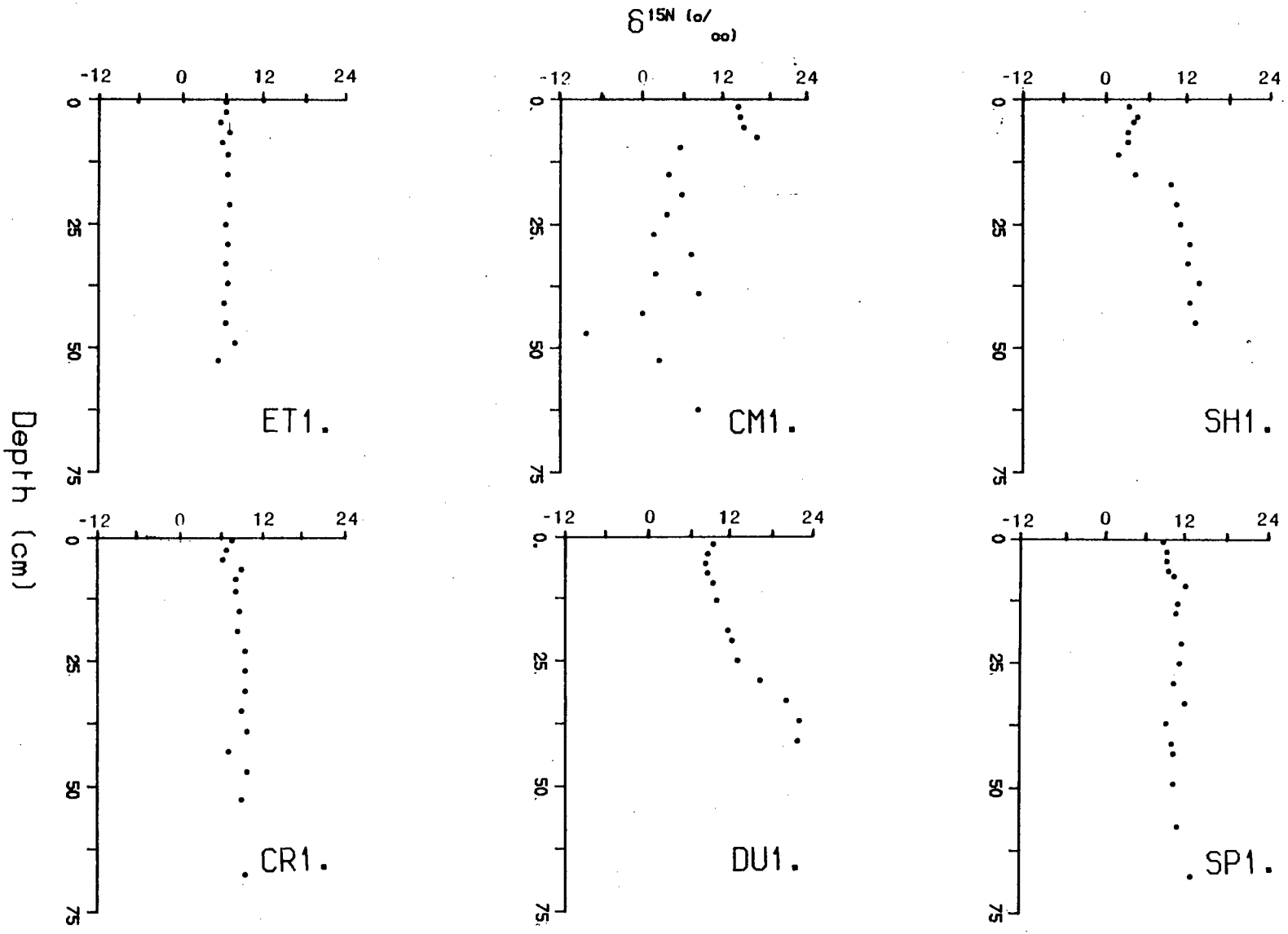

FIGURE 5.2: The patterns of $\delta^{15}N$ in the sediments.

Basin sediments. For this they used $\delta^{15}N$ values of the organic matter from sewerage outfall and from sediment pore water ammonium. They claim these values to be +2.5 $^{o}/_{oo}$ for terrestrial material and +10 $^{o}/_{oo}$ for marine organic matter. These values were subsequently used to plot a mixing curve by which the relative proportions of marine to terrestrial organic matter could be derived for the sediments of the Santa Barbara Basin, assuming there to be no diagenetic fractionation.

Applying the same assumptions and similar end members to the sediments from this study it should be possible to determine the relative influences of marine and terrestrial organic matter in the sediments.

The surface $\delta^{15}N$ value of CM1 would suggest organic matter of entirely marine character. This is consistent with the position of Camas an Thais in the Firth of Lorne. However, below 8cm, the fall in $\delta^{15}N$ to near 0 $^{o}/_{oo}$ at the base of the core suggests that the deeper sediment is more terrestrial in character. If these values are compared with the C/N data (see Figure 5.3) which, despite limitations (see Chapter 4) has been used in the past to differentiate marine and terrestrial organic matter, some similarities can be seen. There is a slight decrease in the C/N values in the top 8cm from 8.8 to 7.6 suggesting possibly some marine influence. Below 8cm, the C/N values increase to a mean of 9.9 which, it could be argued is more terrestrial compared with the surface values.

In SH1 the relatively low $\delta^{15}N$ values would suggest a sediment of a terrestrial character for the top 16cm, with higher values at depth suggesting a greater content of marine organic matter. Comparison of the $\delta^{15}N$ and C/N patterns at station SH1 (Figure 5.3) shows a considerable inconsistency.

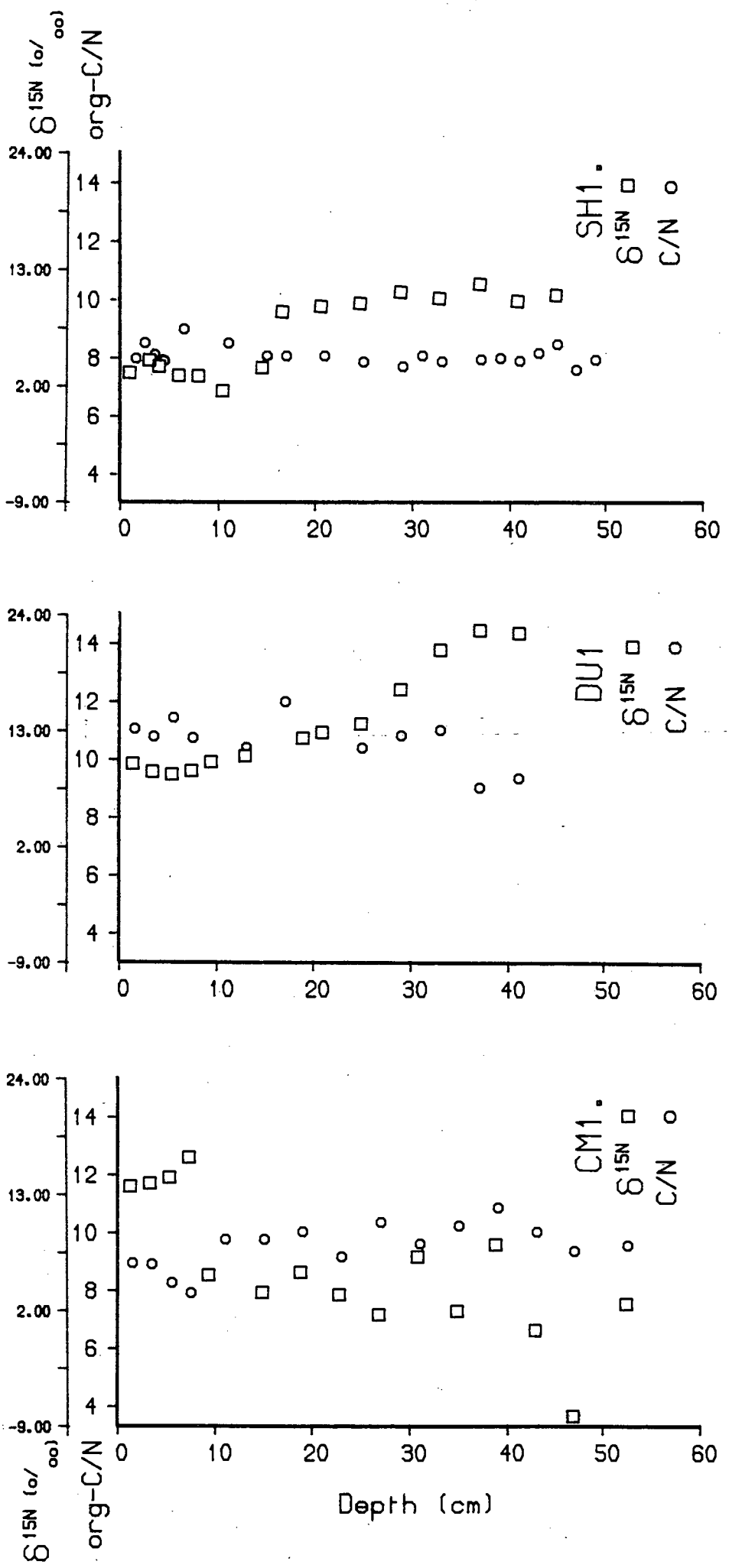

FIGURE 5.3: Comparison of $\delta^{15}N$ and C/N ratios for cores CM1, DU1 and SH1 showing variations in C_{org} source indications.

The upper 6cm shows C/N values of 7.1 to 8.1 which would suggest a marine influence; deeper down the mean C/N value of 8.2 shows little change from that above.

The increasing $\delta^{15}N$ values of core DU1 at depth would suggest an increasing marine influence. However, the base of the core shows very high $\delta^{15}N$ values of over +22 $^{o}/_{oo}$, well in excess of the marine organic matter as demonstrated by Sweeny and Kaplan (1980). These very high values are to be found in the pale grey consolidated clay sediment that occurs below 34cm and probably represents old sediment. The variation in values between +13.3 $^{o}/_{oo}$ at 25cm and +22.3 $^{o}/_{oo}$ at 37cm is probably a result of biomixing of the clay and the overlying sediment during accumulation. In contrast, the C/N ratio of this core (Figure 5.3) does not show such a dramatic change. However, at the sediment surface, the C/N value of 11.7 would imply a much greater terrestrial influence than the $\delta^{15}N$ value would suggest.

In order to examine the sensitivity of $\delta^{15}N$ as an indicator of organic matter provenance, twelve surface sediment samples (0-1cm) collected by Craib corer (Craib, 1965) from Loch Etive by Ridgway (1984) were analysed for $\delta^{15}N$. The samples (see Chapter 4, Figure 4.9 for localities) were collected in summer 1981 and represent a transect down the loch from the head (sample 1c) to the Firth of Lorne (sample 23c). A similar exercise carried out by Malcolm (1981) measuring C/N, found a dramatic difference between C/N values at the head of the loch (C/N 17.3) and at the mouth (C/N 5). This profile is discussed in more detail in Chapter 4. Despite the problems associated with using C/N as a source indicator for organic matter, such high values at the head of the loch will tend to suggest a terrestrial input of C_{org}. The mouth of the loch appears to be influenced to a greater degree by marine

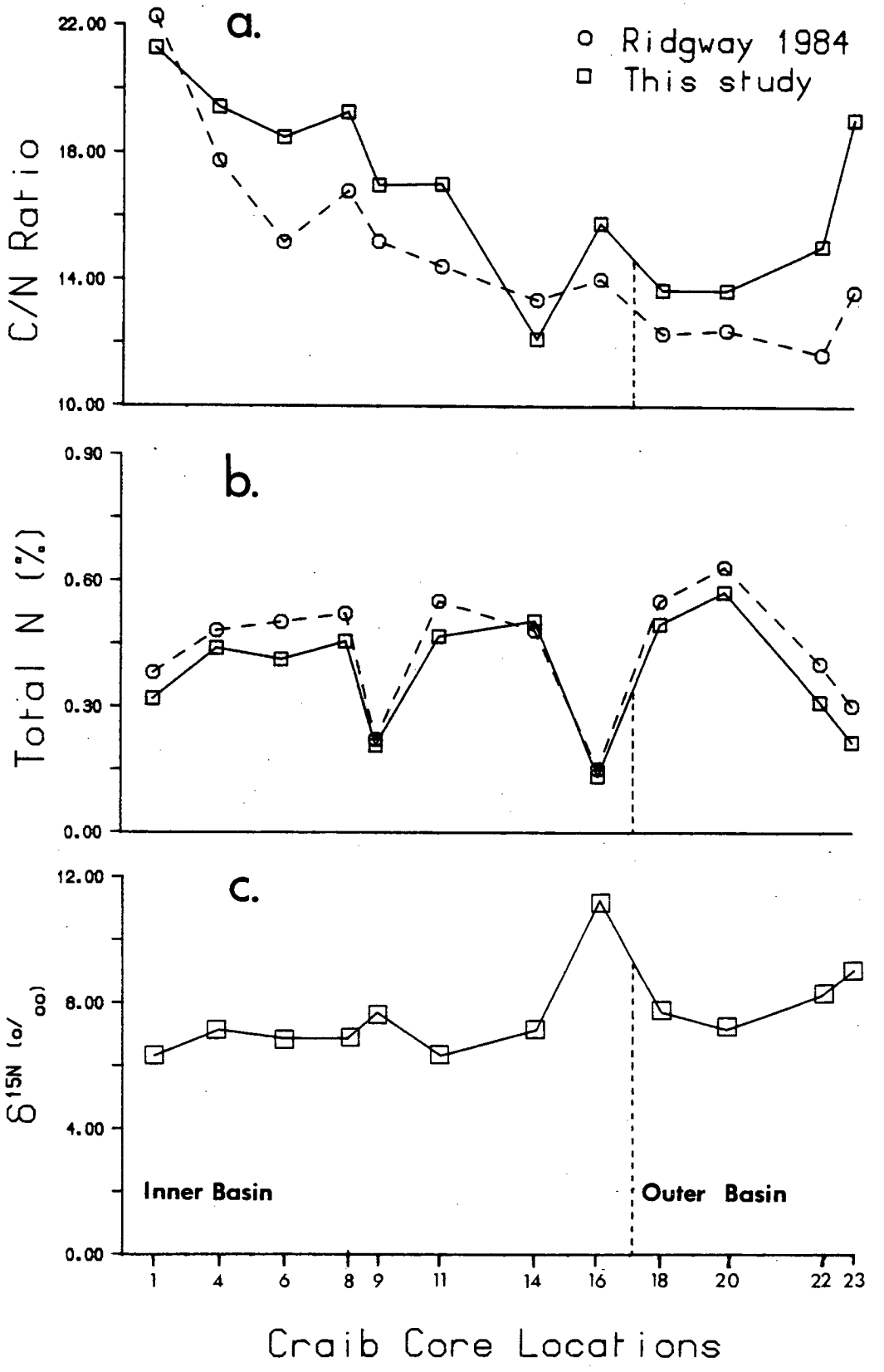

FIGURE 5.4: Profiles of surface values of C/N, total N and $\delta^{15}N$ down Loch Etive.

organic matter. C/N ratios calculated using the N data from this study and the C_{org} for the same stations obtained by Ridgway (1984) (see Table 5.2) show a similar pattern to Malcolm (1981). There is a decline in values from 21.27 at the head of the loch to 13.67 in the outer basin, with a slight rise to 19.05 in the Firth of Lorne. This is illustrated in Figure 5.4(a). Figure 5.4(a) also shows the C/N pattern obtained by Ridgway (1984). The two profiles can be seen to compare well, reflecting the similarity of N values (Figure 5.4(b)). However, the C/N values obtained are much higher than those noted by Malcolm (1981). This can be explained by the fact that the C values reported by Ridgway (1984) are total C, uncorrected for carbonate. Ridgway assumed the influence of carbonate in the sediments of Loch Etive to be very small. The variation between the C values obtained by Malcolm (1981) and Ridgway (1984) suggests this is not the case.

Figure 5.4(c) shows the profile of $\delta^{15}N$ along the loch. There is a slight increase in values overall from the head of the loch (+6.3 $^{o}/_{oo}$) to the mouth (+8.9 $^{o}/_{oo}$) but this is small compared with the variation of organic matter depicted by the trend in C/N ratios. There must, therefore, be other factors influencing the $\delta^{15}N$ values recorded in the sediment.

Two points are worthy of note regarding the $\delta^{15}N$ trend of Figure 5.4(c). Station 11c shows a comparatively low $\delta^{15}N$ value. This station is located off the mouth of the River Kinglass and is likely to receive a sizeable amount of terrestrial organic material. Its value of +6.3 $^{o}/_{oo}$ is similar to that found at the head of the loch an area of maximum terrestrial input. Sediment from Sta. 16c, in the deepest part of the loch has a comparatively high $\delta^{15}N$ value (+11.2 $^{o}/_{oo}$) and is clearly anomalous when compared with adjacent stations. A comparison of the $\delta^{15}N$ value from this station with that of total N shows the

total N content to be anomalously low, 0.1%, suggesting there may be some dependence of $\delta^{15}N$ on total N contents. A similar pattern of $\delta^{15}N$ and N contents occurs in DU1 (Figure 5.5). This trend is not invariable however, as sediments from core CM1 show a wide range of $\delta^{15}N$ values but near constant values of total N.

Interpretation of the data presented is very confusing. $\delta^{15}N$ at depth shows a wide range of values, which could be interpreted as being due to the relative influences of marine and terrestrial organic matter, but they are not always consistent with other indicators such as C/N, which often does not show such wide variation. There may also be some dependence between $\delta^{15}N$ and N content in these sediments.

5.4. Discussion.

The evidence suggests that while the origin of the organic matter in a sediment does play some role in determining the $\delta^{15}N$ values, other factors that have been ignored or dismissed in earlier work may have an important influence. These are now to be considered:

1. Analytical errors.
2. Productivity variations of $\delta^{15}N$.
3. Diagenesis of N during burial and influence of sediment lithology.

Analytical error: All the samples were run in duplicate and the precision was very good. Machine drift was automatically corrected for when the standards were run. There is no dependence in the machine between the amount of total N detected and the $\delta^{15}N$ value. Figure 5.5 shows a plot of

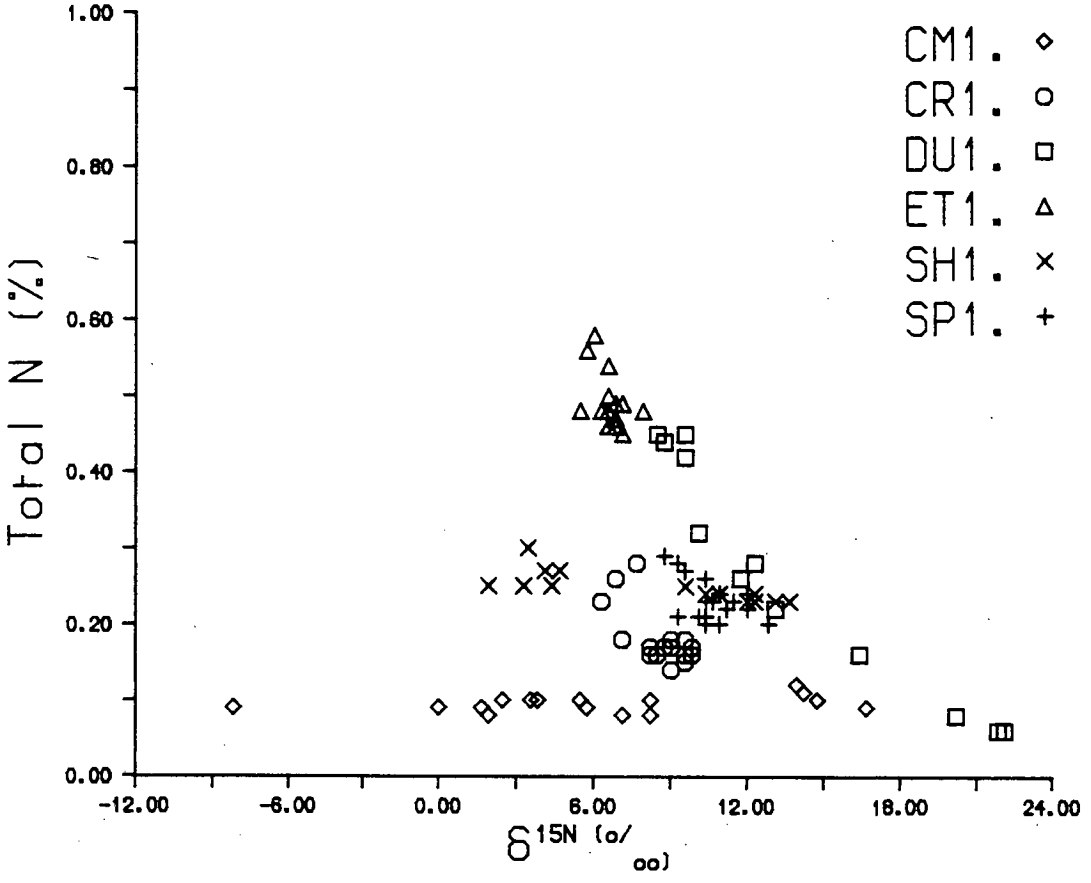

FIGURE 5.5: $\delta^{15}N$ against total N showing spread of points. Note the high values of $\delta^{15}N$ in the low N content clay sediments from the base of core DU1.

$\delta^{15}N$ against total N in which CM1 displays a wide range of $\delta^{15}N$ values but the total N values remain constant. Conversely, ET1 shows a range of N values and a small spread of $\delta^{15}N$ This evidence would discount any machine error.

Productivity: It has been shown by Wada and Hattori (1978) that $\delta^{15}N$ can vary in different species of marine diatom. Moreover, Minagawa and Wada (1984) have shown that there is a stepwise enrichment of $\delta^{15}N$ along the food chain. For instance phytoplankton are found to have ratios of between -2.5 $^{o}/_{oo}$ and +6 $^{o}/_{oo}$, while those of zooplankton are higher, varying between +6 $^{o}/_{oo}$ and +14 $^{o}/_{oo}$. Thus, $\delta^{15}N$ in the surface sediments could be influenced by the type and relative abundances of phytoplankton and zooplankton in the overlying waters.

The variations in $\delta^{15}N$ values of plankton noted by Minagawa and Wada (1984) illustrates a further point. Sweeny and Kaplan (1980) assume two discrete end members to produce their mixing curve. As with C/N ratios it is invalid to assume two discrete values for marine and terrestrial organic matter. Table 5.3 illustrates the range of $\delta^{15}N$ values for a number of natural substances both marine and terrestrial. The overlap of values is very marked. For example, in marine organic matter $\delta^{15}N$ varies between -2.5 $^{o}/_{oo}$ and +14 $^{o}/_{oo}$, while the values for soils can be seen to vary between -0.2 $^{o}/_{oo}$ and +11.7 $^{o}/_{oo}$. With such large variations it seems unlikely that $\delta^{15}N$ can be used as a universal indicator for the source(s) of organic matter in sediments. Nevertheless, at one particular site one would expect to have constant $\delta^{15}N$ values for the different organic matter present

Sediment lithology and diagenesis: Variations in the grain size of a sediment may be due to a variation in the sedimentary input or may be due to

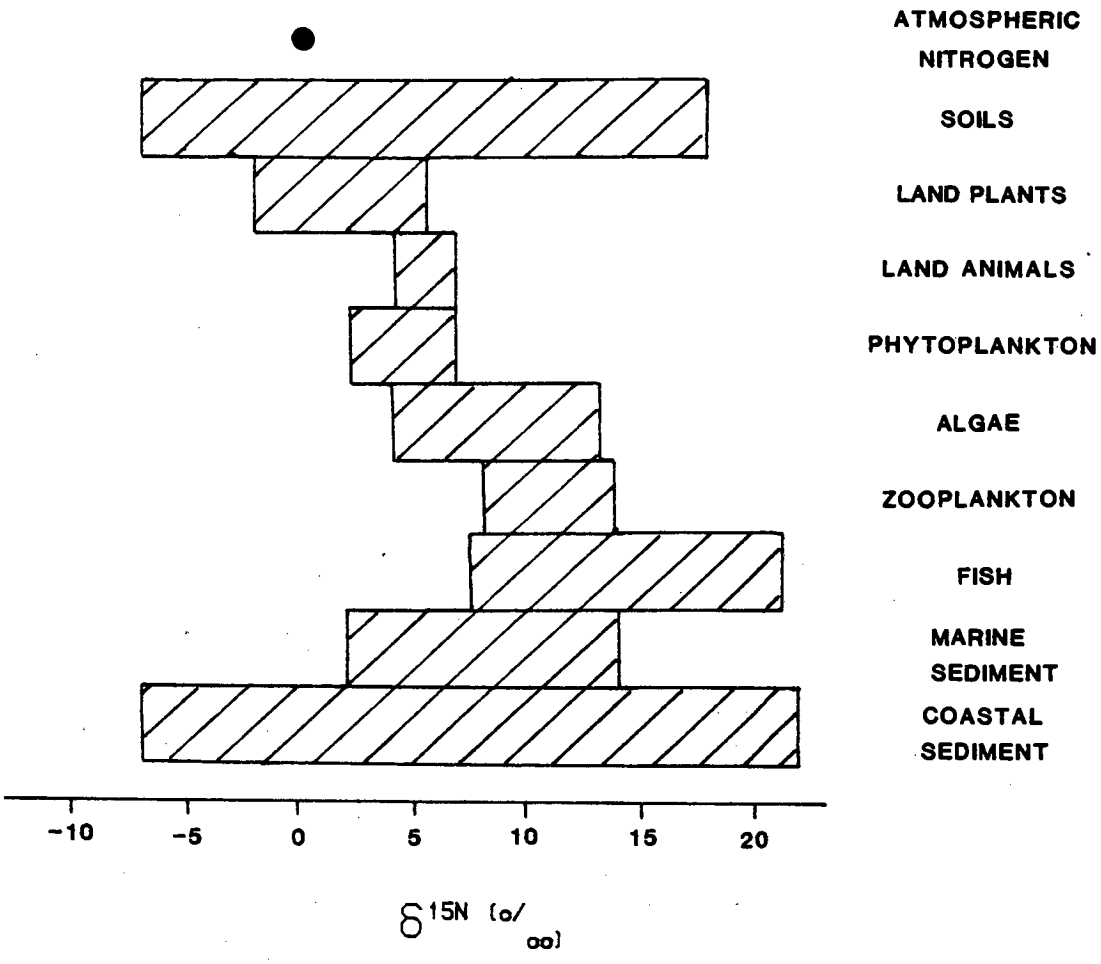

TABLE 5.3: Variation in $\delta^{15}N$ values of natural substances.

Modified after Wlotzka (1972); Kaplan (1975); Miyake and Wada (1967); Sweeny *et al.* (1978).

an erosive phase. Coarse bands in the sediments are often due to the winnowing of finer material by (eroding) currents. Such bands tend to have less organic matter and that remaining tends to be more refractory due to the fact that the more reactive material is associated with the transported finer fraction. This process would have the effect of decreasing the $\delta^{15}N$ values by increasing the relative terrestrial portion of the organic matter. Figure 5.6 shows a comparison between the Zr/Rb ratios and $\delta^{15}N$ patterns in cores CM1, CR1 and SH1. The top 10cm of CM1 (Figure 5.6a) is relatively coarse as indicated by a Zr/Rb ratio of 3.9 to 4.2. The $\delta^{15}N$ values in this section of the core are also high ($>12^{o}/_{oo}$). In CR1, (Figure 5.6b), the Zr/Rb ratio shows coarser sediment in the shell band between 5cm and 12cm. Comparison with the $\delta^{15}N$ pattern again shows the $\delta^{15}N$ values to be higher in the coarser sediments.

Conversely, in Loch Shell (SH1; Figure 5.6c), the Zr/Rb pattern is comparatively invariant with depth (1.31 to 1.4) and suggests a finer grained sediment than those of cores CM1 and CR1. However, the $\delta^{15}N$ values show an increase from +4.5 $^{o}/_{oo}$ to +9.7 $^{o}/_{oo}$ between 14cm and 18cm depth. In DU1 (Figure 5.6(d)), the decrease in Zr/Rb ratios at depth in the sediments above cohesive clay coincides with an increase in the $\delta^{15}N$ values. However, this can be attributed to biomixing of the clay and the overlying sediment. Hence, the evidence from CM1, CR1 and SH1 indicates that variations in lithology do not influence the pattern of $\delta^{15}N$ in the sediments. The possibility of diagenesis and isotope fractionation needs to be considered.

Terrestrial organic matter is believed to be inert in the marine environment and therefore resistant to organic breakdown. With burial, as marine organic matter is degraded, the relative proportions of marine to terrestrial organic

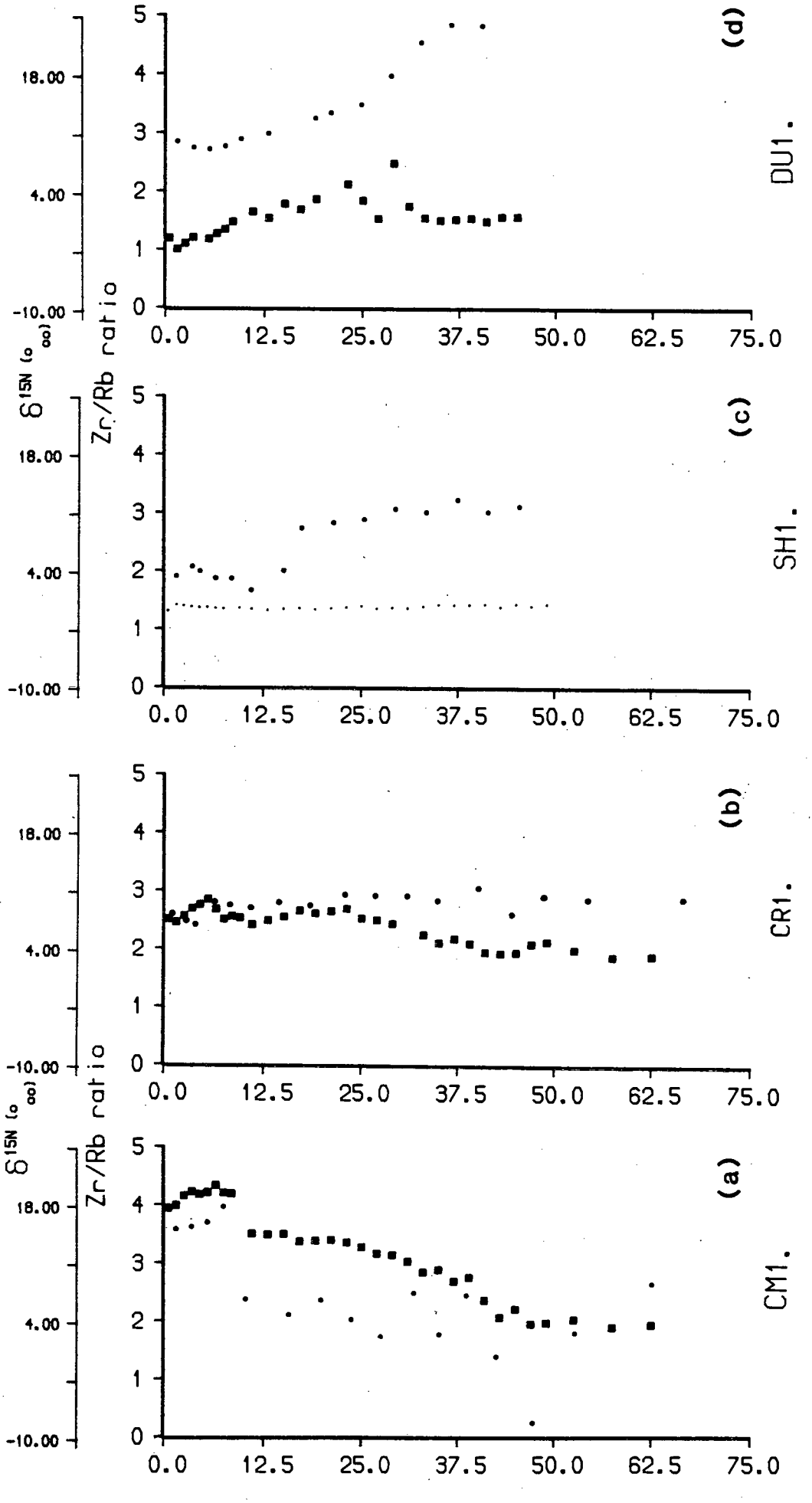

FIGURE 5.6: Comparison of $\delta^{15}N$ with sediment grain size as indicated by Zr/Rb ratio.

matter will decrease. Such behaviour is known to have an effect on the C/N values in the sediments: they would be expected to increase. $\delta^{15}N$ would also be expected to increase as the more labile organic matter is utilised. However, while this may be the case in SH1, other cores (such as CM1) show an increase in $\delta^{15}N$ with depth.

The possibility of isotope fractionation must also be considered. It is difficult to understand why N should not fractionate with burial diagenesis. This was assumed not to occur by Sweeny and Kaplan (1980) because the mean $\delta^{15}N$ values of pore water ammonium from Santa Barbara Basin sediments -derived from organic matter via SO_4 reduction- were similar to those of plankton from the San Pedro shelf area (+8.6$^{o}/_{oo}$). But, this does not take into account the possibility of isotope fractionation during remineralisation reactions. In the water column, denitrification is known to cause fractionation in NO_3^-. $\delta^{15}N$ values have been seen to reach +18.8 $^{o}/_{oo}$ in the active denitrification zone of the Eastern Tropical North Pacific (Cline and Kaplan, 1975).

Fractionation of C isotopes is known to occur in sediment. It has been shown by McCorkle (1985) that sediment pore waters contain isotopically lighter C than sediments and the overlying bottom waters. This is a direct result of organic matter breakdown. Furthermore, the variation in $\delta^{13}C$ is greater; that is, the pore waters become enriched in isotopically lighter C with decreasing bottom water oxygen content and increasing reactive C_{org} input to the sediments. In the sediments from this study, with high rates of organic input compared to deep sea sediments, there is likely to be a high degree of C fractionation. It is possible that N may behave in a similar manner

Sedimenting organic matter in the water column is subject to a considerable degree of alteration before reaching the sediment. Much of the labile organic matter is lost (Berner, 1982). N is known to be more labile than C during organic breakdown and would therefore be expected to be lost preferentially. Since the isotopically lighter ^{14}N would be expected to be preferentially released relative to ^{15}N, the remaining sedimenting organic matter would be isotopically heavier and therefore show an increase in the $\delta^{15}N$. The same process may also occur in the sediments.

Such a hypothesis could be invoked to explain why sediments with very low values of total N appear to show anomalously high isotopic compositions, as seen in DU1. As diagenesis proceeds, ^{14}N is released and ^{15}N becomes increasingly enriched as the total amount of N is reduced. In sediments that have undergone a large amount of diagenesis there is little N remaining, but that which is left is highly enriched in ^{15}N.

A number of conclusions may be drawn from these points. Terrestrial and marine organic matter can display differing $\delta^{15}N$ values, but there may also be considerable overlap and this throws doubt on the use of $\delta^{15}N$ as an organic source indicator. Other factors such as diagenesis, fractionation, and the influences of sediment accumulation, as depicted by lithological changes may be important controls on the $\delta^{15}N$ values at depth. Future work could consider:

a)The $\delta^{15}N$ values of lake sediments to establish whether terrestrial organic material undiluted by marine matter has a recognisable $\delta^{15}N$ signature.

b)The pattern of change of N and C in the sediments and pore waters in terms of $\delta^{13}C$ and $\delta^{15}N$, to investigate whether there is a relationship between $\delta^{15}N$ and the rate of organic matter input.

CHAPTER 6

HALOGEN INPUTS TO THE SEDIMENTS, IODINE AND BROMINE

6.1. Introduction.

In Chapter 3 it was shown that some elements are entirely associated with the terrigenous detrital input and, as such, correlate well with the mineralogical and grain size variation of the sediments. Other elements such as Iodine (I) and Bromine (Br) are derived from the marine environment, in particular sea water and are normally associated with the organic matter of marine sediments. As such, these elements have no direct correlation with sediment mineralogy. However, as I and Br are related to organic matter contents in the sediments they are therefore subject to the processes of diagenetic alteration. In this chapter the patterns of I and Br and their relationship to the organic matter under burial diagenesis, will be discussed.

6.2. Results.

All of the analyses for I and Br were obtained using an X-Ray Fluorescence Spectrometer (See Appendix I, Section 2.2) and the data are expressed on a salt-free basis (Appendix II, Table AII.8).

6.2.1. Iodine.

The surface values of I in the sediments are tabulated in Table 6.1. The lowest surface I concentrations occur in core CM1 (Camas an Thais) (206ppm), with the highest values over (700ppm) being found in core DU1 (Loch Duich). From the surface values, the cores analysed can be divided into three groups (Table 6.1): the highest I concentrations are found in Loch Duich (DU1), Loch Etive (AB1, ET1) and Dunstaffnage (DN1) (435 to >700ppm);

Core	I	Br	I/Br
AB1	540	454	1.32
CM1	206	141	1.46
CR1	342	221	1.55
DN1	435	197	1.42
DU1	579	464	1.25
ET1	486	370	1.31
SH1	376	241	1.56
SP1	388	237	1.64

TABLE 6.1: Surface values of I and Br (0-1cm).

Location	I	Br	I/Br	Author
L. Etive				
Inner Basin	356	360	0.99	Malcolm (1981)
Outer Basin	491	644	0.76	
L. Etive				
Inner Basin	386	237	1.63	Ridgway (1984)
Outer Basin	290	256	1.13	
L.Duich	498	--	--	Krom (1976)
Gulf of Maine	220	188	1.17	Harvey (1980)
Panama Basin	70-400	30-150	2.3-2.6	Pederson & Price (1980)
Gulf of Maine	--	93.5-150	--	Mayer *et al.* (1981)

TABLE 6.2: Comparison of I and Br surface values from other locations.

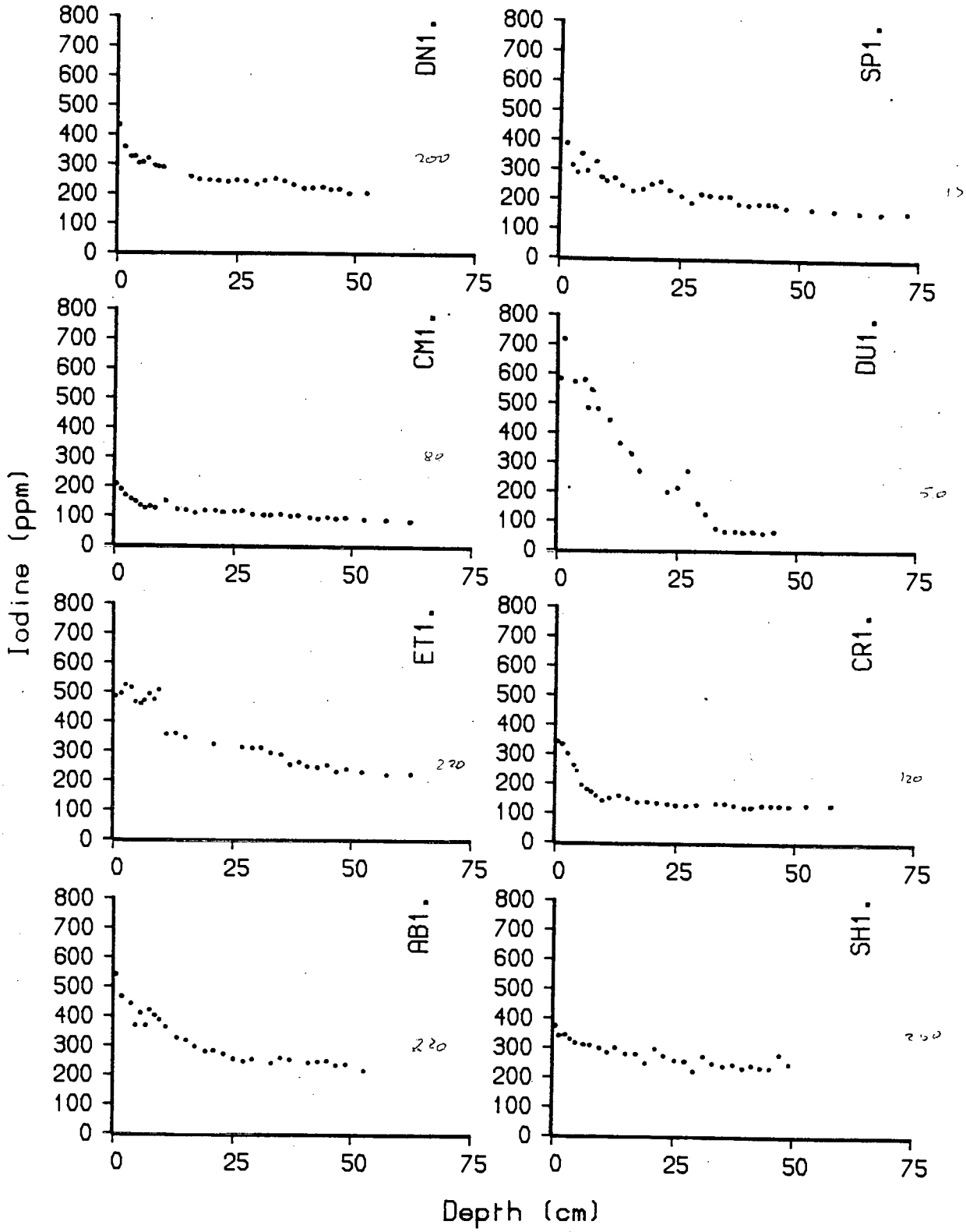

FIGURE 6.1: The patterns of I in the sediments.

Lochs Creran (CR1), Spelve (SP1) and Shell (SH1) form a middle group with I values between 342ppm and 388ppm; the lowest I surface concentration occurs in CM1.

With depth all of the cores display concave downwards profiles (see Figure 6.1), the I values falling to a near constant level at depth. The shape of the profiles varies, as does the I concentration at the base of the cores. For example, ET1 and AB1 a show similar pattern of gradual decline of I to a base level of between 222 and 216ppm at 50cm. Core ET1 shows a marked surficial layer (0-10cm depth) of very erratic values with little decline in I concentration. Below, I contents decrease in a regular manner. In contrast, cores DN1, CM1 and CR1 show the greatest decline in I concentration in the upper 10cm of the sediment, and lower down remain relatively constant with depth. The most conspicuous trend in I is seen in DU1. Surface contents are highest of the cores examined and at depth I is unusually low (50ppm). The pattern of decline appears linear within the interval 4-27cm, implying a sediment mixing between the older consolidated clays and recent surface sediments. The values of I noted in these sediments compare well with values noted from similar localities (Krom, 1976; Malcolm, 1981; Ridgway, 1984) and from similar sediments elsewhere (Pederson and Price, 1980; Harvey, 1980). These values are summarised in Table 6.2.

6.2.2. Bromine.

The patterns of Br in the sediments follow closely those of I. But, owing to the very high concentrations in sea salt, salt free Br contents described below are not as precise as the I analyses. The surface values vary from 141ppm to over 500ppm (see Table 6.1). On these values the cores can be grouped in a

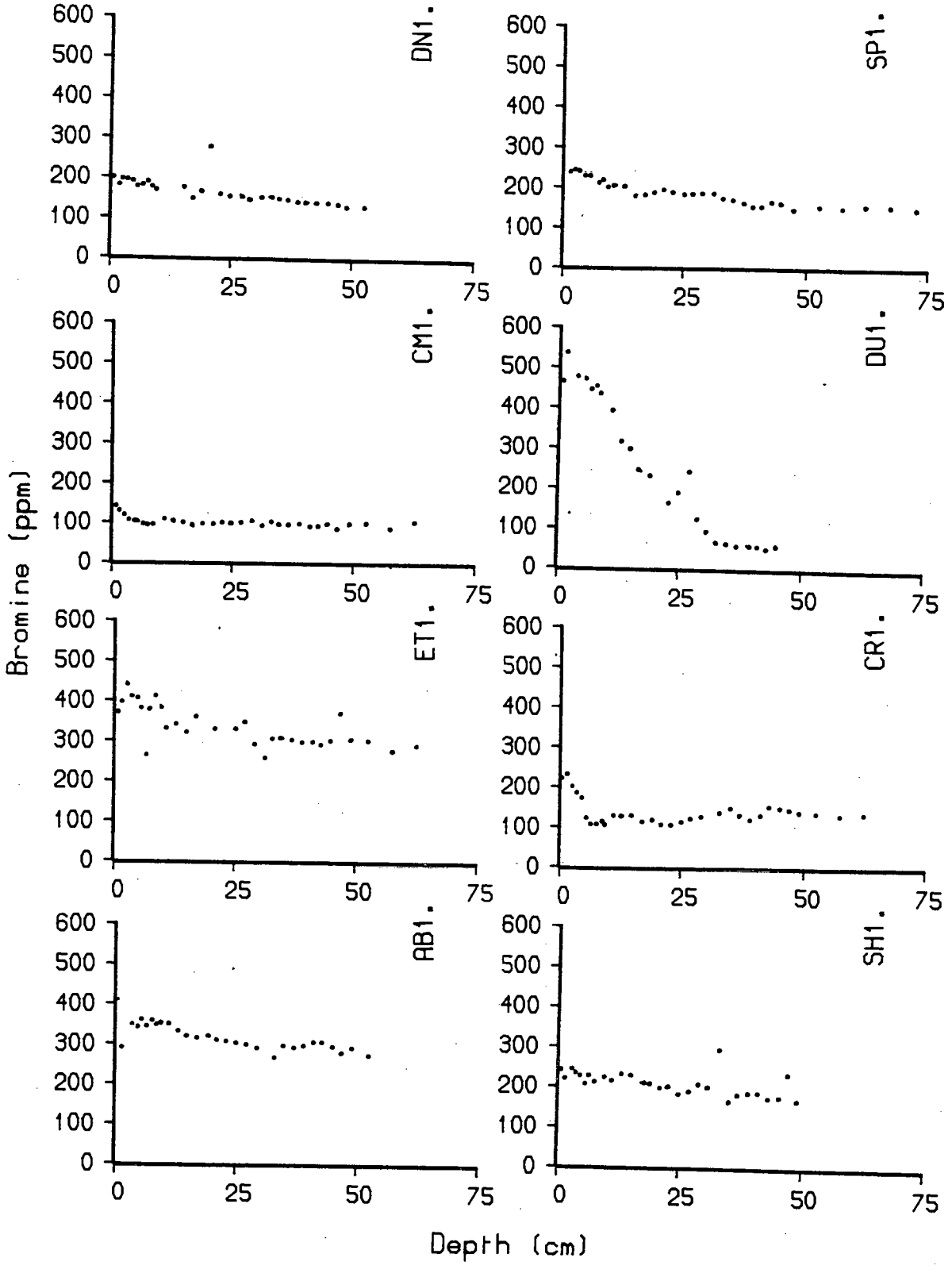

FIGURE 6.2: The patterns of Br in the sediments.

similar manner to I. The highest surface concentrations occur in DU1, AB1 and ET1 (420ppm to 530ppm). Cores CR1, DN1, SH1 and SP1 form a middle group with the lowest concentration occuring in CM1.

At depth there is a similar variation in the Br patterns (see Figure 6.2) as seen from the I data. Cores ET1 and AB1 show similar profiles declining to a background level (278ppm and 273ppm respectively) by 55cm. Surface values tend to be more irregular as seen with I. Conversely, CM1 shows a rapid fall in the 0-10cm interval of the sediment and very little decline in values below this. Core CR1 is unusual in that the greatest fall in Br concentration is in the upper 6cm with low values betweeen 5cm and 12cm depth, coincident with the main shell band in this core. Below this level, Br concentrations are slightly greater and remain relatively constant with depth, except for some decreases in the 36-44cm interval. Br distributions in DU1 follow those of I. Surface contents are the highest seen in these cores and the lowest values can be seen at depth (60ppm). A sediment mixing profile was noted in the I distribution and a very similar pattern is seen in Figure 3.7 for Rb. As with I, the Br values noted compare well with those reported from similar localities and similar sediments elsewhere, summarised in Table 6.2.

6.2.3. I/Br Ratios.

The sediment cores analysed show I/Br ratios of between 0.79 and 2.21 (see Table 6.1). At depth, most cores show a decline in the I/Br ratios relative to the surface values (Figure 6.3). This tends to vary from core to core, but is generally between 0.53 and 0.66. Cores DU1 and SH1 however, show very little decline with depth, 0.20 and 0.11 respectively. In core CR1, within the overall decline in the I/Br ratio, the major shell band (5-12cm) shows increased

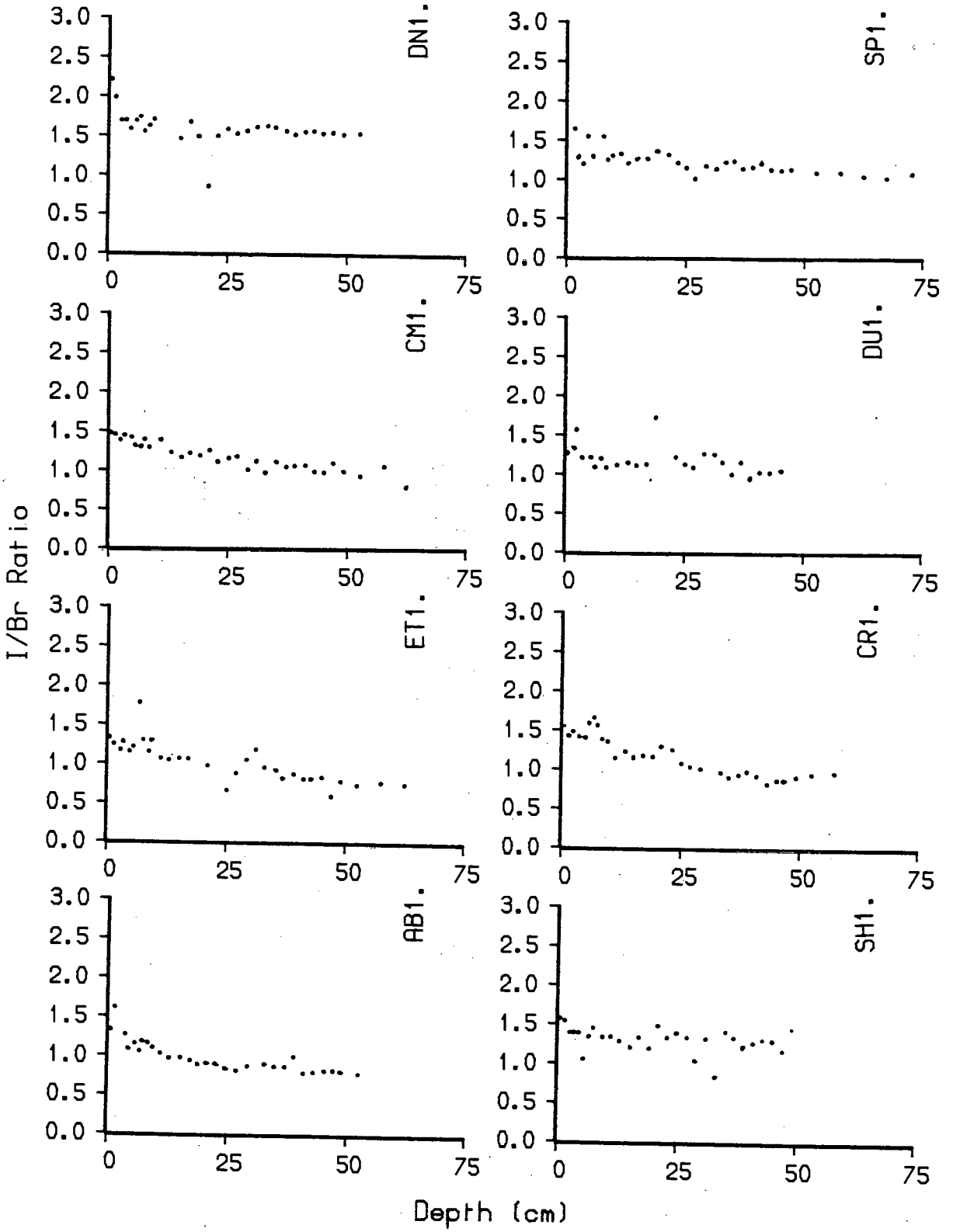

FIGURE 6.3: The patterns of I/Br in the sediments.

I/Br ratios and similar increases can be seen at deeper horizons where shell concentrations are also in evidence. The significance of these trends will be discussed after the associations of halogens and organic matter have been considered.

6.3. The Associations Of Halogens And Organic Matter.

Many workers (Price and Calvert, 1977; Harvey, 1980; Elderfield *et al.*, 1981; Mayer *et al.*, 1981; Ullman and Aller, 1983,1985) have identified that I and Br are intimately associated with organic matter in marine sediments. Under normal marine conditions, the ratio of both I and Br to C assume fairly constant values. At depth however, both elements show a reduction with usually a first order rate decrease. Likewise, all of the sediments except those in Loch Creran show first order reaction rates (for both I and Br) of the form:

$$R_1 = R_o \exp(-\alpha x) \qquad (6.1)$$

Where x = depth

This type of decay is common in metabolic reactions associated with organic matter degradation (Ullman and Aller, 1983). The least squares residuals of I and Br, obtained by fitting the data to equation 6.1 are summarised in Table 6.3, together with the log/linear correlation coefficients. The implication here is that the decline in I and Br with depth is associated with organic matter degradation. Correlations between I and organic matter have been noted by Ullman and Aller (1980, 1983) and Elderfield *et al.* (1981) in microbially mediated reactions following burial. Br diagenesis has been less

Core	I		Br	
	RMS Residual	r	RMS Residual	r
AB1	0.322	-0.899	0.106	-0.804
CM1	0.254	-0.895	0.219	-0.646
CR1	1.017	-0.729	1.034	-0.163
DN1	0.156	-0.899	0.043	-0.952
DU1	0.880	-0.975	0.888	-0.971
ET1	0.195	-0.964	0.104	-0.881
SH1	0.298	-0.864	0.061	-0.888
SP1	0.252	-0.922	0.112	-0.913

TABLE 6.3: Root mean squared residuals and log normal correlation coefficients.

Core	I/C	Br/C	$\delta^{15}N$	C/N
AB1	113.11	85.67	--	--
CM1	254.35	174.09	14.06	8.56
CR1	164.41	106.24	7.24	8.77
DN1	103.60	61.35	--	--
DU1	123.91	99.30	9.15	11.79
ET1	94.93	72.28	6.55	11.64
SH1	185.18	118.70	4.06	8.19
SP1	214.89	131.26	9.01	8.19

TABLE 6.4: Surface values of I/C and Br/C compared with $\delta^{15}N$ and C/N. (-- Not analysed.)

well documented but a similar association with organic matter appears to exist (Price and Calvert, 1977; Harvey, 1980; Mayer *et al*, 1981). Core CR1 is exceptional in that it has very high least squares residual values for both I and Br (1.02 and 1.04 respectively) and correspondingly low correlation coefficients (-0.71 and -0.16). These indicate a very poor fit to the rate equation which is caused in the main, by abrupt changes in the I and Br patterns across the shell band between 5cm and 12cm depth.

Some of the cores show highly variable I and Br values in the upper 10cm, as exemplified in core ET1. This probably reflects the presence of a zone of low biomixing and this is also manifested in pore water SO_4^{2-} and alkalinity profiles (Chapter 4, Section 4.2). In many other cores, for example in the Firth of Lorne cores CM1 and DN1, the most greatest decline in I and Br occurs in the uppermost 10cm of the sediment, implying that the release of halogens is very pronounced within the overall oxic layer of sediments, and probably more intense than in the underlying anoxic sediment. It would seem that the first order loss of halogens from sediments alluded to above is to some extent controlled by oxic rather than anoxic diagenesis. Price and Calvert (1977) noted similar trends in sediment cores showing oxic tops from the Namibian Shelf. This also accounts for the trends noted in Long Island Sound and Winyah Bay sediments by Ullman and Aller (1983,1985).

The I/Br ratios in the sediments (see Figure 6.3) show a decline at depth implying that I is more prone to diagenetic release than Br (Price and Calvert, 1977). This suggests that while both I and Br are associated with the organic matter, the nature of the bond to the organic matter is different. Harvey (1980) showed that I appears to be associated with the nitrogenous components of the organic matter, *i.e.* the polypeptides and the chitin. This

material tends to be preferentially released during degradation (Gordon, 1971; Suess and Muller, 1980; Grundmanis and Murray, 1982). Br tends to form more compounds and is possibly associated with both the nitrogenous and the carbonate fractions. The fact that there appears to be a slightly increased I/Br gradient between anoxic sediment at depth and the uppermost 10cm -which is assumed to be predominantly oxic- indicates that I is preferentially lost from the sediment during biomixing activity.

6.4. Halogen/Organic Carbon Ratios.

It is known that I is associated with the marine organic fraction (Bowen, 1966; Price and Calvert, 1977; Elderfield *et al*, 1981) and that terrigenous organic matter supports little or no I even though I is present in brackish waters such as at the head of Loch Etive (Ridgway, 1984). In contrast, appreciable amounts of Br (roughly 80ppm) are found in terrigenous dominated sediments.

The surface values of Br/C range from 61 in DN1 to 174 in CM1 (Table 6.4). Except for SP1 and CM1, these values are similar to those found in Loch Etive by Ridgway (1984) and the Gulf of Maine (Mayer *et al*, 1981). CM1 and SP1 have ratios which are much higher (174 and 131 respectively) than those noted by the above workers.

In many of the sediments of the study area, particularly those associated with the fjord environments, the organic matter is derived from both terrestrial and marine sources. An attempt has been made to distinguish the relative influences of the two sources using C/N (Chapter 4) and $\delta^{15}N$ (Chapter 5).

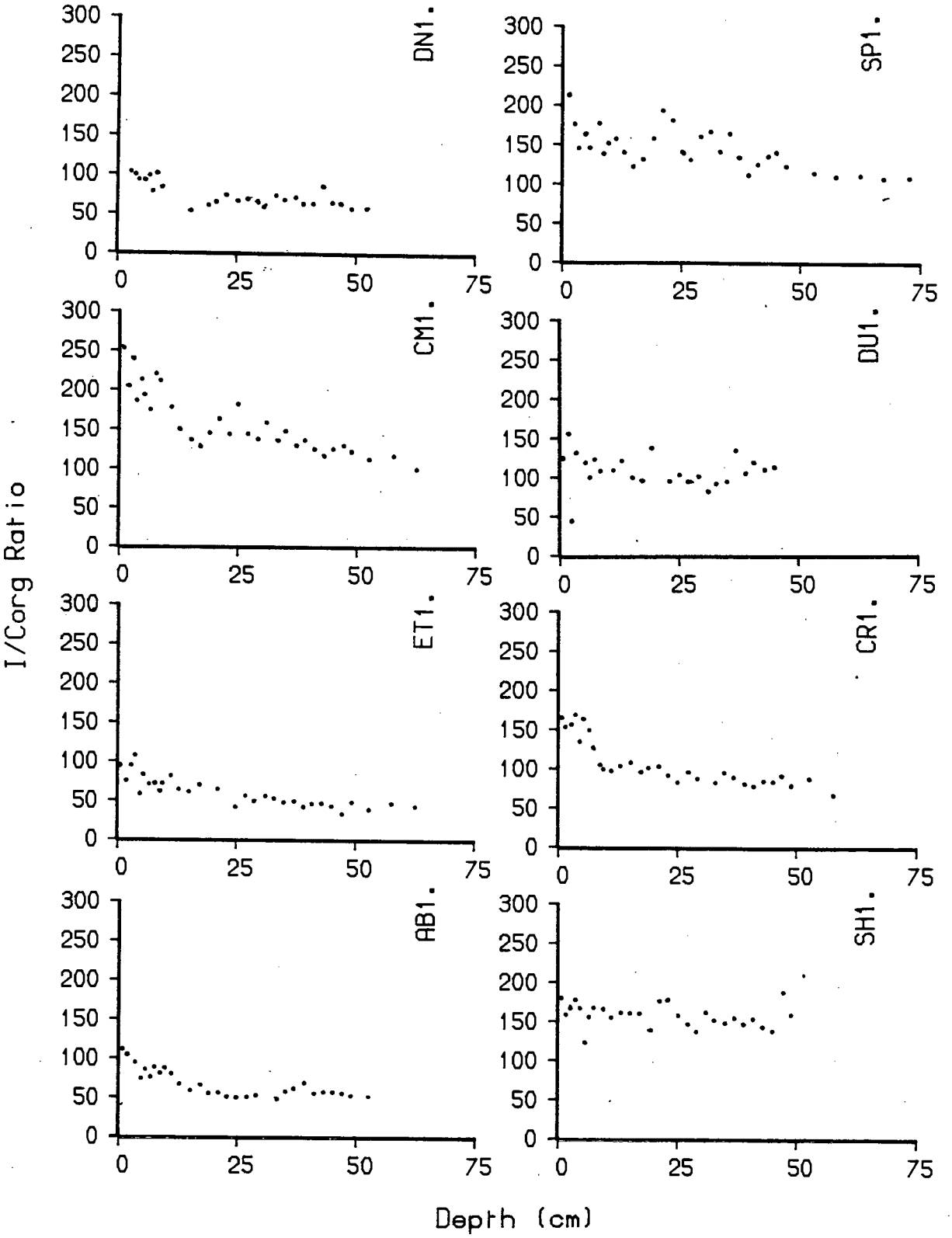

FIGURE 6.4: The patterns of I/C ratios in the sediments.

The association of I with marine organic matter may possibly provide an additional tool for identifying the provenance of organic matter in coastal sediments.

I/C ratios in surface sediments vary from 105 in core ET1 to 254 in CM1 (Table 6.4). Price and Calvert (1977) suggested that an I/C_{org} ratio of 250 was likely for oxic sediments dominated by marine organic matter. This being the case, then CM1, SP1 and SH1 can be seen to be much more marine in character than, for example AB1 and ET1. For comparison the C/N ratios of the sediments are given in Table 6.4. These values are compatible with the trends seen in I/C. Surface C/N ratios are lower in cores CM1, SP1 and SH1 than at depth indicating possibly a greater marine influence at the surface. However, comparison of I/C and C/N ratios with the distribution of $\delta^{15}N$ (see Table 6.4) can show a number of unexplained inconsistencies. Cores CM1 and SP1 showing relatively high $\delta^{15}N$ values also show I/C and C/N values which are consistent with the concept of sediment dominated by marine organic matter. In contrast, ET1 shows $\delta^{15}N$, C/N and I/C ratios that imply greater terrigenous contributions of organic matter. Core SH1 shows much lower positive $\delta^{15}N$ values which contrast with the more marine I/C and C/N patterns. This is likely to be due to external effects of productivity and diagenesis acting upon the $\delta^{15}N$ as discussed in Chapter 5.

At depth, the halogen/C patterns in most cores show a decline in values. The I/C profiles with depth are shown in Figure 6.4. Most of the cores show a concave downward pattern. This is compatible with the release of bound I at a greater rate in the oxic sediments (Price and Calvert, 1977). The decline with depth suggests that the I is mobilised at a greater rate than the bulk of the organic matter.

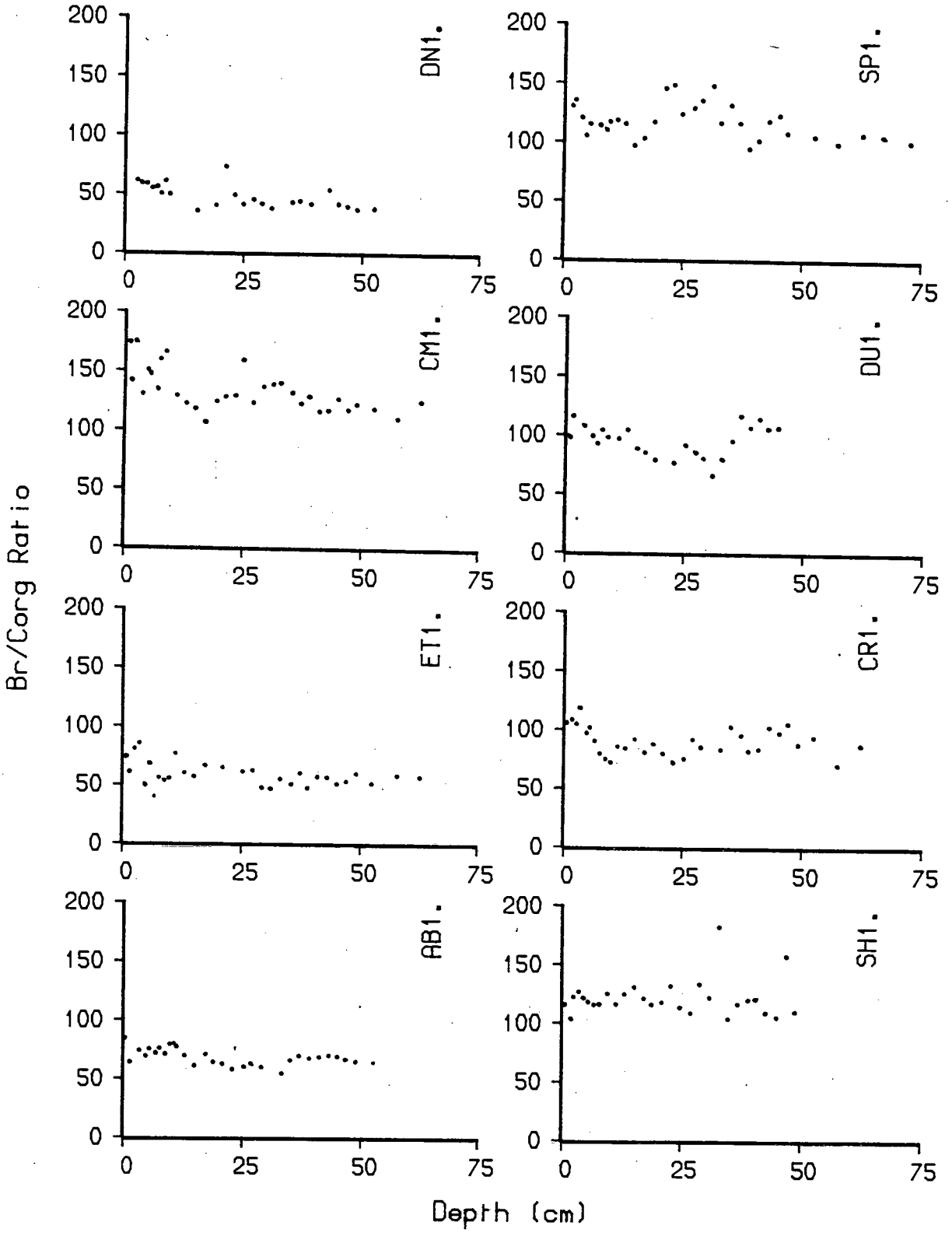

FIGURE 6.5: The patterns of Br/C ratios in the sediments.

Figure 6.5 shows the patterns of Br/C with depth in the sediment cores. The decline is generally much less than that of I/C. The implication here is that Br is less labile than I with burial. This supports the patterns of I/Br in the sediments and is consistent with the findings of Price and Calvert (1977), Harvey (1980) and Ridgway (1984).

CHAPTER 7

COPPER, LEAD AND ZINC IN THE SEDIMENTS

7.1. Introduction.

In this Chapter the Cu, Pb and Zn contents of the sediments will be considered. The relationships of the metals to the geochemistry of other phases, especially lithology, organic matter and halogens will then be discussed.

It was seen in Chapter 6, that the elements such as I and Br were associated with the marine organic fraction of sediments and showed little association with the inorganic detritus. Cu, Pb and Zn however, can be partitioned between detrital and anthropogenic phases. For instance, many workers who have investigated these metals in coastal environments have emphasised the anthropogenic input (Bruland *et al*, 1974; Erlenkeuser *et al*, 1974; Goldberg *et al*, 1977, 1978; Lyons *et al*, 1983). In areas more remote from pollutant input, other workers (Elderfield and Hepworth, 1975; Price, 1976; Krom, 1976; Price *et al*, 1978; Galloway and Likens, 1979) have suggested that the patterns of Cu, Pb and Zn observed at depth in sediments are due more to burial diagenesis.

Recently, Ridgway (1984) has observed a close association between Cu, Pb and Zn, the behaviour of SO_4^{2-} and the I/C ratio in sediments from Loch Etive. In the water column particulate heavy metals are also associated with the non-detrital component. However, Loch Etive is unusual on the West coast of Scotland in that its catchment area is by far the largest of any of the sea lochs. As such, there is much terrigenous input as shown by the nature of the organic matter and its association with halogens. It is possible that the unusual content of heavy metals observed by Ridgway (1984) and Malcolm (1981) may be associated with the relatively large fresh water input. For this

reason, this study has examined sediments over a greater range of environments encompassing sediments from the Northwest coast of Scotland as well as from the Oban area.

7.2. Results.

Heavy metals (Cu, Pb and Zn) were analysed by X-Ray Fluorescence Spectrometry (see Appendix I, Section 2.2). The data is presented in Appendix II, Table AII.9. All of the data has been recalculated on a salt free basis.

The surface values of Copper (Cu) in the sediments vary from 8ppm in CM1 to 31 ppm in ET1 (see Table 7.1). The values found for Loch Etive in this study (AB1 and ET1) are similar to those found by Ridgway (1984). He quotes surface values of 29ppm for the inner basin and 25ppm for the sediments of the outer basin. Table 7.2 shows surface metal contents from other coastal localities. The Cu concentrations seen in this study are similar to those found in; the Southern California coastal zone (Bruland *et al*, 1974), Southern Chesapeake Bay (Goldberg *et al*, 1978), the Savannah River estuary (Goldberg *et al*, 1979) and Ranafjord (Skei and Paus, 1979), but less than the concentrations found in Narragansett Bay (Goldberg *et al*, 1977), the Baltic Sea (Erlenkeuser *et al*, 1974) and Foundry Cove (Bower *et al*, 1978).

At depth Cu concentrations decrease in most cores (Figure 7.1). Those sediment cores showing higher Cu contents show more prominent decreases, whilst sediment cores with surface values of Cu of less than 20ppm, e.g. CM1 show little change. Much of the change in Cu concentration in these cores occurs in sediments immediately below the surface, in or just below the biomixed layer.

Core	Metals (ppm)		
	Cu	Pb	Zn
AB1	26	81	213
CM1	8	31	75
CR1	14	41	117
DN1	21	57	154
DU1	25	55	157
ET1	31	86	243
SH1	19	38	121
SP1	19	49	146

TABLE 7.1: Surface concentrations as a mean of the upper 5cm of sediment.

Location	Metals (ppm)			Author
	Cu	Pb	Zn	
Loch Etive				
(Inner)	29	110	259	Ridgway
(Outer)	23	81	192	(1984)
Firth of Lorne	8	49	118	
Loch Etive				
(Inner)	28	103	265	Malcolm
(Outer)	31	56	266	(1981)
Savannah R.	50	44-53	90-100	Goldberg *et al.* (1979)
S. Chesapeake Bay	22-41	33-61	118-250	Goldberg *et al.* (1978)
Long Island Sound *	9	47	120	Grieg *et al.* (1977)
S. California	30-50	30-40	80-140	Bruland *et al.* (1974)
Baltic Sea	63.6	64.6	316	Erlenkeuser *et al.* (1974)
Foundry Cove	81	186	300	Bower *et al.* (1978)
Ranafjord	57	111	314	Skei & Paus (1979)
Narragansett Bay	202	134	249	Goldberg *et al.* (1977)

* Mean surface values.

TABLE 7.2: Comparison of surface metal contents of sediments from other studies worldwide.

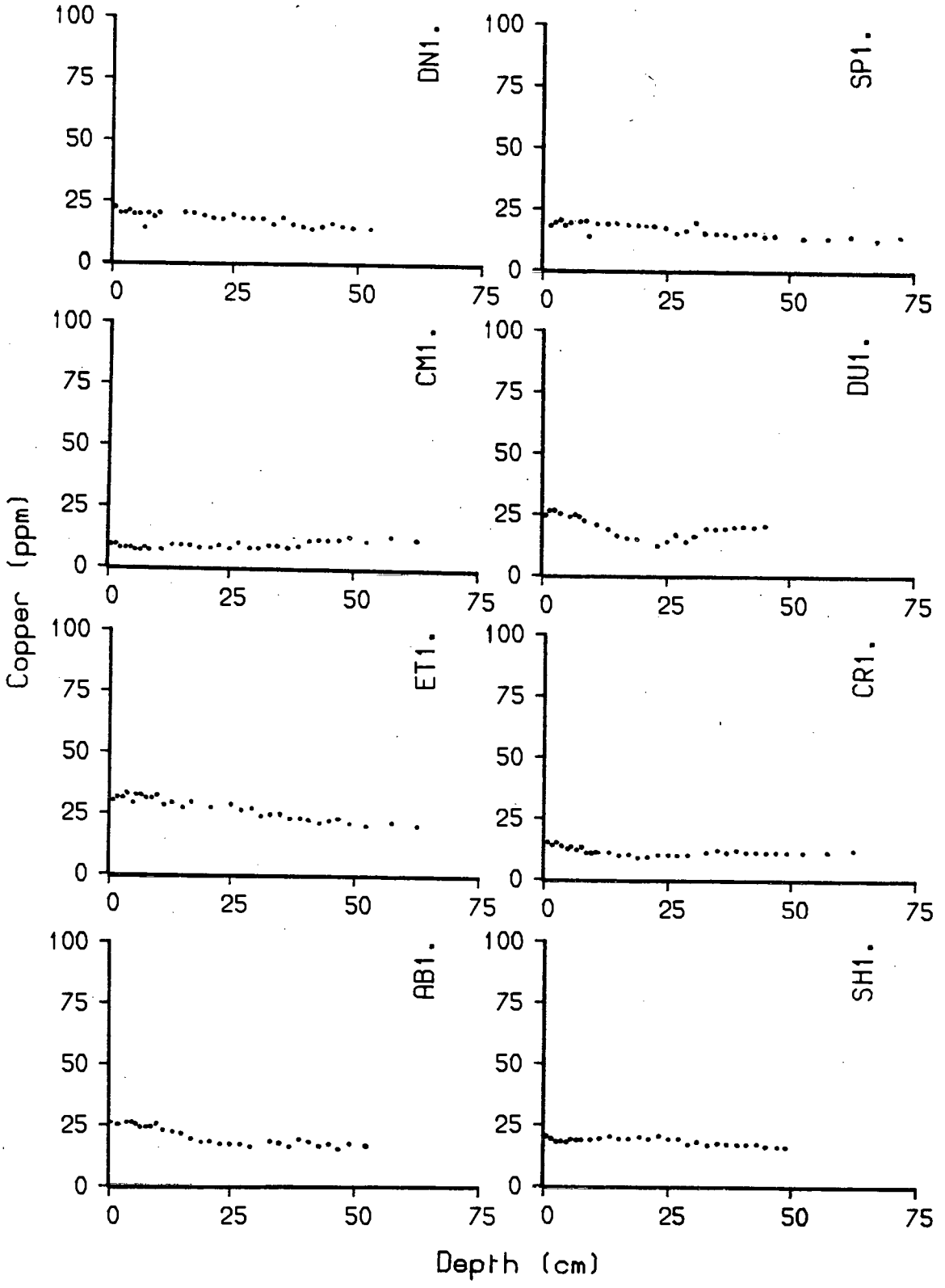

FIGURE 7.1: The patterns of Cu in the sediments.

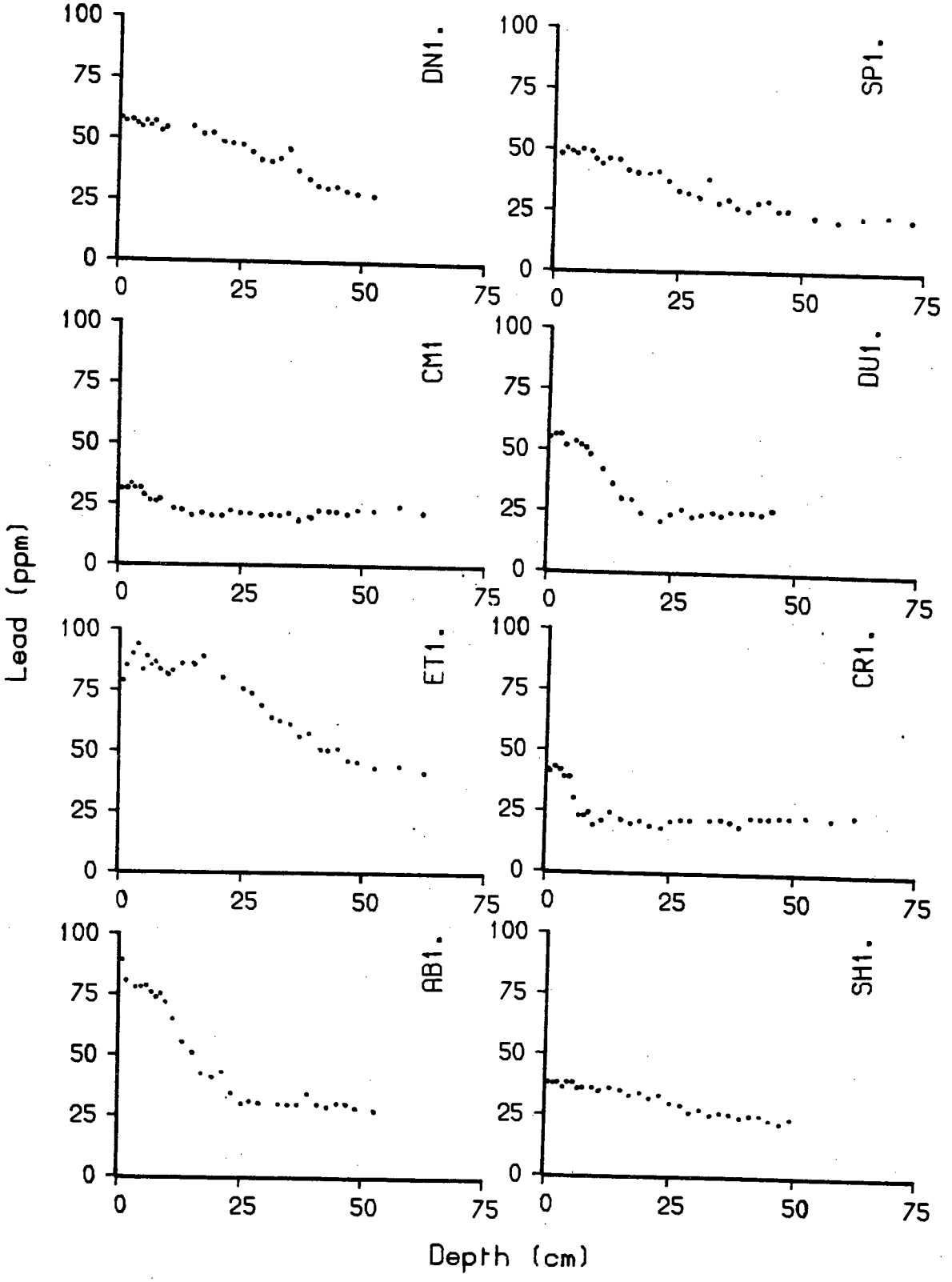

FIGURE 7.2: The patterns of Pb in the sediments.

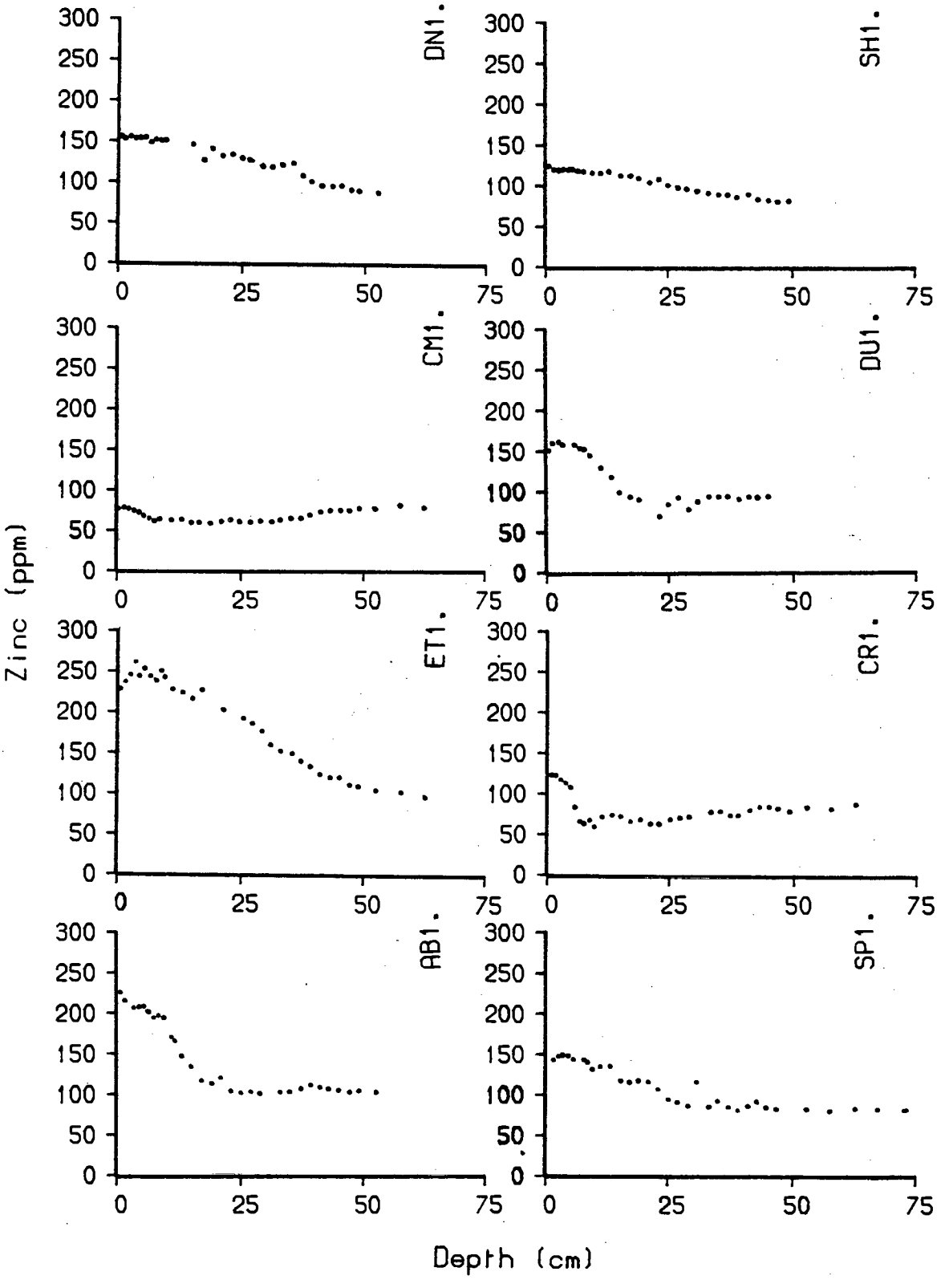

FIGURE 7.3: The patterns of Zn in the sediments.

Lead (Pb) is present in much higher concentrations in the sediments when compared to Cu and often exceeds those found in other sediments quoted in Table 7.2. Pb contents are highly variable in the surface sediments. The highest concentrations occur in the sediments of Loch Etive (ET1 and AB1) and appear to be lowest in the sediments from outside the fjords which have comparatively low organic contents.

In all cores there is a marked decline in Pb concentration with depth (Figure 7.2), but the pattern of decline appears to be quite variable. Nevertheless, in most cores, the most marked change occurs in the sediments immediately below the biomixed zone. In the deeper parts of the cores, the Pb concentration becomes constant and tends to follow the alumina content trends as seen by Zr/Rb. The trends in the upper portions of cores CR1 and DU1 are consistent with the observations that CR1 has a sediment hiatus as marked by the shell band between 5cm and 12cm and DU1 shows a mixing pattern between the older clay and newer sediment above. However, the perturbations in the Pb patterns in these cores can be only partly explained by the lithological variations described in Chapter 3. There is obviously some other fundamental control affecting its distribution, especially its increase in concentration towards the sediment water interface.

The surface values of Zinc (Zn) in the sediments are much higher than Cu or Pb ranging from 76ppm in CM1 to 227ppm in AB1 (Table 7.1). These values, like Pb, are considerably higher than those of average shale (Turekian and Wedepohl, 1961) but are very similar to those found by other authors (Table 7.2) who have associated metal enrichment with anthropogenic inputs (eg Goldberg *et al*, 1978; Bruland *et al*, 1974; Greig *et al*, 1977).

At depth Zinc (Zn) shows a decline in concentration similar to Pb (Figure 7.3). The concentrations at the base of cores ET1, AB1, and DN1 are much higher than in the other cores examined (~90ppm) and tend to follow the trend in Pb contents which exceed 25ppm. These values exceed those of deeply burrowed sediments examined by Malcolm (1981) and Ridgway (1984). The upper section of the sediments show high Zn values which are mainly constant, much of the decrease in content occuring just below the biomixed zone. In DU1, the sediment mixing interval observed in the concentrations of Pb, organic N and other elements can also be seen in the Zn contents

7.3. Metal/Rubidium Ratios.

Heavy metals in these sediments are almost certainly partitioned between authigenic and lithogenic fractions of the sediment. Hence, some of the down core metal variations (Figures 7.1, 7.2 and 7.3) will be caused by lithological variation. In order to reduce the effect of this variability, the heavy metal contents have been normalised to Rb, an element that has often been used to express the aluminosilicate fraction of the sediments (see Chapter 3). Figures 7.4, 7.5 and 7.6 show the metal/Rb patterns in the cores. These emphasise the surface enrichment patterns noted for the Pb and Zn profiles, but the decrease in Cu/Rb ratios is not so well defined. At the base of the cores the Zn/Rb ratios tend to be relatively uniform and except for AB1, show constant ratios between cores. A similar pattern is seen for Pb/Rb ratios, but here there is a more pronounced difference in the ratio at the base of ET1 than in other cores.

Table 7.3 shows factors of surface enrichment over the baseline values as calculated from the metal/Rb ratios. In all the cores Pb is enriched the most

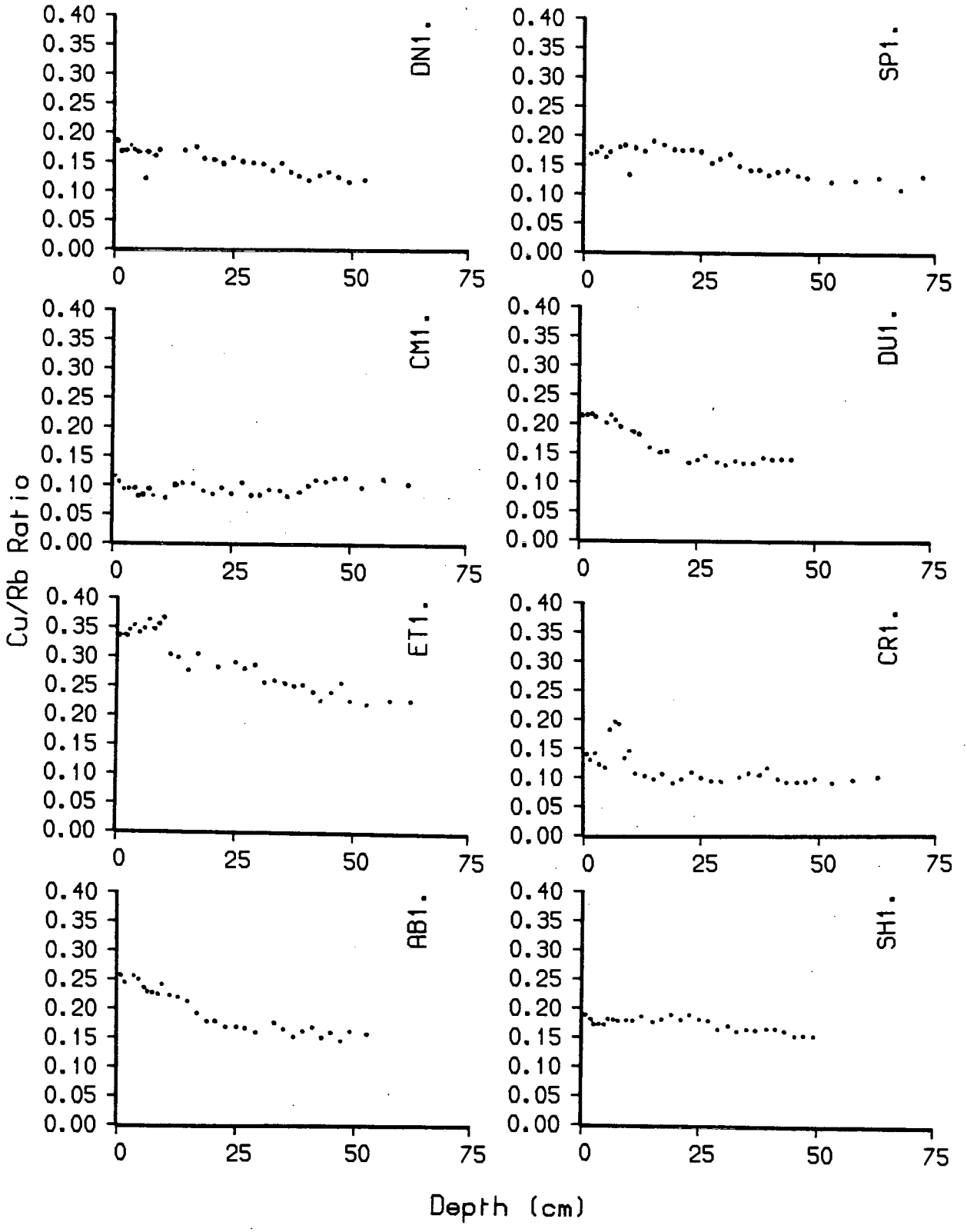

FIGURE 7.4: The patterns of Cu/Rb ratios in the sediments.

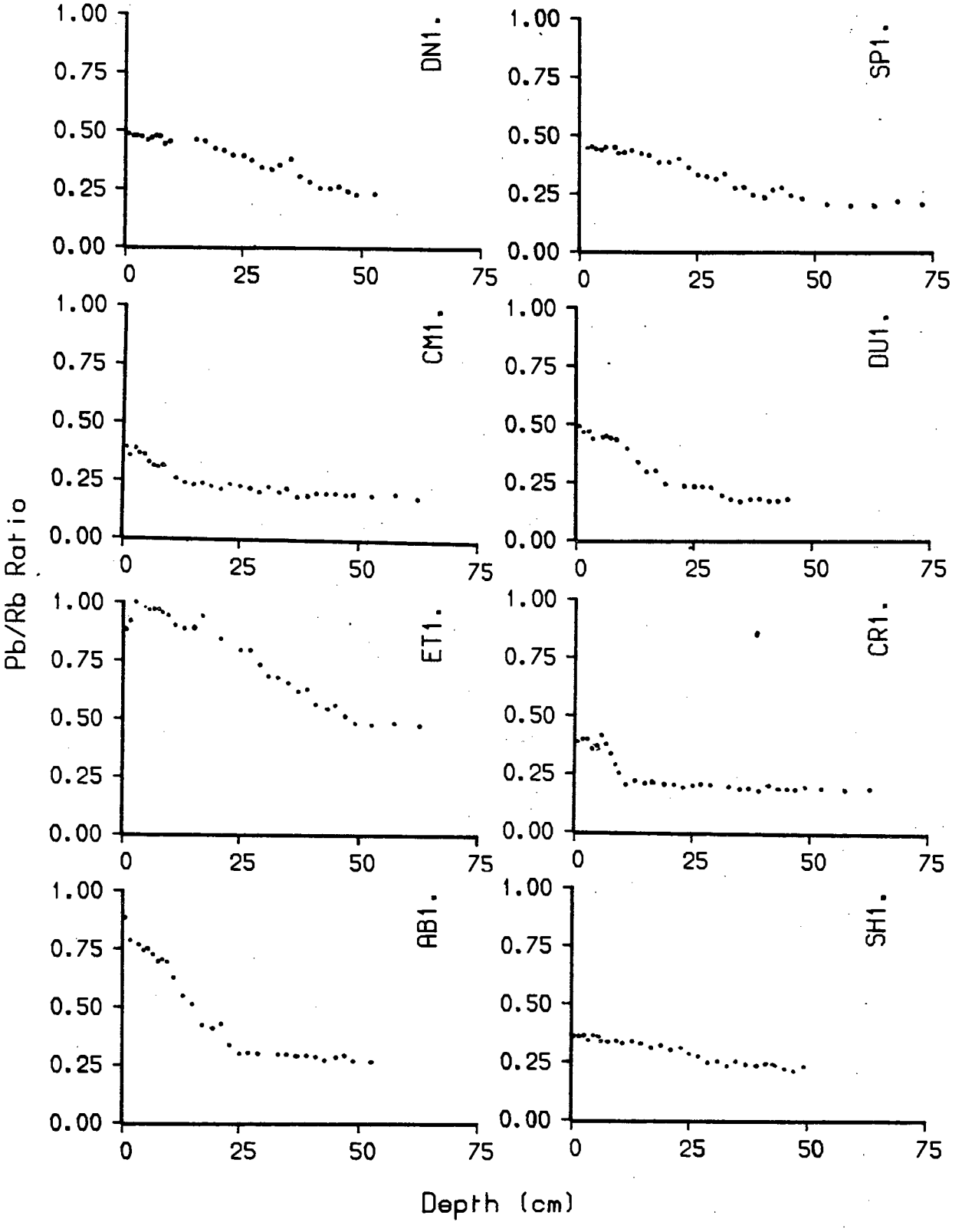

FIGURE 7.5: The patterns of Pb/Rb ratios in the sediments.

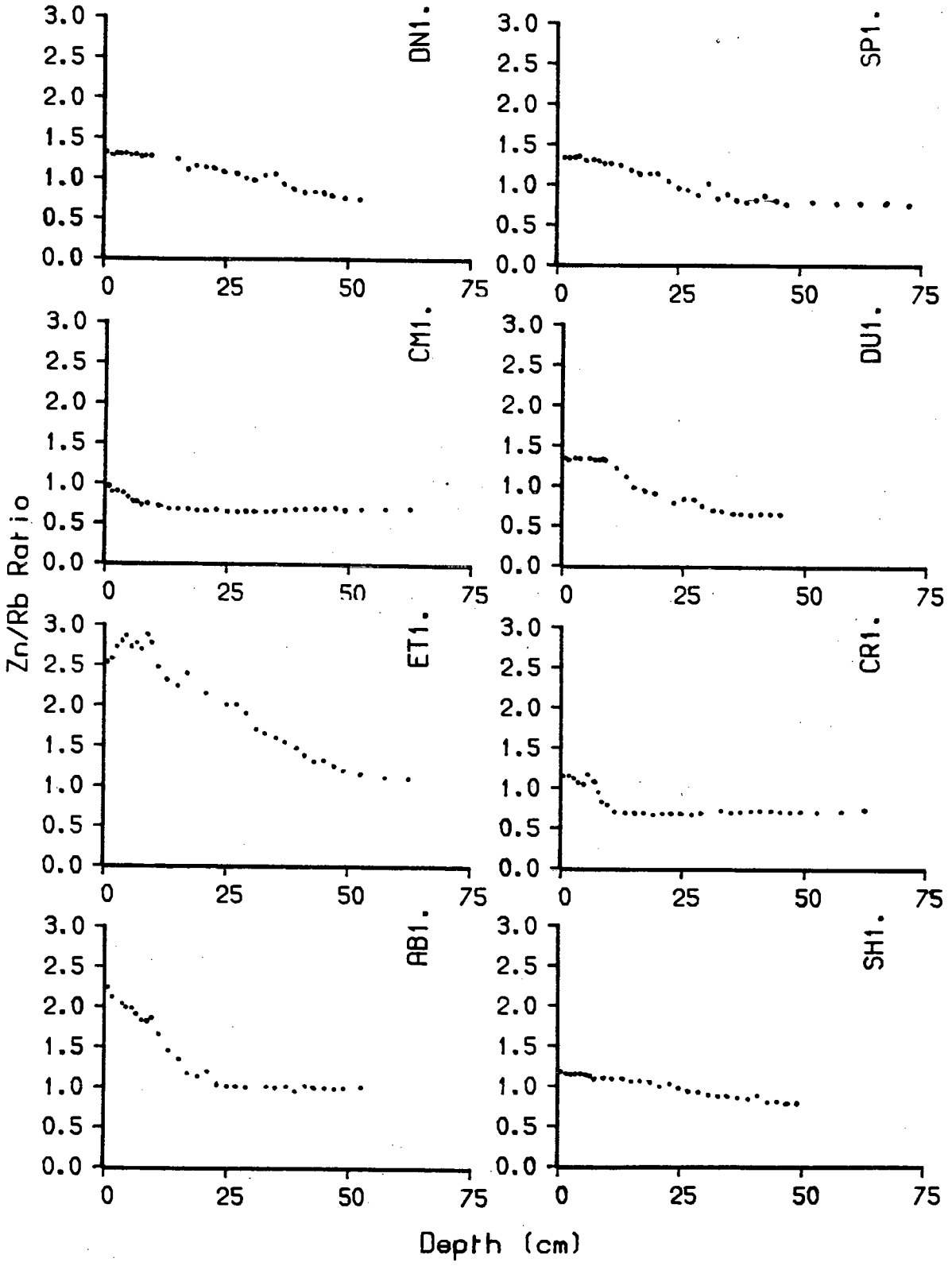

FIGURE 7.6: The patterns of Zn/Rb ratios in the sediments.

Core	Cu	Pb	Zn
AB1	1.61	3.09	2.27
CM1	1.09	2.15	1.42
CR1	1.44	2.01	1.60
DN1	1.56	2.12	1.76
DU1	1.61	2.10	1.72
ET1	1.62	2.17	2.62
SH1	1.21	2.16	1.75
SP1	1.27	2.16	1.75

TABLE 7.3: Surface metal enrichment values as calculated from metal/Rb ratios.

Core	Pb_x	Zn_x	Zn_x/Pb_x	C_{org}
AB1	47	95	2.02	4.67
CM1	18	26	1.44	0.77
CR1	21	42	2.00	1.68
DN1	27	57	2.11	3.23
DU1	26	50	1.92	4.61
ET1	39	135	3.46	6.15
SH1	27	57	2.11	1.86
SP1	26	56	2.15	1.93

$r_{Pb} = 0.798$

$r_{Zn} = 0.869$

TABLE 7.4: Excess metal (ppm), Zn_x/Pb_x and C_{org} (%) concentrations in the biomixed zone of the cores examined with correlation coefficients of excess metal to C_{org}.

followed by Zn, with Cu being the least enriched. As well as varying between metals, the enrichment factors vary across the cores. ET1 and AB1 have the greatest metal enrichment, CM1, SH1 and CR1 the least.

7.4. Origin Of The Metals And Their Behaviour During Burial.

7.4.1. Introduction.

Heavy metal enrichments of surficial sediments have been noted in numerous coastal environments (Chow *et al.* 1973; Bruland *et al.* 1974; Goldberg *et al.* 1977, 1978, 1979; Skei and Paus, 1979). Most authorities have assumed that such enrichments above a baseline concentration represent an anthropogenic presence and furthermore, the patterns of metal enrichment have been used to describe the history of anthropogenic contamination of an environment (Erlenkeuser *et al.* 1974; Bruland *et al.* 1974; Goldberg *et al.* 1977, 1978, 1979). But, Cu, Pb and Zn can be derived from both natural and anthropogenic sources. Much of the metals from the natural sources will enter the sediments associated with the terrestrial detrital material derived from weathering in the catchment area. The sources of anthropogenic metals, their introduction to the sediment and their behaviour during sediment burial are much more complex. They may be derived from direct input from local sources such as industrial and domestic waste. Indeed many previous studies of metals in the environment have concentrated on sediments close to a direct pollutant source (Galloway, 1979; Halcrow *et al.* 1973; Crecelius *et al.* 1975; Bower *et al.* 1978). With sediments enriched in non-detrital heavy metals in areas remote from direct pollutant input, transport from a remote source by aeolian processes and fallout by precipitation is suggested (Bertine and Goldberg, 1971; Swaine, 1977; Goldberg, 1976(b); Franzin *et al.* 1979). Such

fallout of trace metals over land, sea and in remote areas, has been measured (Lazarus *et al*, 1970; Ranticelli and Perkins, 1970; Nraigu, 1979; Shirahata *et al*, 1980; Saule and Patterson, 1981; Boutron and Patterson, 1986). These measurements clearly show that the atmosphere is a major pathway for pollutants to enter remote environments (Galloway and Likens, 1979). Nevertheless, trends in heavy metals, especially in regions removed from industrial sources may not always depict the history of pollution. Other workers studying metals in remote environments (Elderfield and Hepworth, 1975; Price, 1976; Krom, 1976; Price *et al*, 1978; Galloway and Likens, 1979; Ridgway and Price, 1987) have suggested that whilst anthropogenic input of metals to remote sediments occurs, the patterns of Cu, Pb and Zn observed in the sediments may be modified by burial diagenesis. In this study an examination of the heavy metal contents has been made with the intention of identifying their behaviour under oxic, sub-oxic and anoxic burial. Additionally, a close inspection of the patterns of accumulation of the metals in the sediments and their geochemical associations with the major sedimentary constituents, aluminosilicates, organic matter and sulphides may help in identifying the mechanism of accumulation of heavy metals in sediments.

7.4.2. Excess Heavy Metal Contents And Their Incorporation Into The Sediment.

The metal values discussed in Section 7.2 represent either total contents and/or their relationship to the aluminosilicate fraction expressed as metal/Rb ratios. It is unlikely that lithogenic metals play a constituent part in the incorporation of pollutant metals in the sediments. It is therefore desirable to consider the content of the excess metals over and above the lithogenic input before a possible interpretation of their origins is made. In order to do this, the values of Pb and Zn were ratioed to Ni, which from Chapter 3 was seen to

be associated with the detrital fraction and invariant with depth. The association of Cu, Pb and Zn with Ni is probably a more satisfactory normalisation than to Rb as it is assumed that within the alumina related phase all four elements will be concentrated in ferromagnesian detritus rather then aluminosilicates as depicted by Rb. The excess metal (M_{ex}) at each depth in the cores was then calculated using equation 7.1.

$$M_{ex} = (M/Ni_D - M/Ni_B) \cdot Ni_D \qquad (7.1)$$

Where: M/Ni_D = Metal/Nickel ratio at depth (Dcm)

M/Ni_B = Mean background ratio

Ni_D = Nickel concentration at depth (Dcm)

Excess metal values for all the cores are presented in Appendix II, Table AII.10. Surface values of excess Pb and Zn are shown in Table 7.4 together with comparative C_{org} values and Zn_{ex}/Pb_{ex} ratios.

The trends in Cu, Pb and Zn, as expressed by the distribution of excess metal contents, show a different distribution from detrital metals (see Figures 7.7 and 7.8). This comparison, however, does not express the differences in the metal contents at the bottom of the different cores, for instance, the higher metal contents at the base of core ET1. This will be considered later. Excess metal distribution clearly shows an increased loading of the sediment towards the sediment water interface and could imply increased anthropogenic metal loading of all the sediments. These metals have often been associated

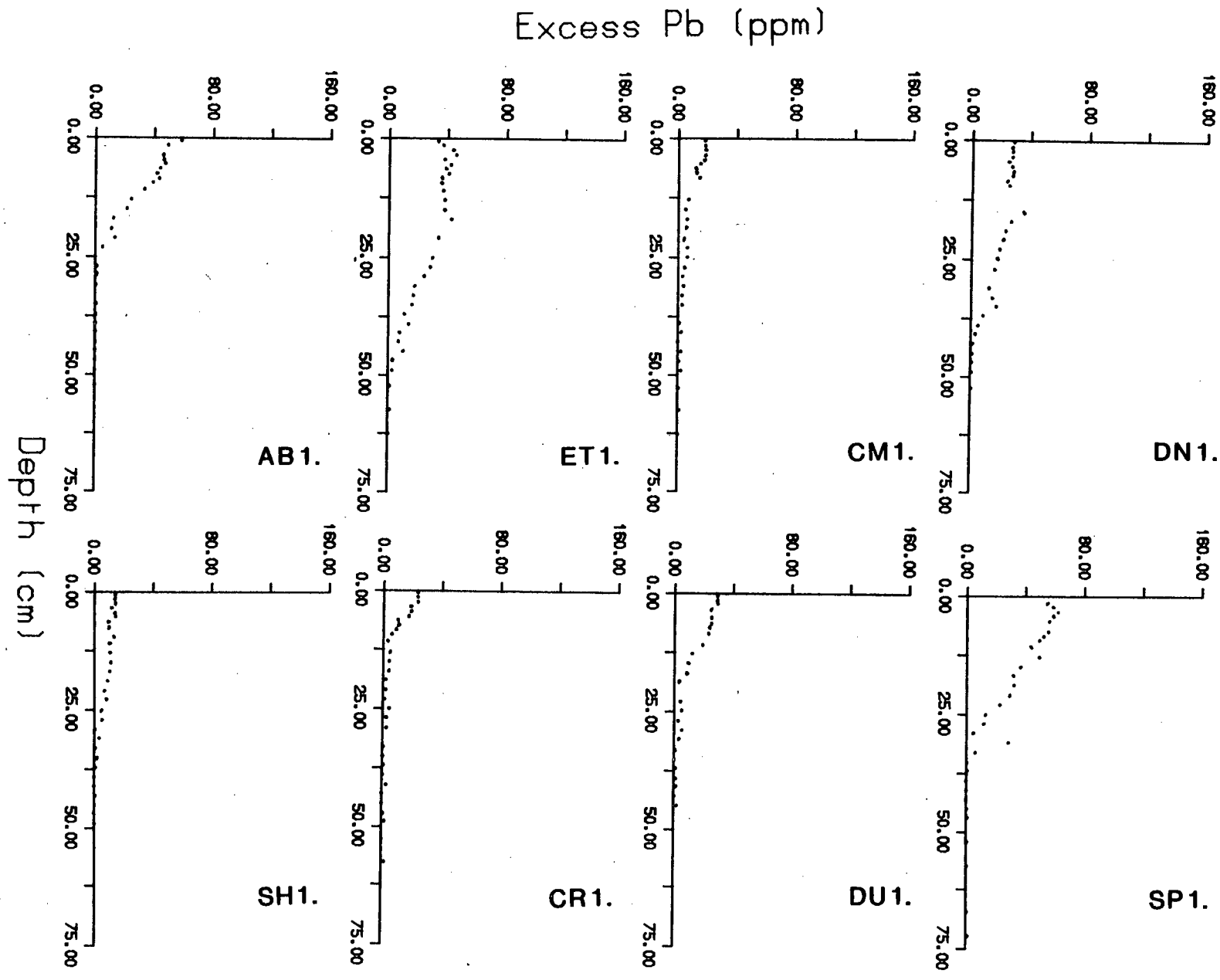

FIGURE 7.7: The patterns of excess Pb in the sediments.

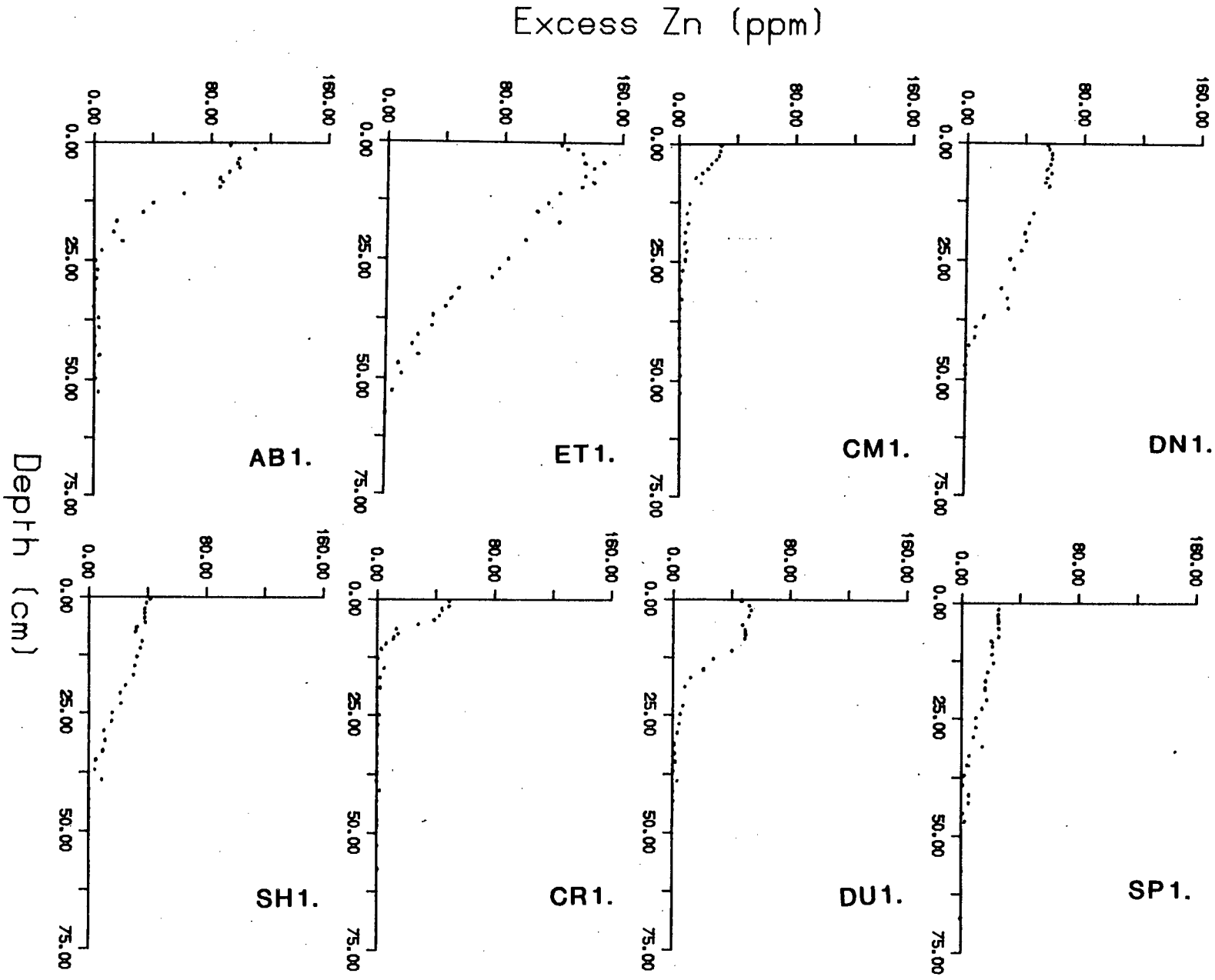

FIGURE 7.8: The patterns of excess Zn in the sediments.

with the organic matter in sediments (Calvert and Price, 1983). However, consideration of the distribution of organic Carbon (Figure 4.1) shows general uniformity with depth in each core and hence there is no obvious relationship between M_{ex} contents and the total organic matter in the sediments. The lack of such correlation may be due to the origin of the organic matter, marine and terrigenous, but it is possibly more related to the quality of the organic matter i.e., the metabolisable content and the change of this down each core. In Chapter 6, the behaviour of I and Br in the sediments have been described and their relationships with C and N have been discussed with respect to organic matter sources and to behaviour with burial diagenesis. Given the observed trends of halogens, it is sensible to consider the patterns of heavy metals at depth in the sediments to be a consequence of diagenetic reactions as well as of anthropogenic loading. Therefore, the excess metal contents of Pb and Zn have been plotted against I as shown in Figures 7.9 and 7.10. These plots are analogous to plots of metal/Rb *vs* I/C used by Ridgway and Price (1987) but are possibly less sensitive to errors caused by detrital variations between different environments. The graphs show that there is a direct positive relationship between I and excess metal as expressed in Table 7.5. However, the relationship between metal and halogen is very different in the surface sediments than at depth. From pore water data, S and halogen patterns, a biomixed layer has been identified in all sediments corresponding to at least 10cm of sediment accumulation. These horizons show a more gradual Zn/I decline than in the sediments below the biomixed zone. It appears that the uppermost sediments showing oxic/sub-oxic character can show appreciable loss of I relative to metal change. Lower down, in the anoxic sediments, the trend of I *vs* M_{ex} is very much the same for most cores except DU1 where sediment mixing is prevalent. The mean Pb_{ex}, Zn_{ex} and I contents for the

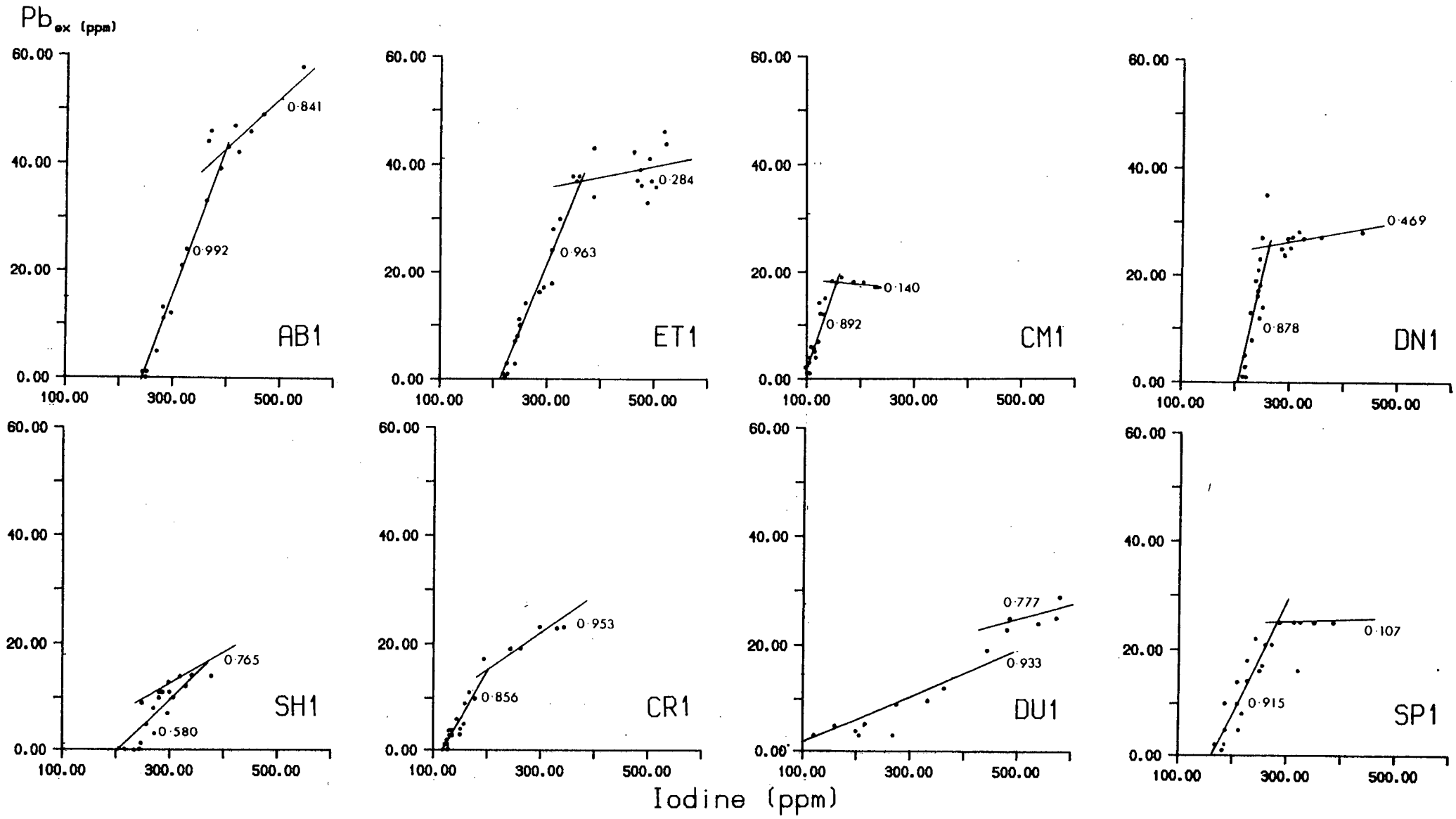

FIGURE 7.9: The relationship of Pb_{ex} to I with depth in the sediments.

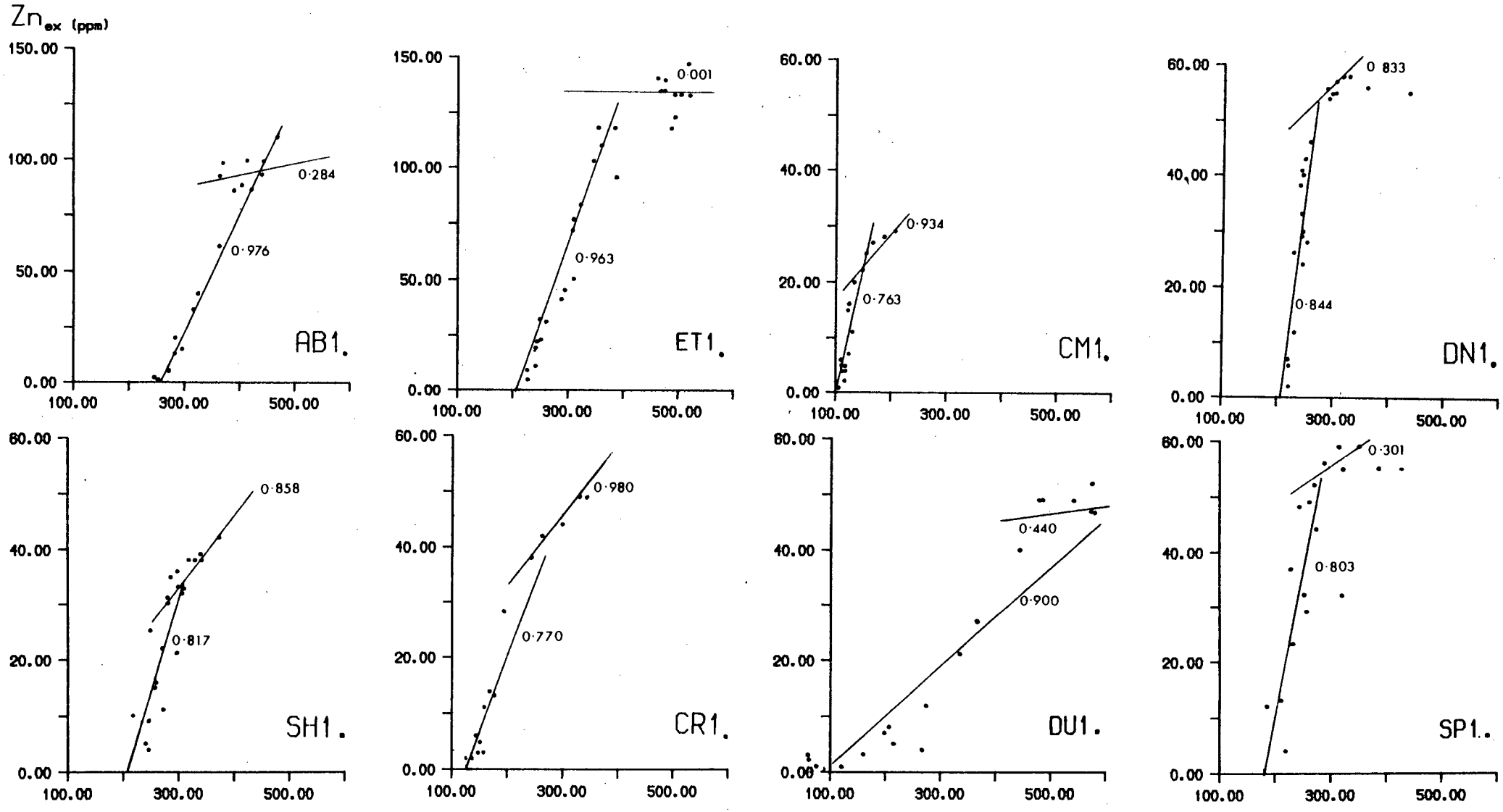

FIGURE 7.10: The relationship of Zn_{ex} to I with depth in the sediments.

Core	Pb		Zn	
	Biomixing	At Depth	Biomixing	At Depth
AB1	0.841	0.992	0.284	0.976
CM1	-0.140	0.892	0.934	0.736
CR1	0.953	0.856	0.980	0.770
DN1	-0.120	0.878	0.833	0.844
DU1	0.777	0.933	0.440	0.900
ET1	0.248	0.963	0.001	0.963
SH1	0.765	0.580	0.858	0.817
SP1	0.107	0.915	0.307	0.803

TABLE 7.5: Correlation coefficients of excess metals against Iodine for sediments both within the biomixed zone and at depth.

	INNER BASIN		OUTER BASIN	
	Surface	Baseline	Surface	Baseline
Cu	0.199	0.081	0.177	0.116
Pb	0.322	0.166	0.551	0.205
Zn	0.935	0.400	1.435	0.723

Fluxes calculated from:

$$F_i = R\,(1-\phi)C\rho\,.10^{-2}$$

Where: F_i = Flux (g m^{-2} yr^{-1})
C = Concentration of metal (ppm)
R = Sedimentation rate (mm yr^{-1})
ϕ = Porosity
ρ = Sediment density (taken as 2.65 g cm^{-3})

The sedimentation rates were taken as 1.37mm yr^{-1} for the inner basin and 1.64mm yr^{-1} for the outer basin (see Ridgway, 1984).

	Cu	Pb	Zn
Atmospheric Input (1971) Wraymires	0.032	0.055	0.12

Data of atmospheric fallout at Windermere, England (1971), (Pierson, 1973.

TABLE 7.6: Metal fluxes needed to create the observed metal levels, both surface and baseline in Loch Etive. With atmospheric fallout data for Windermere for comparison.

biomixed zone have been calculated for each core and are plotted in Figure 7.11. Additional material from Loch Etive (Ridgway, 1984) and Loch Duich (Krom, 1976) and additional cores from the North of the area (NE1, Loch Nevis, HO1, Loch Hourn and SN1, Loch Snizort) are also shown. It is clear from these plots that the concentrations of M_{ex} in cores from the North of the region are different to those from the South. In addition, M_{ex} from Loch Etive have much higher concentrations than sediments collected from coastal regions with no direct input from run-off. These differences are accentuated if one allows for the anomalously high metal concentrations found at the base of cores AB1 and ET1. The trends observed above have a number of implications for the behaviour of excess metals in sediments.

1).

There appears to be a geographical control over the distribution of the metals. SH1, DU1, SN1, NE1 and HO1 in the North appear to receive fewer metals than the sediments further South. In DU1, the high level of I values suggest a high level of marine organic matter, on a par with ET1 or AB1. Data collected by Krom (1976) from Loch Duich and plotted in a similar manner, whilst showing lower I values than this study, still shows relatively lower M_{ex} values, supporting a geographical variation in the trace metal input. This would be expected as the northern sediments are more remote from major industrial sources (the Clyde Valley and England) than are the more southerly cores and are thus less affected by atmospheric fallout.

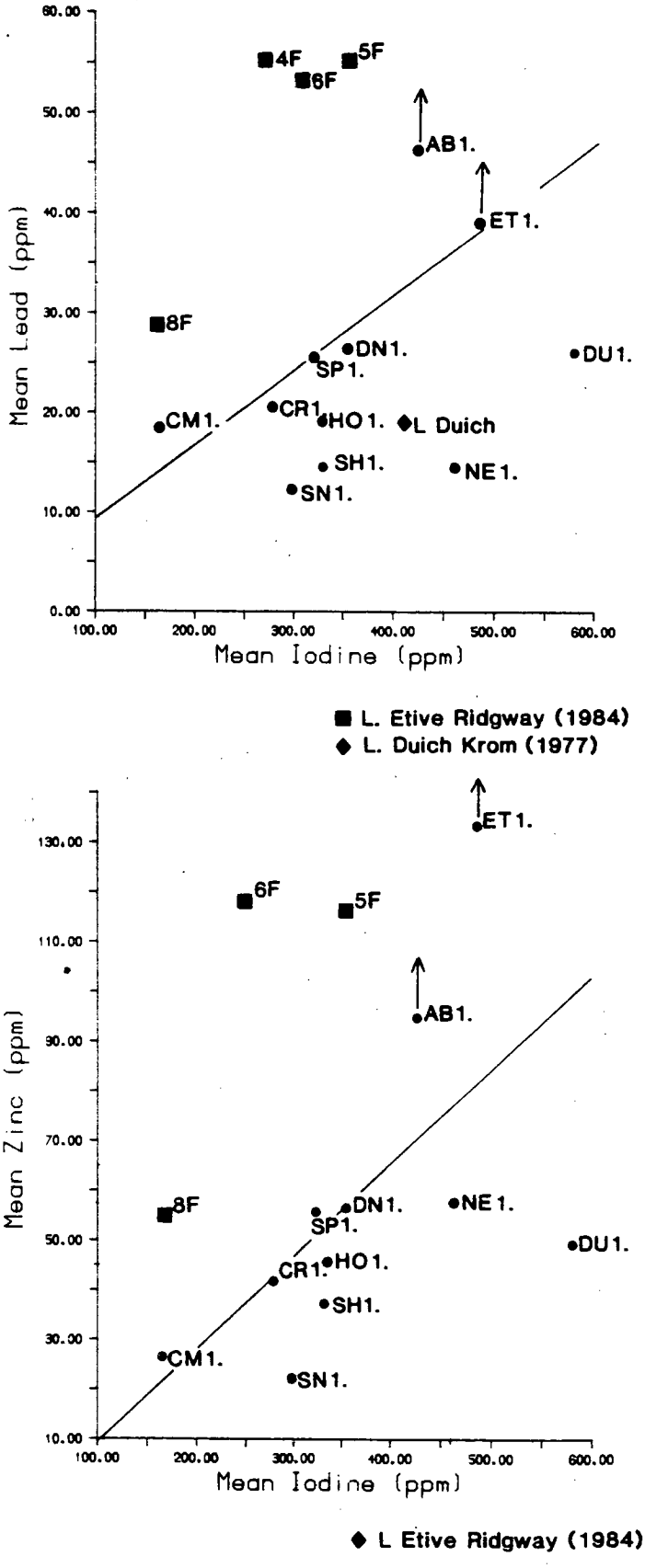

FIGURE 7.11: The relationship of Pb_{ex} and Zn_{ex} to I in the biomixed zone of the sediments. Metal values for AB1 and ET1 may be enhanced due to the depressing effect of the high baseline metal values in these cores.

2).

There is a variation in metal input with the size of catchment area. AB1 and ET1 have much higher metal inputs than the amount of marine organic matter as indicated by I. The catchment area of Loch Etive is the largest in Western Scotland and is an order of magnitude larger than the catchment areas of the other lochs, 1300 Km^2 as opposed to 75 Km^2 for SH1 and 166 Km^2 for Loch Creran. If the atmosphere is a major pathway of metals (Galloway and Likens, 1979), then a larger catchment area will allow a greater amount of metals to enter the loch from surface run-off. Table 7.6 shows the fluxes of anthropogenic metals calculated from the surface excess metal values assuming all of the metals entered the sediments from the overlying water, there being no diagenetic enrichment. No data is available for atmospheric fall-out over the area, but the table includes atmospheric fluxes for Lake Windermere (Pierson *et al*, 1973). These values would be insufficient to produce the amounts of metals seen in the sediments. So, while increased input via a large catchment area may occur, some other mechanism of metal enrichment must also occur.

3).

The ratios of Zn_{ex}/Pb_{ex} in the upper section of the cores are relatively constant at about 2 (Table 7.4). The high ratios at the surface of ET1 (3.46) are caused by neglecting the high baseline values of Pb in this core. If this is taken into account, diagenetic Pb_{ex} will be increased by 20ppm for the whole core. This would reduce the Zn_{ex}/Pb_{ex} ratio to about 2, in line with the other cores. The constancy of Zn_{ex}/Pb_{ex} ratios for all the cores does not necessarily imply that the introduction of these metals to the sediment occurs in the same authigenic or organic phase. Ridgway (1984) showed that in the Loch Etive

particulate matter, the Pb and Zn tended to be preferentially bound to two different phases. While there was some overlap, the Zn appeared to be associated with the particulate organic matter and the Pb was primarily associated with the iron oxides. In the surface sediments this does not appear to be the case. Both Pb and Zn appear to be associated with the organic fraction. Nevertheless, the relationship of the metals to the organic material is obviously different. In Figure 7.11, the best fit line for Zn for the four cores CM1, SP1, CR1 and DN1 has an intercept very close to zero. This would be expected if it was assumed that all of the M_{ex} is associated with the marine organic matter. The best fit line for Pb has a positive intercept, implying that not all of the Pb is associated with the marine organic fraction. In oceanic sediments metals have been seen to be associated with Mn and Fe oxides (Calvert and Piper, 1984; Shimmield, 1984; Balistrieri and Murray, 1986) and these metals are thought to be released as their host phases are reduced. The sediments from this study do not have such high concentrations of Mn or Fe (Ridgway, 1984), nor do the sediments have such oxic surface sediments as oceanic sediments. It is possible that in the sediments of the study area, the FeO is rapidly reduced very close to the sediment water interface allowing Pb to be released and adsorbed onto organic matter.

4).

In the lower sections of the cores the correlation between Zn, Pb and I is excellent with correlation coefficients ranging between 0.76 and 0.98. The slope showing the change of M_{ex} relative to I is mostly uniform apart from the mixing profile observed in DU1. The diagenetic recycling of trace metals at depth in the sediment needs to be considered as a source of metal enrichments. The possible role of redox reactions associated with Mn and Fe

has already been considered, but it is not thought to play as important a role in these sediments as in deep sea sediments where these elements occur in greater concentrations. In coastal sediments the large concentrations of organic matter make this more important. In the next section, the role of the organic matter at depth within the sediment will be considered.

7.4.3. Organic Carbon Diagenesis And Metal Enrichment.

It seems then, that in both the biomixed and the underlying anoxic sediments the trends in excess metals is associated with organic matter degradation depicted in the I profiles. The shallow gradient in the upper portion of the Figures 7.9 and 7.10 reflect organic breakdown in the biomixed zone. The gradients show that the I is released from the organic matter at a faster rate than the metals. At depth the gradients are steeper indicating that the metals are released preferentially to I. This implies that the metals and I are bound to differing organic fractions. From the gradients, it appears that I is more easily released, being preferentially removed in the oxic zone. This is consistent with the findings of Price and Calvert (1977) who suggest that I reacts more rapidly in the oxic environment. A comparison of the gradients for the biomixed region of the cores shows them to be very similar, suggesting that the reaction rates in the oxic zone are similar from core to core. With depth, the gradients of the best fit lines vary. For example, in CM1, there is less metal lost relative to I than in SP1. This may be related to accumulation rate. Where the accumulation rate is slow, for example in CM1, there is less input of organic and detrital material and therefore the reactive organic matter is exposed to rapid oxic breakdown for a longer period. Thus, there is less material incorporated at depth to be reduced anaerobically. Conversely, in ET1, the sedimentation rate is high and much more organic

matter becomes incorporated at depth. This would explain the existence of the higher baseline metal values in ET1 as compared to the lochs with lower sedimentation rates.

CR1 and DU1 show unusual gradients in the best fit lines. In DU1, the shallow gradient suggests than I is being removed, relative to metals, in a similar manner to the reaction in the aerobic zone. This is opposite to that shown by the remaining cores and is interpreted as being due to the influence of the clay at the base of the DU1 core. This clay was responsible for the fall in halogen concentrations with depth (see Chapter 5). It was suggested that the clay, low in organics and halogens, was diluting the sediment above by mixing, possibly caused by bioturbation from deeper burrowing organisms and causing an artificial decline in element concentrations which is not seen in the excess metal values. CR1 is affected by the sediment division at the shell band. The newer sediment above the shell band is probably completely affected by bioturbation.

Comparison of the metal/Rb depth profiles in the sediment with the profiles of solid phase S and pore water SO_4^{2-} shows a distinct pattern. The rapid increase in S correlates well with the zone of metal increase. This is illustrated in AB1, but the pattern can also be seen in CM1 and SP1 (see Figure 7.12(a),(b) and (c)). It was discussed in Chapter 4 that the zone of maximum SO_4^{2-} reduction was actually in or very close to the biomixed zone, but that some SO_4^{2-} reduction occured at depth. This is shown by the increase in S concentration with depth. The correlation of metal values with the SO_4^{2-} reduction was noted in ET1 by both Malcolm (1981) and Ridgway (1984). The amount of SO_4^{2-} reduction occuring at depth in the sediments appears to be controlled by the degree of irrigation of the sediment by deeper burrowing

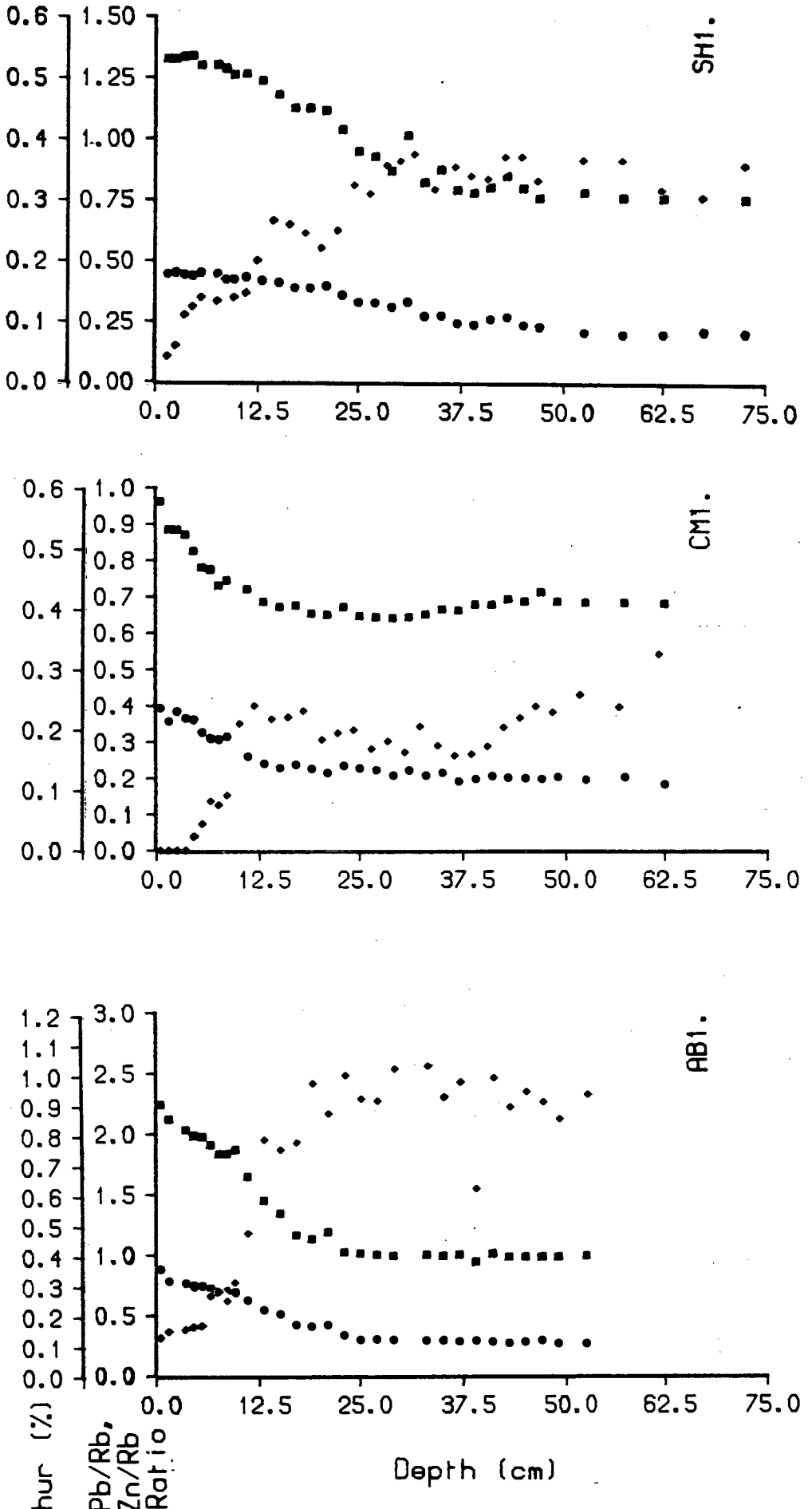

FIGURE 7.12: Patterns of Pb/Rb and Zn/Rb compared to the patterns of solid phase S in cores AB1, CR1 and SH1.

organisms. This in turn controls the anaerobic breakdown of organic matter which regulates the release of the trace metals. Malcolm (1981) suggests that these trace metals once released are free to enter the sediment pore waters causing an observed metal enrichment in the sediment pore waters at depth. This forms a concentration gradient thereby allowing metals to migrate towards the sediment surface where they can be lost to the overlying waters or recycled by adsorption onto organic matter leading to increased metal enrichment at the surface.

CHAPTER 8

SEDIMENT ACCUMULATION RATES

8.1. Introduction.

A number of natural and artificial radio-isotopes have been used to measure accumulation rates in sediments. Koide *et al.* (1972, 1973) applied the decay of ^{210}Pb (a natural isotope) to coastal marine sediments following the work of Krishnaswami (1971) on lacustrine sediments. However, the development of nuclear reactors and the atmospheric testing of nuclear weapons has led to the introduction of a number of artificial radionuclides into the environment. For example, ^{137}Cs derived from atmospheric fall-out of nuclear weapons testing has been used by Ritchie *et al.* (1973), Pennington *et al.* (1973) and Robbins and Edgington (1975) to date sediments. More recently other radio-isotopes such as ^{134}Cs, $^{239,240}Pu$, derived from low-level waste output from nuclear power stations, have been used (Hetherington and Harvey, 1978; Aston and Stanners, 1979; Stanners and Aston, 1981(a) and (b); Bopp *et al*, 1982).

In Western Scotland the sediments are very much influenced by low level nuclear waste discharged from the nuclear fuel reprocessing plant operated by B.N.F.L (British Nuclear Fuels Ltd.) at Sellafield on the Cumbrian coast Livingstone and Bowen, 1979; MacKenzie and Scott, 1982; Swan *et al*, 1982). This site is known to release a number of radionuclides into the environment including; ^{106}Ru, ^{90}Sr, ^{144}Ce, ^{95}Zr, ^{95}Nb and $^{137,134}Cs$.

Cs exists in solution as a monovalent cation. Due to its low reactivitiy, it tends to have a long residence time in the ocean. However, interactions in the coastal environment with particulate, biological and fresh water fluxes results in the incorporation of significant amounts of Cs into the sediments, largely by ion exchange reactions onto clays (Swan *et al*, 1982). In contrast, ^{210}Pb has a

high reactivity and tends to be scavenged by both organic and oxide particulate material (Schell, 1977).

In this study ^{137}Cs has been measured in two cores, DN1 and CR1 and used to estimate the sediment accumulation rate. In addition, ^{137}Cs and ^{210}Pb data obtained from Loch Etive by Ridgway (1984) will be considered. The radionuclide analyses were kindly performed by Dr A.B Mackenzie and Miss T.S Williams at the Scottish Universities Research and Reactor Centre. ^{137}Cs was measured directly by γ-ray counting on a 10cm lead shielded 130cm^3 active volume Ge(Li) detector for 60 hours. The detector was connected to an EG & G Ortec 7032 analyser used for processing the data. The resolution of the detector was 2.1KeV with an absolute efficiency of ~5% for counting. All data are given in Appendix II, Table AII.11.

8.2. Calculation of sediment accumulation rates using ^{137}Cs.

The majority of ^{137}Cs in the sediments in Western Scotland is derived from Sellafield (McKinley *et al*, 1981(a) and (b); McKay and Baxter, 1985). Only a minor proportion is derived from nuclear bomb fall-out (c. 1-3 pCi g^{-1}, Aston and Stanners, 1979; Ritchie *et al*, 1973) and this will be constant over the whole area (Ritchie *et al*, 1973). Sellafield has been discharging radioactive waste since 1952 (Swan *et al*. 1982) and the amount has been increasing with time, although recent years have seen a decrease in discharge (see Table 8.1). As the sediments measured (DN1 and CR1) were collected in 1984, then the appearance of ^{137}Cs in the sediments represents a maximum of 32 years output (Swan *et al*, 1982), assuming there is no post depositional mobilisation of the Cs and little or no bioturbation. In reality this may represent slightly less than 32 years due to the lag time involved in the plume reaching the

Date	^{137}Cs Activity (TBq^{-1})
1964	104
1965	110
1966	181
1967	150
1968	371
1969	444
1970	1154
1971	1325
1972	1289
1973	768
1974	4061
1975	5231
1976	4294
1977	4483
1978	4092
1979	2600
1980	3000
1981	2400
1982	2000
1983	1200
1984	434
1985	325
1986	18

TABLE 8.1: Liquid effluent discharges of ^{137}Cs from Sellafield (1964-1986) (From T.S Williams, Pers Comm).

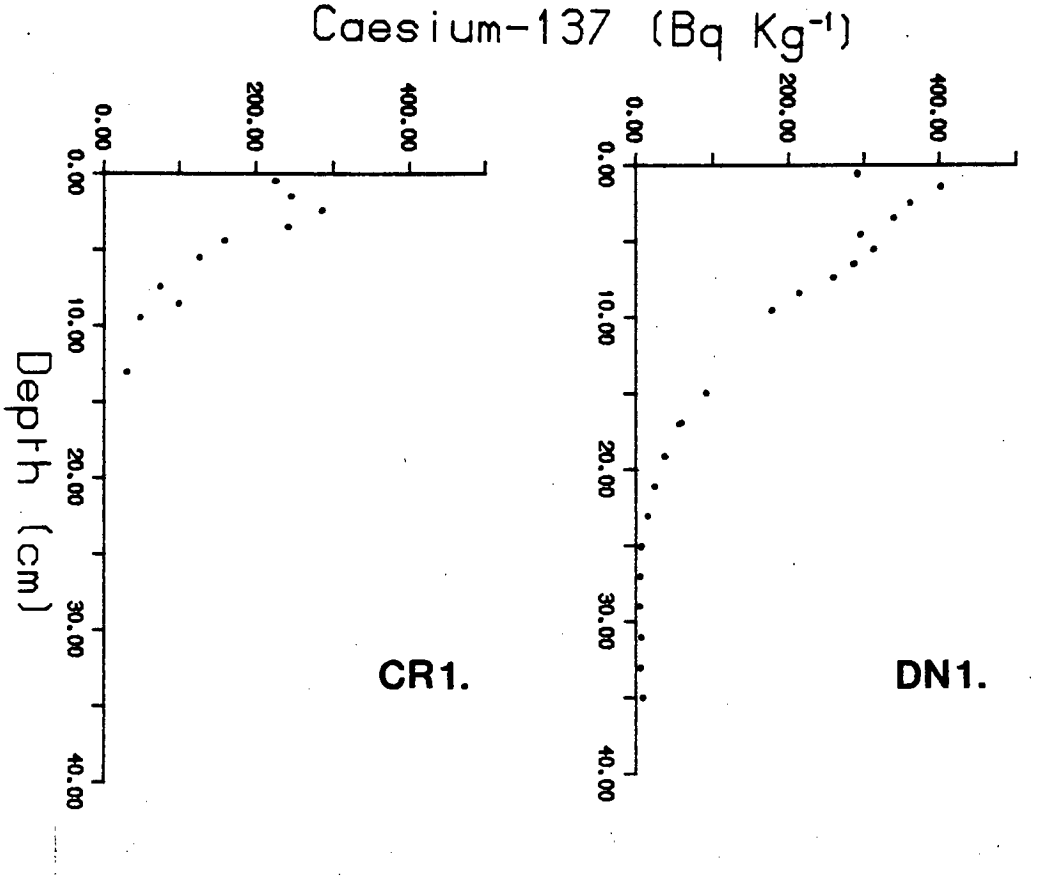

FIGURE 8.1: ^{137}Cs concentrations from cores CR1 (Loch Creran) and DN1 (Dunstaffnage Bay).

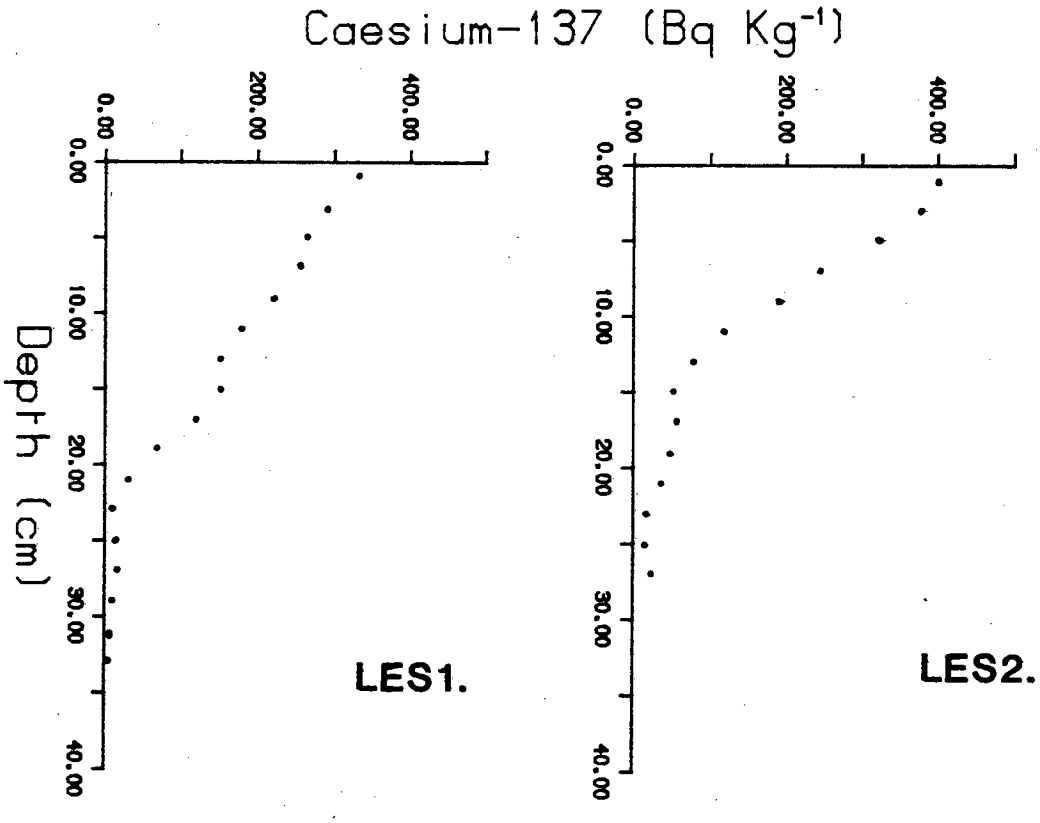

FIGURE 8.2: ^{137}Cs concentrations of two cores from Loch Etive. LES1 (Outer Basin), LES2 (Inner Basin) after Ridgway (1982).

study area. However, McKay *et al.* (1986) suggest that the time for the waste to reach N. Skye from the North Channel is only 4.5 months, thus the lag time may be relatively short.

Figure 8.1 shows the pattern of ^{137}Cs in the sediment cores from DN1 in the Firth of Lorne and CR1. The increasing values towards the sediment surface can be ascribed to increasing Cs discharge (Table 8.1) rather than radioactive decay. The peaks seen in the upper 5cm of the sediments may be ascribed to the 1976-1977 peak in ^{137}Cs discharge. The calculated sediment accumulation rates are given in Table 8.2 together with accumulation rates for Loch Etive measured by Ridgway (1984) using ^{137}Cs, ^{210}Pb and sediment trap methods. Taking the onset of Cs enrichment as 1952, accumulation rates for DN1 and CR1 were calculated at 0.78cm yr^{-1} and 0.68cm yr^{-1} respectively. This is consistent with sediment accumulation rates found by Swan *et al.* (1982) for Gare Loch in the Clyde Estuary (6mm yr^{-1}). However, the values are lower than those calculated by the ^{137}Cs method for Loch Etive by Ridgway (1984) (see Table 8.2), but they are similar to rates obtained by Ridgway using ^{210}Pb and sediment traps (see Table 8.2).

8.3. Discussion.

The large variation in accumulation rates between DN1, CR1 and those of Loch Etive obtained from ^{137}Cs data by Ridgway (1984) is very interesting. There are two possible reasons why this may occur. Firstly, the accumulation rate in Loch Etive may be markedly higher than in the sediments outside the loch. This is possible given the large catchment area and the corresponding input of detrital material to the sediments. (see Chapters 2 and 3). However, the accumulation rates indicated by the sediment trap data are very similar to

Core	Sediment Trap		^{210}Pb		^{137}Cs	
	(a)	(b)	(a)	(b)	(a)	(b)
CR1	--	--	--	--	0.66	5235
DN1	--	--	--	--	0.78	4907
*LES1	0.64	1361	0.33	1311	1.21	4810
*4F	0.64	1361	--	--	1.64	6667
*8F	--	--	--	--	1.50	11035
*LES2	0.80	1061	0.86	2929	1.07	3644
*ET1-A	--	--	--	--	1.07	5884
*5F	--	--	--	--	1.29	3480
*3F	0.80	1061	--	--	1.36	3474

TABLE 8.2: Sediment accumulation rates in cm yr^{-1} and g m^{-2} for sediments from this study and for Ridgway (1984) marked by (*).

Weight of sediment deposited calculated from the expression:

$$z = D(1-\Phi).\rho_s$$

Where: z = total weight of sediment deposited (g cm^{-2})

D = depth (surface = 0)

Φ = mean porosity of the sediments

ρ_s = density of the sediment (2.65 g cm^{-3})

Core	Accumulation Rates		
	1952	1963	1977
CR1	0.66	--	0.29
DN1	0.78	--	0.43
LES1*	0.82	0.86	--
LES2*	0.82	0.94	--

TABLE 8.3: Sediment accumulation rates (cm yr^{-1}) as calculated from known ^{137}Cs peaks observed in the sediments.

(* Corrected accumulation values based on the onset of Cs enrichment rather than on the first appearence of Cs.)

those of DN1 and CR1 from ^{137}Cs. Secondly, there may be errors in the calculation of the accumulation rates in both sets of cores. Sediment cores LES1 and LES2 (Ridgway, 1984) (Figure 8.2) when compared with CR1 and DN1 (Figure 8.1) show similar patterns. The onset of ^{137}Cs enrichment in LES1 and LES2 is slightly higher in the sediment than in DN1. These sediments however, were collected in 1980 and the Cs values, therefore only represent a maximum of 28 years deposition. Recalculating the accumulation rate, assuming 1952 to be indicated by the onset of Cs enrichment, gives sediment accumulation rates of 0.82cm yr^{-1} for both cores. This is much nearer the rates calculated for CN1 and DN1 and closer to the ^{210}Pb and sediment trap data calculated by Ridgway (1984). This casts doubt on the validity of using the first appearance of Cs to calculate accumulation rates (Ridgway, 1984).

A number of problems exist in using radionuclides to calculate sediment accumulation rates. One of the major assumptions is that there is no marked bioturbation in the sediments. This is not the case in these sediments. It was shown in Chapter 4 from SO_4^{2-} and alkalinity data and in Chapter 7 from the change in slope of the excess metal to Iodine plots, that there is an active zone of biomixing down to a depth of at least 10cm in the sediments. It is reasonable to assume that a biomixing zone of similar thickness has been present in the past. This may make using the first appearence of ^{137}Cs as a marker for 1952 (Ridgeway, 1984) a problem. Any ^{137}Cs incorporated into the sediment at that time would be subject to bioturbation and will tend to be dispersed to greater depths. In addition to biomixing diffusion of Cs must be considered. Beasley *et al.* (1982), Santschi *et al.* (1983) and Sholkovitz *et al.* (1983) have noted the mobility of ^{137}Cs in sediments. Sholkovitz and Mann (1984) note enhanced pore water Cs values over those of the

overlying seawater in sediment pore waters from Buzzards Bay. Apparent diffusion rates for ^{137}Cs have been calculated as;

1. 1.1×10^{-8} cm^{-2} s^{-1} (Duursma and Bosch, 1970)
2. 1.3×10^{-8} cm^{-2} s^{-1} (Hess, Smith and Price, 1978)

Applying these diffusion rates to the sediments examined here, diffusion could allow Cs to penetrate up to 13cm deeper in core DN1 and 11cm deeper in cores LES1 and LES2. This is far in excess of the 4.4cm calculated by Ridgway (1984), and coupled with biomixing probably accounts for the relatively constant values of Cs seen at depth in the sediments (Figures 8.1 and 8.2). Calculation of sediment accumulation rate on the first occurence of Cs may, therefore lead to an over estimation. For this reason the 1952 marker in this study was taken to be the point of increasing ^{137}Cs values and not the first occurence of Cs.

Diffusion and bioturbation will have an effect over the whole sediment column. Using box models (Figure 8.3), MacKenzie and Scott (1982) modelled expected profiles of ^{137}Cs in a sediment when acted upon by;

1. Accumulation only.
2. Mixing only.
3. Both mixing and accumulation.

The patterns noted in the sediments in this study tend to conform to either the accumulation only model (Figure 8.3(a)) or both mixing and accumulation (Figure 8.3(c)). The former is illustrated by core LES2 from the

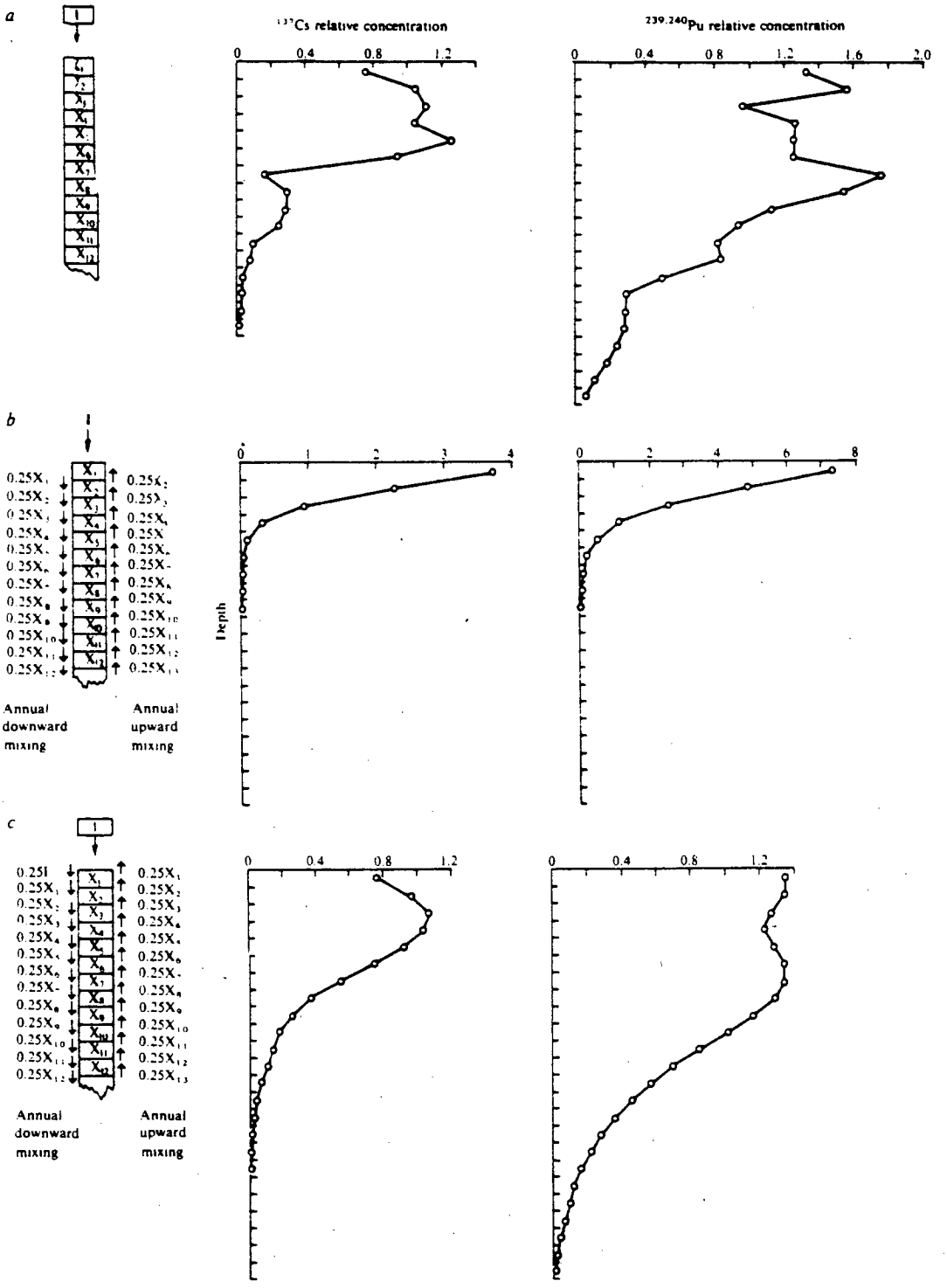

FIGURE 8.3: Box models to show the effect of accumulation and mixing on the pattern of ^{137}Cs in a sediment.

(a) Accumulation only

(b) Mixing only

(c) Mixing and accumulation

(after MacKenzie and Scott, 1982)

inner basin of Loch Etive. The remaining cores tend to conform to the latter model. This would be expected given the low degree of benthic activity observed in the inner basin of Loch Etive compared to that from the outer basin and external to the loch (see Chapter 4). It was seen earlier that variations in the Cs profile in the sediments can be ascribed to specific events. For example; the peaks in the upper 5cm of cores CR1 and DN1 can be attributed to an increase in output of Cs from Sellafield in 1977. Similar peaks in the profiles of cores LES1 and LES2, at 14cm and 16cm depth respectively can possibly be ascribed to the 1962/1963 increase in ^{137}Cs fall-out due to atmospheric nuclear weapons testing. It is possible to use these dated events as a basis for dating sediments. The effects of diffusion and biomixing on the sediments can be seen by comparing the accumulation rates obtained by using the 1952 marker and those obtained by using 1963 and 1977 markers. These are summarised in Table 8.3. In cores LES1 and LES2 the accumulation rates calculated from the bomb peak of 1963 and from the onset of Cs enrichment in 1952 give very similar values. This is not the case in CR1 and DN1. The calculated accumulation rates from the 1977 output peak are much lower than those calculated from 1952. This may be due to a real fall in the rate of sedimentation, but the fact that the sediments from within Loch Etive tend to show little variation, whilst those outside show major variation, would imply that the greater degree of biomixing expected in the sediments from outside Loch Etive is responsible.

It may be concluded then that biomixing can have an appreciable effect on the distribution of Cs in the sediments. This may, therefore, affect the calculation of sediment accumulation rates using the ^{137}Cs distribution.

CHAPTER 9

GEOCHEMISTRY AS A TOOL TO IDENTIFY SEDIMENT INHOMOGENEITY AND BIOMIXING

9.1. Introduction.

Previous chapters have described the geochemical nature of the sediments in terms of, the provenance of the organic matter, the behaviour of the halogens (I and Br) and heavy metals (Cu, Pb and Zn), and their relationship to the patterns of organic matter degradation in the sediments. It has been shown that the behaviour of the organic matter and subsequently that of the halogens and metals tends to be influenced, in part, by the variability of sedimentation. In Chapter 3 the Zr/Rb ratio was used to highlight subtle variations in sediment texture, both temporally and spatially and certain elements, for example Ba and Sr were used to highlight variations in mineralogy. The sediment cores from Loch Creran (CR1) and Loch Duich (DU1) show marked variations which can be seen visually. Other cores which appear to be visually homogenous with depth, for example ET1 and CM1 also show more subtle variation in composition and hence sedimentation.

In the light of the patterns of organic matter and halogens recorded in the sediments, we can now discuss the role that the lithogeochemical trends have in interpreting sediment accumulation, concentrating on the lithological variations displayed by cores CR1 and DU1.

9.2. Discussion.

In core CR1, the shell band between 5cm and 12cm shows a marked increase in the Zr/Rb ratio indicating a coarser sediment. Comparison of the Zr/Rb pattern with those of C_{org}, N, I, and the metals (Cu, Pb and Zn) show that these elements have relatively low concentrations in the shell band. However, the high carbonate content of this zone is indicated by enhanced Sr

values. These patterns are summarised in Figure 9.1. The presence of the shell bands appears to indicate a major hiatus in sedimentation, possibly caused by the winnowing of the finer material to produce a lag deposit of coarse, carbonate rich material, composed principally of residual shell debris of Turritellid gastropods.

Support for an erosive mechanism can be found in the I/C pattern (Figure 9.1). The I/C ratio is constant in the upper 5cm of the sediment, falling rapidly in the shell band and remaining comparatively constant below this. Given that the release of I from sediments is a first order reaction with respect to organic carbon (Chapter 6), the I/C ratios at depth suggest an older unreactive sediment, whilst the values in the upper 5cm of the core are markedly higher indicating the probability of a major hiatus in sedimentation.

An estimate of the total sediment accumulation rate can be gained from the ^{137}Cs data (Chapter 8), basing the measurement on the 1977 output peak of ^{137}Cs (0.4cm yr^{-1}). Assuming that there has been constant accumulation in the upper part of the core. The depth of maximum carbonate content can therefore be dated to 1968–1969, which would coincide with a major hurricane event in the January of 1969.

It is possible to use the pattern of Sr content to quantitatively assess the amount of sediment removed by comparing the background Sr value with the enriched value of the shell band and calculating the amount of sediment removal necessary to cause the observed increase in Sr values. Using this method (summarised in Table 9.1) it is estimated that about 18cm of sediment must have been eroded during this event, this equates to about 7 years of accumulated sediment. However, it is stressed that this can only be

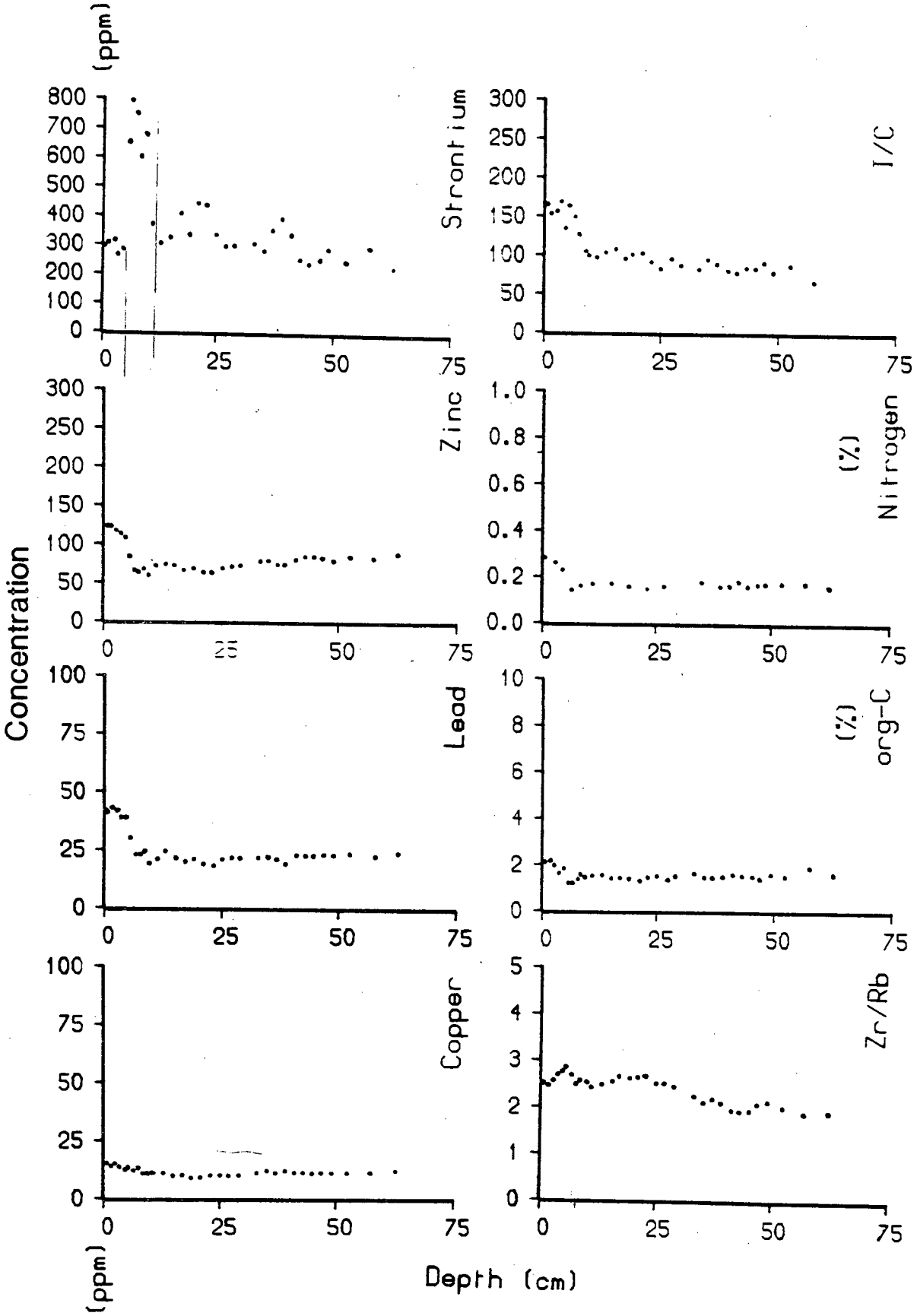

FIGURE 9.1: Profiles of metals, lithogenic and organic indicators in core CR1 showing the effect of the major shell band between 5cm and 12cm depth.

1. $$Sr_B = Sr_o \left(1 - \frac{CaCO_3}{100}\right)$$

2. $$Sr_C = Sr_o^* \cdot \frac{CaCO_3}{100}$$

3. $$Rb_o^* = \frac{Rb_B}{\left(1 - \frac{CaCO_3}{100}\right)}$$

4. $$Clay_{SH} = \frac{Rb_{SH}}{Rb_o^*} \cdot 100$$

5. $$Sr_{CS} = \frac{Sr_o \cdot Clay_{SH}}{100}$$

6. $$Sr_{SC} = Sr_S - Sr_{CS}$$

7. $$C = \frac{CaCO_{3SH}}{CaCO_3}$$

8. $$S = C \cdot d_s$$

9. $$CaCO_{3S} = \frac{Sr_{SC}}{Sr_o^*} \cdot 100$$

C = Contentration of $CaCO_3$ in the shell band over the background. (3.69)
$CaCO_3$ = Mean carbonate of background sediment (from Fig 3.20) (300ppm).
$CaCO_{3SH}$ = Mean carbonate content of the shell band (from Fig 3.20). (42%)
$Clay_{SH}$ = Clay content of the shell band (58%).
d_S = Thickness of shell band (5cm).
Rb_o^* = Rb content in carbonate free clay (123ppm).
Rb_B = Mean Rb content of background sediment (111ppm).
Rb_{SH} = Mean Rb content of the shell band (72ppm).
Sr_B = Mean Sr content of background sediment (300ppm).
Sr_{CS} = Sr content of clay fraction in shell band (87ppm).
Sr_o = Sr content of carbonate free clay (from Fig 3.20) (150ppm).
Sr_o^* = Sr content 100% carbonate (from Fig 3.20) (1593ppm).
Sr_{SC} = Sr content of carbonate fraction of shell band (613ppm).
Sr_S = Mean Sr of shell band (700ppm)
S = Sediment loss (cm)

TABLE 9.1: Summary of expressions for the calculating the amount of sediment eroded from CR1 from the Sr concentration.

a minimum value, as it is impossible to estimate how much carbonate may also have been removed along with the finer material.

Biomixed layers extending to a depth of about 10cm, have been identified in most sediments, from porewater SO_4^{2-} and alkalinity measurements. All of the cores show an excess of sediment S over that which can be accommodated by the observed SO_4^{2-} reduction in the pore water. It is suggested that excess SO_4^{2-} found in sediments must be introduced by biomixing and diffusion (Chapter 4). Sulphur is shown to occur in the biomixed zones of some cores, for example AB1, SP1, and CR1, implying Sulphur fixation in an overall oxic environment. It is likely that the amount of SO_4^{2-} reduction in the biomixed zone is controlled in part by the degree of biomixing, which may in turn be influenced by the sediment accumulation rate and the quality of the organic matter entering the sediment. Thus biomixing appears to have a major control on the degree and position of organic breakdown in the sediments. Where there is a high degree of biomixing, there is a rapid degradation of organic matter and any reduced products are short lived and are likely to be reoxidised. In sediments with a lower degree of biomixing, the reduction products are less likely to be removed through oxidation. Many of the sediments studied do not show an expected 2:1 stoichiometric relationship between A_T and SO_4^{2-}, possibly due to the formation of authigenic sulphides. It is known (Davies, 1977) that some mechanisms of pyrite formation from elemental S (S^o) and pore water Fe can reduce A_T (see Chapter 4). The degree to which this occurs may also be a consequence of biomixing. Most of the S^o needed to convert relatively unstable iron monosulphides into pyrite is formed at or near the sediment water interface from the reoxidation of H_2S (Goldhaber and Kaplan, 1974). Thus in sediments where the rate of biomixing is rapid, more elemental S will

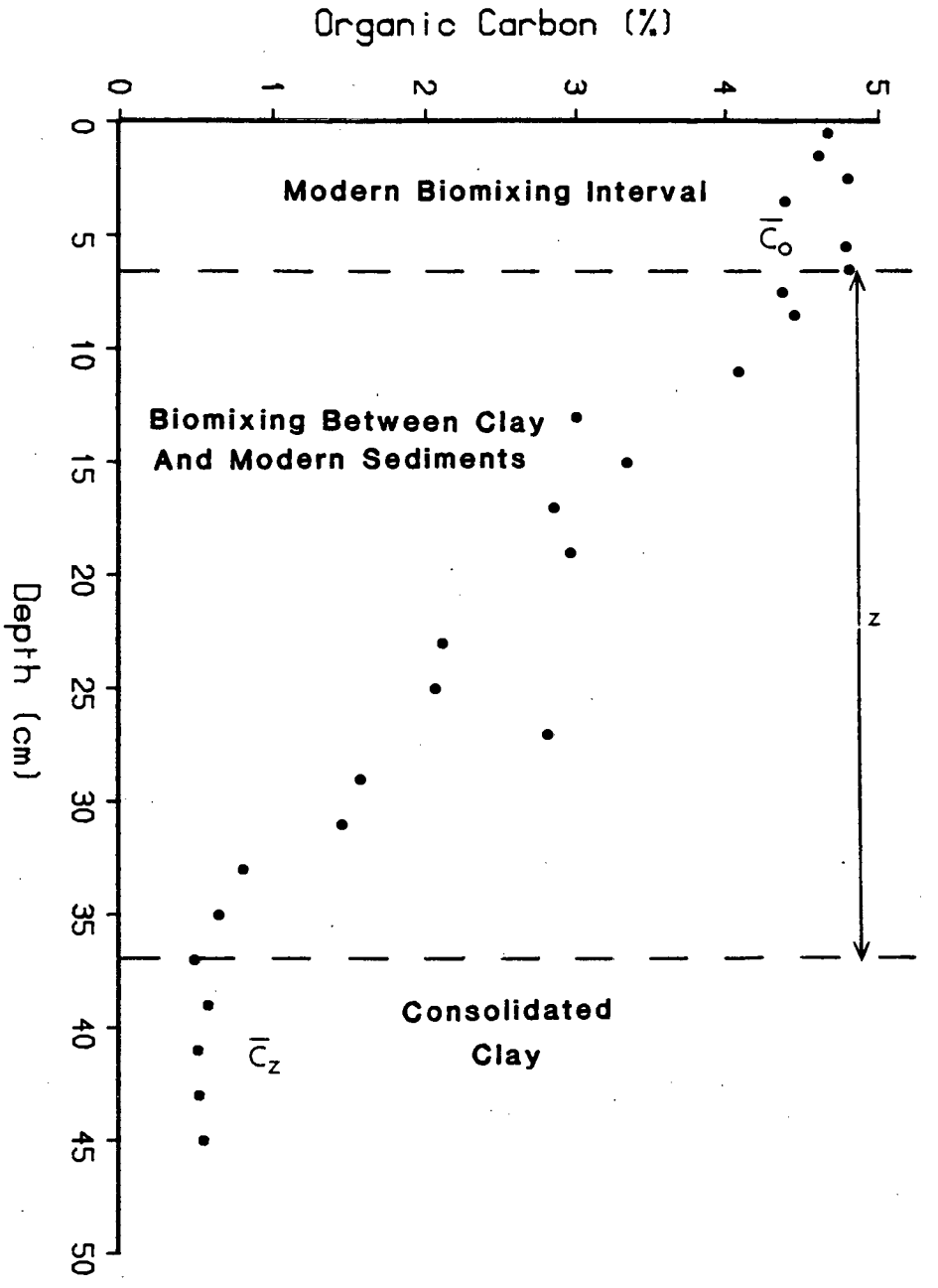

FIGURE 9.2: The pattern of organic Carbon with depth in core DU1 showing the effect of biomixing between the modern sediment and the consolidated clay.

be formed and less monosulphides are likely to be incorporated at depth, most being reduced to pyrite. The converse occurs in sediments with a low degree of biomixing. This is supported by the suggested presence of greigite in dark grey sediments collected from Airds Bay in Loch Etive (Thompson. pers. comm.), which would be expected to have a relatively restricted biomixing rate when compared to sediments outside the loch.

However, the rate of biomixing in these sediments is unknown and would reguire extensive investigation using a family of radioisotopes with appropriate $t_{1/2}$. Nevertheless, it is possible to express the rate of biomixing in one core, DU1 (Loch Duich). In this core, an older clay sediment low in organic matter underlies a more recent sediment which, at the surface has a much higher organic content. It was suggested in previous chapters that the well defined decrease in organic parameters and trace elements is a reflection of the extent of biomixing between these two sediment types. Using the pattern of C_{org} it is possible to estimate the rate of biomixing occuring in this core.

Figure 9.2 shows the pattern of C_{org} with depth in DU1, which can be compared with the patterns of certain radioisotopes, for example ^{210}Pb (e.g. Koide *et al*, 1973; Robbins and Edginton, 1975; Nittrouer *et al*, 197 , 1983; Carpenter *et al*, 1985). Using a box model approach, the relationship of biomixing, sediment accumulation and radioactive decay can be represented by equation 9.1, overleaf:

$$D\,\frac{\partial^2 C}{\partial z^2} - \omega\,\frac{\partial C}{\partial z} - \lambda C = 0 \qquad (9.1)$$

Where: D = rate of biomixing ($cm^2\ yr^{-1}$)

ω = sediment accumulation rate ($cm\ yr^{-1}$)

λ = decay constant of radioisotope

C = concentration of radioisotope

z = depth (cm)

To enable the mixing coefficient to be calculated in sediments where the biomixing exceeds accumulation rate as is likely in these sediments, then equation 9.1 can be simplified equation 9.2 (Nittrouer *et al.*, 1983).

$$D = \lambda \left(\frac{z}{\ln \frac{C_o}{C_z}} \right)^2 \qquad (9.2)$$

The similarity of the pattern of C_{org} in DU1 to that of ^{210}Pb in other cores enables C_{org} to be used in equation 9.2 instead of a radioisotope. The rate of biomixing in DU1 calculated by this method is 134cm^2 yr^{-1}. This is towards the higher end of values for biomixing given by Carpenter *et al.* (1985) for Puget Sound (0.9 - >370cm^2 yr^{-1}) and is much greater than that of 10-12 cm^2 yr^{-1} from continental shelf sediments (Carpenter *et al.*, 1982), and deep-sea sediments (DeMaster and Cochran, 1983). However, it must stressed that this can only be a rough figure as a number of assumptions must be made in the calculation:

1. There is no compaction of the sediments with burial.
2. The rate of biomixing has remained constant with time.
3. The input of C_{org} has been constant during sedimentation of the newer sediment at the level currently seen in the surface sediment.
4. The quality of C_{org} has remained constant.
5. The C_{org} is assumed not to decay, therefore $\lambda = 1$.

It is unlikely that the rate of biomixing has remained constant as biomixing has been shown in Chapter 4 to be dependent to some degree on the quality and amount of organic carbon in the sediment. Even if assumptions 3 and 4 are correct, the clay substrate prior to the onset of modern sediment deposition would have been carbon poor and therefore would possibly have had a lower rate of biomixing. The decay constant (λ) was assumed to be 1 from consideration of the C_{org} contents of the other cores analysed which show little change of C with depth. The decay constant of C_{org} cannot be measured without independent means, as the rate of decay of C_{org} is itself dependent on biomixing (Chapter 4).

Nevertheless, the value of biomixing obtained compares well with quoted biomixing rates (*ibid.*) and illustrates the high degree of biomixing occuring in these sediments.

CHAPTER 10

GENERAL CONCLUSIONS AND DISCUSSION

All of the sediments are composed of a similar suite of minerals consisting of; quartz, a suite of feldspars (mostly albite but containing potassic feldspar, possibly microcline), calcite, and a clay fraction (containing illite, muscovite and chlorite). The proportions of the minerals vary both temporally within individual cores and spatially. It is possible to use geochemistry to identify these mineralogical changes and highlight variations in sediment grain size and therefore changes in the patterns of accumulation in a core. Analysis of the Zr/Rb ratios and Sr patterns in the sediments for example, has shown wide variations in the grain size and carbonate content of the sediments. This indicates that most of the sediments show non-steady state accumulation. For instance examination of the break in sedimentation at the shell band between 5cm and 12cm in Loch Creran (CR1) has shown that about 18cm of sediment accumulation has been removed.

Comparison of the Ni and Cr patterns with those of Rb shows both elements to be associated with the argillaceous fraction in a similar way to Rb. However, from the geochemistries of Ni and Cr (Shiraki, 1978; Turekian, 1978) both elements tend to be concentrated in the ferromagnesian fraction, although some Cr may be associated with the resistate fraction possibly as magnetite. Nevertheless, the association of Ni to the ferromagnesian fraction makes it a useful normalising element when considering the behaviour of Cu, Pb and Zn in the sediments.

The organic matter entering the sediments is known to be composed of varying proportions of marine and terrigenous matter (Pocklington and Leonard, 1979; Lyons and Gaudette, 1979). An attempt has been made to identify the relative proportions of these components in the sediments. The C/N ratio is known to have limitations due to the lability of N relative to C_{org}.

A profile of C/N ratios along Loch Etive, however, has shown there to be a general decrease in the C/N ratio towards the mouth of the loch suggesting that C/N values do reflect variations in the relative proportions of marine and terrigenous organic matter but, this can only be used on a qualitative basis. Considering the C/N ratios of the sediment cores, the surface sediments from the fjordic environments (ET1, DU1) tend to have higher C/N ratios than the shelf sediments (e.g. SP1, SH1) showing the greater terrestrial influence in the lochs. Sweeny *et al.* (1978) suggest the use of $\delta^{15}N$ as an organic source indicator but the use of $\delta^{15}N$ in these sediment highlights a number of problems. Comparison of the $\delta^{15}N$ profile along Loch Etive with a similar profile for C/N does not show such a great increase in values as would be expected from the dramatic fall in C/N values towards the mouth of the loch. Comparing the patterns of δ^{15} and C/N in the sediment cores shows that in some cores, for example DU1, the $\delta^{15}N$ pattern supports that of C/N but, others (e.g. CM1 and SH1) show opposing trends. This suggests that $\delta^{15}N$ may be controlled to some degree by organic matter source, but this may be obscured by overlaps in the isotopic composition of the organic matter types and variations in value due possibly to changes in biological productivity in the overlying waters, fractionation of N whilst still in the water column, and fractionation of N whilst undergoing organic degradation.

In these sediments, the most dominant form of organic matter degradation is anoxic microbial SO_4^{2-} reduction producing iron monosulphides and disulphides. All the sediment cores, however, show relatively constant SO_4^{2-} values in the upper 10cm of the sediment illustrating the presence of an oxic/suboxic biomixed layer. Comparison of the patterns of S and those of SO_4^{2-} in the sediment do not show an expected 1:1 stoichiometric relationship as would be expected from the SO_4^{2-} reduction equation (see Table 4.6).

There is much more S present in the sediments than measured SO_4^{2-}. This implies that SO_4^{2-} is being introduced in the sediment by diffusion, irrigation and biomixing. The presence of S and increasing alkalinity values in the biomixed zone of some sediments (e.g. ET1 and DU1) implies that SO_4^{2-} reduction is occuring in the biomixed zone. The rate of SO_4^{2-} reduction occuring in the sediments and the degree to which reduction products are retained is suggested to be a function of the rate of biomixing, which is in turn controlled by the quality of the organic carbon entering the sediment. The rate of biomixing occuring in the sediments of Loch Duich has been estimated at about $134cm^2\ yr^{-1}$. The degree of biomixing may also influence the production of pyrite relative to monosulphides during SO_4^{2-} reduction. Sediments with a high degree of biomixing for example, cores CM1 and SH1 will tend to produce greater amounts of pyrite relative to monosulphides due to the production of elemental sulphur S^o from the reoxidation of H_2S back to SO_4^{2-} and S^o. Conversely, the more restricted fjords such as Loch Etive will tend to produce greater amounts of monosulphides due to the retention of H_2S and lack of production of S^o.

Iodine is known to be associated with the marine organic fraction of the sediments (Price and Calvert, 1977; Elderfield *et al*, 1981; Harvey, 1980; Ullman and Aller, 1983, 1985) and can therefore be used in addition to C/N as an indicator of marine organic matter. At depth, both I and Br show a loss from the sediments. This has been shown to be first order with respect to depth, a pattern common to metabolic reactions involving organic degradation (Ullman and Aller, 1983). The patterns of halogen/C also show a fall at depth implying a loss of halogens relative to organic carbon. These patterns show that both and I and Br are subject to burial diagenesis. Furthermore, consideration of the I/Br ratios in the sediments shows a loss of I relative to Br. It may

therefore be concluded that while I and Br both show an association with organic matter, I is more weakly bonded than Br. This makes I an ideal indicator of organic matter diagenesis in the sediments.

Cu, Pb and Zn in the sediments are derived from both natural and anthropogenic sources. All of the metals show surface enrichment patterns, Pb being the most enriched and Cu the least. By ratioing the metals to Ni, shown to be associated with the detrital ferromagnesian fraction, the excess metals over the detrital input can be calculated. This can be used as an indicator of the metal input to the sediments from pollution.

From the surface values there appears to be a geographical control over the distribution of the excess metals. The more Northerly cores tend to show less excess metals than those from the South. This would be expected as the North of the region is much more removed from the major industrial pollutant sources, for example the Clyde Valley to the South. There is also a variation in metal input with catchment area size, the cores from Loch Etive (AB1 and ET1) having a greater amount of excess metals than the cores from areas of lower catchment size.

Comparison of the metal enrichments with sediment accumulation rates as depicted by ^{137}Cs shows that the onset of metal enrichment in the sediments generally corresponds to less than 50 years of sediment accumulation. As anthropogenic input of heavy metals to the environment has been occuring since the industrial revolution, the implication is that the metal patterns must be affected by other influences. Comparison of the organic carbon and excess metal contents of the sediments shows that the concentration of excess metals tends to increase with increasing carbon content, suggesting an association between the metals and organic carbon. However, there is a

higher degree of association between the excess metals and I in the sediments. This implies that the heavy metals are more associated with the marine organic fraction. However, the relationship of Pb and Zn to the marine organic matter in the biomixed zone of the sediments appears to be different. The best fit lines for Pb_{ex} and Zn_{ex} against I as calculated from the mean values in the biomixed zones of cores CM1, CR1, DN1 and SP1 are summarised in Figure 7.11. Zn_{ex} can be seen to have an intercept close to zero, which would be expected if all the excess metal was associated with the marine organic fraction. Pb however, has a positive intercept implying that not all of the excess Pb in the surface sediments is associated with the marine organic matter. Nevertheless, the constancy of the Zn_{ex}/Pb_{ex} ratios in the biomixed zone (generally about 2) suggests a marked association between these metals. It is possible that the mechanism of introduction of these metals into the sediments varies. In particulate matter Ridgway (1984) found that Pb and Zn tend to have an association with the marine organic matter, but that Pb is also associated with the iron oxide phase. It appears, however, that once incorporated in the sediments, both metals are taken up by the same phase.

At depth, the patterns of excess metals are similar to those of I, shown to be diagenetically mobile. This implies that the metals behave in a similar manner. When the excess metal and I values are plotted (Figures 7.9, 7.10) a different pattern emerges. A two slope system can be identified. In the upper sediments representing the biomixing interval, I is lost relative to the excess metals. At depth, the excess metals are lost at a greater rate than the I. The onset of I loss has been shown to be close to the sediment/water interface. Conversely, the patterns of excess metals show little loss in the biomixed zone, but a rapid loss in the anoxic sediments below. Comparison of the excess metal and metal/Rb ratios to the patterns of S in the sediments show

the greatest metal loss in the zone of maximum S increase, well illustrated in cores CM1, AB1 and SH1. This suggests that the release of heavy metals from organic matter is associated with the anoxic organic degradation under SO_4^{2-} reduction and is therefore controlled to some degree by sediment accumulation and biomixing. Conversely, the loss of I from the organic matter appears to be more associated with the oxic/suboxic degradation close to the sediment surface.

Comparisons of the halogens and heavy metals would therefore imply that heavy metals are predominantly linked to the marine fraction of the organic matter and are released when this organic matter is degraded. However, the pattern of excess metal to I and the differences in the location of apparent diagenetic release of both I and Br when compared to Pb and Zn would suggest that the metals are bound to different fractions within the marine organic matter and that the strength of these bonds varies, with I being the weakest followed by Br and heavy metals being the most strongly bound.

To conclude, the above points have shown that whilst much of the heavy metal input to the sediments is due to anthropogenic loading, the patterns of metals observed are very much modified by diagenetic action associated with the breakdown of reactive organic carbon. It is therefore invalid to use the heavy metal patterns of a sediment to describe the pollutant history of an area

APPENDICES

APPENDIX I

SAMPLING AND ANALYTICAL METHODS

1. Sample Collection.

The sediment cores were collected using a modified gravity corer (Kemp *et al* 1976). Disturbance of the highly fluid upper section of the sediment core during collection can be a problem. The gravity corer used in this study is designed to reduce the pressure wave in front of the coring device and therefore reduce sediment disturbance. The core barrel is an open perspex tube (I.D. 82mm) with no core catcher, the pressure wave is minimised by the corer allowing a throughflow of water. On removal from the sediment, the valve allowing throughflow is closed, the suction developed holding the collected sediment within the barrel.

Sub-sampling of the cores was carried out in an inert atmosphere of oxygen-free nitrogen to prevent oxidation of the sediments. The core was extruded vertically from its barrel by the insertion of a plunger from below. The extruded sediment was then sub-sectioned with the aid of a perspex guillotine. Constancy of the sub-sections was achieved by the use of formers constructed of core barrel material cut to the required thickness. The upper 10cm of each core was sectioned every cm, the next 40cm every 2cm and there after every 5cm to the base of the core.

From each sub-section a 5ml aliquot of sediment was removed using a modified syringe. This was used to calculate sediment water contents and thus determine porosity (see Chapter 3, Section 3.4).

The remaining sediment was transfered to centrifuge tubes and centrifuged at 3000rpm, in a Sorval GLC 4000 centrifuge, for 20 minutes in order to separate the sediment pore water. Once centrifuged the tubes were again placed under N and the pore water removed from the tubes using PTFE tubing

attached to a 50ml polythene syringe equiped with a PTFE plunger. Fine material suspended in the water was removed by filtering through a 25mm, 0.4µm Sartorious membrane filter during the transfer of the water to acid cleaned glass vials. A 5ml aliquot was removed for SO_4^{2-} analysis. Any sulphide present was stabilised by the adding 0.5ml of 10% Cadmium Acetate solution.

The remaining solid fraction was stored in seal grip polythene bags for subsequent analysis.

All the equipment used was cleaned in 50% HCl, washed four times in de-ionised water and oven dried at 70° C prior to use.

2. Sediment Analysis.

The sediment was oven dried at 70° C for two days prior to grinding by an agate or tungsten carbide TEMA disc mill. The sediment powders were then analysed as described below.

2.1. X-Ray Diffraction.

A small amount of sediment powder was combined with acetone in a pestle and mortar and mixed to a slurry. This was spread on a glass slide and left to evaporate. The slides were then analysed for bulk mineralogy using a Phillips PW 1011/1050 X-Ray Diffractometer with Ni filtered Copper (CuK_α) radiation. Each sample was scanned at a goniometer speed of 2° min^{-1} from 5° (2θ) to 50° (2θ). The peaks obtained were then interpreted using the tables prepared by Chao (1969).

2.2. X-Ray Fluorescence.

37mm and 46mm pressed powder pellets were analysed for minor elements, halogens and sulphur using a Phillips PW1450 Sequential Automatic X-Ray Spectrometer. The pellets were prepared using a method similar to that of Reynolds (1963). 3.5g or 7g (37mm or 46mm diameter pellets respectively) of ground sediment were pressed into a pellet backed by boric acid and consolidated under 10 tons pressure from a hydraulic press. To ensure integrity of the sample surface under the X-Ray beam, the pellets were pressed onto a polished tungsten carbide disc. No binder was added to the powder due to problems with migration of residual sea salt to the pellet surface in the X-Ray beam and the rehydration of clays leading to the destruction of the pellets. To minimise moisture intake, the samples were stored in a dessicator prior to analysis.

All the elements were analysed using a Rh tube and the analytical conditions are given in Table AP1.1. Matrix absorbance coefficients (μ) were determined for all samples and standards by the method of Reynolds (1963) using the Rh K_α Compton Scatter peak. Standardisation was achieved using international and "in house" rock standards prepared in the same way as the sediments. The calibrations were linear. No differences in final element concentrations were observed between the sample analysed using 37mm discs and those using 47mm, the counts being proportional. The analytical precision of the XRF data is as given in Fitton and Dunlop (1985) (see Table AP1.2).

I, Br, Cl and S analyses were made against a synthetic dilution series made by adding a known amount of KIO_4, KBr, NaCl and Na_2SO_4 to a powdered siltstone obtained from a Southern Uplands turbidite sequence. Homogeneity

Elem	Line	Xstal	2θ	Kv	mA	Det	Collim
Ba	$L_{\beta 2}$	LiF_{220}	115.18	60	45	F	c
Sc	K_{α}	LiF_{200}	97.70	60	45	F	c
La	$L_{\alpha 1}$	LiF_{200}	82.91	60	45	F	c
Nd	$L_{\alpha 1}$	LiF_{200}	72.13	60	45	F	c
Ce	$L_{\beta 1}$	LiF_{200}	71.62	60	45	F	c
Cr	K_{α}	LiF_{200}	69.36	60	45	F	c
Ni	K_{α}	LiF_{200}	48.67	60	45	F	c
Cu	K_{α}	LiF_{200}	45.03	60	45	F+S	c
Zn	K_{α}	LiF_{200}	41.80	60	45	F+S	f
Pb	$L_{\beta 2}$	LiF_{200}	28.24	60	45	F+S	f
Rb	K_{α}	LiF_{200}	26.62	60	45	F+S	f
Sr	K_{α}	LiF_{200}	25.15	60	45	F+S	f
Y	K_{α}	LiF_{200}	23.80	60	45	F+S	f
Zr	K_{α}	LiF_{200}	22.55	60	45	F+S	f
S	K_{α}	Ge	110.69	60	45	F	c
Cl	K_{α}	Ge	92.76	60	45	F	c
I	K_{α}	LiF_{200}	12.26	60	45	F+S	c

Crystal: LiF = Lithium Flouride
Ge = Germainium

Detector: F = Flow Counter
S = Scintillation Counter

Collimator: f = Fine
c = Coarse

TABLE AP1.1: Analytical conditions for X-Ray Flourescence Analysis.

p.p.m.	REPRODUCIBILITY on sample ST72		"ACCURACY" (r.m.s.d. from international standards).
Ni	170.9	0.3	4.3
Cr	380.5	2.9	11.0
V	236.6	3.5	11.5
Sc	18.2	0.3	2.4
Cu	48.4	0.4	5.3
Zn	113.9	1.1	5.0
Pb*	-1.8	1.6	4.0
Sr	1129.7	4.0	9.6
Rb	46.7	0.5	3.5
Zr	366.0	1.0	14.8
Nb	92.2	0.5	2.4
Ba	718.4	5.6	39.0
Th	16.6	1.2	2.8
La	78.9	0.8	5.6
Ce	156.7	1.6	13.5
Nd	66.2	0.6	3.6
Y	33.2	0.4	3.4

* Below detection limit. 6 determinations of Pb in andesite MT45 gave a mean concentration of 9.6 p.p.m. with a σ of 0.8 p.p.m.

TABLE AP1.2: Analytical precision for X-Ray Flourescence data.

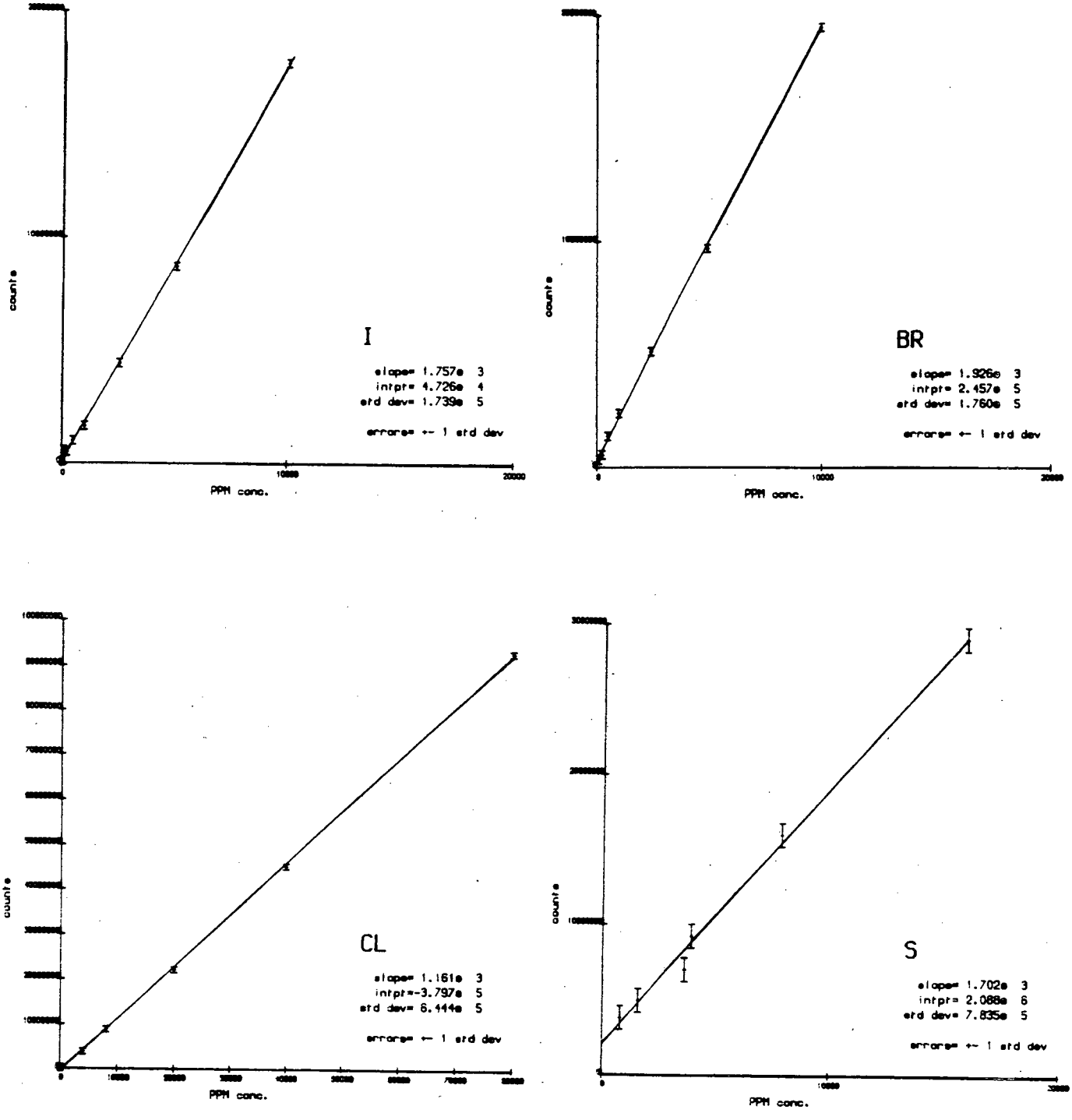

FIGURE AP1.1: X-Ray Flourescence calibration lines for Br, Cl, I and S.

of the standards was ensured by prolonged grinding in a TEMA disc mill. Individual members of the dilution series were created by diluting the original standard with unspiked siltstone. Homogeneity was again ensured by vigourous shaking for 30 minutes on a mechanical shaker. The final calibration lines achieved are summarised in Figure AP1.1.

Iodine was originally analysed using the I L_{α} peak however, a correlation was found between the I data and Sr. This was investigated as such a link has not been previously observed in other sediments. The I L_{α} peak is known to be very close to Ca K_{β} (102.88° and 100.88° respectively). In samples with high Ca contents, two subsidiary peaks were noted on either side of the main Ca K_{β} peak, the high angle subsidiary interfering with the I K_{α}. This was eliminated by reanalysing I using the I K_{α} line. However, a further problem was noted; because I has a high atomic weight (126.9), the amount of sample necessary to obtain a critical depth in the sample disc and thus obtain maximum count response becomes relatively high. The amount of sediment required can be calculated using equation API.1 (see over).

$$M = \frac{4.6\ \pi r^2 \sin\beta}{\mu}$$

(API.1)

Where: M = critical mass of sample required.

r = radius of sample disc (1.85cm for 47mm discs).

β = spectrometer take off angle (40^{o}).

μ = mass absorbance of sample. (In this case at the wavelength of I K_{α}).

μ can be calculated using:

$$\mu = \sum_{n}^{i=1} x_i\ \mu_i$$

(API.2)

Where: x = weight fraction of major element.

μ = measured absorbance of element.

Calculating M for I using a representative major element composition for the sediments derived from; Krom (1976), Malcolm (1981) and Ridgway (1984), and mass-absorbance coefficients from Jenkins and DeVries (1970), a critical mass of 16g of sample is required to produce maximum count response using 47mm discs. This was investigated experimentally using 0.1% I spike in discs

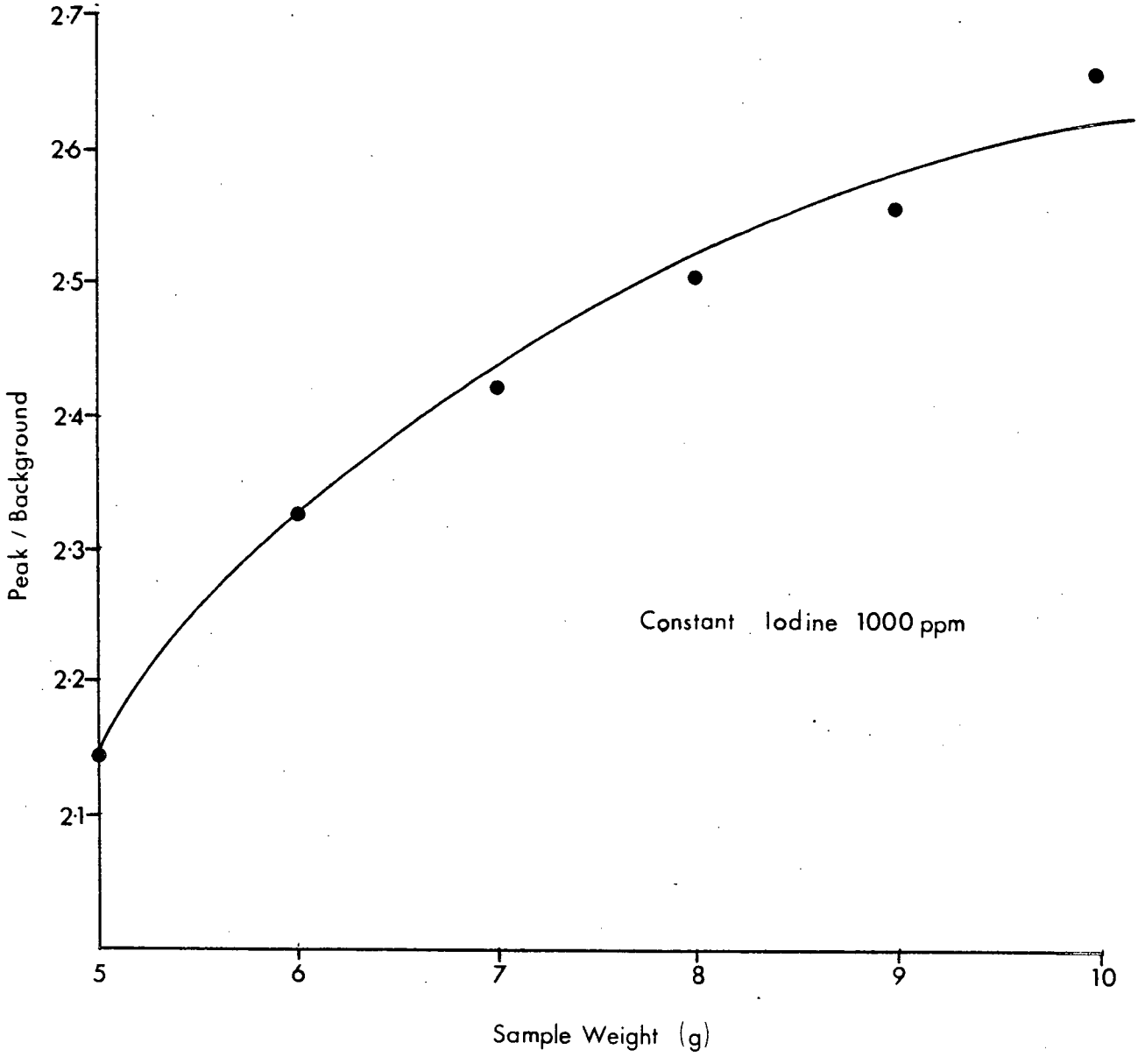

FIGURE AP1.2: Relationship of matrix corrected I counts to sample weight.

of varying weight composed of a matrix of Ordovician siltstone. The results are graphed in Figure AP1.2. The weight of sample used in the 47mm discs analysed was 7g. This does not satisfy the critical weight requirement for I but, as the weight for each sample is consistant, the data set for I is also consistant. Similarly, the sample weight for the 37mm discs is proportional to that in the 47mm discs and therefore these are also consistant. Ridgway (1984) used only 5g of sample per disc and this explains the discrepancy of results between that work and this study, noted in Chapters 5 and 7.

2.3. Carbon and Nitrogen.

Total carbon and nitrogen data was determined on a Perkin-Elmer 240 Elemental Analyser. 10mg of sample was weighed into a platinum boat and combusted. Acetanilide was used as a working standard and conditions were set following the manufacturers recommendations. Precision of the analysis was calculated at ± 6.3% (1σ, n=6) for C and ± 11% (1σ, n=6) for N using a replicate sample taken from depth 48-50cm in core SH1.

2.4. Organic Carbon.

Organic Carbon was measured on sediments from which the carbonate had been removed by acid treatment. 0.25g to 1g of ground sediment, depending on the amount of organic carbon expected was weighed into a ceramic crucible and treated with 50% HCl added dropwise until two treatments after effervescence had ceased. The samples were placed on a hot plate at 150° C and evaporated to dryness. A further treatment with acid followed to ensure total removal of the carbonate fraction. After evaporating to dryness once more, the samples were allowed to cool and then stored in a dessicator prior to analysis.

Organic Carbon wass determined by the ignition of the samples in CO_2 free O_2 in a LECO 521-200 induction furnace. The volume of CO_2 produced was measured using a LECO 572-100 gas burette after absorption by KOH.

Standardisation was acheived against LECO high carbon steel rings. The precision of the analysis was found to be ± 3.05% (1σ, n=8) using a replicate unknown (SH1, 32-34cm).

2.5. Correction For Residual Sea Salt.

The concentrations of elements in marine sediments have to be corrected for the effect of residual sea salt remaining in the sediments after drying. This salt acts as a dilutant and also a contributor of certain elements, the most important being Na, Mg, Ca, K, S, Br and Sr. The X-Ray Fluorescence data was corrected for this effect by assuming that the Cl analysed is associated with the residual salt. The amount of residual sea salt in the sediments can therefore be calcula2ted using equation API.3.

$$Salt = (Cl/10000) \times 1.649 \qquad \text{(API.3)}$$

Individual element corrections for Br and S were then made using API.4 and API.5.

$$ppm\ Br = ppm\ Br_{meas} - Salt \times 19 \qquad \text{(API.4)}$$

$$ppm\ S = ppm\ S_{meas} - Salt \times 260$$

(API.5)

Once the individual element corrections have been made a subsequent correction for dilution should be applied (API.6).

$$Elem_{salt\ free} = Elem_{meas} \cdot \left(\frac{100}{100 - Salt} \right)$$

(API.6)

3. Pore Water Analysis.

3.1. Titration Alkalinity.

Titration Alkalinity was determined by direct potentiometric titration based on the method detailed by Edmond (1970). The sample was titrated with standardised HCl to the second end point of the carbonic system (bicarbonate end point). The volume of acid required is determined from a "Gran Plot" (Gran function versus volume of acid added) (Gran, 1952) and the alkalinity is calculated from the following equation (see over).

$$A_T \text{ (meq } l^{-1}) = \frac{(V_2)\,(N_a).\ 1000 \text{ ml } l^{-1}}{V_o}$$

(API.7)

Where: V_2 = volume of acid needed to reach the bicarbonate endpoint

V_o = original sample volume

N_a = acid normality

3.2. Pore Water Sulphate.

A modified gravimetric technique was used in order to prevent co-precipitation of carbonates and strontium salts (modified from Howarth, 1978). The stabilised 5ml aliquot of pore water (see Section 1.1) was filtered through a 37mm 0.4µm Nuclepore filter to remove the cadmium sulphide precipitate, and 1ml of the filtered water was pipetted into a 50ml beaker, 3ml of 0.4 M HCl and 4ml of 0.1 M EDTA were added. Addition of excess EDTA removes the possibility of co-precipitation of Sr salts. The mixture was gently heated on a hot plate to speed chelation and acid complexing. Watch glasses were used to cover the beakers to reduce evaporation during warming. 10ml of 0.05M HCl was added and the beakers cooled before adding 5ml of 10% $BaCl_2$. The covered beakers were left overnight to allow full preciptation of $BaSO_4$. The samples were then filtered onto pre-weighed 37mm 0.4µm Nuclepore membranes. The beakers were washed twice with deionised water to remove remaining precipitate before the addition of 10ml of 0.05M HCl to remove excess Ba and other soluble salts. The filter was finally washed with

20ml of deionised water, care being taken in these latter stages to prevent loss of $BaSO_4$ due to "creep" of the precipitant up the sides of the filter towers. After removal from the filter apparatus, the filters were stored in clean Millipore petrie slides and dried in a dessicator for several days before re-weighing on a Perkin-Elmer AD-2 Electro-balance to determine the weight of $BaSO_4$ and hence the weight of SO_4. The method was standardised against a dilution series made from IAPSO seawater (chlorinity 19.3775 $^{o}/_{oo}$) and deionised water. The precision of the analysis was ± 5.97% (1σ, n=6).

APPENDIX II

TABULATED DATA

TABLE AII.1

Porosity Data.

Data expressed as percent and calculated from the sediment moisture content using:

$$\phi = \frac{Wds}{Wds + (1 - W)dw}$$

Where:

ϕ = Porosity.

W = % Moisture content ($\times 10^{-2}$).

ds = Mean density of sediment particles (2.65 g cm^{-2}).

dw = Density of pore water (1.02 g cm^{-2}).

(Berner, 1971).

CORE AB1.

Porosity data (%)

AB0-1	0.882
AB1-2	0.874
AB2-3	0.864
AB3-4	0.863
AB4-5	0.866
AB5-6	0.865
AB6-7	0.860
AB7-8	0.866
AB8-9	0.867
AB9-10	0.857
AB10-12	0.844
AB12-14	0.861
AB14-16	0.819
AB16-18	0.856
AB18-20	0.860
AB20-22	0.859
AB22-24	0.848
AB24-26	0.851
AB26-28	0.850
AB28-30	0.849
AB30-32	0.846
AB32-34	0.878
AB34-36	0.836
AB36-38	0.836
AB38-40	0.838
AB40-42	0.844
AB42-44	0.875
AB44-46	0.876
AB46-48	0.838
AB48-50	0.724
AB50-55	0.825

CORE CM1.

Porosity data (%)

CM0-1	0.831
CM1-2	0.801
CM2-3	0.779
CM3-4	0.774
CM4-5	0.776
CM5-6	0.773
CM6-7	0.794
CM7-8	0.767
CM8-9	0.766
CM9-10	0.988
CM10-12	0.744
CM12-14	0.730
CM14-16	0.712
CM16-18	0.706
CM18-20	0.724
CM20-22	0.726
CM22-24	0.745
CM24-26	0.735
CM26-28	0.710
CM28-30	0.677
CM30-32	0.701
CM32-34	0.680
CM34-36	0.733
CM36-38	0.700
CM38-40	0.742
CM40-42	0.706
CM42-44	0.706
CM44-46	0.738
CM46-48	0.757
CM48-50	0.810
CM50-55	0.648
CM55-60	0.707
CM60-65	0.706

CORE CR1.

Porosity Data (%)

CR0-1	0.799
CR1-2	0.864
CR2-3	0.745
CR3-4	0.616
CR4-5	0.693
CR5-6	0.703
CR6-7	0.698
CR7-8	0.665
CR8-9	0.703
CR9-10	0.713
CR10-12	0.716
CR12-14	0.694
CR14-16	0.712
CR16-18	0.687
CR18-20	0.657
CR20-22	0.648
CR22-24	0.659
CR24-26	0.658
CR26-28	0.638
CR28-30	0.705
CR30-32	0.682
CR32-34	0.677
CR34-36	0.676
CR36-38	0.697
CR38-40	0.694
CR40-42	0.696
CR42-44	0.693
CR44-46	0.781
CR46-48	0.699
CR48-50	0.702

CORE DU1.

Porosity data (%)

DU0-1	0.899
DU1-2	0.885
DU2-3	0.860
DU3-4	0.838
DU4-5	0.845
DU5-6	0.833
DU6-7	0.850
DU7-8	0.829
DU8-9	0.841
DU9-10	0.843
DU10-12	0.829
DU12-14	0.782
DU14-16	0.785
DU16-18	0.782
DU18-20	0.765
DU20-22	0.729
DU22-24	0.701
DU24-26	0.766
DU26-28	0.727
DU28-30	0.695
DU30 32	0.663
DU32-34	0.654
DU34-36	0.619
DU36-38	0.621
DU38-40	0.609
DU40-42	0.613
DU42-44	0.618
DU44-46	0.633

CORE DN1.

Porosity data (%)

DN0-1	0.859
DN1-2	0.828
DN2-3	0.813
DN3-4	0.794
DN4-5	0.777
DN5-6	0.780
DN6-7	0.765
DN7-8	0.770
DN8-9	0.749
DN9-10	0.766
DN10-12	0.776
DN12-14	0.745
DN14-16	0.737
DN16-18	0.755
DN18-20	0.755
DN20-22	0.751
DN22-24	0.756
DN24-26	0.731
DN26-28	0.761
DN28-30	0.743
DN30-32	0.747
DN32-34	0.755
DN34-36	0.763
DN36-38	0.765
DN38-40	0.740
DN40-42	0.741
DN42-44	0.803
DN44-46	0.745
DN46-48	0.744
DN48-50	0.736
DN50-55	0.732

CORE ET1.

Porosity data (%)

ET0-1	0.916
ET1-2	0.926
ET2-3	0.932
ET3-4	0.925
ET4-5	0.916
ET5-6	0.911
ET6-7	0.902
ET7-8	0.900
ET8-9	0.904
ET9-10	0.922
ET10-12	0.902
ET12-14	0.895
ET14-16	0.882
ET16-18	0.882
ET18-20	0.894
ET20-22	0.892
ET22-24	0.899
ET24-26	0.893
ET26-28	0.887
ET28-30	0.895
ET30-32	0.893
ET32-34	0.878
ET34-36	0.886
ET36-38	0.885
ET38-40	0.888
ET40-42	0.893
ET42-44	0.883
ET44-46	0.891
ET46-48	0.890
ET48-50	0.899
ET50-55	0.892
ET55-60	0.820
ET60-65	0.885

CORE SH1.

Porosity data (%)

SH0-1	0.853
SH1-2	0.847
SH2-3	0.806
SH3-4	0.815
SH4-5	0.787
SH5-6	0.765
SH6-7	0.771
SH7-8	0.765
SH8-9	0.759
SH9-10	0.776
SH10-12	0.752
SH12-14	0.754
SH14-16	0.746
SH16-18	0.748
SH18-20	0.734
SH20-22	0.749
SH22-24	0.751
SH24-26	0.746
SH26-28	0.744
SH28-30	0.739
SH30-32	0.735
SH32-34	0.732
SH34-36	0.738
SH36-38	0.741
SH38-40	0.733
SH40-42	0.737
SH42-44	0.721
SH44-46	0.728
SH46-48	0.720
SH48-50	0.719

CORE SP1.

Porosity data (%)

SP0-1	0.843
SP1-2	0.836
SP2-3	0.815
SP3-4	0.812
SP4-5	0.774
SP5-6	0.768
SP6-7	0.777
SP7-8	0.747
SP8-9	0.781
SP9-10	0.768
SP10-12	0.766
SP12-14	0.769
SP14-16	0.734
SP16-18	0.755
SP18-20	0.742
SP20-22	0.754
SP22-24	0.761
SP24-26	0.751
SP26-28	0.751
SP28-30	0.733
SP30-32	0.713
SP32-34	0.745
SP34-36	0.759
SP36-38	0.732
SP38-40	0.728
SP40-42	0.747
SP42-44	0.817
SP44-46	0.745
SP46-48	0.733
SP48-50	0.718
SP50-55	0.718
SP55-60	0.736
SP60-65	0.711
SP65-70	0.762
SP70-75	0.728

TABLE AII.2

Lithogenic Minor Element Data.

(Ba, Sc, Cr, Ni, Rb, Sr, Zr)

All data expressed in ppm on a salt free basis.

CORE AB1.

Salt-corrected trace element data, ppm

	Ba	Sc	Cr	Ni	Rb	Sr	Zr
AB0-1	574	14	96	47	101	264	220
AB1-2	601	13	94	48	102	269	231
AB2-3	N.A.	N.A.	N.A.	N.A.	N.A.	N.A.	N.A.
AB3-4	614	12	99	49	102	267	234
AB4-5	571	14	98	50	105	247	219
AB5-6	571	12	99	50	106	253	225
AB6-7	581	15	98	49	105	249	217
AB7-8	545	13	99	49	106	252	219
AB8-9	567	12	97	49	107	248	215
AB9-10	593	16	99	49	104	246	214
AB10-12	606	12	98	50	104	240	211
AB12-14	545	16	92	48	101	252	199
AB14-16	551	12	94	46	100	266	196
AB16-18	539	14	94	46	100	246	192
AB18-20	506	14	94	46	101	238	188
AB20-22	548	15	97	46	102	227	202
AB22-24	516	14	97	45	102	221	201
AB24-26	521	13	98	46	101	222	201
AB26-28	530	16	100	46	103	217	202
AB28-30	494	12	96	45	101	219	192
AB30-32	N.A.	N.A.	N.A.	N.A.	N.A.	N.A.	N.A.
AB32-34	513	17	99	47	103	254	197
AB34-36	543	14	98	47	103	244	199
AB36-38	512	13	99	47	106	220	209
AB38-40	467	10	94	49	118	241	228
AB40-42	476	13	102	49	107	215	209
AB42-44	506	13	103	48	108	209	208
AB44-46	508	17	97	46	107	213	224
AB46-48	485	14	99	46	104	210	223
AB48-50	499	14	97	47	106	213	221
AB50-55	478	14	96	45	103	224	226

CORE CM1.

Salt-corrected trace element data, ppm

	Ba	Sc	Cr	Ni	Rb	Sr	Zr
CM0-1	419	4	58	26	79	450	311
CM1-2	442	10	61	27	87	314	347
CM2-3	452	10	61	27	86	319	357
CM3-4	453	10	60	27	85	315	359
CM4-5	463	9	61	27	86	316	359
CM5-6	463	9	58	26	86	326	362
CM6-7	448	9	59	27	84	337	364
CM7-8	461	8	59	28	85	321	357
CM8-9	431	9	61	27	86	329	360
CM9-10	N.A.	N.A.	N.A.	N.A.	N.A.	N.A.	N.A.
CM10-12	440	9	66	29	89	329	311
CM12-14	416	11	68	31	92	323	320
CM14-16	441	9	66	30	88	352	307
CM16-18	416	9	69	30	89	371	299
CM18-20	390	8	70	30	89	385	300
CM20-22	450	11	71	32	94	317	318
CM22-24	455	10	68	74	94	307	314
CM24-26	453	10	71	31	93	350	303
CM26-28	430	11	72	33	95	333	299
CM28-30	439	12	76	34	97	311	303
CM30-32	411	9	73	34	95	341	286
CM32-34	438	10	75	34	97	338	274
CM34-36	443	12	74	36	98	338	281
CM36-38	423	11	78	35	100	333	267
CM38-40	442	11	81	37	102	301	279
CM40-42	460	13	83	39	108	310	253
CM42-44	421	12	87	43	110	331	225
CM44-46	459	11	88	41	111	295	243
CM46-48	447	12	86	42	107	371	207
CM48-50	442	11	89	42	114	301	223
CM50-55	438	11	87	43	113	295	227
CM55-60	471	14	93	45	119	277	223
CM60-65	431	12	92	42	115	287	220

N.A. Not Analysed

CORE CR1.

Salt-corrected trace element data, ppm

	Ba	Sc	Cr	Ni	Rb	Sr	Zr
CR0-1	500	11	74	35	108	295	270
CR1-2	493	12	74	35	108	307	264
CR2-3	491	13	75	35	106	316	271
CR3-4	508	13	74	34	108	261	290
CR4-5	487	11	75	34	105	284	289
CR5-6	345	1	51	26	72	655	205
CR6-7	266	N.D.	44	23	61	790	163
CR7-8	319	N.D.	48	24	68	751	170
CR8-9	389	2	55	27	83	598	212
CR9-10	358	N.D.	53	26	76	674	192
CR10-12	476	11	73	33	103	370	248
CR12-14	495	12	77	35	108	303	268
CR14-16	463	12	73	32	104	331	265
CR16-18	427	7	66	30	95	408	252
CR18-20	459	12	70	31	101	333	263
CR20-22	393	9	65	31	93	443	246
CR22-24	450	8	65	31	93	436	250
CR24-26	448	8	71	32	102	335	257
CR26-28	511	8	73	35	107	296	267
CR28-30	458	4	78	35	107	298	260
CR30-32	N.A.	N.A.	N.A.	N.A.	N.A.	N.A.	N.A.
CR32-34	448	10	78	37	110	303	247
CR34-36	498	14	84	39	115	282	242
CR36-38	450	8	76	37	107	353	233
CR38-40	414	10	78	35	105	394	220
CR40-42	446	11	82	37	113	337	220
CR42-44	478	15	92	41	121	253	233
CR44-46	506	13	90	42	122	238	237
CR46-48	489	14	88	40	120	250	251
CR48-50	482	13	84	38	115	288	245
CR50-55	512	15	90	42	122	245	243
CR55-60	469	12	88	40	118	295	221
CR60-65	514	15	91	41	124	227	234

CORE DN1.

Salt-corrected trace element data, ppm

	Ba	Sc	Cr	Ni	Rb	Sr	Zr
DN0-1	408	14	104	51	119	338	168
DN1-2	413	14	101	49	119	333	168
DN2-3	416	12	98	49	119	336	162
DN3-4	378	14	98	48	119	333	160
DN4-5	416	16	98	49	119	333	164
DN5-6	382	14	101	50	121	331	166
DN6-7	375	15	94	46	115	323	160
DN7-8	416	12	100	49	120	329	162
DN8-9	380	14	100	49	119	327	165
DN9-10	392	14	98	48	119	341	164
DN10-12			No Sample				
DN12-14			No Sample				
DN14-16	575	16	135	68	163	459	218
DN16-18	300	7	76	42	113	311	156
DN18-20	422	15	103	48	122	332	169
DN20-22	415	15	97	47	117	331	156
DN22-24	417	15	99	48	121	327	157
DN24-26	426	16	101	50	122	330	160
DN26-28	404	14	99	48	121	332	158
DN28-30	426	14	98	48	121	331	163
DN30-32	372	15	99	48	122	338	162
DN32-34	404	11	99	47	118	360	160
DN34-36	416	16	103	48	121	335	164
DN36-38	392	15	102	49	120	338	164
DN38-40	398	16	100	48	120	337	168
DN40-42	358	15	97	46	119	346	166
DN42-44	392	14	100	48	118	342	166
DN44-46	418	15	98	49	119	347	167
DN46-48	422	15	100	47	120	347	163
DN48-50	402	13	99	48	120	344	163
DN50-55	379	16	97	45	118	350	172

N.D. - Not detectable

N.A. Not Analysed

CORE DU1.

Salt-corrected trace element data, ppm

	Ba	Sc	Cr	Ni	Rb	Sr	Zr
DU0-1	455	16	104	52	112	336	133
DU1-2	457	15	108	54	121	319	121
DU2-3	485	14	108	54	120	310	132
DU3-4	461	16	106	53	119	315	143
DU4-5	N.A.	N.A	N.A	N.A.	N.A.	N.A.	N.A
DU5-6	500	16	107	56	119	298	140
DU6-7	477	17	105	53	117	300	149
DU7-8	478	15	106	52	116	314	156
DU8-9	477	15	99	49	112	315	165
DU9-10	N.A.	N.A.	N.A.	N.A.	N.A.	N.A.	N.A
DU10-12	527	14	98	45	107	330	176
DU12-14	539	13	95	46	106	335	163
DU14-16	568	11	82	39	101	360	180
DU16-18	577	12	84	41	100	388	169
DU18-20	549	12	88	41	99	361	185
DU20-22	N.A.	N.A.	N.A.	N.A.	N.A.	N.A.	N.A
DU22-24	580	13	74	34	90	439	191
DU24-26	561	14	85	39	102	354	188
DU26-28	558	13	98	44	111	329	170
DU28-30	642	12	82	37	104	351	258
DU30-32	695	16	88	42	125	313	218
DU32-34	731	16	95	47	140	274	216
DU34-36	761	14	96	47	144	265	216
DU36-38	723	17	95	46	143	267	217
DU38-40	742	15	94	47	142	267	218
DU40-42	770	14	94	46	144	266	213
DU42-44	789	16	95	47	143	269	223
DU44-46	779	15	96	47	143	270	223

CORE ET1.

Salt-corrected trace element data, ppm

	Ba	Sc	Cr	Ni	Rb	Sr	Zr
ET0-1	593	13	89	46	89	309	197
ET1-2	637	13	88	48	92	301	184
ET2-3	608	13	89	47	90	313	156
ET3-4	602	14	95	48	93	299	156
ET4-5	495	14	84	46	85	267	166
ET5-6	581	12	91	47	92	284	180
ET6-7	529	12	85	46	88	272	172
ET7-8	551	11	85	45	89	349	166
ET8-9	513	12	90	47	87	281	172
ET9-10	565	13	84	46	87	275	176
ET10-12	552	14	88	46	92	269	183
ET12-14	589	14	91	48	97	268	171
ET14-16	622	15	90	48	97	273	178
ET16-18	600	15	88	46	95	273	171
ET18-20				No Sample			
ET20-22	624	11	86	46	95	282	186
ET22-24				No Sample			
ET24-26	607	15	88	46	96	287	181
ET26-28	601	13	86	46	93	283	177
ET28-30	616	14	88	45	94	285	185
ET30-32	577	14	87	46	94	300	196
ET32-34	644	14	85	45	92	303	204
ET34-36	667	14	83	45	93	298	205
ET36-38	604	15	81	45	91	294	179
ET38-40	625	16	84	43	91	296	187
ET40-42	630	12	82	43	91	297	188
ET42-44	662	14	85	43	92	299	197
ET44-46	646	12	84	41	91	300	189
ET46-48	591	12	86	43	89	271	163
ET48-50	611	13	87	42	93	273	175
ET50-55	631	14	84	42	91	288	177
ET55-60	622	14	85	43	92	295	174
ET60-65	603	12	78	41	88	301	184

N.A. Not Analysed

CORE SH1.

Salt-corrected trace element data, ppm

	Ba	Sc	Cr	Ni	Rb	Sr	Zr
SH0-1	321	10	93	48	106	453	138
SH1-2	297	10	95	48	105	445	148
SH2-3	322	12	95	48	105	444	146
SH3-4	331	12	100	48	105	443	144
SH4-5	304	13	97	48	105	444	143
SH5-6	314	11	99	48	106	444	145
SH6-7	306	13	99	50	106	443	143
SH7-8	312	12	95	50	107	447	144
SH8-9	N.A.	N.A.	N.A.	N.A.	N.A.	N.A.	N.A.
SH9-10	292	12	97	48	106	445	144
SH10-12	293	14	98	48	106	445	142
SH12-14	308	10	98	49	107	448	141
SH14-16	305	12	96	48	107	445	143
SH16-18	294	15	95	48	106	444	143
SH18-20	280	12	99	49	106	449	141
SH20-22	336	12	97	49	105	451	142
SH22-24	284	13	97	49	106	452	145
SH24-26	309	8	97	50	105	455	146
SH26-28	323	13	95	49	106	457	143
SH28-30	305	11	98	50	104	451	142
SH30-32	312	11	97	48	106	457	144
SH32-34	322	9	100	48	106	462	147
SH34-36	310	12	94	47	103	460	146
SH36-38	284	12	97	49	104	465	147
SH38-40	249	13	96	48	103	475	146
SH40-42	270	11	95	48	103	465	147
SH42-44	307	13	100	49	105	465	145
SH44-46	293	14	100	48	104	467	149
SH46-48	320	11	95	48	103	468	144
SH48-50	318	11	99	49	104	464	149

CORE SP1.

Salt-corrected trace element data, ppm

	Ba	Sc	Cr	Ni	Rb	Sr	Zr
SP0-1	N.A.	N.A.	N.A.	N.A.	N.A.	N.A.	N.A.
SP1-2	333	15	103	49	108	346	159
SP2-3	377	13	105	49	111	311	166
SP3-4	370	15	104	48	111	308	162
SP4-5	362	13	105	49	110	315	162
SP5-6	382	16	106	49	111	312	165
SP6-7	N.A.	N.A.	N.A.	N.A.	N.A.	N.A.	N.A.
SP7-8	358	16	103	49	110	317	163
SP8-9	358	14	105	49	109	329	168
SP9-10	340	17	100	46	104	325	163
SP10-12	340	13	99	50	106	349	167
SP12-14	369	17	106	49	110	320	165
SP14-16	342	11	94	45	100	416	157
SP16-18	358	15	101	47	103	369	165
SP18-20	337	12	99	47	103	359	169
SP20-22	354	12	103	48	103	348	173
SP22-24	350	15	102	47	103	343	180
SP24-26	325	14	98	46	100	380	168
SP26-28	344	13	96	44	98	355	164
SP28-30	329	14	99	46	100	364	176
SP30-32	403	15	106	48	114	288	164
SP32-34	399	13	100	47	102	346	173
SP34-36	295	16	102	48	105	337	177
SP36-38	375	15	101	47	106	342	174
SP38-40	337	12	101	47	105	348	174
SP40-42	341	11	102	47	107	338	172
SP42-44	359	11	99	48	107	343	172
SP44-46	340	14	103	47	105	344	171
SP46-48	357	12	101	46	108	352	169
SP48-50	N.A.	N.A.	N.A.	N.A.	N.A.	N.A.	N.A.
SP50-55	365	12	101	46	106	353	169
SP55-60	329	13	99	46	105	354	171
SP60-65	346	14	99	46	109	343	168
SP65-70	337	14	99	46	108	351	168
SP70-75	365	13	99	46	107	359	168

CORE HO1.

Salt-corrected trace element data, ppm

	Ba	Sc	Cr	Ni	Rb	Sr	Zr
HO0-1	401	18	106	49	118	287	160
HO1-2	375	20	105	50	117	287	154
HO2-3	330	18	91	41	102	241	136
HO3-4	411	18	113	58	115	354	153
HO4-5	417	22	116	56	113	348	165
HO5-6	406	19	116	57	117	348	155
HO6-7	418	17	116	56	113	348	160
HO7-8	413	18	118	57	111	354	162
HO8-9	429	17	119	58	106	358	152
HO9-10	453	17	119	59	108	358	153
HO10-12	449	17	121	57	109	361	162
HO12-14	445	16	126	63	97	406	148
HO14-16	454	14	129	67	91	390	143
HO16-18	430	15	124	66	93	415	146
HO18-20	430	17	125	61	104	372	152
HO20-22	443	17	123	58	99	389	151
HO22-24	437	12	141	65	76	414	154
HO24-26	504	12	155	63	70	427	172
HO26-28	561	12	114	48	82	382	187
HO28-30	447	16	146	66	98	374	159
HO30-32	N.A	N.A.	N.A.	N.A.	N.A.	N.A.	N.A.
HO32-34	458	16	146	64	100	383	162
HO34-36	428	18	131	61	100	381	153
HO36-38	371	18	124	57	106	384	169
HO38-40	436	17	132	57	107	381	157

CORE NE1.

Salt-corrected trace element data, ppm

	Ba	Sc	Cr	Ni	Rb	Sr	Zr
NE0-1	393	17	116	67	124	353	131
NE1-2	372	19	102	53	116	393	132
NE2-3	398	20	106	55	123	345	133
NE3-4	383	20	103	51	123	350	134
NE4-5	404	20	102	53	123	349	134
NE5-6	376	21	102	53	124	352	138
NE6-7	418	19	104	53	123	353	134
NE7-8	395	20	104	52	123	348	136
NE8-9	413	20	99	52	124	355	134
NE9-10	386	22	102	52	123	355	136
NE10-12	423	21	102	51	123	354	135
NE12-14	399	19	102	52	124	359	133
NE14-16	388	19	102	53	123	350	135
NE16-18	392	21	105	52	123	364	133
NE18-20	383	20	104	52	124	361	134
NE20-22	410	18	100	52	123	361	132
NE22-24	385	21	99	49	120	355	129
NE24-26	377	21	102	52	123	361	133
NE26-28	415	20	100	51	124	360	133
NE28-30	376	21	102	52	122	366	132
NE30-32	391	20	103	52	124	372	134
NE32-34	396	23	101	51	122	372	134
NE34-36	368	20	100	52	122	378	133
NE36-38	346	21	101	51	121	375	134
NE38-40	398	21	99	51	122	386	132

N.A. Not Analysed

CORE SN1.

Salt-corrected trace element data, ppm

	Ba	Sc	Cr	Ni	Rb	Sr	Zr
SN0-1			No Sample				
SN1-2			No Sample				
SN2-3	193	3	71	29	51	709	152
SN3-4	202	N.D.	67	27	47	745	150
SN4-5	193	3	74	29	51	700	153
SN5-6	350	20	131	65	100	374	147
SN6-7	323	18	132	65	101	376	145
SN7-8	306	19	134	65	97	393	147
SN8-9	321	18	129	64	97	375	148
SN9-10	337	18	127	64	98	375	147
SN10-12	322	18	125	63	98	376	145
SN12-14	333	20	132	65	99	381	148
SN14-16	286	19	128	64	97	381	145
SN16-18	314	21	130	66	98	387	143
SN18-20	304	18	129	66	97	391	145
SN20-22	313	18	131	66	97	392	143
SN22-24	310	19	134	65	97	391	143
SN24-26	330	21	134	67	97	391	147
SN26-28	313	20	131	66	97	395	146
SN28-30	321	16	133	63	96	396	145
SN30-32	316	21	133	64	93	396	149
SN32-34	301	16	135	64	94	402	148
SN34-36	327	17	127	61	97	409	146
SN36-38	316	19	128	63	97	406	147
SN38-40	326	19	127	62	96	407	146
SN40-42	326	17	128	62	98	413	147

N.D. - Not detectable

TABLE AII.3

Lithogenic Minor Element Ratios.

(Zr/Rb, Ni/Cr, Ni/Rb, Cr/Rb, Sc/Rb)

CORE AB1.

Salt free minor element ratios

	Zr/Rb	Ni/Cr	Ni/Rb	Cr/Rb	Sc/Rb
AB0-1	2.17	0.49	0.47	0.95	0.14
AB1-2	2.26	0.51	0.47	0.92	0.13
AB2-3	N.A.	N.A.	N.A.	N.A.	N.A.
AB3-4	2.29	0.50	0.48	0.97	0.12
AB4-5	2.08	0.51	0.48	0.93	0.14
AB5-6	2.12	0.51	0.47	0.93	0.12
AB6-7	2.07	0.50	0.47	0.93	0.15
AB7-8	2.07	0.50	0.46	0.93	0.13
AB8-9	2.02	0.51	0.48	0.92	0.12
AB9-10	2.05	0.50	0.47	0.95	0.16
AB10-12	2.02	0.51	0.48	0.94	0.12
AB12-14	1.97	0.52	0.48	0.91	0.16
AB14-16	1.96	0.49	0.46	0.94	0.12
AB16-18	1.91	0.49	0.46	0.94	0.14
AB18-20	1.87	0.49	0.46	0.93	0.14
AB20-22	1.99	0.47	0.45	0.95	0.16
AB22-24	1.97	0.46	0.44	0.95	0.14
AB24-26	1.99	0.47	0.46	0.97	0.13
AB26-28	1.97	0.46	0.45	0.97	0.17
AB28-30	1.91	0.47	0.45	0.95	0.12
AB30-32	N.A.	N.A.	N.A.	N.A.	N.A.
AB32-34	1.92	0.48	0.46	0.96	0.17
AB34-36	1.93	0.48	0.46	0.95	0.14
AB36-38	1.98	0.48	0.44	0.93	0.13
AB38-40	1.93	0.52	0.42	0.79	0.10
AB40-42	1.95	0.49	0.46	0.95	0.12
AB42-44	1.92	0.47	0.44	0.91	0.12
AB44-46	2.09	0.47	0.43	0.95	0.16
AB46-48	2.14	0.47	0.44	0.95	0.13
AB48-50	2.08	0.49	0.44	0.92	0.14
AB50-55	2.19	0.47	0.44	0.93	0.14

CORE CM1.

Salt free minor element ratios

	Zr/Rb	Ni/Cr	Ni/Rb	Cr/Rb	Sc/Rb
CM0-1	3.93	0.45	0.33	0.73	0.05
CM1-2	3.98	0.44	0.31	0.71	0.12
CM2-3	4.17	0.44	0.31	0.71	0.12
CM3-4	4.20	0.45	0.32	0.71	0.12
CM4-5	4.16	0.44	0.31	0.71	0.11
CM5-6	4.23	0.45	0.30	0.67	0.11
CM6-7	4.35	0.46	0.32	0.70	0.11
CM7-8	4.22	0.48	0.33	0.70	0.11
CM8-9	4.20	0.44	0.31	0.71	0.11
CM9-10	N.A.	N.A.	N.A.	N.A.	N.A.
CM10-12	3.48	0.44	0.33	0.74	0.10
CM12-14	3.48	0.46	0.34	0.74	0.12
CM14-16	3.47	0.46	0.34	0.75	0.10
CM16-18	3.34	0.44	0.34	0.78	0.10
CM18-20	3.37	0.43	0.34	0.79	0.09
CM20-22	3.38	0.45	0.34	0.76	0.12
CM22-24	3.33	0.43	0.34	0.79	0.11
CM24-26	3.27	0.44	0.33	0.76	0.11
CM26-28	3.14	0.46	0.35	0.76	0.12
CM28-30	3.11	0.45	0.35	0.78	0.12
CM30-32	3.02	0.47	0.36	0.77	0.10
CM32-34	3.81	0.45	0.35	0.77	0.10
CM34-36	2.86	0.49	0.37	0.76	0.12
CM36-38	2.67	0.45	0.35	0.78	0.10
CM38-40	2.72	0.46	0.36	0.79	0.11
CM40-42	2.34	0.47	0.36	0.77	0.12
CM42-44	2.04	0.49	0.39	0.79	0.11
CM44-46	2.18	0.47	0.37	0.79	0.10
CM46-48	1.93	0.49	0.39	0.80	0.11
CM48-50	1.96	0.47	0.37	0.78	0.10
CM50-55	2.02	0.49	0.38	0.77	0.12
CM55-60	1.88	0.48	0.38	0.78	0.12
CM60-65	1.91	0.47	0.37	0.80	0.10

N.A. Not Analysed

CORE CR1.

Salt free minor element ratios

	Zr/Rb	Ni/Cr	Ni/Rb	Cr/Rb	Sc/Rb
CR0-1	2.51	0.47	0.32	0.69	0.10
CR1-2	2.44	0.47	0.32	0.69	0.11
CR2-3	2.55	0.47	0.33	0.71	0.12
CR3-4	2.69	0.46	0.32	0.69	0.12
CR4-5	2.75	0.45	0.32	0.71	0.11
CR5-6	2.83	0.51	0.32	0.71	0.01
CR6-7	2.66	0.52	0.38	0.72	N.D.
CR7-8	2.50	0.50	0.35	0.71	N.D.
CR8-9	2.56	0.49	0.33	0.66	0.02
CR9-10	2.52	0.49	0.34	0.70	N.D.
CR10-12	2.41	0.45	0.32	0.71	0.11
CR12-14	2.47	0.46	0.32	0.71	0.11
CR14-16	2.54	0.44	0.31	0.70	0.12
CR16-18	2.64	0.46	0.32	0.70	0.07
CR18-20	2.59	0.43	0.31	0.69	0.12
CR20-22	2.66	0.48	0.33	0.70	0.10
CR22-24	2.69	0.48	0.33	0.70	0.08
CR24-26	2.51	0.45	0.30	0.70	0.08
CR26-28	2.49	0.48	0.33	0.68	0.08
CR28-30	2.42	0.45	0.33	0.73	0.04
CR30-32	N.A.	N.A.	N.A.	N.A.	N.A.
CR32-34	2.24	0.47	0.34	0.71	0.09
CR34-36	2.10	0.46	0.34	0.73	0.12
CR36-38	2.18	0.49	0.35	0.71	0.08
CR38-40	2.10	0.45	0.33	0.74	0.10
CR40-42	1.95	0.45	0.33	0.73	0.10
CR42-44	1.92	0.45	0.34	0.76	0.12
CR44-46	1.94	0.47	0.34	0.74	0.11
CR46-48	2.10	0.46	0.33	0.73	0.12
CR48-50	2.14	0.45	0.33	0.73	0.12
CR50-55	1.99	0.47	0.34	0.74	0.12
CR45-60	1.88	0.46	0.34	0.75	0.10
CR60-65	1.88	0.45	0.33	0.73	0.12

CORE DN1.

Salt free minor element ratios

	Zr/Rb	Ni/Cr	Ni/Rb	Cr/Rb	Sc/Rb
DN0-1	1.42	0.49	0.43	0.87	0.12
DN1-2	1.42	0.49	0.41	0.85	0.12
DN2-3	1.36	0.50	0.41	0.82	0.10
DN3-4	1.34	0.49	0.40	0.82	0.12
DN4-5	1.38	0.50	0.41	0.82	0.13
DN5-6	1.37	0.49	0.41	0.84	0.12
DN6-7	1.39	0.49	0.40	0.82	0.13
DN7-8	1.36	0.49	0.41	0.83	0.10
DN8-9	1.38	0.48	0.41	0.84	0.12
DN9-10	1.38	0.50	0.40	0.82	0.12
DN10-12			No Sample		
DN12-14			No Sample		
DN14-16	1.34	0.55	0.42	0.83	0.10
DN16-18	1.38	0.47	0.37	0.68	0.16
DN18-20	1.38	0.49	0.39	0.84	0.12
DN20-22	1.33	0.49	0.40	0.83	0.13
DN22-24	1.30	0.50	0.40	0.82	0.12
DN24-26	1.31	0.49	0.41	0.83	0.13
DN26-28	1.30	0.49	0.40	0.82	0.12
DN28-30	1.35	0.49	0.40	0.81	0.12
DN30-32	1.33	0.49	0.40	0.81	0.12
DN32-34	1.36	0.48	0.40	0.84	0.09
DN34-36	1.36	0.46	0.40	0.85	0.13
DN36-38	1.36	0.48	0.41	0.85	0.13
DN38-40	1.40	0.47	0.41	0.83	0.13
DN40-42	1.39	0.47	0.40	0.82	0.13
DN42-44	1.40	0.48	0.41	0.85	0.12
DN44-46	1.40	0.50	0.41	0.82	0.13
DN46-48	1.36	0.47	0.40	0.83	0.13
DN48-50	1.36	0.45	0.40	0.83	0.11
DN50-55	1.46	0.46	0.38	0.82	0.14

N.A. Not Analysed

CORE DU1.

Salt free minor element ratios

	Zr/Rb	Ni/Cr	Ni/Rb	Cr/Rb	Sc/Rb
DU0-1	1.19	0.50	0.46	0.93	0.14
DU1-2	1.00	0.50	0.45	0.89	0.12
DU2-3	1.10	0.50	0.45	0.90	0.12
DU3-4	1.20	0.50	0.45	0.89	0.13
DU4-5	N.A.	N.A.	N.A.	N.A.	N.A.
DU5-6	1.18	0.52	0.47	0.90	0.13
DU6-7	1.27	0.51	0.45	0.90	0.15
DU7-8	1.35	0.49	0.45	0.91	0.13
DU8-9	1.47	0.50	0.44	0.88	0.13
DU9-10	N.A.	N.A.	N.A.	N.A.	N.A.
DU10-12	1.64	0.46	0.42	0.92	0.13
DU12-14	1.54	0.48	0.43	0.90	0.12
DU14-16	1.78	0.48	0.39	0.81	0.11
DU16-18	1.69	0.49	0.41	0.84	0.12
DU18-20	1.86	0.47	0.41	0.89	0.12
DU20-22	N.A.	N.A.	N.A.	N.A.	N.A.
DU22-24	2.13	0.46	0.38	0.82	0.14
DU24-26	1.84	0.46	0.38	0.83	0.14
DU26-28	1.53	0.45	0.40	0.88	0.12
DU28-30	2.49	0.45	0.36	0.79	0.12
DU30 32	1.75	0.48	0.34	0.70	0.13
DU32-34	1.54	0.50	0.34	0.68	0.11
DU34-36	1.50	0.49	0.33	0.67	0.10
DU36-38	1.51	0.48	0.32	0.66	0.12
DU38-40	1.53	0.50	0.33	0.66	0.11
DU40-42	1.48	0.49	0.32	0.65	0.10
DU42-44	1.56	0.50	0.33	0.66	0.11
DU44-46	1.56	0.49	0.33	0.67	0.11

CORE ET1.

Salt free minor element ratios

	Zr/Rb	Ni/Cr	Ni/Rb	Cr/Rb	Sc/Rb
ET0-1	2.21	0.52	0.52	1.00	0.15
ET1-2	2.00	0.55	0.52	0.96	0.14
ET2-3	1.74	0.53	0.52	0.99	0.14
ET3-4	1.68	0.55	0.52	1.02	0.15
ET4-5	1.96	0.52	0.54	0.99	0.17
ET5-6	1.95	0.54	0.51	0.99	0.13
ET6-7	1.95	0.53	0.52	0.97	0.14
ET7-8	1.87	0.52	0.51	0.96	0.12
ET8-9	1.98	0.55	0.54	1.03	0.14
ET9-10	2.02	0.52	0.53	0.97	0.15
ET10-12	1.99	0.53	0.50	0.96	0.15
ET12-14	1.77	0.53	0.50	0.94	0.14
ET14-16	1.83	0.52	0.50	0.93	0.16
ET16-18	1.80	0.54	0.48	0.93	0.16
ET18-20		No Sample			
ET20-22	1.97	0.52	0.48	0.91	0.12
ET22-24		No Sample			
ET24-26	1.89	0.54	0.48	0.92	0.16
ET26-28	1.90	0.51	0.50	0.93	0.14
ET28-30	1.97	0.53	0.48	0.94	0.15
ET30-32	2.09	0.53	0.49	0.93	0.15
ET32-34	2.21	0.53	0.49	0.92	0.15
ET34-36	2.21	0.54	0.48	0.89	0.15
ET36-38	1.97	0.56	0.49	0.89	0.17
ET38-40	2.05	0.51	0.47	0.92	0.18
ET40-42	2.07	0.52	0.47	0.90	0.13
ET42-44	2.14	0.51	0.47	0.92	0.15
ET44-46	2.09	0.49	0.45	0.92	0.13
ET46-48	1.83	0.50	0.48	0.97	0.14
ET48-50	1.88	0.48	0.45	0.94	0.14
ET50-55	1.95	0.51	0.46	0.92	0.15
ET55-60	1.90	0.52	0.47	0.92	0.15
ET60-65	2.09	0.53	0.47	0.89	0.14

N.A. Not Analysed

CORE SH1.

Salt free minor element ratios

	Zr/Rb	Ni/Cr	Ni/Rb	Cr/Rb	Sc/Rb
SH0-1	1.56	0.52	0.46	0.88	0.09
SH1-2	1.41	0.51	0.46	0.91	0.09
SH2-3	1.40	0.51	0.46	0.91	0.11
SH3-4	1.37	0.48	0.46	0.95	0.11
SH4-5	1.36	0.50	0.46	0.92	0.12
SH5-6	1.37	0.50	0.45	0.93	0.10
SH6-7	1.35	0.51	0.47	0.93	0.12
SH7-8	1.35	0.53	0.47	0.89	0.11
SH8-9	N.A.	N.A.	N.A.	N.A.	N.A.
SH9-10	1.36	0.50	0.45	0.92	0.11
SH10-12	1.33	0.49	0.45	0.93	0.13
SH12-14	1.31	0.50	0.46	0.92	0.09
SH14-16	1.34	0.50	0.45	0.90	0.11
SH16-18	1.35	0.51	0.45	0.90	0.14
SH18-20	1.34	0.50	0.46	0.93	0.11
SH20-22	1.35	0.51	0.47	0.92	0.11
SH22-24	1.36	0.51	0.46	0.92	0.12
SH24-26	1.40	0.52	0.48	0.92	0.08
SH26-28	1.35	0.52	0.46	0.90	0.12
SH28-30	1.36	0.51	0.48	0.94	0.11
SH30-32	1.36	0.50	0.43	0.92	0.10
SH32-34	1.39	0.48	0.43	0.95	0.09
SH34-36	1.42	0.50	0.46	0.91	0.12
SH36-38	1.42	0.51	0.47	0.93	0.12
SH38-40	1.42	0.50	0.47	0.93	0.13
SH40-42	1.42	0.51	0.47	0.92	0.11
SH42-44	1.38	0.49	0.47	0.95	0.12
SH44-46	1.44	0.48	0.46	0.96	0.14
SH46-48	1.40	0.51	0.47	0.92	0.11
SH48-50	1.43	0.50	0.47	0.95	0.11

N.D. - Not detectable

N.A. Not analysed

CORE SP1.

Salt free minor element ratios

	Zr/Rb	Ni/Cr	Ni/Rb	Cr/Rb	Sc/Rb
SP0-1			No Sample		
SP1-2	1.47	0.46	0.45	0.95	0.14
SP2-3	1.50	0.47	0.44	0.95	0.12
SP3-4	1.46	0.46	0.43	0.94	0.14
SP4-5	1.47	0.47	0.45	0.96	0.12
SP5-6	1.49	0.46	0.44	0.96	0.14
SP6-7	N.A.	N.A.	N.A.	N.A.	N.A.
SP7-8	1.48	0.48	0.45	0.94	0.15
SP8-9	1.54	0.47	0.45	0.96	0.13
SP9-10	1.57	0.47	0.44	0.96	0.16
SP10-12	1.58	0.51	0.47	0.93	0.12
SP12-14	1.49	0.46	0.45	0.96	0.16
SP14-16	1.56	0.48	0.45	0.94	0.11
SP16-18	1.60	0.47	0.45	0.98	0.15
SP18-20	1.64	0.48	0.45	0.96	0.13
SP20-22	1.68	0.47	0.47	1.00	0.13
SP22-24	1.75	0.46	0.46	0.99	0.15
SP24-26	1.67	0.47	0.46	0.98	0.14
SP26-28	1.68	0.46	0.45	0.97	0.13
SP28-30	1.76	0.48	0.46	0.98	0.14
SP30-32	1.43	0.45	0.42	0.93	0.13
SP32-34	1.70	0.47	0.46	0.98	0.13
SP34-36	1.69	0.47	0.46	0.97	0.15
SP36-38	1.64	0.47	0.44	0.95	0.14
SP38-40	1.65	0.47	0.45	0.96	0.11
SP40-42	1.61	0.46	0.44	0.95	0.10
SP42-44	1.60	0.49	0.45	0.93	0.10
SP44-46	1.62	0.46	0.45	0.98	0.13
SP46-48	1.57	0.46	0.43	0.94	0.11
SP48-50	N.A.	N.A.	N.A.	N.A.	N.A.
SP50-55	1.60	0.46	0.43	0.95	0.11
SP55-60	1.63	0.46	0.44	0.94	0.12
SP60-65	1.54	0.46	0.42	0.91	0.13
SP65-70	1.56	0.46	0.43	0.92	0.13
SP70-75	1.57	0.46	0.43	0.93	0.12

CORE HO1.

Salt free minor element ratios

	Zr/Rb	Ni/Cr	Ni/Rb	Cr/Rb	Sc/Rb
HO0-1	1.36	0.47	0.43	0.90	0.16
HO1-2	1.32	0.48	0.43	0.90	0.17
HO2-3	1.33	0.46	0.41	0.90	0.17
HO3-4	1.33	0.51	0.50	0.99	0.15
HO4-5	1.46	0.48	0.50	1.02	0.20
HO5-6	1.32	0.49	0.49	0.99	0.16
HO6-7	1.42	0.49	0.51	1.03	0.15
HO7-8	1.46	0.48	0.51	1.07	0.17
HO8-9	1.44	0.48	0.55	1.14	0.16
HO9-10	1.41	0.49	0.54	1.10	0.16
HO10-12	1.49	0.47	0.52	1.11	0.16
HO12-14	1.52	0.50	0.65	1.30	0.17
HO14-16	1.57	0.52	0.73	1.42	0.16
HO16-18	1.58	0.53	0.70	1.34	0.16
HO18-20	1.46	0.48	0.58	1.20	0.17
HO20-22	1.53	0.48	0.59	1.25	0.17
HO22-24	2.03	0.46	0.88	1.87	0.15
HO24-26	2.47	0.40	0.90	2.22	0.17
HO26-28	2.27	0.42	0.58	1.38	0.15
HO28-30	1.63	0.45	0.68	1.50	0.16
HO30-32	N.A	N.A.	N.A.	N.A.	N.A.
HO32-34	1.63	0.44	0.64	1.47	0.15
HO34-36	1.52	0.47	0.61	1.30	0.18
HO36-38	1.59	0.46	0.53	1.16	0.17
HO38-40	1.47	0.44	0.54	1.24	0.16
HO40-42	1.49	0.44	0.54	1.22	0.17

CORE NE1.

Salt free minor element ratios

	Zr/Rb	Ni/Cr	Ni/Rb	Cr/Rb	Sc/Rb
NE0-1	1.06	0.58	0.55	0.94	0.14
NE1-2	1.14	0.52	0.46	0.87	0.17
NE2-3	1.08	0.52	0.45	0.86	0.16
NE3-4	1.09	0.50	0.41	0.84	0.16
NE4-5	1.09	0.53	0.44	0.83	0.17
NE5-6	1.12	0.53	0.43	0.83	0.17
NE6-7	1.09	0.51	0.43	0.84	0.15
NE7-8	1.10	0.50	0.42	0.84	0.17
NE8-9	1.08	0.53	0.42	0.80	0.17
NE9-10	1.11	0.51	0.43	0.83	0.18
NE10-12	1.09	0.50	0.41	0.83	0.17
NE12-14	1.08	0.52	0.43	0.83	0.15
NE14-16	1.10	0.52	0.43	0.83	0.19
NE16-18	1.08	0.50	0.42	0.85	0.17
NE18-20	1.08	0.50	0.42	0.84	0.16
NE20-22	1.08	0.52	0.43	0.82	0.14
NE22-24	1.08	0.50	0.41	0.83	0.18
NE24-26	1.08	0.51	0.42	0.83	0.17
NE26-28	1.07	0.51	0.41	0.81	0.16
NE28-30	1.09	0.51	0.43	0.84	0.17
NE30-32	1.08	0.51	0.42	0.84	0.17
NE32-34	1.10	0.51	0.42	0.84	0.19
NE34-36	1.09	0.52	0.43	0.82	0.16
NE36-38	1.10	0.51	0.42	0.83	0.17
NE38-40	1.08	0.52	0.42	0.82	0.18

CORE SN1.

Salt free minor element ratios

	Zr/Rb	Ni/Cr	Ni/Rb	Cr/Rb	Sc/Rb
SN0-1			No Sample		
SN1-2			No Sample		
SN2-3	2.99	0.41	0.57	1.39	0.06
SN3-4	3.17	0.40	0.57	1.43	N.D.
SN4-5	2.99	0.39	0.57	1.45	0.06
SN5-6	1.47	0.49	0.65	1.31	0.20
SN6-7	1.44	0.49	0.64	1.31	0.18
SN7-8	1.51	0.49	0.67	1.38	0.20
SN8-9	1.53	0.50	0.66	1.33	0.19
SN9-10	1.50	0.50	0.65	1.30	0.18
SN10-12	1.48	0.50	0.64	1.28	0.18
SN12-14	1.49	0.49	0.66	1.33	0.20
SN14-16	1.49	0.50	0.66	1.32	0.20
SN16-18	1.46	0.51	0.67	1.33	0.21
SN18-20	1.50	0.51	0.68	1.33	0.19
SN20-22	1.47	0.50	0.68	1.35	0.19
SN22-24	1.48	0.49	0.67	1.38	0.20
SN24-26	1.52	0.50	0.69	1.38	0.22
SN26-28	1.51	0.50	0.68	1.35	0.21
SN28-30	1.51	0.47	0.66	1.39	0.17
SN30-32	1.60	0.48	0.69	1.43	0.23
SN32-34	1.57	0.47	0.68	1.44	0.17
SN34-36	1.51	0.48	0.63	1.31	0.18
SN36-38	1.52	0.49	0.65	1.32	0.20
SN38-40	1.52	0.49	0.65	1.32	0.20
SN40-42	1.51	0.49	0.63	1.31	0.17

N.D. Not Detectable

TABLE AII.4

Rare Earth Element Data.

(Y, La, Ce, Nd)

All values given as ppm on a salt free basis.

CORE AB1.

Rare earth element data

	Y	La	Ce	Nd
AB0-1	27	52	118	43
AB1-2	27	53	106	42
AB2-3	N.A.	N.A.	N.A.	N.A.
AB3-4	27	56	118	46
AB4-5	29	50	126	44
AB5-6	29	49	115	42
AB6-7	28	59	122	42
AB7-8	28	51	117	46
AB8-9	28	55	118	46
AB9-10	29	57	122	45
AB10-12	28	55	122	45
AB12-14	27	50	115	39
AB14-16	27	53	120	42
AB16-18	26	47	115	42
AB18-20	26	51	112	43
AB20-22	27	52	117	43
AB22-24	27	52	109	42
AB24-26	27	52	117	42
AB26-28	27	53	112	42
AB28-30	27	52	109	44
AB30-32	N.A.	N.A.	N.A.	N.A.
AB32-34	26	53	112	41
AB34-36	27	51	109	41
AB36-38	28	55	117	41
AB38-40	26	40	84	42
AB40-42	27	48	116	29
AB42-44	27	47	113	41
AB44-46	28	45	113	42
AB46-48	26	46	108	42
AB48-50	28	51	114	39
AB50-55	27	49	119	42

CORE CM1.

Rare earth element data

	Y	La	Ce	Nd
CM0-1	24	22	59	24
CM1-2	25	25	72	26
CM2-3	25	27	67	24
CM3-4	26	32	62	26
CM4-5	25	24	66	26
CM5-6	25	29	65	29
CM6-7	25	31	70	26
CM7-8	26	27	66	26
CM8-9	25	31	60	24
CM9-10	N.A.	N.A.	N.A.	N.A.
CM10-12	25	30	71	28
CM12-14	25	28	69	30
CM14-16	25	25	69	23
CM16-18	24	28	65	30
CM18-20	24	25	68	28
CM20-22	26	29	64	27
CM22-24	26	27	68	28
CM24-26	25	30	71	27
CM26-28	25	33	72	28
CM28-30	26	32	73	31
CM30-32	25	28	74	30
CM32-34	25	28	73	30
CM34-36	26	28	68	31
CM36-38	26	34	71	32
CM38-40	26	29	71	28
CM40-42	26	30	69	30
CM42-44	26	34	68	29
CM44-46	26	31	73	31
CM46-48	24	28	71	31
CM48-50	26	35	79	33
CM50-55	27	32	77	29
CM55-60	26	34	79	33
CM60-65	26	40	81	32

CORE CR1.

Rare earth element data

	Y	La	Ce	Nd
CR0-1	28	38	84	34
CR1-2	28	38	85	34
CR2-3	27	36	85	37
CR3-4	29	39	88	37
CR4-5	29	36	92	36
CR5-6	21	20	67	27
CR6-7	17	16	57	24
CR7-8	19	19	60	27
CR8-9	23	23	70	29
CR9-10	21	24	68	26
CR10-12	26	32	76	33
CR12-14	27	40	81	33
CR14-16	26	35	81	34
CR16-18	25	29	78	31
CR18-20	28	33	80	30
CR20-22	25	30	82	32
CR22-24	26	35	73	30
CR24-26	27	31	79	32
CR26-28	28	32	76	32
CR28-30	27	39	86	34
CR30-32	N.A.	N.A.	N.A.	N.A.
CR32-34	27	38	77	35
CR34-36	27	39	87	36
CR36-38	27	37	82	36
CR38-40	25	32	80	33
CR40-42	27	37	89	35
CR42-44	29	36	96	36
CR44-46	29	43	92	37
CR46-48	29	36	92	37
CR50-55	29	42	96	38
CR55-60	28	36	89	35
CR60-65	29	40	88	38

N.A. Not Analysed

CORE DU1.

Rare Earth Element data

	Y	La	Ce	Nd
DU0-1	24	47	110	39
DU1-2	25	48	122	45
DU2-3	27	52	117	40
DU3-4	27	48	113	40
DU4-5	N.A.	N.A.	N.A.	N.A.
DU5-6	27	45	115	45
DU6-7	27	44	120	44
DU7-8	27	47	120	42
DU8-9	27	47	120	42
DU9-10	N.A.	N.A.	N.A.	N.A.
DU10-12	27	46	126	42
DU12-14	27	50	122	43
DU14-16	26	45	111	44
DU16-18	27	44	114	42
DU18-20	28	46	125	42
DU20-22	N.A.	N.A.	N.A.	N.A.
DU22-24	25	42	111	40
DU24-26	29	45	117	46
DU26-28	29	51	129	51
DU28-30	29	50	115	47
DU30 32	30	45	106	47
DU32-34	32	57	103	50
DU34-36	33	48	107	46
DU36-38	32	50	115	49
DU38-40	33	47	113	51
DU40-42	32	55	104	50
DU42-44	32	56	109	50
DU44-46	33	52	116	50

Rare earth element data

	Y	La	Ce	Nd
DN0-1	24	36	64	29
DN1-2	24	31	74	28
DN2-3	24	30	74	31
DN3-4	24	34	77	34
DN4-5	23	34	80	29
DN5-6	25	37	79	32
DN6-7	24	34	78	29
DN7-8	23	39	78	30
DN8-9	25	35	82	34
DN9-10	25	35	75	32
DN10-12		No Sample		
DN12-14		No Sample		
DN14-16	34	51	109	48
DN16-18	23	24	57	22
DN18-20	25	32	75	33
DN20-22	25	33	75	32
DN22-24	25	34	74	30
DN24-26	25	33	81	31
DN26-28	24	37	83	30
DN28-30	25	34	78	30
DN30-32	25	36	75	32
DN32-34	25	30	72	30
DN34-36	25	32	80	30
DN36-38	25	30	73	31
DN38-40	25	33	74	26
DN40-42	25	32	75	32
DN42-44	25	36	75	33
DN44-46	25	30	75	30
DN46-48	24	30	73	32
DN48-50	25	36	68	30
DN50-55	25	29	77	30

Rare earth element data

	Y	La	Ce	Nd
ET0-1	26	52	120	44
ET1-2	27	49	127	45
ET2-3	27	52	126	46
ET3-4	27	57	134	46
ET4-5	26	58	120	45
ET5-6	28	60	125	47
ET6-7	27	56	125	48
ET7-8	26	48	127	48
ET8-9	28	54	125	46
ET9-10	28	58	125	48
ET10-12	28	55	132	49
ET12-14	28	57	137	50
ET14-16	28	55	133	47
ET16-18	27	59	135	48
ET18-20		No Sample		
ET20-22	28	60	122	46
ET22-24		No Sample		
ET24-26	28	54	141	48
ET26-28	27	57	123	45
ET28-30	27	55	125	43
ET30-32	29	53	126	46
ET32-34	28	52	127	45
ET34-36	28	58	137	46
ET36-38	27	55	127	44
ET38-40	28	55	128	46
ET40-42	27	58	131	47
ET42-44	27	55	129	45
ET44-46	27	55	134	46
ET46-48	26	56	134	44
ET48-50	27	60	133	49
ET50-55	27	54	125	45
ET55-60	27	62	134	51
ET60-65	27	51	129	47

N.A. Not Analysed

CORE SP1.

Rare earth element data

	Y	La	Ce	Nd
SP0-1		No Sample		
SP1-2	23	33	69	29
SP2-3	24	34	81	30
SP3-4	24	37	75	30
SP4-5	24	36	73	30
SP5-6	25	32	81	32
SP6-7	N.A.	N.A.	N.A.	N.A.
SP7-8	24	37	69	32
SP8-9	24	31	75	32
SP9-10	24	34	76	29
SP10-12	24	33	73	28
SP12-14	25	37	83	29
SP14-16	23	31	66	28
SP16-18	23	33	64	28
SP18-20	24	30	73	27
SP20-22	24	32	76	28
SP22-24	25	33	75	30
SP24-26	24	27	71	30
SP26-28	22	35	69	28
SP28-30	24	30	64	27
SP30-32	25	37	75	33
SP32-34	24	30	66	27
SP34-36	24	32	68	30
SP36-38	24	28	71	33
SP38-40	25	31	57	27
SP40-42	24	27	68	29
SP42-44	24	33	67	29
SP44-46	24	31	79	29
SP46-48	25	36	74	29
SP48-50	N.A.	N.A.	N.A.	N.A.
SP50-55	24	26	64	27
SP55-60	24	31	75	27
SP60-65	24	32	75	30
SP65-70	24	31	67	31
SP70-75	24	30	74	31

CORE SH1.

Rare earth element data

	Y	La	Ce	Nd
SH0-1	23	25	63	26
SH1-2	23	30	67	26
SH2-3	24	34	64	27
SH3-4	23	30	60	29
SH4-5	23	26	68	27
SH5-6	23	27	61	26
SH6-7	23	26	72	27
SH7-8	23	33	67	28
SH8-9	N.A.	N.A.	N.A.	N.A.
SH9-10	23	28	62	26
SH10-12	23	29	62	29
SH12-14	23	25	59	24
SH14-16	23	32	64	25
SH16-18	22	28	63	25
SH18-20	23	25	64	28
SH20-22	23	26	61	28
SH22-24	23	29	63	29
SH24-26	23	30	69	27
SH26-28	23	34	67	28
SH28-30	23	29	64	27
SH30-32	23	27	61	30
SH32-34	23	27	68	28
SH34-36	22	28	61	26
SH36-38	24	27	64	32
SH38-40	22	29	62	29
SH40-42	23	27	63	29
SH42-44	24	35	67	28
SH44-46	23	28	59	27
SH46-48	22	25	59	27
SH48-50	23	27	60	28

N.A. Not Analysed

TABLE AII.5

Organic Data.

(S, C, N, C/N)

All data expressed on a salt free basis.

C and N given as %

S given as ppm

C/N given as atomic ratio

CORE AB1.

Salt free organic data

	S (ppm)	C (%)	N (%)	C/N (atm)
AB0-1	961	4.63	N.A.	N.A.
AB1-2	1672	4.33	N.A.	N.A.
AB2-3	N.A.	N.A.	N.A.	N.A.
AB3-4	1232	4.53	N.A.	N.A.
AB4-5	1315	4.75	N.A.	N.A.
AB5-6	1358	4.59	N.A.	N.A.
AB6-7	2346	4.61	N.A.	N.A.
AB7-8	2490	4.54	N.A.	N.A.
AB8-9	2175	4.70	N.A.	N.A.
AB9-10	2745	4.28	N.A.	N.A.
AB10-12	4374	4.38	N.A.	N.A.
AB12-14	7667	4.61	N.A.	N.A.
AB14-16	7330	5.03	N.A.	N.A.
AB16-18	7586	4.29	N.A.	N.A.
AB18-20	9528	4.79	N.A.	N.A.
AB20-22	8547	4.75	N.A.	N.A.
AB22-24	9820	5.02	N.A.	N.A.
AB24-26	9036	4.76	N.A.	N.A.
AB26-28	8981	4.63	N.A.	N.A.
AB28-30	10052	4.64	N.A.	N.A.
AB30-32	N.A.	N.A.	N.A.	N.A.
AB32-34	10157	4.65	N.A.	N.A.
AB34-36	9132	4.33	N.A.	N.A.
AB36-38	9642	4.02	N.A.	N.A.
AB38-40	6099	4.20	N.A.	N.A.
AB40-42	9781	4.22	N.A.	N.A.
AB42-44	8824	4.17	N.A.	N.A.
AB44-46	9332	4.14	N.A.	N.A.
AB46-48	8994	4.06	N.A.	N.A.
AB48-50	8447	4.30	N.A.	N.A.
AB50-55	9262	4.08	N.A.	N.A.

CORE CM1.

Salt free organic data

	S (ppm)	C (%)	N (%)	C/N (atm)
CM0-1	N.D.	0.81	N.A.	N.A.
CM1-2	N.D.	0.91	0.12	8.85
CM2-3	N.D.	0.69	N.A.	N.A.
CM3-4	N.D.	0.83	0.11	8.80
CM4-5	224	0.69	N.A	N.A.
CM5-6	429	0.69	0.10	8.05
CM6-7	810	0.71	N.A.	N.A.
CM7-8	745	0.59	0.10	7.65
CM8-9	913	0.58	N.A.	N.A.
CM9-10	N.A.	N.A.	N.A.	N.A.
CM10-12	2109	0.84	0.10	9.80
CM12-14	2385	0.83	N.A.	N.A.
CM14-16	2134	0.84	0.10	9.80
CM16-18	2139	0.84	N.A.	N.A.
CM18-20	2221	0.78	0.09	10.11
CM20-22	1718	0.73	N.A.	N.A.
CM22-24	1805	0.78	0.10	9.10
CM24-26	1833	0.62	N.A.	N.A.
CM26-28	1505	0.81	0.09	10.50
CM28-30	1618	0.76	N.A.	N.A.
CM30-32	1413	0.66	0.08	9.63
CM32-34	1824	0.75	N.A.	N.A.
CM34-36	1490	0.71	0.08	10.36
CM36-38	1306	0.77	N.A.	N.A.
CM38-40	1322	0.76	0.08	11.09
CM40-42	1440	0.78	N.A.	N.A.
CM42-44	1742	0.78	0.09	10.11
CM44-46	1891	0.78	N.A.	N.A.
CM46-48	2071	0.72	0.09	9.33
CM48-50	1964	0.78	N.A.	N.A.
CM50-55	2230	0.82	0.10	9.57
CM55-60	2011	0.77	N.A.	N.A.
CM60-65	2876	0.83	0.10	9.69

N.A. Not Analysed.

CORE CR1.

Salt free organic data

	S (ppm)	C (%)	N (%)	C/N (atm)
CR0-1	644	2.08	0.28	8.67
CR1-2	1077	2.14	N.A.	N.A.
CR2-3	1111	1.91	0.26	8.56
CR3-4	1413	1.56	N.A.	N.A.
CR4-5	1710	1.79	0.23	9.08
CR5-6	1696	1.19	N.A.	N.A.
CR6-7	1940	1.19	0.14	9.92
CR7-8	2360	1.35	N.A.	N.A.
CR8-9	2783	1.51	0.16	11.01
CR9-10	3016	1.45	N.A.	N.A.
CR10-12	4365	1.53	0.17	10.50
CR12-14	4055	1.52	N.A.	N.A.
CR14-16	4085	1.40	0.17	9.61
CR16-18	4077	1.42	N.A.	N.A.
CR18-20	4048	1.34	0.16	9.73
CR20-22	3598	1.32	N.A.	N.A.
CR22-24	4183	1.45	0.15	11.28
CR24-26	4228	1.53	N.A.	N.A.
CR26-28	4500	1.34	0.18	9.73
CR28-30	4933	1.51	N.A.	N.A.
CR30-32	N.A.	N.A.	N.A.	N.A.
CR32-34	4252	1.62	N.A.	N.A.
CR34-36	4398	1.43	0.18	9.27
CR36-38	3945	1.40	N.A.	N.A.
CR38-40	4063	1.48	0.16	10.74
CR40-42	3778	1.57	N.A.	N.A.
CR42-44	3426	1.51	0.18	9.78
CR44-46	3930	1.50	N.A.	N.A.
CR46-48	3915	1.39	0.17	9.54
CR48-50	4060	1.56	N.A.	N.A.
CR50-55	4365	1.46	0.17	10.02
CR55-60	4442	1.87	N.A.	N.A.
CR60-65	4463	1.58	0.18	11.47

CORE DN1.

Salt free organic data

	S (ppm)	C (%)	N (%)	C/N (atm)
DN0-1	N.D.	N.A.	N.A.	N.A.
DN1-2	N.D.	N.A.	N.A.	N.A.
DN2-3	N.D.	3.15	N.A.	N.A.
DN3-4	N.D.	3.25	N.A.	N.A.
DN4-5	N.D.	3.24	N.A.	N.A.
DN5-6	4	3.25	N.A.	N.A.
DN6-7	26	3.27	N.A.	N.A.
DN7-8	91	3.79	N.A.	N.A.
DN8-9	141	2.88	N.A.	N.A.
DN9-10	459	3.40	N.A.	N.A.
DN10-12		No Sample		
DN12-14		No Sample		
DN14-16	N.D.	5.05	N.A.	N.A.
DN16-18	393	N.A.	N.A.	N.A.
DN18-20	1224	4.04	N.A.	N.A.
DN20-22	51	3.75	N.A.	N.A.
DN22-24	504	3.23	N.A.	N.A.
DN24-26	394	3.70	N.A.	N.A.
DN26-28	688	3.48	N.A.	N.A.
DN28-30	534	3.48	N.A.	N.A.
DN30-32	567	3.96	N.A.	N.A.
DN32-34	577	3.37	N.A.	N.A.
DN34-36	544	3.52	N.A.	N.A.
DN36-38	626	3.26	N.A.	N.A.
DN38-40	571	3.44	N.A.	N.A.
DN40-42	1202	3.41	N.A.	N.A.
DN42-44	937	2.59	N.A.	N.A.
DN44-46	982	3.32	N.A.	N.A.
DN46-48	971	3.48	N.A.	N.A.
DN48-50	1224	3.56	N.A.	N.A.
DN50-55	1113	3.44	N.A.	N.A.

N.A. Not Analysed

CORE DU1.

Salt free organic data

	S (ppm)	C (%)	N (%)	C/N (atm)
DU0-1	903	4.67	N.A.	N.A.
DU1-2	1181	4.61	0.45	11.21
DU2-3	1127	4.80	N.A.	N.A.
DU3-4	1589	4.39	0.44	11.02
DU4-5	N.A	N.A.	N.A.	N.A.
DU5-6	2115	4.79	0.45	1.87.
DU6-7	2325	4.81	N.A.	N.A.
DU7-8	2064	4.37	0.42	11.07
DU8-9	2169	4.45	N.A.	N.A.
DU9-10	N.A.	N.A.	N.A.	N.A.
DU10-12	2390	4.08	N.A.	N.A.
DU12-14	2430	3.00	0.32	10.72
DU14-16	2912	3.34	N.A.	N.A.
DU16-18	2740	2.85	0.26	12.61
DU18-20	3401	2.96	N.A.	N.A.
DU20-22	N.A.	N.A.	N.A.	N.A.
DU22-24	4186	2.11	N.A.	N.A.
DU24-26	4494	2.06	0.22	9.12
DU26-28	4314	2.81	N.A.	N.A.
DU28-30	3827	1.57	0.16	11.30
DU30 32	3173	1.45	N.A.	N.A.
DU32-34	2529	0.80	0.08	11.53
DU34-36	1934	0.64	N.A.	N.A.
DU36-38	2015	0.48	0.06	9.32
DU38-40	2038	0.57	N.A.	N.A.
DU40-42	2086	0.50	0.66	9.71
DU42-44	2370	0.51	N.A.	N.A.
DU44-46	2257	0.54	N.A.	N.A.

CORE ET1.

Salt free organic data

	S (ppm)	C (%)	N (%)	C/N (atm)
ET0-1	1188	5.12	0.50	11.49
ET1-2	1153	6.77	N.A.	N.A.
ET2-3	801	5.53	0.54	11.32
ET3-4	736	4.89	N.A.	N.A.
ET4-5	4971	8.33	0.56	16.47
ET5-6	1524	5.71	N.A.	N.A.
ET6-7	588	6.95	1.49	16.22
ET7-8	1228	6.95	N.A.	N.A.
ET8-9	4291	7.89	0.58	15.09
ET9-10	4588	7.18	N.A.	N.A.
ET10-12	2785	4.40	0.49	10.07
ET12-14	2306	5.78	N.A.	N.A.
ET14-16	1910	5.86	0.46	14.55
ET16-18	2101	5.57	N.A.	N.A.
ET18-20	No Sample			
ET20-22	2527	5.14	0.45	13.03
ET22-24	No Sample			
ET24-26	3093	5.53	0.46	13.44
ET26-28	4539	5.71	N.A.	N.A.
ET28-30	4103	6.28	0.47	14.95
ET30-32	4245	5.60	N.A.	N.A.
ET32-34	5116	5.82	0.46	14.14
ET34-36	4935	6.29	N.A.	N.A.
ET36-38	7393	5.13	0.46	15.71
ET38-40	7647	6.35	N.A.	N.A.
ET40-42	7572	5.37	0.48	12.79
ET42-44	6112	5.39	N.A.	N.A.
ET44-46	7504	6.04	0.48	14.38
ET46-48	11775	7.05	N.A.	N.A.
ET48-50	6782	5.15	0.48	12.26
ET50-55	7396	6.09	N.A.	N.A.
ET55-60	6363	4.82	0.48	11.48
ET60-65	7808	5.11	N.A.	N.A.

N.A. Not Analysed.

CORE SH1.

Salt free organic data

	S (ppm)	C (%)	N (%)	C/N (atm)
SH0-1	729	2.03	N.A.	N.A.
SH1-2	541	2.10	0.30	7.90
SH2-3	636	2.01	N.A.	N.A.
SH3-4	728	1.86	0.27	7.75
SH4-5	921	1.90	0.27	7.92
SH5-6	734	1.78	N.A.	N.A.
SH6-7	829	1.98	0.25	9.24
SH7-8	916	1.83	N.A.	N.A.
SH8-9	N.A.	N.A.	N.A.	N.A.
SH9-10	1050	1.80	0.25	N.A.
SH10-12	1201	1.86	N.A.	8.68
SH12-14	1234	1.84	N.A.	N.A.
SH14-16	1226	1.75	0.25	8.17
SH16-18	1469	1.75	N.A.	N.A.
SH18-20	2170	1.81	N.A.	N.A.
SH20-22	1678	1.68	0.24	8.17
SH22-24	1437	1.53	N.A.	N.A.
SH24-26	1839	1.64	0.24	7.97
SH26-28	2276	1.75	N.A.	N.A.
SH28-30	1933	1.58	0.24	7.68
SH30-32	2035	1.68	N.A.	N.A.
SH32-34	2365	1.63	0.24	7.92
SH34-36	2272	1.64	N.A.	N.A.
SH36-38	2157	1.58	0.23	8.01
SH38-40	1914	1.60	N.A.	N.A.
SH40-42	2342	1.57	0.23	7.96
SH42-44	2442	1.64	N.A.	N.A.
SH44-46	2586	1.71	0.23	8.67
SH46-48	1509	1.50	N.A.	N.A.
SH48-50	2524	1.58	N.A.	8.01

CORE SP1.

Salt free organic data

	S (ppm)	C (%)	N (%)	C/N (atm)
SP0-1	No Sample			
SP1-2	506	1.81	N.A.	N.A.
SP2-3	679	1.78	0.28	7.16
SP3-4	1195	1.98	N.A.	N.A.
SP4-5	1330	2.15	0.28	8.96
SP5-6	1485	1.98	N.A.	N.A.
SP6-7	N.A.	N.A.	N.A.	N.A.
SP7-8	1421	1.84	0.27	7.96
SP8-9	1775	1.95	0.26	8.96
SP9-10	1476	1.71	0.24	8.31
SP10-12	1554	1.73	N.A.	N.A.
SP12-14	2120	1.75	0.24	8.51
SP14-16	2776	1.85	N.A.	N.A.
SP16-18	2715	1.76	0.23	8.93
SP18-20	2571	1.59	N.A.	N.A.
SP20-22	2330	1.33	0.23	9.11
SP22-24	2621	1.27	N.A.	N.A.
SP24-26	3369	1.48	0.22	9.18
SP26-28	3229	1.43	N.A.	N.A.
SP28-30	3688	1.37	0.23	8.37
SP30-32	3565	1.26	N.A.	N.A.
SP32-34	3677	1.49	0.22	7.78
SP34-36	3217	1.29	N.A.	N.A.
SP36-38	3607	1.39	0.21	8.56
SP38-40	3465	1.63	N.A.	N.A.
SP40-42	3427	1.51	0.21	11.22
SP42-44	3804	1.39	N.A.	N.A.
SP44-46	3823	1.31	0.21	7.06
SP46-48	3433	1.38	N.A.	N.A.
SP48-50	N.A.	N.A.	N.A.	N.A.
SP50-55	3795	1.47	N.A.	9.62
SP55-60	3808	1.53	0.20	8.98
SP60-65	3342	1.48	N.A.	N.A.
SP65-70	3244	1.48	0.20	8.28
SP70-75	3793	1.48	N.A.	N.A.

N.A. Not Analysed.

TABLE AII.6

Pore Water Data.

Sulphate values expressed as mM.

Alkalinity values expressed as meq l^{-1}.

CORE AB1.

Pore water data

	SO4 (mM)	AT (meq/l)
AB0-1	16.65	2.62
AB1-2	20.47	5.45
AB2-3	N.A.	N.A.
AB3-4	21.53	3.90
AB4-5	20.47	5.50
AB5-6	16.48	6.22
AB6-7	21.58	6.90
AB7-8	19.59	6.85
AB8-9	20.30	7.41
AB9-10	18.47	8.36
AB10-12	19.73	8.32
AB12-14	17.96	9.58
AB14-16	16.66	10.91
AB16-18	18.72	11.85
AB18-20	17.12	11.25
AB20-22	18.19	11.36
AB22-24	14.30	14.88
AB24-26	14.85	15.58
AB26-28	11.32	17.34
AB28-30	14.57	19.93
AB30-32	N.A.	N.A.
AB32-34	16.09	21.36
AB34-36	14.88	31.98
AB36-38	14.01	24.26
AB38-40	16.39	25.35
AB40-42	13.76	26.24
AB42-44	12.66	26.93
AB44-46	9.90	27.68
AB46-48	13.07	28.55
AB48-50	11.73	29.25
AB50-55	12.33	28.70

CORE CM1.

Pore water data

	SO4 (mM)	AT (meq/l)
CM0-1	30.64	2.21
CM1-2	28.58	2.07
CM2-3	32.74	2.14
CM3-4	28.28	2.15
CM4-5	29.53	2.36
CM5-6	25.84	2.22
CM6-7	31.69	2.45
CM7-8	28.99	2.57
CM8-9	27.94	2.77
CM9-10	N.A.	N.A.
CM10-12	28.74	2.91
CM12-14	29.92	2.93
CM14-16	29.58	3.02
CM16-18	36.02	2.97
CM18-20	33.05	3.20
CM20-22	30.76	3.32
CM22-24	32.31	3.23
CM24-26	31.04	3.31
CM26-28	28.80	3.28
CM28-30	28.89	4.00
CM28-30	27.65	3.43
CM30-32	28.32	3.16
CM32-34	27.42	3.88
CM34-36	27.80	3.90
CM36-38	27.17	4.06
CM38-40	27.85	3.96
CM40-42	25.97	4.89
CM42-44	26.59	4.38
CM44-46	27.06	4.73
CM46-48	27.94	4.13
CM48-50	29.29	5.33
CM50-55	29.20	5.00

N.A. Not Analysed

CORE CR1.

Pore water data

	SO4 (mM)	AT (meq/l)
CR0-1	28.66	6.34
CR1-2	27.61	7.51
CR2-3	27.60	7.51
CR3-4	N.A.	N.A.
CR4-5	26.61	7.98
CR5-6	28.88	7.51
CR6-7	28.34	7.50
CR7-8	28.51	6.85
CR8-9	26.46	8.59
CR9-10	26.55	8.51
CR10-12	29.99	8.66
CR12-14	25.88	9.29
CR14-16	24.68	10.52
CR16-18	25.54	11.01
CR18-20	27.44	11.01
CR20-22	24.00	11.34
CR22-24	26.54	13.07
CR24-26	24.07	11.31
CR26-28	25.56	13.46
CR28-30	23.49	13.26
CR30-32	22.82	13.38
CR32-34	22.23	17.54
CR34-36	23.09	19.35
CR36-38	24.83	14.93
CR38-40	23.82	18.44
CR40-42	24.75	18.34
CR42-44	23.52	19.79
CR44-46	24.30	20.76
CR46-48	N.A.	N.A.
CR48-50	22.80	21.58

CORE DN1.

Pore water data

	SO4 (mM)	AT (meq/l)
DN0-1	29.84	2.51
DN1-2	31.05	1.77
DN2-3	32.65	2.65
DN3-4	29.92	3.07
DN4-5	32.21	3.12
DN5-6	30.79	2.57
DN6-7	30.60	2.59
DN7-8	29.77	3.72
DN8-9	29.24	3.63
DN9-10	31.55	3.56
DN10-12	28.87	3.10
DN12-14	No Sample	
DN14-16	No Sample	
DN16-18	26.25	3.10
DN18-20	29.61	3.52
DN20-22	26.91	4.17
DN22-24	28.47	3.59
DN24-26	28.40	3.70
DN26-28	30.22	3.52
DN28-30	28.57	3.87
DN30-32	29.93	3.77
DN32-34	29.38	4.04
DN34-36	28.17	3.98
DN36-38	27.72	3.96
DN38-40	28.63	4.27
DN40-42	28.83	2.88
DN42-44	28.75	4.37
DN44-46	34.71	4.84
DN46-48	26.74	3.39
DN48-50	28.15	4.41

CORE DU1.

Pore water data

	SO4 (mM)	AT (meq/l)
DU0-1	27.12	N.A.
DU1-2	27.50	N.A.
DU2-3	26.65	N.A.
DU3-4	N.A.	N.A.
DU4-5	N.A.	N.A.
DU5-6	22.68	N.A.
DU6-7	26.98	N.A.
DU7-8	27.97	N.A.
DU8-9	27.46	N.A.
DU9-10	29.37	N.A.
DU10-12	28.92	N.A.
DU12-14	28.12	N.A.
DU14-16	28.71	N.A.
DU16-18	28.39	N.A.
DU18-20	29.59	N.A.
DU20-22	N.A.	N.A.
DU22-24	28.62	N.A.
DU24-26	28.17	N.A.
DU26-28	29.44	N.A.
DU28-30	29.41	N.A.
DU30 32	27.37	N.A.
DU32-34	27.90	N.A.
DU34-36	24.42	N.A.
DU36-38	27.33	N.A.
DU38-40	26.07	N.A.
DU40-42	26.95	N.A.
DU42-44	24.14	N.A.

N.A. Not Analysed

CORE ET1.

Pore water Data

	SO4 (mM)	AT (meq/l)
ET0-1	16.66	5.81
ET1-2	19.87	5.64
ET2-3	20.02	6.78
ET3-4	20.53	7.10
ET4-5	18.88	7.45
ET5-6	19.26	7.45
ET6-7	20.08	7.40
ET7-8	20.23	7.42
ET8-9	20.62	8.14
ET9-10	20.24	8.60
ET10-12	18.28	10.14
ET12-14	17.19	12.46
ET14-16	17.38	14.66
ET16-18	15.97	16.51
ET18-20	16.47	18.07
ET20-22	16.43	19.68
ET22-24	16.69	21.62
ET24-26	16.90	20.18
ET26-28	16.21	20.82
ET28-30	16.46	20.00
ET30-32	16.13	22.70
ET32-34	15.53	22.79
ET34-36	15.10	24.13
ET36-38	13.93	25.14
ET38-40	13.43	22.26
ET40-42	12.14	23.87
ET42-44	10.88	28.50
ET44-46	12.14	30.75
ET46-48	12.77	44.27
ET48-50	10.49	43.96
ET50-55	9.07	56.09
ET55-60	5.62	59.36

CORE SH1.

Pore water data

	SO4 (mM)	AT (meq/l)
SH0-1	26.39	N.A.
SH1-2	26.71	N.A.
SH2-3	25.06	N.A.
SH3-4	25.98	N.A.
SH4-5	25.01	N.A.
SH5-6	26.40	N.A.
SH6-7	25.38	N.A.
SH7-8	25.18	N.A.
SH8-9	26.17	N.A.
SH9-10	26.01	N.A.
SH10-12	25.73	N.A.
SH14-16	23.62	N.A.
SH16-18	24.11	N.A.
SH18-20	24.91	N.A.
SH20-22	25.01	N.A.
SH22-24	24.39	N.A.
SH24-26	24.03	N.A.
SH26-28	24.03	N.A.
SH28-30	22.39	N.A.
SH30-32	22.60	N.A.
SH32-34	21.29	N.A.
SH34-36	21.21	N.A.
SH36-38	19.09	N.A.
SH38-40	14.97	N.A.
SH40-42	N.A.	N.A.
SH42-44	17.46	N.A.
SH44-46	15.76	N.A.
SH46-48	N.A.	N.A.
SH48-50	N.A.	N.A.
SH50-55	15.37	N.A.

N.A. Not analysed

CORE SP1.

Pore water data

	SO4 (mM)	AT (meq/l)
SP0-1	29.89	N.A.
SP1-2	27.40	N.A.
SP2-3	27.22	N.A.
SP3-4	28.00	N.A.
SP4-5	28.41	N.A.
SP5-6	26.19	N.A.
SP6-7	26.62	N.A.
SP7-8	27.41	N.A.
SP8-9	24.39	N.A.
SP9-10	26.74	N.A.
SP10-12	26.89	N.A.
SP12-14	29.97	N.A.
SP14-16	30.75	N.A.
SP16-18	29.19	N.A.
SP18-20	26.06	N.A.
SP20-22	28.37	N.A.
SP22-24	25.95	N.A.
SP24-26	31.01	N.A.
SP26-28	28.18	N.A.
SP28-30	28.77	N.A.
SP30-32	27.60	N.A.
SP32-34	26.21	N.A.
SP34-36	N.A.	N.A.
SP36-38	N.A.	N.A
SP38-40	26.09	N.A.
SP40-42	25.84	N.A.
SP42-44	24.20	N.A.
SP44-46	N.A.	N.A.
SP46-48	27.52	N.A
SP48-50	23.73	N.A.
SP50-55	22.02	N.A.
SP55-60	20.01	N.A.
SP60-65	17.44	N.A.
SP65-70	16.40	N.A.
SP70-75	15.32	N.A.

TABLE AII.7

$\delta^{15}N$ Data.

All values calculated as $^{o}/_{oo}$ from:

$$\delta^{15}N = \frac{(\text{at\% } ^{15}N)_x - (\text{at\% } ^{15}N)_{atm}}{(\text{at\% } ^{15}N)_{atm}} \cdot 1000$$

CORE CM1. DN15		CORE CR1. DN15		CORE DU1. DN15		CORE ET1. DN15		CORE SH1. DN15		CORE SP1. DN15	
CM0-1	N.A.	CR0-1	7.64	DU0-1	N.A.	ET0-1	6.55	SH0-1	N.A.	SP0-1	8.74
CM1-2	13.92	CR1-2	N.A.	DU1-2	9.56	ET1-2	N.A.	SH1-2	3.45	SP1-2	N.A.
CM2-3	N.A.	CR2-3	6.83	DU2-3	N.A.	ET2-3	6.55	SH2-3	N.A.	SP2-3	9.28
CM3-4	14.20	CR3-4	N.A.	DU3-4	8.74	ET3-4	N.A.	SH3-4	4.67	SP3-4	N.A.
CM4-5	N.A.	CR4-5	6.28	DU4-5	N.A.	ET4-5	5.73	SH4-5	4.10	SP4-5	9.28
CM5-6	14.74	CR5-6	N.A.	DU5-6	8.46	ET5-6	N.A.	SH5-6	N.A.	SP5-6	N.A.
CM6-7	N.A.	CR6-7	9.01	DU6-7	N.A.	ET6-7	7.10	SH6-7	3.28	SP6-7	9.56
CM7-8	16.65	CR7-8	N.A.	DU7-8	8.74	ET7-8	N.A.	SH7-8	N.A.	SP7-8	10.37
CM8-9	N.A.	CR8-9	8.19	DU8-9	N.A.	ET8-9	6.01	SH8-9	3.28	SP8-9	N.A.
CM9-10	5.46	CR9-10	N.A.	DU9-10	9.56	ET9-10	N.A.	SH9-10	N.A.	SP9-10	12.01
CM10-12	N.A.	CR10-12	8.19	DU10-12	N.A.	ET10-12	6.83	SH10-12	1.91	SP10-12	N.A.
CM12-14	N.A.	CR12-14	N.A.	DU12-14	10.10	ET12-14	N.A.	SH12-14	N.A.	SP12-14	10.92
CM14-16	3.82	CR14-16	8.74	DU14-16	N.A.	ET14-16	6.83	SH14-16	4.37	SP14-16	N.A.
CM16-18	N.A.	CR16-18	N.A.	DU16-18	11.74	ET16-18	N.A.	SH16-18	9.56	SP16-18	10.65
CM18-20	5.73	CR18-20	8.46	DU18-20	N.A.	ET18-20	N.A.	SH18-20	N.A.	SP18-20	N.A.
CM20-22	N.A.	CR20-22	N.A.	DU20-22	12.29	ET20-22	7.10	SH20-22	10.37	SP20-22	11.47
CM22-24	3.55	CR22-24	9.56	DU22-24	N.A.	ET22-24	N.A.	SH22-24	N.A.	SP22-24	N.A.
CM24-26	N.A.	CR24-26	N.A.	DU24-26	13.10	ET24-26	6.55	SH24-26	10.92	SP24-26	11.19
CM26-28	1.64	CR26-28	9.56	DU26-28	N.A.	ET26-28	N.A.	SH26-28	N.A.	SP26-28	N.A.
CM28-30	N.A.	CR28-30	N.A.	DU28-30	16.38	ET28-30	6.83	SH28-30	12.29	SP28-30	10.37
CM30-32	7.10	CR30-32	9.56	DU30 32	N.A.	ET30-32	N.A.	SH30-32	N.A.	SP30-32	N.A.
CM32-34	N.A.	CR32-34	N.A.	DU32-34	20.20	ET32-34	6.55	SH32-34	12.01	SP32-34	12.01
CM34-36	1.91	CR34-36	9.01	DU34-36	N.A.	ET34-36	N.A.	SH34-36	N.A.	SP34-36	N.A.
CM36-38	N.A.	CR36-38	N.A.	DU36-38	22.11	ET36-38	6.83	SH36-38	13.65	SP34-36	9.28
CM38-40	8.19	CR38-40	9.83	DU38-40	N.A.	ET38-40	N.A.	SH38-40	N.A.	SP38-40	N.A.
CM40-42	N.A.	CR40-42	N.A.	DU40-42	21.84	ET40-42	6.28	SH40-42	12.29	SP40-42	10.10
CM42-44	-12.83	CR42-44	7.10	DU42-44	N.A.	ET42-44	N.A.	SH42-44	N.A.	SP42-44	N.A.
CM44-46	N.A.	CR44-46	N.A.			ET44-46	6.55	SH44-46	13.10	SP44-46	10.37
CM46-48	-8.19	CR46-48	9.83			ET46-48	N.A.	SH46-48	N.A.	SP46-48	N.A.
CM48-50	N.A.	CR48-50	N.A.			ET48-50	7.92	SH48-50	N.A.	SP48-50	10.37
CM50-55	2.46	CR50-55	N.A.			ET50-55	N.A.			SP50-55	N.A.
CM55-60	N.A.					ET55-60	5.46			SP55-60	10.92
CM60-65	8.19									SP60-65	N.A.
										SP65-70	12.83
										SP70-75	N.A.

N.A. Not Analysed

TABLE AII.8

Halogen Data.

(Br, Cl, I)

All values expressed as ppm on a salt free basis.

CORE AB1.

Salt-corrected halogen data, ppm

	I	Br	Cl
AB0-1	540	409	18324
AB1-2	467	290	15546
AB2-3	N.A.	N.A.	N.A.
AB3-4	443	349	15371
AB4-5	369	344	14930
AB5-6	414	359	15352
AB6-7	364	345	16764
AB7-8	421	358	18985
AB8-9	402	350	13330
AB9-10.	388	352	14015
AB10-12	363	352	13973
AB12-14	324	333	19097
AB14-16	316	321	14646
AB16-18	296	316	14926
AB18-20	283	321	19807
AB20-22	282	312	12855
AB22-24	271	306	13967
AB24-26	251	302	14759
AB26-28	244	299	12256
AB28-30	252	291	14062
AB30-32	N.A.	N.A.	N.A.
AB32-34	241	297	14913
AB34-36	259	297	13580
AB36-38	252	291	12091
AB38-40	295	290	11714
AB40-42	243	305	14345
AB42-44	243	297	10522
AB44-46	245	296	13432
AB46-48	233	280	15288
AB48-50	236	293	11977
AB50-55	216	273	13489

CORE CM1.

Salt-corrected halogen data, ppm

	I	Br	Cl
CM0-1	206	141	7423
CM1-2	186	129	5555
CM2-3	166	120	5328
CM3-4	155	108	5171
CM4-5	147	104	4617
CM5-6	133	101	4083
CM6-7	124	96	5171
CM7-8	130	94	4141
CM8-9	122	96	4851
CM9-10	N.A.	N.A.	N.A.
CM10-12	121	108	6280
CM12-14	123	101	5262
CM14-16	115	99	5553
CM16-18	109	90	5369
CM18-20	114	97	6061
CM20-22	118	94	2946
CM22-24	112	101	5719
CM24-26	113	99	6495
CM26-28	117	100	6345
CM28-30	104	104	8381
CM30-32	104	92	4713
CM32-34	102	105	8202
CM34-36	104	94	5946
CM36-38	99	95	5745
CM38-40	104	98	5785
CM40-42	97	91	4956
CM42-44	91	92	6332
CM44-46	97	99	7536
CM46-48	93	85	9210
CM48-50	95	96	7433
CM50-55	92	98	7252
CM55-60	89	85	4741
CM60-65	84	104	8544

CORE CR1.

Salt-corrected halogen data, ppm

	I	Br	Cl
CR0-1	342	221	8791
CR1-2	329	232	11047
CR2-3	298	201	7732
CR3-4	262	184	7452
CR4-5	241	172	7980
CR5-6	194	121	6934
CR6-7	177	107	6662
CR7-8	168	107	7336
CR8-9	158	114	8730
CR9-10	143	105	7874
CR10-12	149	131	8030
CR12-14	157	128	6653
CR14-16	151	129	7805
CR16-18	136	114	8040
CR18-20	136	117	7286
CR20-22	136	105	5664
CR22-24	132	105	7028
CR24-26	126	116	6991
CR26-28	128	124	6551
CR28-30	130	128	7090
CR30-32	N.A.	N.A.	N.A.
CR32-34	132	136	6732
CR34-36	135	148	9558
CR36-38	126	133	7306
CR38-40	119	121	5185
CR40-42	122	131	5654
CR42-44	127	154	6367
CR44-46	127	147	7110
CR46-48	127	146	8368
CR48-50	124	136	7604
CR50-55	128	136	7517

N.A. Not Analysed.

CORE DN1.

Salt-corrected halogen data, ppm

	I	Br	Cl
DN0-1	435	197	9384
DN1-2	358	180	7490
DN2-3	326	193	11959
DN3-4	325	193	10945
DN4-5	302	191	10878
DN5-6	302	179	10289
DN6-7	317	182	12377
DN7-8	297	190	10783
DN8-9	289	178	9968
DN9-10	286	168	11208
DN10-12	No Sample		
DN12-14	No Sample		
DN14-16	356	178	8847
DN16-18	247	147	6475
DN18-20	244	165	13722
DN20-22	242	178	6512
DN22-24	239	160	10983
DN24-26	245	154	7363
DN26-28	241	158	11041
DN28-30	229	147	7854
DN30-32	245	152	9482
DN32-34	252	154	10011
DN34-36	243	150	8301
DN36-38	231	146	7641
DN38-40	220	144	7490
DN40-42	221	141	9907
DN42-44	222	141	11021
DN44-46	216	140	9463
DN46-48	218	139	8650
DN50-55	203	131	8856

CORE DU1.

Salt-corrected halogen data, ppm

	I	Br	Cl
DU0-1	579	464	22423
DU1-2	718	535	24908
DU2-3	211	135	14710
DU3-4	571	476	19142
DU4-5	N.A.	N.A.	N.A.
DU5-6	573	472	13660
DU6-7	484	447	16459
DU7-8	539	444	14082
DU8-9	479	414	13570
DU9-10	N.A.	N.A.	N.A.
DU10-12	444	395	13342
DU12-14	364	315	11329
DU14-16	333	297	11558
DU16-18	274	243	9136
DU18-20	206	234	9590
DU20-22	N.A.	N.A.	N.A.
DU22-24	199	163	8109
DU24-26	215	190	11240
DU26-28	268	243	10464
DU28-30	160	127	7906
DU30-32	120	95	5853
DU32-34	74	64	4493
DU34-36	61	61	5341
DU36-38	65	56	4882
DU38-40	59	61	5422
DU40-42	59	57	4547
DU42-44	56	54	4486
DU44-46	61	58	4542

N.A. Not Analysed

CORE ET1.

Salt-corrected halogen data, ppm

	I	Br	Cl
ET0-1	486	370	24587
ET1-2	493	399	24857
ET2-3	522	444	32142
ET3-4	517	410	24511
ET4-5	467	406	24945
ET5-6	461	382	25110
ET6-7	473	265	12543
ET7-8	491	380	27194
ET8-9	475	412	27277
ET9-10	503	387	24424
ET10-12	355	332	19971
ET12-14	359	341	20712
ET14-16	347	324	19058
ET16-18	386	363	19022
ET18-20	No sample		
ET20-22	322	328	18130
ET22-24	No sample		
ET24-26	223	333	20354
ET26-28	311	348	21818
ET28-30	308	292	20517
ET30-32	309	257	25897
ET32-34	294	308	16228
ET34-36	288	308	14396
ET36-38	249	303	19496
ET38-40	261	298	20714
ET40-42	245	299	18168
ET42-44	240	293	18350
ET44-46	250	302	19838
ET46-48	226	372	22669
ET48-50	241	304	14504
ET50-55	227	303	17842
ET55-60	219	278	17994
ET60-65	222	290	22767

CORE SH1.

Salt-corrected halogens data, ppm

	I	Br	Cl
SH0-1	376	241	28235
SH1-2	340	222	21558
SH2-3	341	245	11879
SH3-4	329	236	10905
SH4-5	318	229	12247
SH5-6	220	209	11272
SH6-7	308	228	11340
SH7-8	307	212	10380
SH8-9	N.A.	N.A.	N.A.
SH9-10	299	224	10332
SH10-12	287	216	11220
SH12-14	299	232	11677
SH14-16	281	230	11362
SH16-18	281	221	9745
SH18-20	249	209	7192
SH20-22	296	198	9672
SH22-24	271	202	9404
SH24-26	258	185	8234
SH28-30	257	191	10458
SH28-30	271	210	10273
SH30-32	273	204	11973
SH32-34	247	297	11891
SH34-36	241	170	10391
SH36-38	246	184	8921
SH38-40	234	190	7607
SH40-42	242	191	9509
SH42-44	234	178	8044
SH44-46	233	179	8867
SH46-48	248	237	8199
SH48-50	250	172	7886

CORE SP1.

Salt-corrected halogen data, ppm

	I	Br	Cl
SP0-1	N.A.	N.A.	N.A.
SP1-2	388	237	11952
SP2-3	314	241	10771
SP3-4	287	238	11253
SP4-5	351	228	10287
SP5-6	289	227	11456
SP9-7	N.A.	N.A.	N.A.
SP7-8	325	210	10897
SP8-9	272	217	11783
SP9-10	262	201	9181
SP10-12	N.A	N.A.	N.A.
SP12-14	244	201	9872
SP14-16	228	179	8554
SP16-18	232	183	7715
SP18-20	252	186	9631
SP20-22	257	195	10843
SP22-24	229	189	9502
SP24-26	210	183	10504
SP26-28	187	184	10445
SP28-30	219	186	9859
SP30-32	211	187	12115
SP32-34	212	173	8888
SP34-36	212	170	9281
SP36-38	186	163	9313
SP38-40	182	155	8208
SP40-42	188	154	12263
SP42-44	188	165	9673
SP44-46	182	161	7730
SP46-48	169	148	12094
SP40-50	N.A.	N.A.	N.A.
SP50-55	169	155	10006
SP55-60	166	152	9318
SP60-65	164	158	8508
SP65-70	158	155	8591
SP70-75	160	149	8143

CORE HO1.

Salt-corrected halogen data, ppm

	I	Br	Cl
HO0-1	455	277	15079
HO1-2	412	239	10691
HO2-3	420	253	11588
HO3-4	381	222	10202
HO4-5	374	223	11610
HO5-6	323	212	12617
HO6-7	334	216	10449
HO7-8	314	192	9322
HO8-9	252	164	8897
HO9-10	228	133	5425
HO10-12	233	152	9125
HO12-14	257	170	7913
HO14-16	243	159	8343
HO16-18	159	96	3652
HO18-20	123	73	4217
HO20-22	178	46	2024
HO22-24	215	143	6604
HO24-26	215	152	7508
HO26-28	226	154	9305
HO28-30	223	151	10043
HO30-32	N.A.	N.A.	N.A.
HO32-34	236	158	8601
HO34-36	239	156	8137
HO36-38	233	145	8890
HO38-40	226	152	9335
HO40-42	202	142	8382

N.A. Not Analysed

CORE NE1.

Salt-corrected halogen data, ppm

	I	Br	Cl
NE0-1	546	243	12158
NE1-2	474	225	9984
NE2-3	457	237	10513
NE3-4	504	250	13251
NE4-5	480	254	14103
NE5-6	441	232	11677
NE6-7	420	234	13242
NE7-8	432	231	11776
NE8-9	435	251	15035
NE9-10	420	227	12698
NE10-12	402	229	11930
NE12-14	389	233	15788
NE14-16	362	224	11923
NE16-18	367	208	8701
NE18-20	362	210	9433
NE20-22	361	237	13575
NE22-24	350	249	12105
NE24-26	360	214	11019
NE26-28	363	215	12493
NE28-30	335	206	12200
NE30-32	361	211	11552
NE32-34	356	202	11056
NE34-36	353	206	11674
NE36-38	341	208	10331
NE38-40	364	225	12904

CORE SN1.

Salt-corrected halogen data, ppm

	I	Br	Cl
SN0-1		No Sample	
SN1-2		No Sample	
SN2-3	336	205	11352
SN3-4	353	204	10997
SN4-5	242	161	11220
SN5-6	296	183	9861
SN6-7	297	178	8987
SN7-8	306	178	12998
SN8-9	289	181	8613
SN9-10	290	173	10975
SN10-12	268	174	10909
SN12-14	262	145	10966
SN14-16	268	168	10948
SN16-18	253	167	9915
SN18-20	256	160	9074
SN20-22	245	155	9122
SN22-24	260	156	10104
SN24-26	253	156	10173
SN26-28	239	148	10180
SN28-30	229	155	11345
SN30-32	233	155	10645
SN32-34	217	141	9805
SN34-36	230	159	9776
SN36-38	217	137	8423
SN38-40	209	133	8655
SN40-42	197	136	9761

N.A. Not Analysed.

TABLE AII.9

Total Metals And Metal/Rb Ratios.

(Cu, Pb, Zn, Cu/Rb, Pb/Rb, Zn/Rb)

All values expressed on a salt free basis.

Metal values given as ppm.

CORE AB1.

Salt free metal data and ratios

	Cu	Pb	Zn	Cu/Rb	Pb/Rb	Zn/Rb
AB0-1	26	89	226	0.26	0.88	2.24
AB1-2	25	80	216	0.25	0.78	2.12
AB2-3	N.A.	N.A.	N.A.	N.A.	N.A.	N.A.
AB3-4	26	78	207	0.26	0.77	2.03
AB4-5	26	78	208	0.25	0.74	1.98
AB5-6	25	79	209	0.25	0.75	1.97
AB6-7	24	76	200	0.30	0.72	1.91
AB7-8	24	74	194	0.23	0.70	1.83
AB8-9	24	75	196	0.22	0.71	1.83
AB9-10	25	72	194	0.24	0.62	1.87
AB10-12	23	65	171	0.22	0.63	1.64
AB12-14	22	55	146	0.22	0.55	1.45
AB14-16	21	51	134	0.21	0.51	1.34
AB16-18	19	42	116	0.19	0.42	1.16
AB18-20	18	41	114	0.18	0.41	1.29
AB20-22	18	43	121	0.18	0.42	1.67
AB22-24	17	34	104	0.17	0.33	1.02
AB24-26	17	30	102	0.17	0.30	1.01
AB26-28	17	31	103	0.18	0.30	1.00
AB28-30	16	30	100	0.16	0.30	0.99
AB30-32	N.A.	N.A.	N.A.	N.A.	N.A.	N.A.
AB32-34	18	30	103	0.18	0.29	1.00
AB34-36	17	30	102	0.17	0.29	0.99
AB36-38	16	30	106	0.15	0.28	1.00
AB38-40	19	34	111	0.16	0.29	0.94
AB40-42	18	30	108	0.17	0.28	1.01
AB42-44	16	29	106	0.15	0.27	0.98
AB44-46	17	30	105	0.16	0.28	0.98
AB46-48	15	30	102	0.14	0.29	0.98
AB48-50	17	28	104	0.16	0.26	0.98
AB50-55	16	27	102	0.16	0.26	0.99

N.A. Not Analysed

CORE CM1.

Salt free metal data and ratios

	Cu	Pb	Zn	Cu/Rb	Pb/Rb	Zn/Rb
CM0-1	9	31	76	0.11	0.39	0.96
CM1-2	9	31	77	0.10	0.36	0.89
CM2-3	8	33	76	0.09	0.38	0.88
CM3-4	8	31	74	0.09	0.37	0.87
CM4-5	8	31	71	0.09	0.36	0.83
CM5-6	7	28	67	0.08	0.33	0.78
CM6-7	7	26	65	0.83	0.31	0.77
CM7-8	8	26	62	0.09	0.31	0.73
CM8-9	7	27	64	0.08	0.31	0.74
CM9-10	N.A.	N.A.	N.A.	N.A.	N.A.	N.A.
CM10-12	7	23	64	0.08	0.26	0.72
CM12-14	9	22	63	0.10	0.24	0.69
CM14-16	9	20	59	0.10	0.23	0.67
CM16-18	9	21	60	0.10	0.24	0.67
CM18-20	8	20	58	0.09	0.23	0.65
CM20-22	8	20	61	0.09	0.21	0.65
CM22-24	9	22	63	0.10	0.23	0.67
CM24-26	8	21	60	0.09	0.23	0.65
CM26-28	10	21	61	0.10	0.22	0.64
CM28-30	8	20	62	0.08	0.21	0.64
CM30-32	8	21	61	0.08	0.22	0.64
CM32-34	9	20	63	0.09	0.21	0.65
CM34-36	9	21	65	0.09	0.21	0.66
CM36-38	8	19	66	0.08	0.19	0.66
CM38-40	9	20	69	0.09	0.20	0.68
CM40-42	11	22	73	0.10	0.20	0.68
CM42-44	12	22	76	0.11	0.20	0.69
CM44-46	12	22	76	0.11	0.20	0.69
CM46-48	12	21	76	0.11	0.20	0.71
CM48-50	13	23	78	0.11	0.20	0.68
CM50-55	11	22	77	0.10	0.20	0.68
CM55-60	13	24	81	0.11	0.20	0.68
CM60-65	12	21	78	0.10	0.18	0.68

CORE CR1.

Salt free metal data and ratios

	Cu	Pb	Zn	Cu/Rb	Pb/Rb	Zn/Rb
CR0-1	15	42	123	0.14	0.40	1.14
CR1-2	14	43	123	0.13	0.40	1.14
CR2-3	15	42	118	0.14	0.40	1.11
CR3-4	13	39	114	0.12	0.36	1.06
CR4-5	12	39	109	0.11	0.37	1.04
CR5-6	13	30	83	0.18	0.42	1.15
CR6-7	12	23	66	0.26	0.37	1.08
CR7-8	13	23	64	0.19	0.34	0.94
CR8-9	11	24	68	0.13	0.30	0.82
CR9-10	11	19	60	0.15	0.25	0.79
CR10-12	11	21	72	0.17	0.20	0.70
CR12-14	11	24	74	0.10	0.22	0.69
CR14-16	10	22	72	0.10	0.21	0.69
CR16-18	10	20	65	0.11	0.21	0.68
CR18-20	9	21	67	0.19	0.21	0.66
CR20-22	9	19	63	0.10	0.20	0.68
CR22-24	10	18	63	0.11	0.19	0.67
CR24-26	10	21	69	0.10	0.21	0.68
CR26-28	10	22	72	0.09	0.21	0.68
CR28-30	10	22	73	0.09	0.21	0.68
CR30-32	N.A.	N.A.	N.A.	N.A.	N.A.	N.A.
CR32-34	11	22	78	0.10	0.20	0.71
CR34-36	12	22	79	0.10	0.19	0.69
CR36-38	11	21	75	0.10	0.20	0.70
CR38-40	12	19	74	0.11	0.18	0.71
CR40-42	11	23	80	0.10	0.20	0.71
CR42-44	11	23	85	0.09	0.19	0.70
CR44-46	11	23	85	0.09	0.19	0.70
CR46-48	11	23	83	0.92	0.19	0.69
CR48-50	11	23	80	0.10	0.20	0.70
CR50-55	11	23	85	0.09	0.19	0.70
CR55-60	11	22	83	0.09	0.19	0.70
CR60-65	12	24	88	0.10	0.19	0.71

CORE DN1.

Salt free metal data and ratios.

	Cu	Pb	Zn	Cu/Rb	Pb/Rb	Zn/Rb
DN0-1	22	58	156	0.19	0.49	1.31
DN1-2	20	57	153	0.17	0.48	1.29
DN2-3	20	57	155	0.17	0.48	1.30
DN3-4	21	56	153	0.18	0.47	1.29
DN4-5	20	55	154	0.17	0.46	1.29
DN5-6	20	57	154	0.17	0.47	1.27
DN6-7	14	55	149	0.12	0.48	1.30
DN7-8	20	57	152	0.17	0.48	1.27
DN8-9	19	53	151	0.18	0.45	1.27
DN9-10	20	54	150	0.17	0.45	1.26
DN10-12			No Sample			
DN12-14			No Sample			
DN14-16	27	76	200	0.17	0.47	1.23
DN16-18	20	52	126	0.18	0.46	1.12
DN18-20	19	52	141	0.16	0.43	1.16
DN20-22	18	49	133	0.15	0.42	1.14
DN22-24	18	48	134	0.15	0.40	1.11
DN24-26	19	48	130	0.16	0.39	1.07
DN26-28	18	45	126	0.15	0.37	1.04
DN28-30	18	42	121	0.15	0.35	1.00
DN30-32	18	41	119	0.15	0.34	0.98
DN32-34	16	42	121	0.14	0.36	1.03
DN34-36	18	46	125	0.15	0.38	1.03
DN36-38	16	37	109	0.13	0.31	0.91
DN38-40	15	34	102	0.13	0.28	0.85
DN40-42	14	31	97	0.12	0.26	0.82
DN42-44	15	30	97	0.13	0.25	0.82
DN44-46	16	31	97	0.13	0.26	0.82
DN46-48	15	29	93	0.13	0.24	0.78
DN48-50	14	28	90	0.12	0.23	0.75
DN50-55	14	27	88	0.12	0.23	0.75

N.A. Not Analysed

CORE DU1.

Salt free metal data and ratios

	Cu	Pb	Zn	Cu/Rb	Pb/Rb	Zn/Rb
DU0-1	24	55	150	0.21	0.49	1.34
DU1-2	26	56	159	0.22	0.46	1.31
DU2-3	26	56	160	0.22	0.47	1.33
DU3-4	25	52	157	0.21	0.44	1.32
DU4-5	N.A.	N.A.	N.A.	N.A.	N.A.	N.A.
DU5-6	24	53	158	0.20	0.45	1.33
DU6-7	25	52	154	0.21	0.44	1.32
DU7-8	24	51	152	0.21	0.44	1.31
DU8-9	22	48	146	0.20	0.43	1.30
DU9-10	N.A.	N.A	N.A.	N.A.	N.A.	N.A.
DU10-12	20	42	129	0.19	0.39	1.21
DU12-14	19	36	118	0.18	0.34	1.11
DU14-16	16	30	98	0.16	0.30	0.97
DU16-18	15	30	93	0.15	0.30	0.93
DU18-20	15	24	89	0.15	0.24	0.90
DU20-22	N.A.	N.A.	N.A.	N.A.	N.A.	N.A.
DU22-24	12	21	70	0.13	0.23	0.79
DU24-26	14	24	84	0.14	0.24	0.82
DU26-28	16	26	92	0.14	0.23	0.83
DU28-30	14	23	77	0.14	0.22	0.74
DU30 32	16	24	86	0.13	0.19	0.69
DU32-34	19	25	94	0.14	0.18	0.67
DU34-36	19	24	94	0.13	0.70	0.65
DU36-38	19	25	93	0.13	0.18	0.65
DU38-40	20	25	91	0.14	0.18	0.64
DU40-42	20	25	94	0.14	0.17	0.65
DU42-44	20	24	93	0.14	0.17	0.65
DU44-46	20	26	93	0.14	0.18	0.65

CORE ET1.

Salt free metal data and ratios

	Cu	Pb	Zn	Cu/Rb	Pb/Rb	Zn/Rb
ET0-1	30	79	227	0.34	0.88	2.55
ET1-2	31	85	237	0.34	0.92	2.58
ET2-3	31	90	245	0.34	1.00	2.72
ET3-4	33	94	261	0.36	1.01	2.81
ET4-5	29	83	244	0.34	0.98	2.87
ET5-6	32	89	252	0.35	0.97	2.74
ET6-7	32	85	244	0.36	0.92	2.77
ET7-8	31	86	240	0.35	0.97	2.70
ET8-9	31	83	251	0.60	0.95	2.89
ET9-10	32	82	242	0.37	0.94	2.78
ET10-12	28	83	227	0.30	0.90	2.46
ET12-14	29	86	224	0.30	0.89	2.31
ET14-16	27	86	217	0.28	0.89	2.24
ET16-18	29	89	227	0.31	0.96	2.39
ET18-20	N.A.	N.A.	N.A.	N.A.	N.A.	N.A.
ET20-22	27	80	204	0.28	0.84	2.15
ET22-24	N.A.	N.A.	N.A.	N.A.	N.A.	N.A.
ET24-26	28	76	192	0.29	0.79	2.00
ET26-28	26	74	186	0.28	0.80	2.00
ET28-30	27	69	178	0.29	0.73	1.89
ET30-32	24	64	159	0.26	0.68	1.69
ET32-34	24	62	151	0.26	0.67	1.64
ET34-36	24	61	148	0.26	0.98	1.59
ET36-38	23	56	139	0.25	0.62	1.53
ET38-40	23	57	133	0.25	0.63	1.46
ET40-42	22	51	124	0.24	0.56	1.36
ET42-44	21	50	120	0.23	0.54	1.31
ET44-46	22	51	120	0.24	0.56	1.32
ET46-48	23	46	111	0.26	0.52	1.25
ET48-50	21	45	110	0.23	0.48	1.18
ET50-55	20	43	105	0.22	0.47	1.15
ET55-60	21	44	102	0.23	0.48	1.11
ET60-65	20	41	97	0.23	0.47	1.10

N.A. Not Analysed.

CORE SH1.

Salt free metal data and ratios

	Cu	Pb	Zn	Cu/Rb	Pb/Rb	Zn/Rb
SH0-1	20	38	124	0.19	0.36	1.17
SH1-2	19	38	121	0.18	0.36	1.15
SH2-3	18	38	120	0.17	0.36	1.14
SH3-4	18	36	120	0.17	0.34	1.14
SH4-5	18	38	120	0.17	0.36	1.14
SH5-6	19	38	120	0.18	0.36	1.13
SH6-7	19	36	118	0.18	0.34	1.11
SH7-8	19	36	117	0.18	0.34	1.09
SH8-9	N.A.	N.A.	N.A.	N.A.	N.A.	N.A.
SH9-10	19	36	117	0.18	0.34	1.04
SH10-12	19	35	116	0.18	0.33	1.09
SH12-14	20	36	116	0.19	0.34	1.08
SH14-16	19	35	113	0.18	0.33	1.06
SH16-18	19	33	112	0.18	0.31	1.06
SH18-20	20	34	109	0.19	0.32	1.03
SH20-22	19	32	104	0.18	0.31	0.99
SH22-24	20	33	108	0.19	0.31	1.02
SH24-26	19	30	101	0.18	0.29	0.96
SH26-28	17	29	98	0.18	0.27	0.93
SH28-30	17	26	95	0.16	0.25	0.91
SH30-32	18	27	93	0.17	0.26	0.88
SH32-34	17	25	91	0.16	0.24	0.86
SH34-36	17	26	89	0.17	0.25	0.86
SH36-38	17	25	88	0.16	0.24	0.85
SH38-40	17	24	86	0.17	0.23	0.84
SH40-42	17	25	90	0.17	0.24	0.87
SH42-44	17	25	83	0.16	0.24	0.79
SH44-46	16	23	82	0.15	0.22	0.79
SH46-48	16	22	80	0.16	0.21	0.77
SH48-50	16	24	81	0.15	0.23	0.78

N.A. Not Analysed

CORE SP1.

Salt free metal data and ratios

	Cu	Pb	Zn	Cu/Rb	Pb/Rb	Zn/Rb
SP0-1			No Sample			
SP1-2	18	48	143	0.17	0.44	1.32
SP2-3	19	50	147	0.17	0.45	1.32
SP3-4	20	49	148	0.18	0.44	1.35
SP4-5	18	48	147	0.16	0.44	1.34
SP5-6	19	50	144	0.17	0.45	1.30
SP6-7	N.A.	N.A.	N.A.	N.A.	N.A.	N.A.
SP7-8	20	49	143	0.18	0.44	1.30
SP8-9	20	46	140	0.18	0.42	1.28
SP9-10	14	44	131	0.14	0.42	1.26
SP10-12	19	46	134	0.18	0.43	1.26
SP12-14	19	46	136	0.17	0.42	1.24
SP14-16	19	41	118	0.19	0.41	1.18
SP16-18	19	40	116	0.18	0.39	1.30
SP18-20	18	40	116	0.18	0.39	1.30
SP20-22	18	41	115	0.18	0.40	1.12
SP22-24	18	37	107	0.18	0.36	1.04
SP24-26	17	33	95	0.17	0.33	0.95
SP26-28	15	32	91	0.15	0.33	0.93
SP28-30	16	31	87	0.16	0.31	0.87
SP30-32	19	38	116	0.17	0.33	1.02
SP32-34	15	28	84	0.18	0.28	0.82
SP34-36	15	29	92	0.14	0.28	0.88
SP36-38	15	26	84	0.14	0.25	0.99
SP38-40	14	25	82	0.13	0.24	0.78
SP40-42	15	28	86	0.14	0.26	0.80
SP42-44	15	29	91	0.14	0.27	0.85
SP44-46	14	25	84	0.13	0.24	0.80
SP46-48	14	25	82	0.13	0.23	0.76
SP48-50	N.A.	N.A.	N.A.	N.A.	N.A.	N.A.
SP50-55	13	22	83	0.12	0.21	0.78
SP55-60	13	21	80	0.12	0.20	0.76
SP60-65	14	22	83	0.13	0.20	0.76
SP65-70	12	23	82	0.11	0.21	0.76
SP70-75	14	22	81	0.13	0.21	0.76

CORE NE1.

Salt free metal data and ratios

	Cu	Pb	Zn	Cu/Rb	Pb/Rb	Zn/Rb
NE0-1	20	44	140	0.17	0.36	1.16
NE1-2	20	45	132	0.18	0.40	1.16
NE2-3	21	47	140	0.17	0.39	1.16
NE3-4	20	47	139	0.17	0.39	1.15
NE4-5	21	46	139	0.18	0.38	1.16
NE5-6	20	47	135	0.17	0.39	1.16
NE6-7	21	46	131	0.17	0.38	1.12
NE7-8	20	45	133	0.17	0.37	1.14
NE8-9	21	46	131	0.17	0.38	1.10
NE9-10	21	44	134	0.18	0.37	1.10
NE10-12	20	43	132	0.17	0.36	1.10
NE12-14	20	42	129	0.17	0.35	1.06
NE14-16	19	43	132	0.17	0.36	1.08
NE16-18	20	42	131	0.17	0.35	1.00
NE18-20	20	39	132	0.16	0.32	0.97
NE20-22	19	38	129	0.16	0.32	0.95
NE22-24	19	38	129	0.16	0.32	0.94
NE24-26	19	37	131	0.16	0.31	0.93
NE26-28	19	37	130	0.16	0.31	0.93
NE28-30	18	36	130	0.15	0.30	0.94
NE30-32	17	36	131	0.14	0.30	0.89
NE32-34	18	34	131	0.15	0.29	0.89
NE34-36	17	34	130	0.14	0.28	0.85
NE36-38	18	34	132	0.14	0.29	0.84
NE38-40	18	33	129	0.14	0.28	0.81

CORE HO1.

Salt free metal data and ratios

	Cu	Pb	Zn	Cu/Rb	Pb/Rb	Zn/Rb
HO0-1	14	28	89	0.12	0.24	0.77
HO1-2	13	28	89	0.11	0.24	0.77
HO2-3	6	27	79	0.01	0.27	0.79
HO3-4	20	45	130	0.18	0.40	1.15
HO4-5	20	44	124	0.18	0.40	1.12
HO5-6	21	47	132	0.18	0.41	1.15
HO6-7	19	45	125	0.17	0.41	1.13
HO7-8	18	44	122	0.17	0.40	1.12
HO8-9	18	40	111	0.17	0.39	1.07
HO9-10	19	41	115	0.18	0.38	1.08
HO10-12	19	40	112	0.18	0.37	1.05
HO12-14	17	35	94	0.18	0.18	0.98
HO14-16	15	33	85	0.17	0.37	0.94
HO16-18	16	33	82	0.17	0.36	0.89
HO18-20	20	32	88	0.19	0.31	0.85
HO20-22	15	30	82	0.15	0.31	0.84
HO22-24	11	27	57	0.15	0.35	0.76
HO24-26	9	23	46	0.13	0.33	0.67
HO26-28	9	25	44	0.11	0.31	0.53
HO28-30	14	26	70	0.15	0.27	0.73
HO30-32	N.A	N.A.	N.A.	N.A.	N.A.	N.A.
HO32-34	14	26	73	0.14	0.27	0.75
HO34-36	13	26	73	0.13	0.26	0.74
HO36-38	12	28	74	0.11	0.27	0.71
HO38-40	15	26	79	0.14	0.25	0.75
HO40-42	14	26	77	0.14	0.25	0.74

N.A. Not Analysed

CORE SN1.

Salt free metal data and ratios

	Cu	Pb	Zn	Cu/Rb	Pb/Rb	Zn/Rb
SN0-1			No Sample			
SN1-2			No Sample			
SN2-3	12	26	58	0.24	0.51	1.14
SN3-4	9	22	45	0.19	0.47	0.96
SN4-5	11	21	48	0.22	0.41	0.64
SN5-6	24	39	119	0.24	0.39	1.19
SN6-7	24	40	119	0.24	0.40	1.18
SN7-8	21	28	83	0.22	0.29	0.86
SN8-9	23	38	114	0.24	0.39	1.18
SN9-10	22	38	112	0.22	0.39	1.14
SN10-12	21	38	110	0.21	0.39	1.12
SN12-14	24	37	112	0.24	0.37	1.13
SN14-16	21	34	102	0.22	0.35	1.05
SN16-18	22	32	98	0.22	0.33	1.00
SN18-20	21	31	92	0.22	0.32	0.95
SN20-22	21	31	91	0.22	0.32	0.94
SN22-24	20	30	92	0.21	0.31	0.95
SN24-26	22	29	90	0.23	0.30	0.93
SN26-28	21	28	85	0.22	0.29	0.88
SN28-30	21	28	86	0.22	0.22	0.88
SN30-32	22	29	90	0.24	0.31	0.97
SN32-34	19	28	85	0.20	0.30	0.90
SN34-36	19	26	80	0.20	0.30	0.83
SN36-38	18	25	80	0.19	0.26	0.83
SN38-40	17	24	80	0.18	0.25	0.83
SN40-42	18	27	81	0.18	0.28	0.83

TABLE AII.10

Excess Metal Data.

(Pb/Ni, Zn/Ni, Pb_{ex}, Zn_{ex})

Values expressed on a salt free basis, calculated from:

$$M_{ex} = (M/Ni_D - M/Ni_B) \cdot Ni_D$$

Where:

M/Ni_D = Metal/Nickel ratio at depth, Dcm.

M/Ni_B = Mean background Metal/Nickel ratio.

Ni_D = Nickel concentration at depth, Dcm.

CORE AB1.

Salt free excess metal data

	Pb/Ni	Zn/Ni	Pbx	Znx
AB0-1	1.89	4.81	58	93
AB1-2	1.67	4.50	49	110
AB2-3	N.A.	N.A.	N.A.	N.A.
AB3-4	1.59	4.22	46	99
AB4-5	1.56	4.16	46	98
AB5-6	1.58	4.18	47	99
AB6-7	1.55	4.08	44	92
AB7-8	1.51	3.96	42	86
AB8-9	1.53	4.00	43	88
AB9-10	1.45	3.96	39	86
AB10-12	1.30	3.42	33	61
AB12-14	1.15	3.04	24	40
AB14-16	1.11	2.91	21	33
AB16-18	0.91	2.52	12	15
AB18-20	0.89	2.48	11	13
AB20-22	0.93	2.63	13	20
AB22-24	0.76	2.31	5	5
AB24-26	0.65	2.22	0	1
AB26-28	0.67	2.24	1	2
AB28-30	0.67	2.22	1	1
AB30-32	N.A.	N.A.	N.A.	N.A.
AB32-34	0.64	2.19	0	0
AB34-36	0.64	2.17	0	0
AB36-38	0.64	2.26	0	3
AB38-40	0.69	2.27	0	3
AB40-42	0.61	2.20	0	0
AB42-44	0.60	2.21	0	0
AB44-46	0.65	2.28	0	3
AB46-48	0.65	2.22	0	0
AB48-50	0.60	2.21	0	0
AB50-55	0.60	2.27	0	3

CORE CM1.

Salt free excess metal data

	Pb/Ni	Zn/Ni	Pbx	Znx
CM0-1	1.19	2.92	18	29
CM1-2	1.15	2.85	18	28
CM2-3	1.22	2.81	19	27
CM3-4	1.15	2.74	18	25
CM4-5	1.15	2.63	18	22
CM5-6	1.08	2.58	15	20
CM6-7	0.96	2.41	12	16
CM7-8	0.93	2.21	12	11
CM8-9	1.00	2.37	14	15
CM9-10	N.A.	N.A.	N.A.	N.A.
CM10-12	0.79	2.21	8	12
CM12-14	0.71	2.03	7	7
CM14-16	0.67	1.97	5	5
CM16-18	0.70	2.00	6	6
CM18-20	0.67	1.93	5	4
CM20-22	0.63	1.91	4	4
CM22-24	0.69	1.97	6	5
CM24-26	0.68	1.94	6	4
CM26-28	0.64	1.85	4	2
CM28-30	0.59	1.82	3	1
CM30-32	0.62	1.79	4	0
CM32-34	0.59	1.85	3	2
CM34-36	0.58	1.81	3	0
CM36-38	0.54	1.89	1	0
CM38-40	0.54	1.86	1	0
CM40-42	0.56	1.87	2	0
CM42-44	0.51	1.77	0	0
CM44-46	0.54	1.85	2	0
CM46-48	0.50	1.81	0	0
CM48-50	0.55	1.86	2	0
CM50-55	0.51	1.79	0	0
CM55-60	0.53	1.80	1	0
CM60-65	0.50	1.86	0	0

CORE CR1.

Salt free excess metal data

	Pb/Ni	Zn/Ni	Pbx	Znx
CR0-1	1.20	3.51	23	49
CR1-2	1.20	3.51	23	49
CR2-3	1.20	3.37	23	44
CR3-4	1.10	3.35	19	42
CR4-5	1.10	3.21	19	38
CR5-6	1.20	3.19	17	28
CR6-7	1.00	2.67	10	13
CR7-8	0.96	2.67	11	14
CR8-9	0.89	2.52	9	11
CR9-10	0.73	2.31	6	6
CR10-12	0.64	2.18	3	3
CR12-14	0.69	2.11	5	0.3
CR14-16	0.69	2.25	4	5
CR16-18	0.67	2.17	4	2
CR18-20	0.68	2.16	2	2
CR20-22	0.61	2.03	2	0
CR22-24	0.58	2.03	1	0
CR24-26	0.66	2.16	4	2
CR26-28	0.63	2.06	3	0
CR28-30	0.63	2.09	3	0
CR30-32	N.A.	N.A.	N.A.	N.A.
CR32-34	0.59	2.11	1	0.3
CR34-36	0.56	2.03	0	0
CR36-38	0.57	2.03	1	0
CR38-40	0.54	2.11	0	0.3
CR40-42	0.62	2.16	3	2
CR42-44	0.56	2.07	0	0
CR44-46	0.55	2.02	0	0
CR46-48	0.58	2.08	1	0
CR48-50	0.61	2.11	2	0
CR50-55	0.55	2.02	0	0
CR55-60	0.55	2.08	2	0
CR60-65	0.59	2.15	0	0

N.A. Not Analysed

CORE DU1.

Salt free excess metal data

	Pb/Ni	Zn/Ni	PbX	Znx
DU0-1	1.06	2.88	29	47
DU1-2	1.04	2.94	29	52
DU2-3	1.04	2.96	29	53
DU3-4	0.98	2.96	25	52
DU4-5	N.A.	N.A.	N.A.	N.A.
DU5-6	0.95	2.82	25	47
DU6-7	0.98	2.91	25	49
DU7-8	0.98	2.92	24	49
DU8-9	0.98	2.98	23	49
DU9-10	N.A.	N.A.	N.A.	N.A.
DU10-12	0.93	2.87	19	40
DU12-14	0.78	2.57	12	27
DU14-16	0.77	2.51	10	21
DU16-18	0.73	2.27	9	12
DU18-20	0.59	2.17	3	8
DU20-22	N.A.	N.A.	N.A.	N.A.
DU22-24	0.62	2.06	4	7
DU24-26	0.62	2.15	5	5
DU26-28	0.59	2.09	3	4
DU28-30	0.62	2.08	5	3
DU30 32	0.57	2.05	3	1
DU32-34	0.53	2.00	1	1
DU34-36	0.51	2.00	0	2
DU36-38	0.54	2.02	1	0
DU38-40	0.53	1.94	1	3
DU40-42	0.54	2.04	1	0
DU42-44	0.51	1.98	0	0
DU44-46	0.55	1.98	2	0

CORE DN1.

Salt free excess metal data

	Pb/Rb	Zn/Rb	Pbx	Znx
DN0-1	1.14	3.06	28	55
DN1-2	1.16	3.12	27	56
DN2-3	1.16	3.16	27	58
DN3-4	1.17	3.19	27	58
DN4-5	1.12	3.14	25	57
DN5-6	1.14	3.08	27	55
DN6-7	1.20	3.24	28	58
DN7-8	1.16	3.10	27	55
DN8-9	1.08	3.08	24	54
DN9-10	1.13	3.13	25	56
DN10-12		No Sample		
DN12-14		No Sample		
DN14-16	1.12	2.94	35	46
DN16-18	1.24	3.00	27	43
DN18-20	1.08	2.94	23	40
DN20-22	1.04	2.83	21	41
DN22-24	1.00	2.79	19	38
DN24-26	0.96	2.60	18	30
DN26-28	0.94	2.63	16	33
DN28-30	0.88	2.52	13	26
DN30-32	0.85	2.48	12	24
DN32-34	0.89	2.57	14	28
DN34-36	0.96	2.60	17	29
DN36-38	0.76	2.22	8	12
DN38-40	0.71	2.13	5	7
DN40-42	0.67	2.11	3	6
DN42-44	0.63	2.02	1	2
DN44-46	0.63	1.98	1	0
DN46-48	0.62	1.98	1	0
DN48-50	0.58	1.88	0	0
DN50-55	0.60	1.96	0	0

N.A. Not Analysed

CORE ET1.

Salt free excess metal data

	Pb/Ni	Zn/Ni	Pbx	Znx
ET0-1	1.72	4.93	33	118
ET1-2	1.77	4.94	37	123
ET2-3	1.94	5.21	44	133
ET3-4	1.96	5.44	46	147
ET4-5	1.80	5.30	37	135
ET5-6	1.89	5.36	42	141
ET6-7	1.85	5.30	39	135
ET7-8	1.91	5.33	41	133
ET8-9	1.77	5.34	36	140
ET9-10	1.78	5.26	36	133
ET10-12	1.80	4.93	37	118
ET12-14	1.79	4.67	38	110
ET14-16	1.79	4.52	38	103
ET16-18	1.93	4.93	43	118
ET18-20		No Sample		
ET20-22	1.74	4.43	34	95
ET22-24		No Sample		
ET24-26	1.65	4.17	30	83
ET26-28	1.61	4.04	28	77
ET28-30	1.53	3.96	24	72
ET30-32	1.39	3.46	18	50
ET32-34	1.38	3.36	17	45
ET34-36	1.36	3.29	16	41
ET36-38	1.24	3.09	11	32
ET38-40	1.33	3.09	14	31
ET40-42	1.19	2.88	8	22
ET42-44	1.16	2.79	7	18
ET44-46	1.24	2.93	10	23
ET46-48	1.07	2.58	3	9
ET48-50	1.07	2.62	3	11
ET50-55	1.02	2.50	1	5
ET55-60	1.02	2.37	1	0
ET60-65	1.00	2.37	0	0

CORE SH1.

Salt free excess metal data

	Pb/Ni	Zn/Ni	Pbx	Znx
SH0-1	0.79	2.58	14	42
SH1-2	0.79	2.50	14	39
SH2-3	0.79	2.50	14	38
SH3-4	0.75	2.50	12	38
SH4-5	0.79	2.50	14	38
SH5-6	0.79	2.50	14	38
SH6-7	0.70	2.50	10	33
SH7-8	0.70	2.36	10	32
SH8-9	N.A.	N.A.	N.A.	N.A.
SH9-10	0.75	2.34	13	36
SH10-12	0.73	2.44	11	35
SH12-14	0.73	2.42	11	33
SH14-16	0.73	2.37	11	31
SH16-18	0.70	2.35	10	30
SH18-20	0.69	2.33	9	25
SH20-22	0.65	2.22	7	21
SH22-24	0.67	2.12	8	22
SH24-26	0.60	2.20	5	16
SH26-28	0.59	2.02	5	15
SH28-30	0.50	2.00	0	10
SH30-32	0.56	1.90	3	11
SH32-34	0.52	1.93	1	9
SH34-36	0.55	1.89	2	5
SH36-38	0.51	1.80	0	4
SH38-40	0.50	1.79	0	9
SH40-42	0.52	1.88	0	0
SH42-44	0.51	1.69	0	0
SH44-46	0.48	1.71	0	0
SH46-48	0.46	1.67	0	0
SH48-50	0.49	1.65	0	0

CORE SP1.

Salt free excess metal data

	Pb/Ni	Zn/Ni	Pbx	Znx
SP0-1	No Sample			
SP1-2	1.00	2.92	55	25
SP2-3	1.02	3.00	59	25
SP3-4	1.12	3.08	62	25
SP4-5	1.00	3.00	59	25
SP5-6	1.02	2.94	56	25
SP6-7	N.A.	N.A.	N.A.	N.A.
SP7-8	1.00	2.92	55	25
SP8-9	0.93	2.86	52	21
SP9-10	0.96	2.85	49	21
SP10-12	0.92	2.68	44	21
SP12-14	0.94	2.78	49	22
SP14-16	0.91	2.62	37	18
SP16-18	0.85	2.47	32	16
SP18-20	0.85	2.47	32	16
SP20-22	0.85	2.40	29	17
SP22-24	0.79	2.28	23	14
SP24-26	0.72	2.07	13	10
SP26-28	0.73	2.07	12	10
SP28-30	0.67	1.89	5	8
SP30-32	0.79	2.42	29	14
SP32-34	0.60	1.79	6	5
SP34-36	0.60	1.92	0	5
SP36-38	0.55	1.79	0	2
SP38-40	0.53	1.75	0	1
SP40-42	0.60	1.83	0	5
SP42-44	0.60	1.90	0	5
SP44-46	0.53	1.79	0	1
SP46-48	0.54	1.78	0	2
SP48-50	N.A.	N.A.	N.A.	N.A.
SP50-55	0.48	1.80	0	0
SP55-60	0.46	1.74	0	0
SP60-65	0.48	1.80	0	0
SP65-70	0.50	1.78	0	0
SP70-75	0.48	1.76	0	0

N.A. Not Analysed

CORE NE1.

Salt free excess metal data

	Pb/Ni	Zn/Ni	Pbx	Znx
NE0-1	0.67	2.12	5	41
NE1-2	0.87	2.53	14	54
NE2-3	0.87	2.60	15	61
NE3-4	0.94	2.78	17	65
NE4-5	0.89	2.68	15	62
NE5-6	0.91	2.68	16	62
NE6-7	0.89	2.60	15	59
NE7-8	0.89	2.69	15	62
NE8-9	0.90	2.64	16	59
NE9-10	0.87	2.60	14	57
NE10-12	0.86	2.63	13	57
NE12-14	0.83	2.50	12	52
NE14-16	0.83	2.49	12	53
NE16-18	0.81	2.37	11	45
NE18-20	0.75	2.31	8	42
NE20-22	0.75	2.25	8	39
NE22-24	0.78	2.30	9	40
NE24-26	0.73	2.19	7	36
NE26-28	0.75	2.24	7	38
NE28-30	0.71	2.19	6	36
NE30-32	0.71	2.14	6	33
NE32-34	0.69	2.12	4	32
NE34-36	0.65	2.00	2	26
NE36-38	0.69	2.00	4	26
NE38-40	0.65	1.92	2	22

CORE HO1.

Salt free excess metal data

	Pb/Ni	Zn/Ni	Pbx	Znx
HO0-1	0.59	1.86	12	32
HO1-2	0.58	1.82	12	31
HO2-3	0.53	1.95	7	31
HO3-4	0.80	2.28	26	62
HO4-5	0.80	2.25	25	59
HO5-6	0.84	2.35	28	66
HO6-7	0.79	2.23	25	59
HO7-8	0.79	2.16	25	55
HO8-9	0.69	1.95	20	43
HO9-10	0.71	1.97	21	45
HO10-12	0.72	2.00	21	46
HO12-14	0.56	1.51	13	19
HO14-16	0.51	1.28	11	6
HO16-18	0.50	1.24	10	3
HO18-20	0.53	1.46	11	16
HO20-22	0.52	1.41	10	15
HO22-24	0.40	0.88	3	0
HO24-26	0.38	0.75	2	0
HO26-28	0.52	0.94	8	0
HO28-30	0.41	1.08	4	0
HO30-32	0.41	1.16	4	0
HO32-34	0.43	1.21	5	0
HO34-36	0.51	1.32	9	0
HO36-38	0.46	1.40	6	0
HO38-40	0.46	1.36	6	0

CORE SN1.

Salt free excess metal data

	Pb/Rb	Zn/Rb	Pbx	Znx
SN0-1	No Sample			
SN1-2	No Sample			
SN2-3	0.90	2.00	14	19
SN3-4	0.82	1.67	11	9
SN4-5	0.72	1.66	9	9
SN5-6	0.60	1.83	14	31
SN6-7	0.62	1.83	14	31
SN7-8	0.43	1.28	2	0
SN8-9	0.59	1.78	12	28
SN9-10	0.59	1.75	13	25
SN10-12	0.60	1.75	11	26
SN12-14	0.57	1.72	11	24
SN14-16	0.53	1.59	8	16
SN16-18	0.49	1.48	5	9
SN18-20	0.47	1.39	4	3
SN20-22	0.47	1.38	2	2
SN22-24	0.46	1.42	2	5
SN24-26	0.43	1.34	2	0
SN26-28	0.42	1.29	0	0
SN28-30	0.44	1.37	0	0
SN30-32	0.45	1.41	0	0
SN32-34	0.44	1.33	0	0
SN34-36	0.43	1.33	0	0
SN36-38	0.40	1.31	0	0
SN38-40	0.39	1.27	0	0
SN40-42	0.44	1.29	0	0

N.A. Not Analysed

TABLE AII.11

^{137}Cs Data.

Including data from Ridgway, (1984).

All values expressed in Becquerels Kg^{-1}

BDL Below detection limit.

CORE CR1.

137Cs Data (Bq/Kg)

CR0-1	228.4
CR1-2	232.7
CR2-3	267.6
CR3-4	227.3
CR4-5	148.5
CR5-6	130.0
CR6-7	N.A.
CR7-8	79.2
CR8-9	94.0
CR9-10	48.3
CR10-12	N.A.
CR12-14	30.2
CR14-16	N.A.
CR16-18	N.A.
CR18-20	N.A.
CR20-22	N.A.
CR22-24	N.A.
CR24-26	N.A.
CR26-28	N.A.
CR28-30	N.A.
CR30-32	N.A.
CR32-34	N.A.
CR34-36	N.A.
CR36-38	N.A.
CR38-40	N.A.
CR40-42	N.A.
CR42-44	N.A.
CR44-46	N.A.
CR46-48	N.A.
CR48-50	N.A.
CR50-55	N.A.

CORE DN1.

137Cs Data (Bq/Kg)

DN0-1	291.1
DN1-2	402.3
DN2-3	361.8
DN3-4	339.3
DN4-5	296.8
DN5-6	311.5
DN6-7	284.5
DN7-8	258.0
DN8-9	214.6
DN9-10	177.1
DN10-12	N.A.
DN12-14	N.A.
DN14-16	90.7
DN16-18	55.7
DN18-20	37.6
DN20-22	23.5
DN22-24	16.8
DN24-26	7.3
DN26-28	6.5
DN28-30	5.4
DN30-32	8.6
DN32-34	6.1
DN34-36	9.1
DN36-38	N.A.
DN38-40	N.A.
DN40-42	N.A.
DN42-44	N.A.
DN44-46	N.A.
DN46-48	N.A.
DN48-50	N.A.

137Cs Data (Bq/Kg)
(After Ridgway, 1984)

	LES1	LES2
0-2	330	401
2-4	292	377
4-6	263	321
6-8	255	244
8-10	222	192
10-12	177	117
12-14	153	77
14-16	153	53
16-18	120	55
18-20	68	47
20-22	30	37
22-24	10	17
24-26	13	15
26-28	17	23
28-30	10	ND
30-32	7	
32-34	5	
34-36	BDL	

N.A. Not Analysed

N.D. Not Detectable

ACKNOWLEDGEMENTS.

During the period of this study I have asked and received a great many favours from innumerable people. My thanks must go to all of these people over the last three years.

I would especially like to thank Dr. Brian Price for his conscientious supervision throughout this project and especially during the writing of this thesis. Thanks also to Dr. Graham Shimmield for his help in sample collection and for his patient explanations and criticisms.

I must also thank the skippers and crew of the vessels *R.V. Calanus* and *R.V. Seol Mara* and the staff at the Scottish Marine Biological Association at Dunstaffnage for allowing me to use their facilities.

Thanks must also go to Dr. Godfrey Fitton and Mrs Doreen James for their invaluable work on the XRF, to Dr. Gus MacKenzie at Scottish Universities Reactor and Research Centre for allowing the use of the counters to analyse ^{137}Cs, Miss Tracy Williams for running the said samples, and to Dr. Keith Smith and the technical staff of the Soil Science Department in the School of Agriculture for allowing time on the Nitrogen Analyser. Lastly in this section I would like to thank the technical staff at the Grant Institute for their help, especially Mr. Mike Saunders for his assistance with the wet chemical analysis techniques.

On a personal note, I would like to thank Mrs. Denise Wilson for kindly typing the references, thereby saving me alot of pain, Miss Tracy Watson for proof reading the manuscript, and my house mates, Miss Helen Stebbens and Dr. Philip Bentley, also for proof reading but mostly for putting up with me.

Lastly, I cannot thank enough my mother, Audrey, and my step-father, Albert, for their unflagging belief in my ability and their occasionally more concrete support.

Finally, I would like to acknowledge N.E.R.C for furnishing the grant under which this work was carried out.

BIBLIOGRAPHY

Aller, R.C. 1980. Diagenetic processes near the sediment water interface of LIS. I Decomposition and nutrient element geochemistry (S,N,P). Adv. Geophys. 22, p.237-350.

Altabet, M.A., Deuser, W.G. 1985. Seasonal variations in natural abundance of ^{15}N in particles sinking to the deep Sargasso Sea. Nature, London, 315, p.218-219.

Altabet, M.A., McCarthy, J.J. 1985. Temporal and spatial variations in the natural abundance of ^{15}N in PON from a warm core ring. Deep Sea Res. 32, p.755-772.

Altabet, M.A., McCarthy, J.J. 1986. Vertical patterns in ^{15}N natural abundance in PON from the surface waters of warm-core rings. J. Mar. Res., 44, p.185-201.

Aston, S.R., Stanners, D.A. 1979. The determination of estuarine sedimentation rates by $^{134}Cs/^{137}Cs$ and other artificial radionuclide profiles. Est. & Coast. Mar. Sci., 9, p.529-541.

Arrhenius, G. 1952. Sediment cores from the East Pacific. In: Reports of the Swedish Deep Sea Expedition 1947-1948. H. Patterson (ed), V, p.1-227, Göteburg.

Arrhenius, G., Bonatti, E. 1965. Neptunism and vulcanism in the ocean. In: Progress in Oceanography 3, p.7-22, (Ed. M. Sears). Pergamon Press, Oxford, London, Edin. N.Y.

Bader, R.G. 1955. Carbon and Nitrogen relations. In: surface and subsurface marine sediments. Geochim et Cosmochim Acta, 7, p.205-211.

Balistrieri, L.S., Murray, J.W. 1986. The Surface Chemistry of Sediments from the Panama Basin: The influence of Mn oxides on metal absorption. Geochim et Cosmochim. Acta, 50, p.2235-2243.

Baturin, G.N., Kockemov, A.V., Shinkus, K.M. 1967. Uranium and rare metals in the sediments of the Black and Mediterranean Seas. Geochem. Internat., 4, pp29.

Beasley, T.M., Carpenter, R., Jennings, C.D. 1982. Plutonium, ^{241}Am and ^{137}Cs, ratios, inventories and vertical profiles in Washington and Oregon Continental Shelf sediments. Geochim. et Cosmochim. Acta., 46, p.1931-1946.

Berner, R.A. 1964. Distribution and diagenesis of sulphur in the sediment from the Gulf of California. Mar. Geol., 1, 117-140.

Berner, R.A. 1970. Sedimentary pyrite formation. Am. J. Sci., 268, p.1-23.

Berner, R.A. 1971. Principles of Chemical Sedimentology. McGraw-Hill, New York, pp240.

Berner, R.A. 1978. Sulphate reduction and the rate of deposition of marine sediments. Earth Planet. Sci. Lett., 37, p.492-498.

Berner, R.A. 1979. A new look at biogenous material in deep sea sediments. Ambio. Sp. Rep., 6, p.5-10.

Berner, R.A. 1980. Early diagenesis: A theoretical approach. Princeton University Press, Princeton, N.J., pp241.

Berner, R.A. 1982. Burial of organic carbon and pyrite sulphur in modern oceanic sediments. Amer. J. Sci., 282, p.451-473.

Berner, R.A. 1984. Sedimentary pyrite formation: An update. Geochim et Cosmochim. Acta., 48, p.605-615.

Berner, R.A., Scott, M.R., Thomlinson, C. 1970. Carbonate alkalinity in the pore waters of anoxic marine sediment. Limnol. Oceanogr., 15, p.544-549.

Berner, R.A., Westrich, J.T. 1985. Bioturbation and the early diagenesis of C and S. Am. J. Sci., 285, p.193-206.

Bertine, K.K., Goldberg, E.D. 1971. Fossil fuel combustion and the major sedimentation cycle. Science, 173, p.233-235.

Bertine, K.K., Mendeck, M.F. 1978. Industrialisation of New Haven, Conn, as recorded in reservoir sedimentation. Environ. Sci. & Tech., 12, p.201-207.

Biscaye, P.E. 1965. Mineralogy and sedimentation of recent deep sea clay in the Atlantic Ocean and adjacent seas and oceans. Geol. Soc. Amer. Bull., 76, p.803-832.

Bopp, R.F., Simpson, H.J., Olsen, G.R., Kostyk, N. 1981. Polychlorinated biphyenyls in sediments of the tidal Hudson River, New York. Environ. Sci. & Tech., 15, p.210-276.

Bopp, R.F., Simpson, H.J., Olsen, C.R., Treir, R.M., Kostyk, N. 1982. Chlorinated hydrocarbons and radionuclide chronologies in sediments of the Hudson River and Estuary, New York. Environ. Sci. & Tech., 16, p.666-676.

Bordovskiy, O.K. 1965. Transformation and diagenesis of organic matter in sediments. Mar. Geol., 3, p.83-114.

Boutron, C., Patterson, C.C. 1986. Lead concentration changes in Antarctic ice during the Wisconsin/Holocene Transition. Nature, 323, p.222-227.

Bowen, H.J.M. 1966. Trace elements in biochemistry. Academic Press, pp241.

Bower, P.M., Simpson, H.J., Williams, S.C., Li, Y.H. 1978. Heavy metals in the sedimentation of Foundry Cove, Cold Spring, N.Y. Environ. Sci. & Tech., 12, p.683-687.

Brown, F.S., Baedecker, M.J., Nissebaum, A., Kaplan, I.R. 1972. Early diagenesis in a reducing fjord Saanich Inlet, British Columbia-III: Changes in organic constituents of sediment. Geochim. et Cosmochim. Acta., 36, p.1185-1203.

Bruland, K.W., Bertine, K.W., Koide, M., Goldberg, E.D. 1974. History of metal pollution in the Southern California coastal zone. Environ. Sci. & Tech., 8, p.425-432.

Calvert, S.E. 1976. Mineralogy and geochemistry of near-shore sediments. In: Chemical oceanography, vol 6. 2nd Ed J.P. Riley & R. Chester (eds). Academic Press, London.

Calvert, S.E. & Piper, D.Z. 1984. Geochemistry of ferromanganese nodules from DOMES site A, Northern equatorial Pacific: Multiple diagenetic sources in the deep sea. Geochim. et Cosmochim. Acta., 48, p.1913-1928.

Calvert, S.E., Price, N.B. 1983. Geochemistry of Namibian Shelf Sediments. In: Coastal Upwelling Pt. A. NATO conference series IV, Marine sciences; 10.A E. Suess & J. Theide (Eds).

Carpenter, R., Peterson, M.L., Bennett, J.T. 1982. ^{210}Pb derived sediment accumulation and mixing rates for the Washington Continental Slope. Mar. Geol., 48, p.135-164.

Carpenter, R., Peterson, M.L., Bennett, J.T. 1985. ^{210}Pb derived sediment accumulation and mixing rates for the greater Puget Sound Region. Mar. Geol., 64, p.291-312.

Chao, G.Y. 1969. 2θ (Cu) table for common minerals. Carleton University Geological Paper 69-2. Ottawa, Canada.

Chow, T.J., Bruland, K.W., Bertine, K., Soutar, A., Koide, M., Goldberg, E.D. 1973. Lead pollution: Records in S. California Coast sedimentation. Science, 181, p.551-552.

Cline, J.D., Kaplan, I.R. 1975. Isotopic fractionation of dissolved nitrate during denitrification in the Eastern Tropical North Pacific Ocean. Mar. Chem., 3, p.271-299.

Craib, J.S. 1965. Craib corer, A short sediment corer. J. Cons. Perm. Int. Explor. Mar., 30, p.34-39.

Crecelius, E.A., Piper, D.Z. 1973. Particulate Pb contamination recorded in sedimentary cores from Lake Washington, Seattle. Environ. Sci. & Tech., 7, 11, p.1053-1055.

Crecelius, E.A., Bothner, M.H., Carpenter, R. 1975. Geochemistries of As, Sb, Hg and related elements in sediments of Puget Sound. Environ. Sci. & Tech., 9, 4, p.325-333.

Davies, I.M. 1977. Chemical diagenesis of coastal sediments. Ph.D. Thesis (Unpub.) University of Edinburgh, pp235.

Degens, E.T., Mopper, K. 1976. Factors controlling the distribution and early diagenesis of organic material in marine sediments. In: Chemical Oceanography, vol 6, 2nd edition J.P. Riley & R. Chester (Eds). Academic Press, London.

De Master, D.J., Cochran, J.K. 1983. Particle mixing rates in deep-sea sediments determined from excess ^{210}Pb and ^{32}Si profiles. Earth Planet. Sci. Lett., 61, p.257-271.

Duchesne, J.C. 1968. Strontium vs calcium, barium vs potassium relationships in plagioclases from South Rogaland anorthosites. Ann. Soc. Geol. Belg. Bull., 90, pp643.

Duursma, E.K., Bosch, C.J. 1970. Theoretical, experimental and field studies concerning diffusion of radioisotopes in sediments and suspended particles of the sea. Part B: Methods and experiments. Neth. J. Sea. Res., 4, p.395-469.

Edmond, J. 1970. High precision determination of titration alkalinity and total carbon dioxide content of sea water by potentiometric titration. Deep Sea Res., 17, p.737-750.

Edwards, A, Xu, Z., Thompson, R. 1987. Sediments and physical oceanography of Airds Bay, Loch Etive. Marine Physics Group Report No 38, SMBA.

Eisenrich, S.J., Hollod, G.J., Johnson, T.C. 1979. Accumulation of PCB's in surficial Lake Superior sediments: Atmospheric deposition. Environ. Sci. & Tech., 13, p.596-573.

Elderfield, H., Hepworth, A. 1975. Diagenesis, metals and pollution in estuaries. Mar. Pol. Bull., 6, p.85-87.

Elderfield, H., McCaffrey, R.J., Luedtke, N., Bender, M., Truesdale, V.M. 1981. Chemical diagenesis in Narragansett Bay sediments. Am. J. Sci., 281, p.1021-1055.

El Ghobary, H., Latouche, C. 1986. Distribution of certain metals in lithochemical fractions of sediments from the Archachon Basin SW France: Authigenic mineral formation and pollution. Chem. Geol., 54 (1986), p.295-309.

Erlank, A.J., Smith, H.S., Marchant, J.N., Cardoso, M.P., Ahrens, L.H. 1978. Zirconium abundance in common sediments and sedimentary rocks. In: Handbook of Geochemistry II/4. Wedepohl et al. (Eds) Springer Verlag, Heidelberg, New York.

Erlenkeuser, H., Suess, E., Willkomm, H. 1974. Industrialisation effects heavy metal and carbon isotope concentrations in recent Baltic Sea sediments. Geochim. et Cosmochim. Acta., 38, p.832-842.

Farmer, J.G. 1983. Metal pollution in marine sediment cores in the west coast of Scotland. Mar. Environ. Res., 8, p.1-28.

Fitton, J.G., Dunlop, H.M. 1985. The Cameroon Line, West Africa, and its bearing on the origin of oceanic and continental alkali basalt. Earth Planet. Sci. Lett., 72, p.23-38.

Francis, P.W., Moorbath, S., Welke, H.J. 1971. Isotopic age data from Scourian Intrusive rocks on the Isle of Barra, Outer Hebrides, NW Scotland. Geol. Mag., 108, p.13-22.

Franzin, W.G., McFarlane, G.A., Lutz, A. 1979. Atmospheric fall-out in the vicinity of a base metal smelter at Flin Flon, Manitoba, Canada. Environ. Sci. & Tech., 13, p.1513-1522.

Froelich, P.N., Klinkhammer, G.P., Bender, M.L., Luedtke, N.A., Heath, G.R., Cullen, D., Dauphin, P., Hammond, D., Hartmann, B., Maynard, V. 1979. Early oxidation of organic matter in pelagic sediments of the eastern equatorial Atlantic: Suboxic diagenesis. Geochim. et Cosmochim. Acta., 43, p.1075-1090.

Frondel, C. 1978. Scandium. In: Handbook of geochemistry vol II/2. Wedepohl et al. (Eds). Springer-Verlag, Berlin, Heidelberg, New York.

Füchtbauer, H., Reineck, H-E. 1963. Porositt und verdichtung rezenter, mariner sedimente. Sedimentology, 2, p.294-306.

Galloway, J.N. 1979. Alteration of trace metal geochemical cycles due to marine discharge of wastewater. Geochim. et Cosmochim. Acta., 43, p.207-218.

Galloway, J.N., Likens, G.E. 1979. Atmospheric enhancement of metal deposition in Adirondack Lake sediments. Limnol. Oceanogr., 24, p.427-433.

Goldberg, E.D. 1976(a). The Health of the Oceans. Unesco Press, Paris, pp172.

Goldberg, E.D. 1976(b). Pollution History of Estuarine Sediments. Oceanus, p.18-26.

Goldberg, E., Gamble, E., Griffin, J.J., Koide, M. 1977. Pollution history of Narragansett Bay as recorded in its sediments. Est. & Coast mar. Sci., 5, p.549-561.

Goldberg, E., Hodge, V., Koide, M. Griffen, J., Gamble, E., Bricker, O.P., Matisoff, G., Holdren, G.R. (Jnr)., Braun, R. 1978. A pollution history of Chesapeake Bay. Geochim. et Cosmochim. Acta., 42, p.1413-1425.

Goldberg, E.D., Griffin, J.J., Hodge, V., Koide, M., Windam, H. 1979. Pollution history of the Savannah River Estuary. Env. Sci. & Technol., 13, p.588-593.

Goldhaber, M.B. 1974. Equilibrium and dynamic aspects of the marine geochemistry of sulphur. Ph.D. thesis, UCLA, pp399.

Goldhaber, M.B., Kaplan, I.R. 1975. Controls and consequences of sulphate reduction rates on recent marine sediments. Soil. Sci., 119,p.42-55.

Goldhaber, M.B., Aller, R.C., Cochran, J.K., Rosenfeld, J.K., Martens, C.S., Berner, R.A. 1977. Sulphate reduction, diffusion and bioturbation in Long Island sound sediments: Report of the FOAM Group. Amer. J. Sci., 277, p.193-237.

Goldhaber, M.B., Kaplan, I.R. 1974. The sulphur cycle. In: The Sea. E.D. Goldberg (ed), Wiley, New York, p.569-655.

Goldhaber, M.B., Kaplan, I.R. 1980. Mechanisms of sulphur incorporation and isotope fractionation during early diagenesis in sediments of the Gulf of California. Mar. Chem., 9, p.95-143.

Goldschmidt, V.M. 1954. Geochemistry. Clarendon Press, Oxford pp730.

Gordon, D.C. 1971. Distribution of organic carbon and nitrogen at an oceanic station in the Central Pacific. Deep Sea Res., 18, p.1127-1134.

Gran, G. 1952. Determination of the equivalence point in potentiometric titrations part II. Analyst, 77, p.661-671.

Greig, R.A., Reid, R.N., Wenzloff, D.R. 1977. Trace metal concentrations in sediments from Long Island Sound. Mar. Poll. Bull. 8, p.183-188.

Grundmanis, V., Murray, J.W. 1982. Aerobic respiration in pelagic marine sediments. Geochim. et Cosmochim. Acta., 46, p.1101-1120.

Halcrow, W., Mackay, D.W., Thornton, I. 1973. The distribution of trace metals and fauna in the Firth of Clyde in relation to disposal of sewage sludge. J. Mar. Biol. Ass. UK, 53, p.721-739.

Hamilton-Taylor. 1979. Enrichments of Zn, Pb, Cu in recent sediments of Windermere, England. Environ. Sci. & Tech., 13, p.693-697.

Harker, A. 1941. The west Highlands and the Hebrides. Cambridge.

Harvey, G.R. 1980. A study of the chemistry of I and Br in marine sediments. Mar. Chem., 8, p.327-332.

Haskin, M., Haskin, L.A. 1966. Rare earth elements in European shales: a redetermination. Science, 154, p.507-509.

Heier, K.S., Billings, G.K. 1978. Rubidium; abundance in common sediments and sedimentary rock types. In: Handbook of Geochemistry II4 Wedepohl et al. (Eds). Springer-Verlag Heidelberg, New York.

Hess, C.T., Smith, C.W., Price, A.H. 1978. Radionuclide loss from marine sediment. Nature, 272, p.807-809.

Hetherington, J.A., Harvey, B.R. 1978. Uptake of radioactivity by marine sediments and implications for monitoring metal pollutants. Mar. Pol. Bull., 9, p.102-106.

Herrmann, A.G. 1978. Yttrium and the Lanthanides. In: Handbook of Geochemistry. Vol II/5. K.H. Wedepohl et al. (Eds). Springer-Verlag, Heidelberg, New York.

Hill, P.A., Parker, A. 1970. Tin and zirconium in the sediments around the British Isles: A preliminary reconnaisance. Econ. Geol., 65, p.409-416.

Hom, W., Riseborough, R.W., Soutar, A., Young, D.R. 1974. Deposition of DDE and polychlorinated biphenyls in dated sediments of the Santa Barbara Basin. Science, 184, p.1197-1199.

Howarth 1978. A precise method for determining sulfate in seawater estuarine waters, and sediment pore waters. Limnol. Oceanogr., 23, p.1066-1069.

Hunt, C.D. 1981. Regulation of sedimentary cation exchange capacity by organic matter. Chem. Geol., 34, p.131-149.

Hunt, C.D., Fitzgerald, W.F. 1983. The capacity of marine plankton, macrophytes and particulate matter to adsorb Cu^{2+} in the presence of Mg^{2}. Mar. Chem., 12, p.255-280.

Ittekot, V. 1987. Nature of organic matter in rivers suspensions: Global trends and implications for marine organic carbon burial. (In Press).

Jenkins, R., De Vries, J.L. 1970. Practical X-Ray spectrometry. 2nd Edition, Phillip's Technical Library. Macmillan, London.

Johnson, M.R.W. 1983. Torridonian-Moine. In: Geol. of Scot. G.Y. Craig (Ed.)., 2nd Edition Scottish Academic Press, 1982.

Jones, G.B., Jordan, M.B. 1979. Distribution of organic matter and trace metals in sediment from R. Liffey estuary, Dublin. Est. Coast. Mar. Sci., 8, p.37-47.

Jorgensen, B.B. 1977. The sulphur cycle of a coastal marine sediment (Limfjorden Denmark). Limnol. oceanogr., 22, p.814-832.

Jorgensen, B.B. 1982. Ecology of the bacteria of the sulphur cycle with special reference to anoxoic-oxic interface environments. Phil. Trans. Roy. Soc. London, B298, p.543-561.

Kaplan, I.R. 1975. Stable isotopes as a guide to biogeochemical processes. Proc. Roy. Soc. Lond. (B), 189, p.183-211.

Kaplan, I.R., Emergy, K.O., Rittenberg, S.C. 1963. The marine sediments of Southern California. Geochim. et Cosmochim. Acta., 27, p.297-331.

Keeny, D.R., Bremner, J.M. 1967. Determination and isotope ratio analysis of different forms of nitrogen in soils 7-Urea. Soil. Sci. Soc. Amer. Proc., 31, p.317-321.

Kemp, A.L.W., Thomas, R.L., Dell, C.I., Jaquet, J.M. 1976. Cultural impact on the geochemistry of the sediments in Lake Erie. J. Fish. Res. Board. Can., 33, p.440-462.

King, G.M., Howes, B.L., Dacey, J.W.H. 1985. Short term end products of SO_4 reduction in a salt marsh: formation of acid volatile sulphides, elemental sulphur and pyrite. Geochim. et Cosmochim. Acta., 49, p.1561-1566.

Klump, J.V., Martens, C.S. 1987. Biogeochemical cycling in an organic rich coastal marine basin 5: Sedimentary N and P budgets based upon kinetic models, mass balances and the stoichiometry of nutrient regeneration. Geochim. et Cosmochim. Acta, 51, p.1161-1173.

Kochenov, A.V., Zonov'ev, V.V. 1960. Distribution of rare earth elements in phosphatic remains of fish from the Maikop deposits. Geochemistry (USSR) English Transl. p.860-873.

Kohl, D.H., Shearer, G., Commoner, B. 1971. Fertiliser nitrogen: Contribution of NO_3 in surface waters in a corn belt watershed. Science, 174, p.1331-1334.

Koide, M., Soutar, A., Goldberg, E.D. 1972. Marine geochronology with ^{210}Pb. Earth Planet. Sci. Lett., 14, p.442-446.

Koide, M., Bruland, K.W., Goldberg, E.D. 1973. $^{228}Th/^{232}Th$ and ^{210}Pb geochronologies in marine and lake sediments. Geochim. et Cosmochim. Acta., 37, p.1171-1187.

Koide, M., Goldberg, E.D., Hodge, V.F. 1980. ^{241}Pu and ^{241}Am in sediments from coastal basins off California and Mexico. Earth Planet. Sci. Lett., 48, p.250-256.

Krishnaswami, S., Lah, D., Martin, J.M., Meybeck, M. 1971. Geochronology in lake sediments. Earth Planet. Sci. Lett., 11, p.407-414.

Krom, M.D. 1976. The geochemistry of Loch Duich, Scotland. Ph.D. thesis, University of Edinburgh (Unpublished) pp250.

Krom, M.D., Berner, R.A. 1980. Diffusion coefficients of SO_4, NH_3, PO_4 ions in anoxic marine sediments. Limnol. Oceanogr., 25, p.327-337.

Krom, M.D., Sholkovitz, E.R. 1977. Nature and reactions of dissolved organic matter in the interstitial waters of marine sediments. Geochim. et Cosmochim. Acta., 41, p.1565-1573.

Lazarus, A.K., Lorange, E., Lodge, J.P. 1970. Lead and other metal ions in U.S. precipitation. Environ. Sci. Technol., 4, p.55-58.

Livingston, H.D., Bowen, V.T. 1979. Plutonium and ^{137}Cs in coastal sediments. Earth Planet. Sci. Lett., 43, p.29-45.

Lord, III C.J., Church, T.M. 1983. The geochemistry of salt marshes: Sedimentary iron, diffusion, SO_4 reduction and pyritisation. Geochim. et Cosmochim. Acta., 47, p.1381-1391.

Lyons, W.B., Gaudette, H.E. 1979. Sulphate reduction and the nature of estuarine sediments. Org. Geochim., 1, p.151-155.

Lyons, W.B., Armstrong, P.B., Gaudette, H.E. 1983. Trace metal concentrations and fluxes in Bermuda sediments. Mar. Pol. Bull., 14, p.65-68.

Mackenzie, A.B., Scott, R.D. 1982. Radiocaesium and intertidal sediments from Southern Scotland. Nature, 299, p.613-616.

Mackenzie, A.B., Scott, R.D., Williams, T.M. 1987. Mechanisms for northwards dispersal of Sellafield waste. Nature, 329, p.42-45.

Malcolm, S.J. 1981. The chemistry of sediments of Loch Etive, Scotland. Ph.D. Thesis, University of Edinburgh pp183 .

Malcolm, S.J., Battersby, N.S., Stanley, S.O., Brown, C.M. 1986. Organic degradation, sulphate reduction and ammonia production in the sediment of Loch Eil, Scotland. Est. Coast & Shelf Sci., 23, p.689-706.

Manheim, F.T. 1976. Interstitial waters in marine sediment. In: Chemical Oceanography, vol 6, 2nd Edition. J.P. Riley, R. Chester (eds). Academic Press, London.

Mariotti, A. 1983. Atmospheric nitrogen is a reliable standard for natural ^{15}N abundance measurements. Nature, London, 303, p.685-687.

Martens, C.S., Berner, R.A., Rosenfeld, J.K. 1978. Interstitial water chemistry of anoxic Long Island sound sediments. 2. Nutrient regeneration and phosphate removal. Limnol. Oceanogr. 23(4), p.605-617.

Martens, C.S., Klump, V.J. 1984. Biogeochemical cycling in an organic rich coastal marine basin 4: An organic C budget for sediment dominated by SO_4 reduction and methanogenesis. Geochim. et Cosmochim. Acta., 48, p.1987-2004.

Matzat, E. 1978. Chromium: Crystal chemistry. In: Handbook of Geochemistry vol II/3 K.H. Wedepohl et al. (Eds) Springer-Verlag, Heidelberg, New York.

Mayer, L.M., Macko, S.A. Mook, W.H., Murray, S. 1981. The distribution of bromine in coastal sediments and its use as a source indicator for organic matter. Org. Geochem., 3, p.37-42.

McCorkle, D.C., Emerson, S.R., Quay, P.D. 1985. Stable carbon isotopes in marine pore waters. Earth Planet. Sci. Lett., 74, p.13-26.

McKay, W.A., Baxter, M.S. 1985. The partitioning of Sellafield derived radiocaesium in Scottish coastal sediments. J. Environ. Rad., 2, p.93-115.

McKay, W.A., Baxter, M.S., Ellet, D.J., Meldrum, D.T. 1986. Radiocaesium and circulation patterns West of Scotland. J. Environ. Reactivity, 4, p.205-232.

McKinley, I.G., Baxter, M.S., Jack, W. 1981(a). A simple model of radiocaesium transport from Windscale to the Clyde Sea. Est. Coast. & Shelf Sci., 13, p.59-68.

McKinley, I.G., Baxter, M.S., Ellet, D.J., Jack, W. 1981(b). Tracer applications of radiocaesium in the sea of the Hebrides. Est. Coast. & Shelf Sci., 13, p.69-82.

Minagawa, M., Wada, E. 1984. Stepwise enrichment of ^{15}N along food chains: Further evidence and the relation between ^{15}N and animal age. Geochim. et Cosmochim. Acta., 48, p.1135-1140.

Miyakie, Y., Wada, E. 1967. The abundance ratio of $^{15}N/^{14}N$ in marine environments. Records of oceanographic works in Japan, 9, p.37-53.

Moorbath, S., Powell, J.L., Taylor, P.N. 1975. Isotopic evidence for the age and origin of the grey gneiss complex of the S. Outer Hebrides. J. Geol. Soc. Lond., 131, p.213-222.

Morse, J.W., Millero, F.J., Cornwell, J.C., Rickard, D. 1987. The chemistry of the hydrogen sulphide and iron sulphide systems in natural waters. Earth Sci. Rev., 24, p.1-42.

Müller, P.J. 1977. C/N ratios in Pacific Deep Sea sediments: Effect of inorganic ammonium and organic nitrogen compounds sorbed by clays. Geochim. et Cosmochim. Acta., 41, p.765-776.

Musset, A.E., Brown, G.C., Eckford, M., Charlton, S.R. 1973. The British Tertiary igneous province: K-Ar ages of some dykes and lavas from Mull, Scotland. Geophys. J.R. Astr. Soc., 30, p.405-414.

Musset, A.E., Dagley, P., Skelhorn, R.R. 1980. Magneto-stratigraphy of the Tertiary igneous succession of Mull, Scotland. J. Geol. Soc. Lond., 137, p.349-357.

Nicholls 1950. The Glenelg-Ratagan igneous complex. Q. J. Geol. Soc. Lond., 106, p.309-344.

Nissenbaum, A., Presley, B.J., Kaplan, I.R. 1972. Early diagenesis in a reducing fjord. Saanich Inlet, British Columbia, I. Chemical and isotopic changes in major components of interstitial water. Geochim. et Cosmochim. Acta., 36, p.1007-1027.

Nittrouer, C.A., Sternberg, R.W., Carpenter, R., Bennett, J.T. 1979. The use of ^{210}Pb geochronology as a sedimentological tool: Application to the Washington continental shelf. Mar. Geol., 31, p.297-316.

Nittrouer, C.A., De Master, D.J., McKee, B.A., Cutshall, N.H. 1983. The effect of sediment mixing on ^{210}Pb accumulation rates for the Washington Continental Shelf. Mar. Geol., 54, p.201-221.

Nraigu, J.O. 1979. Global inventory of natural and anthropogenic emission of trace metals to the atmosphere. Nature, 279, p.409-411.

Peach, B.N., Horne, J. 1930. Chapters on the geology of Scotland. Oxford University Press.

Peacock, J.D., Graham, D.K., Wilkinson, I.P. 1978. Late glacial and post-glacial marine environment at Ardyne Scotland, and their significance in the interpretation of the Clyde Sea area. Rep. Inst. Geol. Sci. London, 78/17.

Pederson, T.F., Price, N.B. 1980. The geochemistry of iodine and bromine in sediments of the Panama Basin. J. Mar. Res., 38, p.397-411.

Pennington, W., Cambray, R.S., Fisher, E.M. 1973. Observations on lake sediments using fallout ^{137}Cs as a tracer. Nature, 242, p.324-326.

Peters, K.E., Sweeny, R.E., Kaplan, I.R. 1978. Correlation of C and N stable isotope ratios in sedimentary organic matter. Limnol. Oceanogr., 23, p.598-604.

Pettijohn, F.J. 1975. Sedimentary rocks. 3rd edition. Harper & Row, New York, pp628.

Pierson, D.H., Cawse, P.A., Salmon, L., Cambray, R.S. 1973. Trace elements in the atmospheric environment. Nature, 241, p.252-256.

Pocklington, R., Leonard, J.D. 1979. Terrigenous organic matter in sediments of the St Lawrence estuary and Saguenay Fjord. J. Fish. Res. Board Can., 36, p.1250-1255.

Potter, P.E., Shimp, N.F., Witters, J. 1963. Trace elements in marine and fresh water argillaceous sediments. Geochim. et Cosmochim. Acta., 27, p.669-694.

Price, N.B. 1976. Chemical diagenesis in sediments. In: Chemical Oceanography vol 6 2nd Edition J.P. Riley & R. Chester (Eds). Academic Press, London.

Price, N.B., Calvert, S.E. 1977. The contrasting geochemical behaviours of iodine and bromine in recent sediments from the Namibian Shelf. Geochim. et Cosmochim. Acta., 41, p.1769-1775.

Price, N.B., Malcolm, S.J., Hamilton-Taylor, J. 1978. Environmental impact of Pb and Zn in recent sediments. In: Biogeochemistry of Estuarine sediments. Unesco Paris, pp293.

Puchelt, H. 1967. Zur geochimie des Bariums im exogenes Zyklus. Sitzugsber. Heidelb. Akad. Wiss. Matt-Nat. K1, 4 Abh.

Puchelt, H. 1978. Barium: Abundance in rock forming minerals (I) and Barium minerals (II). In: Handbook of Geochemistry vol II/4, Wedepohl et al. (eds). Springer-Verlag, Heidelberg, Berlin, New York.

Pyzik, A.J., Sommer, S.E. 1981. Sedimentary iron monosulphides kinetics and mechanism of formation. Geochim. et Cosmochim. Acta., 45, p.687-698.

Ranticelli, L.A., Perkins, R.W. 1970. Trace element concentrations in the Troposphere and Lower Stratosphere. J. Geophys. Res., 75, p.3055-3064.

Redfield, A.C., Ketchum, B.H., Richards, F.A. 1963. The influence of organisms on the composition of sea water. In: The Sea vol 2,, M.N. Hill (ed), J. Wiley, 1963, pp26-77.

Reynolds, R.C. (Jnr) 1963. Matrix corrections in trace element analysis by X-Ray flourescence: Estimation of the mass absorption coefficient by Compton scattering. Amer. Min., 48, p.1133-1143.

Ridgway, I.M. 1984. Behaviour of organic material and minor elements in Scottish Sea lochs. Ph.D. Thesis University of Edinburgh pp227.

Ridgway, I.M., Price, N.B. 1987. Geochemical associations and post-depositional mobility of heavy metals in coastal sediments. Loch Etive, Scotland. Mar. Chem., 21, p.229-248.

Ritchie, J.C., McHenry, J.R., Gill, A.C. 1973. Dating recent reservoir sediments. Limnol. Oceanogr., 18, p.254-263.

Rittenberg, S.C., Emery, K.O., Orr, W.L. 1955. Regeneration of nutrients in sediments of marine basins. Deep Sea Res., 3, p.23-45.

Robbins, J.A., Edgington, D.N. 1975. Determination of recent sedimentation rates in Lake Michigan using ^{210}Pb and ^{137}Cs. Geochim. et Cosmochim. Acta., 39, p.285-304.

Rosenfeld, J.K. 1979(a). Ammonium adsorption in nearshore anoxic sediments. Limnol. & Oceanogr., 24, p.356-364.

Rosenfeld, J.K. 1979(b). Interstitial water and sediment chemistry of two cores from Florida Bay. J. Sed. Pet., 49:3, p.989-994.

Saino, T., Hattori, A. 1980. ^{15}N natural abundance in oceanic suspended particulate matter. Nature, 283, p.752-754.

Santschi, P.H., Li, Y.H., Adler, D.M., Amdurer, M., Bell, J.J., Nyffeler, U.P. 1983. The relative mobility of natural (Th, Pb and Po) and fallout (Pu, Am and Cs) radionuclide in the coastal marine environment: results from model ecosystems (MERL) and Narragansett Bay. Geochim. et Cosmochim. Acta., 47, p.201-210.

Sayles, F.L., Mannheim, F.T. 1975. Interstitial solutions and diagenesis in deeply buried marine sediments: results from the DSDP. Geochim. et Cosmochim. Acta., 39, p.103-127.

Schell, W.R. 1977. Concentrations, physico-chemical states and mean residence times of ^{210}Pb and ^{210}Po in marine and estuarine waters. Geochim. et Cosmochim. Acta., 41, p.1019-1031.

Shaule, B.K., Patterson, C.C. 1981. Lead concentrations in the NE Pacific. Evidence for global anthropogenic perturbation. Earth Planet. Sci. Lett., 54, p.97-116.

Shearer, G., Kohl, D.H., Commoner, B. 1973. Variation of ^{15}N in corn and soil following application of fertiliser Nitrogen. Soil. Sci. Amer. Proc., 37, p.888-892.

Shearer, G., Kohl, D.H., Commoner, B. 1979. Nitrogen-15 abundance in N-fixing and Non N-fixing plants. 4 Int. Symposium on Mass Spectrometry in Biochem. & Medicine. Riva del Garda, Italy, 20-22 June 1979.

Shimmield, G.B. 1984. The geochemistry and mineralogy of Pacific sediments Baja California. Unpubl. Ph.D. Thesis, University of Edinburgh.

Shirahata, H., Eleas, R.W., Patterson, C.C., Koide, M. 1980. Chronological variations in concentrations and isotopic compositions of anthropogenic atmospheric Pb in sediments of a remote sub-alpine pond. Geochim. et Cosmochim. Acta., 37, p.2043-2073.

Shiraki, K. 1966. Some aspects of the geochemistry of chromium. J. Earth Sci. Nagoya University, 14.

Shiraki, K. 1978. Chromium: Abundance in common sediments and sedimentary rock types. In: Handbook of Geochemistry, II/3. 5th edition, K.H. Wedepohl et al.(eds), Springer Verlag, Heidelberg, New York.

Sholkovitz, E.R. 1973. Interstitial water chemistry of the Santa Barbera basin sediments. Geochim. et Cosmochim. Acta., 37, p.2043-2073.

Sholkovitz, E.R., Cochran, J.K., Carey, A.E. 1983. Laboratory studies of the diagenesis and mobility of $^{239,240}Pu$ and ^{137}Cs in nearshore sediment. Geochim. et Cosmochim. Acta., 47, p.1369-1379.

Sholkovitz, E.R., Mann, D.R. 1984. The pore water chemistry of $^{239,240}Pu$ and ^{137}Cs in sediments in Buzzards Bay, Massachusetts. Geochim. et Cosmochim. Acta., 48, p.1107-1114.

Sigg, L, Sturm, M., Kistler, D. 1987. Vertical transport of heavy metals by settling particles in Lake Zurich. Limnol. oceanogr., 32, p.112-130.

Sissons, J.B. 1967. The evolution of Scotland's scenery. Oliver and Boyd Ltd, London pp259.

Skei, J., Paus, P.E. 1979. Surface metal enrichment and partitioning of metals in a dated sediment core from a Norwegian Fjord. Geochim. et Cosmochim. Acta., 43, p.239-246.

Stanners, D.A., Aston, S.R. 1981(a). An improved method of determining sedimentation rates by the use of artificial radionuclides. Est. Coast. & Shelf Sci., 13, p.101-106.

Stanners, D.A., Aston, S.R. 1981(b). ^{134}Cs:^{137}Cs and ^{106}Ru:^{137}Cs ratios in intertidal sediments from the Cumbria and Lancashire coasts, England. Est. Coast & Shelf Sci., 13, p.409-417.

Stevenson, F.T., Cheng, C.N. 1972. Organic geochemistry of the Argentine Basin sediments: C/N relationship and Quaternary correlations. Geochim. et Cosmochim. Acta., 36, p.653-671.

Stueber, A.M. 1978. Strontium abundance in rock forming minerals; strontium minerals. In: Handbook of Geochemistry, K.H. Wedepohl et al. (eds), 5th Edition, Springer-Verlag, Heidelberg, New York.

Stumm, W. & Morgan, J.J. 1970. Aquatic Chemistry. New York, John Wiley & Sons, New York pp583.

Suess, E., Müller, P.J. 1980. Productivity, sedimentation rate and sedimentary organic matter in the oceans-II: Elemental fractionation. Proceedings CNRS Symposium on the Benthic Boundary Layer, Marsielle, France, p.17-26.

Swaine, D.J. 1977. Trace elements in fly ash. In: Geochemistry 1977 (Ellis, A.J. Compiler) DSIR Bull. p.127-131.

Swan, D.S., Baxter, M.S., McKinley, I.G., Jack, W. 1982. Radiocaesium and ^{210}Pb in Clyde Sea Loch sediments. Est. Coast. & Shelf Sci., 15, p.515-536.

Sweeny, R.E., Liu, K.K., Kaplan, I.R. 1978. Oceanic nitrogen isotopes and their uses in determining the source of sedimentary nitrogen. In: Stable isotopes in the Earth Sciences, p.9-26 DSIR Bull. B.W. Robinson (Ed).

Sweeny, R.E. & Kaplan, I.R. 1980. Natural abundances of ^{15}N as a source indicator for near shore marine sedimentary and dissolved nitrogen. Mar. Chem., 9, p.81-94.

Toth, D.J., Lerman, A. 1977. Organic matter reactivity and sedimentation rates in the Ocean. Am. J. Sci., 277, p.465-85.

Turekian, K.K. 1978. Nickel abundance in rock-forming minerals, nickel minerals and phase equilibria. In: Handbook of Geochemistry II/3 K.H. Wedepohl et al. (Eds). Springer-Verlag, Heidelberg, New York.

Turekian, K.K. & Wedepohl, K.H. 1961. Distribution of the elements in some major units of the Earth's crust. Geol. Soc. Am. Bull., 72, p.175-192.

Ullman, W.J., Aller, R.C. 1980. Dissolved I flux from estuarine sediments and implications for enrichment at the sediment/water interface. Geochim. et Cosmochim. Acta., 44, p.1177-1184.

Ullman, W.J., Aller R.C. 1983. Rates of iodine remineralisation in terrigenous near-shore sediments. Geochim. et Cosmochim. Acta., 47, p.1423-1432.

Ullman, W.J., Aller, R.C. 1985. The geochemistry of iodine in nearshore carbonate sediments. Geochim. et Cosmochim. Acta., 49, p.967-978.

Vaccaro, R.F. 1965. Inorganic nitrogen in sea water. In: Chemical Oceanography, vol 1 Riley & Skirrow (Eds), p.365-408.

Wada, E., Hattori, A. 1978. Nitrogen isotope effects in the assimilation of inorganic nitrogenous compounds in marine diatoms. Geomicrobiol. J., 1, p.85-101.

Walsh, J.N., Beckinsale, R.D., Skelhorn, R.R., Thorpe, R.S. 1979. Geochemistry and petrogenesis of Tertiary granitic rocks from the island of Mull, NW Scotland. Contrib. Mineral. Petrol., 71, p.99-116.

Waples, D.W. 1985. Organic and inorganic N in sediment from Leg 80 DSDP. Init. Rep. DSDP Leg 80 Brest-Southampton PtII P.C. de Gacionsky, C.W. Poag (eds).

Willey, J.D. & Fitzgerald, R.A. 1980. Trace metal geochemistry in sediment from Miramichi Estuary, New Brunswick. Can. J. Earth Sci., 17, p.254-265.

White, S.M. 1970. Mineralogy and geochemistry of continental shelf sediments off the Washington, Oregon Coast. J. Sedim. Petrol, 40, p.38-54.

Wlotzka, F. 1972. Nitrogen Chapter 7 In: Handbook of Geochemistry vol II/1, K.H. Wedepohl et al. (Eds), Springer-Verlag, Heidelberg, New York.